



University
of Glasgow

McCully, Mark Alan (2015) The delivery of small regulatory RNAs by gold nanoparticles. PhD thesis.

<http://theses.gla.ac.uk/6478/>

Copyright and moral rights for this thesis are retained by the author

A copy can be downloaded for personal non-commercial research or study, without prior permission or charge

This thesis cannot be reproduced or quoted extensively from without first obtaining permission in writing from the Author

The content must not be changed in any way or sold commercially in any format or medium without the formal permission of the Author

When referring to this work, full bibliographic details including the author, title, awarding institution and date of the thesis must be given.

The Delivery of Small Regulatory RNAs by Gold Nanoparticles

Mark Alan McCully

For the degree of Doctor of Philosophy

March 2015



University
of Glasgow

Centre for Cell Engineering

College of Medical, Veterinary and Life Sciences

University of Glasgow

UK, G12 8QQ

Abstract

The traditional paradigm relying on drug discovery to treat and heal the body is changing. Medicine for the 21st century is moving towards using the body's internal language of DNA and RNA to cure disease and repair injuries to the body.

We now appreciate the complexity of signalling through the genome and its transcribed RNA. The role of micro RNAs and short interfering RNAs are gaining much interest as potential therapeutics. This interest has been sparked by the discovery that the dysregulation of micro RNAs is the origin for a spectrum of diseases from cancer through to osteoporosis.

Small regulatory RNAs have been shown to influence stem cell maintenance, proliferation and differentiation, offering the potential to produce new tissue by manipulating RNA levels.

However delivery of these molecules is fraught with difficulties. Without protection these molecules are quickly degraded *in vivo* and *in vitro* before reaching their intended target. With this in mind, this thesis aims to investigate the potential role for gold nanoparticles to deliver small regulatory RNAs and in turn produce a non-toxic and physiologically significant effect upon the cells.

Initial investigations revealed the importance of PEG density and AuNP concentration; with lower PEG densities, allowing attached therapeutic siRNA against C-Myc to reduce C-Myc protein levels and cell proliferation. Subsequently we determined that modulating the expression of osteo-suppressive miRNA, with a nucleic antagonist sequence was able to influence osteogenesis in two cell models (MG63s and hMSCs). This thesis has shown that AuNPs can be used to effectively deliver therapeutically active small molecules to cells *in vitro*.

Table of Contents

The Delivery of Small Regulatory RNAs by Gold Nanoparticles	1
Abstract.....	2
Table of Contents.....	3
List of Tables	7
List of Figures.....	8
Acknowledgement	12
Author's Declaration	13
Abstracts and Publications.....	14
1 Chapter 1: Introduction.....	15
1.1 Nanoparticle Overview.....	15
1.1.1 Cellular Uptake of NPs.....	16
1.1.2 Multivalency	18
1.1.3 Multivalency Leading Towards a Theranostic Nanoparticle..	24
1.2 Gold Nanoparticles	26
1.2.1 Gold Nanoparticle Uptake	27
1.2.2 Regulation of Cells by RNA	32
1.2.3 Nanoparticle-Mediated Delivery of Oligonucleotides	40
1.3 Targeting Cancers Using an siRNA-Nanoparticle Delivery Platform	42
1.3.1 Targeting Genetic Disease	42
1.3.2 C-Myc Protein and Cancer	44
1.3.3 C-Myc Oncogene Addiction	45
1.3.4 Targeting the C-Myc Protein by RNAi-siRNA	46
1.3.5 Nanoparticles as siRNA Delivery Vehicles for Cancer	48
1.4 MiRNA and Mesenchymal Stem Cells	50
1.4.1 Stem Cells.....	50
1.4.2 Mesenchymal Stem Cells (MSCs).....	54
1.4.3 Artificial Control of MSC Differentiation.....	62
1.4.4 Targeting MSC Differentiation by MiRNAs	63
1.5 Project Outline and Aims.....	65
2 Chapter 2: Materials and Methods	68
2.1 Materials.....	68
2.1.1 Antibodies	68
2.1.2 Cell Culture	70
2.1.3 Electron Microscopy (EM)	71
2.1.4 General Reagents	72

2.1.5	Microscopes	74
2.1.6	Quantitative Real-Time PCR (qRT-PCR)	75
2.1.7	Scientific Instruments	75
2.2	General Solutions.....	76
2.3	Cell Culture	77
2.3.1	Human Cell Lines	77
2.3.2	Primary Culture.....	78
2.3.3	Media	78
2.4	General Methods.....	78
2.4.1	Synthesis and Functionalization of Gold Nanoparticles.....	78
2.4.2	Toxicity Testing (MTT Assay)	82
2.4.3	Uptake Analysis	83
2.4.4	Functional Assays.....	84
2.4.5	Osteocalcin Nodule Formation via Fluorescence	91
3	Chapter 3: Gold Nanoparticle-mediated Knockdown of C-Myc in the Osteosarcoma Cell Line MG63 via siRNA	92
3.1	Introduction	93
3.2	Materials and Methods.....	96
3.2.1	Synthesis and Functionalisation of Gold Nanoparticles.....	96
3.2.2	Cell Culture	98
3.2.3	Glutathione (GSH) Assay.....	98
3.2.4	Nanoparticle Toxicity	98
3.2.5	Cellular Uptake of Gold Nanoparticles	99
3.2.6	In Cell Western (ICW).....	99
3.2.7	Brdu Proliferation assay	100
3.2.8	Statistics.....	100
3.3	Results	100
3.3.1	Intracellular GSH Levels.....	100
3.3.2	Cellular Uptake of AuNPs via TEM	102
3.3.3	ICP-MS	105
3.3.4	siRNA-mediated C-Myc Knockdown.....	105
3.3.5	BrdU Analysis	107
3.4	Discussion.....	110
3.5	Conclusion	113
3.6	Supplemental	114
4	Chapter 4: Gold Nanoparticle-mediated Blocking of Mir-31 to Influence Osterix Expression in the Osteosarcoma Cell Line MG6	115
4.1	Introduction	116

4.2	Materials and Methods	123
4.2.1	Synthesis and Functionalisation of Gold Nanoparticles.....	123
4.2.2	Cell Culture	127
4.2.3	Toxicity	127
4.2.4	Cellular Uptake of Gold Nanoparticles	127
4.2.5	Fluidigm Analysis of Osterix and Related Gene RNA Levels 128	
4.2.6	In Cell Western Analysis of Osterix Protein Levels.....	129
4.2.7	Theoretical Binding of Antagomir-31 Sequences	129
4.2.8	Statistics	129
4.3	Results	130
4.3.1	Cell Toxicity : MTT Assay	130
4.3.2	Cellular Uptake : TEM	130
4.3.3	Cellular Uptake : ICP-MS	133
4.3.4	Osterix and Related Gene Expression via Fluidigm	133
4.3.5	Osterix Protein Levels via In-Cell Western	136
4.4	Discussion.....	137
4.4.1	Mir-31 : Osterix and Osteogenesis.....	137
4.4.2	Antagomir Sequence Directionality: 5A Vs 3A	138
4.4.3	Off Target Effects	144
4.5	Conclusion	145
5	Chapter 5:Gold Nanoparticle-mediated Blocking of Mir-31 to Influence Osterix Expression in Human Mesenchymal Stem Cells	146
5.1	Introduction	147
5.2	Materials and Methods.....	151
5.2.1	Cell Culture	151
5.2.2	Toxicity	151
5.2.3	Cellular Uptake of Gold Nanoparticles	152
5.2.4	Fluidigm.....	152
5.2.5	In Cell Western	152
5.2.6	Osteocalcin Nodule Formation by Immuno Fluorescence..	153
5.2.7	Statistics	153
5.3	Results	154
5.3.1	Cell Toxicity: MTT Assay	154
5.3.2	Cellular Uptake : TEM	154
5.3.3	Cellular Uptake : ICP-MS	157
5.3.4	Osterix and Related Gene Expression via Fluidigm	157
5.3.5	Osterix Protein Levels via ICW	161

5.3.6	Osteocalcin Nodule Formation by Immunofluorescence ...	162
5.4	Discussion.....	167
5.4.1	Influencing Differentiation	167
5.4.2	Why Do PEG AuNPs Affect MSC Cell Gene Expression?	168
5.4.3	The Variability Between Osterix RNA and Protein Levels ..	169
5.4.4	Positive Downstream Effects of Increased Osterix.....	170
5.5	Conclusion	172
6	Chapter 6: Discussion	173
6.1	Gold Nanoparticles: A Future in Clinic?	173
6.2	The Use of siRNA and miRNA in Current Therapies	175
6.2.1	SiRNA Therapeutics	175
6.2.2	MiRNA Therapeutics.....	176
6.2.3	Oncology.....	184
6.2.4	Encouraging Bone Formation	185
6.3	Future Work.....	187
	List of References	188

List of Tables

Table 1-1. Stem cell type, tissue of origin and differentiation potential.	51
Table 1-2. Advantages and disadvantages of different stem cell types and their origins.....	53
Table 1-3. Common MSC stem cell markers used in biomedical research as described by Casado-Díaz <i>et al</i> (2011). Positive markers highlighted in yellow, are markers that have been selected and used for the experimental work carried out for this investigation.....	55
Table 2-1. Primer list used for fluidigm analysis, detailing the gene function and the forward and reverse sequences used. Those with * indicate housekeeping genes.	86
Table 3-1. The AuNPs used in this chapter with the corresponding PEG ligand densities and siRNA strands per nm ² . Please note that B denotes biotin and S denotes siRNA.....	97
Table 4-1 Specific miRNAs involved in different cancer types.....	117
Table 4-2 Role of miRNAs in the different bone cell types. Adapted from Lain and Stein <i>et al</i> , 2012 and Baglio and DeVescovi <i>et al</i> , 2013.	119
Table 4-3. Oligomer sequences used for AuNPs-antagomir functionalization. GC % relates to the melting temperature, the greater the GC content the higher the melting temperature. Antagomir-31 5', is designed to bind with perfect complementarity to the corresponding mir-31 5' sequence. The same principle relates to antagomir-31 3', which binds with perfect complementarity to the mir-31 3' sequence.....	124
Table 4-4. Physical-chemical properties of the gold nanoparticles employed in this chapter. Please note that 5A denotes the 5' end of the antagonist sequence of mir-31, and 3A denotes the 3' end of the antagonist sequence of mir-31. NS is a nonsense strand used as a negative control. SPR corresponds to the AuNP surface plasmon resonance.	126
Table 4-5. The predicted structures of the single stranded RNA sequences, based on the minimal free energy (MFE) method (an established method to predict RNA structure). Complimentary regions are evaluated to predict the most energetically stable molecule. The stability of the structure is given in kcal/mol, the more negative the value equates to a more stable structure.	140
Table 6-1. A conclusive list of current siRNA treatments undergoing clinical trials. All information was taken from clinicaltrials.gov. SNALPs (Stable Nucleic Acid Lipid Particles) LODER polymer (biodegradable polymeric matrix).	177

List of Figures

- Figure 1-1. Mechanisms of endocytosis. The three main mechanisms of endocytosis are (i) clathrin-mediated, (ii) caveolae and (iii) macropinocytosis. Endocytosis is a naturally occurring process whereby a cell uptakes external material. It is readily capitalised upon to enhance the uptake of therapeutic nanoparticles. (© 2012 Maude Boisvert, Peter Tijssen. Adapted from (Boisvert and Tijssen, 2012); originally published under CC BY 3.0 license. Available from: <http://dx.doi.org/10.5772/45821> 18
- Figure 1-2. Schematic of the multiple types of ligand that can be attached to create a multivalent NP. 19
- Figure 1-3. Timeline of major advances for miRNA studies, with particular focus on stem cells and osteogenesis (personal image). 34
- Figure 1-4 Diagram comparing antagomir, miRNA and siRNA pathways and routes. SiRNA and antagomirs are made exogenously. A) Antagomirs enter the cell and bind to miRNA, blocking miRNA expression. B) MiRNA made in the nucleus are processed into hairpin structures, exported from the nucleus and cut with dicer to silence mRNA. C) SiRNA enters the cell and is processed by dicer, cutting the double stranded RNA into single stranded RNA. This RNA is loaded into the RISC complex silencing mRNA targets. Routes A and C will be used in this thesis. Adapted from (Rana, 2007). 36
- Figure 1-5. Effect of stimuli on C-Myc expression in healthy and dysregulated cells. Figure adapted from (Cassinelli and Supino *et al.*, 2004) 44
- Figure 1-6. Differentiation potential of MSCs harvested from bone marrow, showing the most established stem cell positive cell markers 56
- Figure 1-7. Interplay between the endosteal and sinusoid niches, in bone marrow. The endosteal niche is located near the osteoblast lined endosteal bone, which supports MSC quiescence and self-renewal. The sinusoidal niche normally located near blood vessels, supports proliferation and differentiation. HSCs migrate and bind to the nestin markers on MSCs. Blue cells show MSCs, pink indicate HSCs, Green osteoblasts and yellow endothelial capillary cells. Image adapted from Zhang *et al* (2003)..... 57
- Figure 1-8. Osteogenic pathways found in hMSCs, combining BMP, Hedgehog, MAP and Wnt signalling. Red circles indicated a phosphorylated protein and red arrows indicate protein inhibition. This diagram is not an exhaustive list, and highlights only some of the complexity of signalling during osteogenesis. The area within the blue dotted line corresponds to the events within the nucleus, outside this represents the cytoplasm and the two parallel lines signify the plasma membrane. 60
- Figure 2-1. Gold nanoparticle characterization. (A) TEM image of citrate-gold nanoparticles (scale bar = 100 nm). Inset: size distribution histogram showing an average diameter of 14.4 ± 2.0 nm. (B) UV-Vis spectra of the synthesized gold nanoparticles with a

characteristic surface plasmon resonance (SPR) peak at 519 nm. Provided by J. Conde (2015).....	79
Figure 2-2. (A) Absorbance spectra of DTNB after reaction with the thiolated PEG. (B) Standard calibration curve for PEG chains, whose concentration can be calculated via the following equation $Abs_{412} = 26.229 \times [HS-PEG, \text{mg/mL}] + 0.0671$. (C) Variation of the excess of PEG thiolated chains as a function of the initial concentration in the incubation with 10 mM AuNPs. The dashed vertical line indicates the 100% saturation, i.e. the PEG concentration above which no more PEG can be bonded to the AuNPs surface. (D) Ratio between non-aggregated (at 520 nm) and aggregated NPs (at 600 nm) of AuNPs after functionalization with increasing amounts (0-0.035 mg/mL) of thiolated PEG. Provided by J. Conde (2015).....	81
Figure 3-1 Panel of the four types of AuNP used: 1) Au-B-25% PEG, 2) Au-B-S-25% PEG, 3) Au-B-40% PEG, 4) Au-B-S-40% PEG.	97
Figure 3-2. Glutathione (GSH) levels in MG63, MCF-7 and HeLa cancer cell lines. Cell number was normalised to 1×10^6 cells and values were plotted onto a GSH standard curve ($n=3$). Crosses indicate GSH standards, whilst the squares correspond to the cell type. Dashed areas around cell type indicate standard deviation. MTT Assay.....	101
Figure 3-3. MTT analysis of MG63 cells treated with 15 nM and 2 nM of each AuNP, with 40% or 25% PEG coverage for 24 hours. (B = biotin; S = siRNA) ($n=3$; error bars indicate SD).....	102
Figure 3-4. TEM images of MG63 cells treated with 15 nM and 2 nM AuNPs, with 25% PEG after 24-hour incubation. Clusters of the AuNPs are evident within the cell body. Scale bar = 1 μm	103
Figure 3-5. TEM images of MG63 cells treated with 15 nM and 2 nM AuNPs, with 40% PEG after 24-hour incubation. As with the 25%, clusters of the AuNPs are evident within the cell body.	104
Figure 3-6. ICP-MS analysis of MG63 cells treated with 2nM and 15 nM of AuNPs, with 25% or 40% PEG coverage for 24 hours (each lysate has $n=3$, error bars denote SD). All values have been normalised to ultrapure water. ANOVA analysis comparing all treatments to MG63s without AuNPs, found a significant increase in elemental gold within cells treated with AuNPs $p < 0.0001$	105
Figure 3-7. ICW data comparing C-Myc protein levels in MG63 cells with AuNP treatments, normalised to GAPDH. Cells were serum starved for 24 hours before treatment to synchronise cell division. The NPs were added at both 2nM and 15nM, with both 25% and 40% PEG coverage. The standard control reflects cells without AuNPs added, additional controls included lipofectamine treatment, C-Myc siRNA with lipofectamine (CL), Allstar nonsense siRNA with lipofectamine (AL), or C-Myc siRNA or Allstar siRNA added directly to the media (CN & AN) ($n=6$; error bars denote standard error, asterisk denotes significance based on Anova analysis, with a Dunnet post test normalising to control. Hash marks relate to an unpaired two tailed t-test, with a welchs correction ## = $p < 0.005$, ### = $p < 0.0005$).....	106

- Figure 3-8. BrdU incorporation into cells treated with 2 nM and 15 nM of AuNPs, with either 40% or 25% PEG coverage for 48 hours. Cells were stained for nuclei (DAPI:blue) and actively dividing cells (BrdU:red). Additional controls included C-Myc with lipofectamine (CL), Allstar nonsense siRNA with lipofectamine (AL), or C-Myc and Allstar siRNA added directly to the media (CN & AN). Scale bar = 20 μm 108
- Figure 3-9. Graphical representation of the BrdU images as determined by CellProfiler, normalised to nuclei number, comparing the level of MG63 cells in S-phase with different treatments. Control cells are MG63s with AuNPs. CL= C-Myc siRNA with lipofectamine, CN= C-Myc siRNA only, AL= Allstar siRNA with lipofectamine, AN= Allstar siRNA only. Results from 10 images per sample, n=3 replicates, error bars denote standard error, asterisk denotes significance based on Anova analysis, with a Dunnet post test compared to control. Hash marks relate to an unpaired two tailed t-test, with a Welchs correction $p < 0.05$). 109
- Figure 4-1. The interaction of mir-31 within an osteogenic pathway; green arrows indicate interacting factors, with a dashed line showing a simplified interaction, whilst red bars indicate an inhibitory effect (personal image). 121
- Figure 4-2. TEM image of antagomir-gold nanoparticles (scale bar = 200 nm). Panel A shows nonsense (NS)-AuNPs; B shows 5A-AuNPs, and C shows 3A-AuNPs. 125
- Figure 4-3. MTT analysis of MG63 cells treated with each AuNP (50nM oligo, 30% PEG) type for 24 hours (PEG, NS, 3A, 5A) (n=3; error bars indicate SD)..... 130
- Figure 4-4. TEM images of MG63 cells treated with AuNPs (50nM, 30% PEG) after 1 (A) and 48 hours (B). Black arrowheads denote AuNPs. Scale bar =0.2 μm 132
- Figure 4-5. ICP-MS analysis of MG63s treated with AuNPs (50nM, 30%) for 48 hours. Each lysate has an n=3, error bars denote SD. 133
- Figure 4-6. Heat-Map of MG63s treated with the AuNPs for 48 hours (green reflects a decrease in expression, whilst red reflects an increase). The data was analysed using PermutMatrix and ordered into hierarchy based on expression similarity using McQuitty's criteria. 5A and 3A are the most related. After 48 hours 3A appears to activate a wide array of osteogenic factors, whereas 5A has appeared to up-regulate RUNX2 very strongly whilst down regulating C-Myc expression. 135
- Figure 4-7. ICW data comparing osterix levels in MG63s after 48 hours with AuNP treatments normalised to cell number, and in MCF-7 cells. (n=6; error bars denote standard deviation)..... 136
- Figure 4-8. miRNA binding sequence geometries based on base pairing and minimum free energy using RNAhybrid. The stability of the structure is measured in kcal/mol (ie. the energy required to break the structure). The greater the energy needed the more stable the structure. Linearity infers stability, whilst loops indicate incompatibility and lack of binding. The antagomirs and their

- corresponding miRNA sequence form the strongest and most stable structure. 143
- Figure 5-1 Key miRNAs involved in MSC differentiation. Figure adapted from Guo *et al* (2011) and Baglìo *et al* (2013)..... 148
- Figure 5-2. MTT analysis of hMSCs treated with each AuNP type (50nM oligo, 30% PEG saturation) for 48 hours (PEG,NS, 5A, 3A) (n=3; error bars indicate SD)..... 154
- Figure 5-3. TEM images of hMSCs cells treated with AuNPs (50nM, 30%) after 1 (A) and 48 (B) hours. PEG=Cells treated with AuNPs functionalised with PEG only. NS=AuNPs with PEG and nonsense antagomir strands. 5A= AuNPs with PEG and antagonist sequences targeting 5' of mir-31. 3A=AuNPs with PEG and antagonist sequences targeting 5' of mir-31. Scale bar =0.2µm. Arrows indicate AuNP clusters..... 156
- Figure 5-4. ICP-MS analysis of hMSCs treated with AuNPs (50nM, 30% PEG saturation) for 48 hours. Each lysate has an n=3, error bars denote SD. 157
- Figure 5-5. Heat map of hMSCs treated with AuNPs for 5 days showing stem cell associated factors. The data was analysed using PERMUT and ordered into hierarchy based on similarity. 5A,3A and NS are the most related. After 5 days PEG appears to activate a wide array of stem cell associated factors. Whereas 5A was able to down regulate the stem cell markers..... 159
- Figure 5-6. Heat-Map of hMSCs treated with AuNPs for 5 days and showing oestrogenic markers. The data was analysed using PERMUT and ordered into hierarchy based on similarity. 5A and 3A are the most related in terms of gene expression. 160
- Figure 5-7. ICW data comparing osterix levels in hMSCs over several time points. A) AuNP treatments are shown as 5A= Red, 3A Green, NS= Purple (normalised to cell number and then PEG-AuNPs) B) Control cells (no AuNPs) normalised to cell number are shown in (n=6; error bars denote standard error)..... 162
- Figure 5-8 Representative images from each replicate of AuNP treatment cultured with hMSCs after 3 weeks. Staining indicates actin (green), nucleus (blue) and osteocalcin nodules (red). Scale bar= 5µm..... 164
- Figure 5-9 Representative images from each replicate of AuNP treatment cultured with hMSCs after 5 weeks. Staining indicates actin (green), nucleus (blue) and osteocalcin nodules (red). Scale bar= 5µm..... 165
- Figure 5-10 Semi-quantification of osteocalcin staining in hMSCs after treatment with AuNPs for 3 and 5 weeks (A and B respectively). All treatments have been normalised to control cells treated with no AuNPs. (n=3, error bars denote SEM) ***= $p < 0.001$ 166

Acknowledgement

Firstly I would like to thank my supervisor, Dr Catherine Berry. Catherine has always been very supportive and given excellent advice over the years. As my supervisor she has created an enormous array of opportunities for me, from visiting collaborators, to presenting my work and developing my teaching through lab demonstrating.

I would also like to thank Professor Matthew Dalby, as my second supervisor his input has been invaluable. His lectures and discussions in my 4th year indirectly led to me studying an MRes at Glasgow and ultimately my PhD in the CCE. This has been a fantastic stage of my life and I'm very grateful for Matt's advice, which led me to here.

Dr Mathis Riehle also requires an acknowledgement. Mathis is a fantastic source of new ideas and has helped me numerous times with troubleshooting problems. Although a very busy man, his ability to make time to help others has always been greatly appreciated.

I would like to thank everyone else at the CCE. To thank everyone personally for his or her help would be a mini thesis in itself. Briefly I would like to thank Carol-Anne Smith for her humour and solutions to any problems that arose in the lab. To Dr Monica Tsimbouri, who was always at hand to advise on experiments and help make things more efficient. Mr Niall Crawford is also owed a special mention; his sense of humour and our lively discussions have been a highlight (despite his delusions about Ms Aguilera) and will be missed.

To everyone else in the CCE and beyond, it has been a pleasure working with you and I hope in the future our paths will cross again.

Finally I would like to thank my friends, family and partner Neil for their kind words, encouragement and support. This truly has been a team effort. Thank you.

Author's Declaration

I hereby declare that the research reported within this thesis is my own work, unless otherwise stated, and that at the time of submission is not being considered elsewhere for any other academic qualification.

Mark McCully

20 March 2015

Abstracts and Publications

Original research publications authored by the candidate on work relating to this thesis.

MCCULLY, M., HERNANDEZ, Y., CONDE, J., BAPTISTA, P. V., DE LA FUENTE, J. M., HURSTHOUSE, A., STIRLING, D., BERRY, C.C. 2015
The Significance of the Balance Between Intracellular Glutathione and Polyethylene Glycol (PEG) for Successful siRNA Release from Gold Nanoparticles. (Manuscript submitted to Nano Research, under review)

MCCULLY, M., CONDE, J., BAPTISTA, P. V., OLIVE, V., BERRY, C.C. 2015. Blocking Mir-31 with Antagomirs to Accelerate Osteogenesis. (Manuscript in progress)

Conference Proceedings

2012 Tissue and Cellular Engineering Society

'Using Functionalised Gold Nanoparticles for the Delivery of siRNA to Bone Cancer Cells *In Vitro*'. Liverpool, UK (poster presentation)

2013 Tissue and Cellular Engineering Society

'Delivery of Therapeutically Active siRNA Against C-Myc in Bone Cancer Cells'. Cardiff, UK (Oral presentation)

2014 Tissue Engineering and Regenerative Medicine International Society (TERMIS)

'Gold Nanoparticle Design: Silencing C-Myc expression in Bone Cancer Cells with siRNA' Genoa, Italy (poster presentation)

2015 Multifunctional, Hybrid and Nanomaterials

'Blocking Mir-31 with Antisense RNA Conjugated Gold Nanoparticles Drives an Increase in Osteogenic Markers'. Sitges, Spain (poster presentation)

1 Chapter 1: Introduction

1.1 Nanoparticle Overview

Nanoparticles have been hailed as revolutionary vehicles for biomedical research in the 21st century. Nanoparticles (NPs) can be defined as a material that has at least one dimension less than 100nm (Bosselmann S Fau - Williams and Williams, 2004). At the nanoscale, materials develop novel properties that are distinctive to the bulk material. Indeed, NPs develop unique and often advantageous properties including optical, magnetic, catalytic, thermodynamic and electrochemical properties (Levy and Shaheen *et al.*, 2010).

At present there are a multitude of NP types, with an inherent range of functions and capabilities. These particles are generally sub-divided into either organic NPs, such as organic polymers, liposomes (Torchilin, 2005) and dendrimers (Lee and MacKay *et al.*, 2005); or inorganic NPs including quantum dots (Medintz and Uyeda *et al.*, 2005) magnetic iron oxides (Lu and Salabas *et al.*, 2007), gold NPs (Huang and Jain *et al.*, 2007.,Sanvicens and Marco, 2008) and mixed alloy NPs (Liong and Lu *et al.*, 2008.,Sun and Kandalam *et al.*, 2006). Each type of NP has different properties that infer advantages depending on the biomedical application being considered (Ferrari, 2005). These unique properties allow better imaging, delivery and remote activation of the NP, allowing for a more intelligent delivery system (Bosselmann S Fau - Williams and Williams, 2004.,Jokerst Jv Fau - Gambhir and Gambhir, 2011).

When considering inorganic particles, a main advantage of their use as a delivery platform are their inherent optical and imaging properties, whether *in vitro* or *in vivo*; which is hugely beneficial in a clinical setting as it allows remote NP tracking. For example, quantum dots (QDs), which are fluorescent inorganic nanocrystals with a broad absorption spectra, can be tailored to release a narrow band of emission frequencies; producing better signal brightness and a greater resistance to photo bleaching of samples when compared with traditional organic

dyes (Liu and Yang *et al.*, 2012). Gold NPs are more established, having been used for decades in biological imaging, including *via* immunogold labelling in transmission electron microscopy. A further example is the use of magnetic NPs, such as iron oxide, which are employed as contrast agents in magnetic resonance imaging to aid image generation (Ghosh and Han *et al.*, 2008). These imaging technologies play a crucial role in disease diagnoses and their subsequent treatment (Na and Song *et al.*, 2009., Leduc and Jung *et al.*, 2011).

Aside from the benefits of allowing remote imaging, inorganic NPs provide researchers and clinicians with a multifunctional tool that can be used as a cellular or tissue delivery system. The control of NP design and assembly, through recent advantages in nanotechnology, can help tailor the properties of a NP towards a particular application (Aili and Gryko *et al.*, 2011). The success of NPs in this regard is due to multivalency; a property that allows a NP to have a range of attachments or ligands that can facilitate a multitude of tasks (see section 1.1.2).

Nanoparticles have gained more interest for medical application than larger particles for a number of reasons. Larger particles such as micro particles have poor circulation *in vivo*, have difficulty crossing membranes and can aggregate producing complications like embolisms or ischemic events (Kohane, 2007).

1.1.1 Cellular Uptake of NPs

Before the successful application of biomedical NPs, the issue of delivery must be addressed, whereby cells must first uptake the NPs. Uptake can naturally happen through the process of phagocytosis (occurs only in specialised cells), passive diffusion and endocytosis (Kuhn and Vanhecke *et al.*, 2014). Here we focus on endocytosis, which can be loosely divided into three main mechanisms: i) clathrin mediated endocytosis, ii) caveolin mediated endocytosis, iii) macropinocytosis. Endocytosis can be receptor mediated, as shown in Figure 1-1, and

when considering the uptake of NPs, generally relies on either clathrin-mediated uptake or caveolin-mediated uptake (Benfer and Kissel, 2012.,Chithrani and Chan, 2007.,McMillan and Batrakova et al., 2011).

Clathrin mediated endocytosis involves small 100 nm vesicles that are a complex of proteins associated with the cytosolic protein Clathrin (Mukherjee and Ghosh *et al.*, 1997.,Mellman, 1996). Found in virtually all cells, clathrin-coated vesicles are formed from initial invaginations in the cell membrane, to which clathrin is recruited. Clathrin coated pits are then generated, which are pinched off from the membrane to form vesicles *via* dynamin. Large extracellular molecules have different receptors responsible for clathrin-receptor-mediated endocytosis such as antibodies, transferrin and growth factors.

Caveolin mediated endocytosis is also a common feature of many cell types and includes Vip21 a cholesterol-binding protein (Doherty and McMahon, 2009.,Conner and Schmid, 2003). Caveolin-mediated uptake is characterised by ~50 nm diameter pits in the membrane with up to a third of the plasma membrane covered in these pits in some cells such as smooth muscle and fibroblasts. It is thought that extracellular uptake of molecules/nanoparticles is mediated *via* receptors in the caveolae.

As indicated in Figure 1-1, macropinocytosis also occurs. This is essentially cell drinking, with general uptake of the surrounding fluid (Swanson and Watts, 1995). It occurs within highly ruffled areas in the plasma membrane; these invaginations in the cell membrane form a pocket, which closes over to form a vesicle (0.5–5 μm in diameter) filled extracellular fluid, unintentionally containing any added NPs. This allows around 100 times more extracellular fluid to enter the cells compared to clathrin-mediated endocytosis and is a non-specific uptake mechanism.

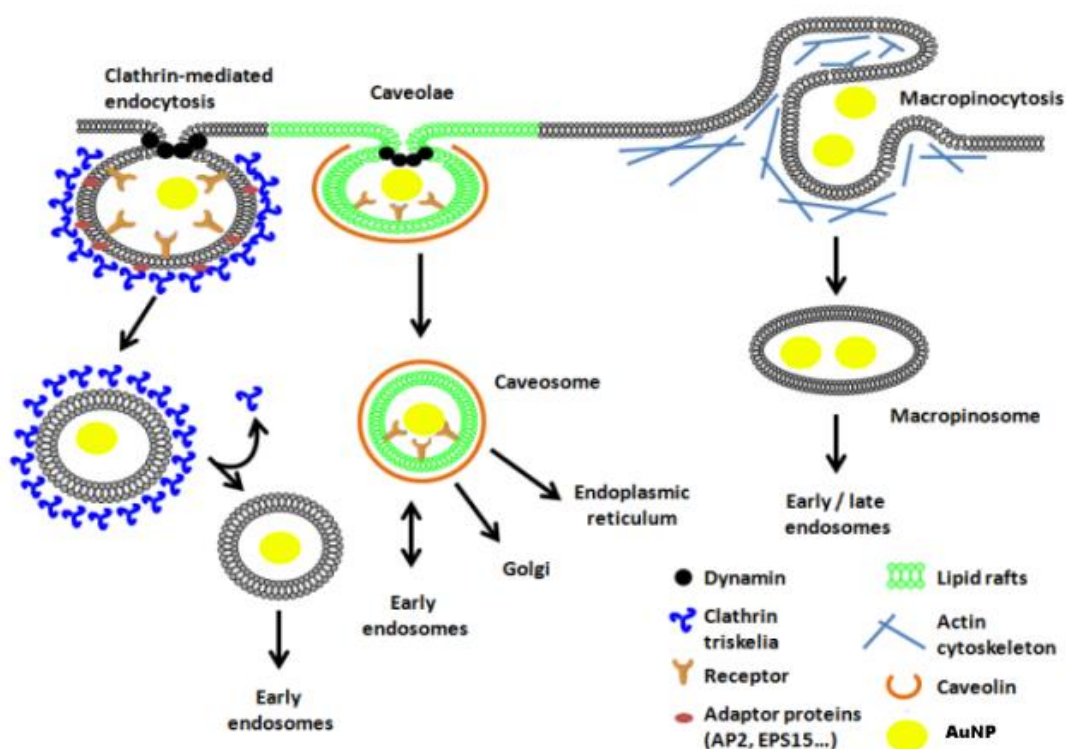


Figure 1-1. Mechanisms of endocytosis. The three main mechanisms of endocytosis are (i) clathrin-mediated, (ii) caveolae and (iii) macropinocytosis. Endocytosis is a naturally occurring process whereby a cell uptakes external material. It is readily capitalised upon to enhance the uptake of therapeutic nanoparticles. (© 2012 Maude Boisvert, Peter Tijssen. Adapted from (Boisvert and Tijssen, 2012); originally published under CC BY 3.0 license. Available from: <http://dx.doi.org/10.5772/45821>)

1.1.2 Multivalency

Multivalency describes our ability to use a NP surface as a platform to attach ligands, in particular the capability of attaching multiple individual ligands. This allows us to functionalise a NP with specific cargo or to provide certain beneficial properties, such as genetic material (e.g. DNA or RNA sequences), peptides and drugs, or cell-targeting ligands respectively. This creates a multifunctional NP, allowing us to combine the inherent NP properties (e.g., in terms of imaging *etc.*) with further benefits in terms of molecule delivery to cells

and tissues. This ability to produce a particle with a number of different ligands or tags allows for a wide range of both diagnostic and therapeutic capabilities (Figure 1-2) (Cheng and Meyers *et al.*, 2011).

Gold NPs (AuNPs) are particularly well situated in this regard. They are well established in cell biology, and are known to be relatively inert and therefore very applicable in biomedicine, with a history of use that spans decades both *in vivo* and *in vitro*. AuNPs are easily produced in a range of diameters and easily functionalised with a number of different components using thiol linkage (Levy and Shaheen *et al.*, 2010). A variety of ligands are typically considered when designing a NP for biomedical applications.

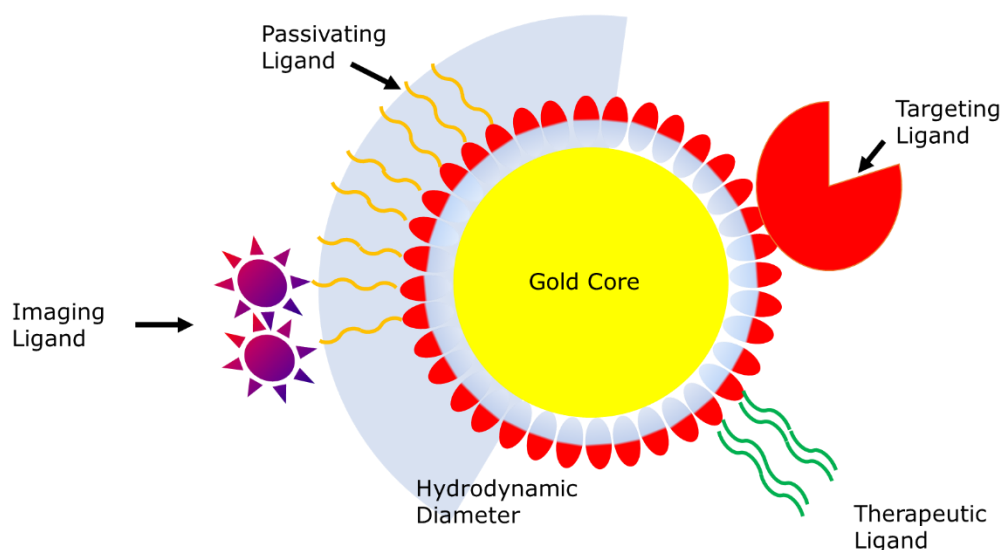


Figure 1-2. Schematic of the multiple types of ligand that can be attached to create a multivalent NP.

1.1.2.1 Passivating Ligand

Passivating ligands are attached to NPs with the aim of both conferring NP stability in solution and also shielding the NP from the immune system *in vivo*, allowing for a longer half-life. Various arrays of sugars and polymers have been used to date, however the most widely used is polyethylene glycol, PEG, (a polymer of ethylene oxide) (Wang and Wei *et al.*, 2013, Simpson and Agrawal *et al.*, 2011, Sant and Poulin *et al.*,

2008.,Rahme and Chen et al., 2013.,Pittella and Zhang et al., 2011.,Oishi and Nakaogami et al., 2001b.,Kah and Wong et al., 2009.,Jokerst and Lobovkina et al., 2011.,Free and Shaw et al., 2009). Adding PEG to the NP surface a process known as PEGylation, is known to increase the circulation time of NPs by resisting opsonisation, leading to PEG being described as having 'stealth' properties. Opsonisation is a process involving the absorption of proteins on to the surface of the material, leading to the NPs being recognised, phagocytised and cleared (Juliano and Alam *et al.*, 2008). PEG is amphipathic, has a range of molecular weights depending on polymer length and can be further functionalised with other reactive groups. Indeed, organic polymers such as PEG, are invaluable for increasing the stability of the NP and in turn increasing the therapeutic potential (Liu and Shipton *et al.*, 2007). Additionally PEG has a low toxicity, is FDA approved and has been used in biomedical applications for decades (Jokerst and Lobovkina *et al.*, 2011). Varying the chain length of PEG, the density of PEG on the NP particle and the conformation of the PEG can alter the level of steric hindrance exhibited by a NP. Steric hindrance is the reduction or blocking of intra- and intermolecular interactions due to the spatial arrangement of passivating molecules. By using steric hindrance, NPs can be produced with a low aggregation potential.

1.1.2.2 Targeting Ligand

Targeting ligands are selected with a view towards localising NPs to the cell surface and encouraging cellular uptake, thereby increasing the potency of the drug/gene cargo. The integrin-binding motif RGD (Arginine-Glycine-Aspartic acid), which ubiquitously binds to specific integrins on the plasma membrane of many cell types, has been used as a potential targeting molecule to aid cell-nanoparticle binding and allow for greater uptake (Kumar and Ma *et al.*, 2012a). Cell penetrating peptides such as TAT peptide (derived from the transactivator of transcription sequence) isolated from the HIV virus, have been used

extensively to increase NP uptake (Meade and Dowdy, 2008.,Berry, 2008)

In addition, targeting ligands are also selected to associate with specific cell surface receptors, allowing cell-type targeting (Gao and Dagnaes-Hansen *et al.*, 2009.,Leamon and Low, 1991.,Davis and Zuckerman *et al.*, 2010). For example CRGDK (a peptide sequence that binds to neuropilin-1, a receptor over expressed in certain cancers) was used to target AuNPs and a therapeutic payload to cancer cells, and folate has also been adopted for cancer cell targeting (Kumar and Ma *et al.*, 2012b).

1.1.2.3 Imaging Ligand

Depending on the type of NP, some have innate imaging properties, such as magnetic NPs (viewed by NMR) and QDs (viewed by NIR imaging) (Medintz and Uyeda *et al.*, 2005.,Jokerst and Gambhir, 2011.,Weng and Song *et al.*, 2006.,Liong and Lu *et al.*, 2008.,Derfus and Chen *et al.*, 2007), however others, such as gold NPs, may require additional ligands to allow NP imaging *in vitro* and *in vivo*. These have ranged from attaching biotin onto the NP and using streptavidin-linked fluorophores, to directly conjugating fluorescent tags to the NP, such as fluorescein, cy- dyes and dylight to name a few (Conde and Ambrosone *et al.*, 2012).

1.1.2.4 Therapeutic Ligand

Whilst passivating, targeting and imaging ligands are important, the attachment of a therapeutic ligand is perhaps the more interesting, as this opens up the potential for NPs to be used in nanomedicine. There have been many types of therapeutic ligands used to date, ranging from small molecules, such as siRNA and miRNA, through to larger drug entities. Some NPs however have innate therapeutic potential, e.g. using an NIR laser on AuNPs can induce heating, with the resulting

thermal ablation killing tumour cells (Huang and El-Sayed, 2010). The mechanism of attachment to the NP is critical, and can determine the success or failure of the NP as a delivery platform. For example ionic attachment has been shown to be weaker than covalent attachment, with the resulting payload dissociating too quickly, often in the extracellular space before gaining cellular entry (Conde and Ambrosone et al., 2012). Covalent attachment is generally much stronger and when considering AuNPs, using a thiol linkage is an excellent method, allowing for very high association with the NP, whilst also permitting intracellular dissociation *via* glutathione in the cell cytoplasm (Lushchak, 2012., Meister and Anderson, 1983., Wu and Fang *et al.*, 2004., Lei, 2002., Fang and Yang *et al.*, 2002., Meister, 1988). Glutathione is a common antioxidant found within cells. The reduced form of glutathione (GSH) prevents damage to intracellular components from free radicals. GSH has been shown to reduce thiol bonds and is the main mechanism for release of components attached by thiol bonds to the AuNP surface (Kumar and Meenan et al., 2012).

The point of attachment is also of importance, if attached directly to the NP and shielded by the passivating ligand, the payload remains stable and functional for longer, whereas direct attachment onto the passivating ligand surface can result in degradation, and poor functional effects for the targeting ligand (Conde and Ambrosone et al., 2012).

1.1.2.5 Benefits of Multivalency

When designing multifunctional NPs it is important to consider the optimal concentration of each ligand on the NP surface, and how these functional groups could interact with each other. A study by Derfus *et al* investigated the optimal number of siRNA per QD NP to induce efficient protein down regulation coupled with anti-cancer peptides. They found that a single siRNA molecule in conjunction with 15 or more anti-cancer peptides attached to a PEGylated QD gave optimal silencing. Doubling the siRNA molecules attached to the NP achieved the same level of

silencing, but required less than 10 targeting peptides (Derfus and Chen *et al.*, 2007).

As described above, multivalency offers benefits, not only in terms of delivery into cells (using targeting ligands), but also as a protection against degradation of the payload. For example, the delivery of siRNA, with a view to silencing specific target genes, has much potential. However siRNA molecules with no delivery vector are rapidly removed from the blood system by the kidneys. By attaching the siRNA directly to a NP, the half-life of these siRNA molecules can be significantly extended (Derfus and Chen *et al.*, 2007.,Juliano and Alam *et al.*, 2008.,Soutschek and Akinc *et al.*, 2004). In 2010 a multifunctional NP was employed in human phase I clinical trials (Davis and Zuckerman *et al.*, 2010). The NP was a cyclodextran-based polymer (CDP) NP, stabilized with polyethylene glycol (PEG), with siRNA cargo and a cell targeting peptide (transferrin). The NP was administered to patients with solid tumors, resulting in an intracellular accumulation of NPs predominantly within the tumors. The siRNA conjugated NPs were shown to be functional, *via* reduced levels of the target mRNA and its protein by quantitative real-time PCR and western blotting. Immunostaining of tumour biopsy pre- and post-treatment, show an acute reduction in the spread of the melanised tumour. This groundbreaking study showed that by using RNAi technology *via* a multifunctional NP as delivery agent, oncogene expression in humans could be altered.

Multivalency also presents us with the opportunity to create a NP to broadly target and knockdown multiple genes at once (Juliano and Alam *et al.*, 2008). The potential to create multi-therapeutic vectors is believed by Paciotti *et al* (2004) to be vitally important for treating many disease states, being particularly effective with potential cancer treatments (Paciotti and Myer *et al.*, 2004). Tumours do not exist in a homogenous environment; they are composed of multiple cancerous cell types, requiring an effective NP to target a broad spectrum of cells present within the tumour (Spremulli and Dexter, 1983.,Dexter and

Kowalski *et al.*, 1978). This could be achieved, for example, by attaching multiple siRNA sequences against a variety of oncogenic proteins, or by a combination of siRNA and anti-cancer drugs such as paclitaxel (a chemotherapy drug, from the taxane family) working in partnership to increase the potency of the NP (Iwase and Shimada *et al.*, 2006).

Song *et al* studied the functional properties of a multivalent protamine-antibody fused protein with multiple siRNAs targeting three oncogenes *in vivo* (Song and Zhu *et al.*, 2005). In their study they used siRNA targeting C-Myc, MDM2 and VEGF; three well established oncogenes. C-Myc induces cell proliferation (de Nigris and Balestrieri *et al.*, 2006), MDM2 silences p53 (a cell cycle check point protein)(Halaby and Yang, 2007) and VEGF is a growth factor predominantly found up regulated in tumour cells to promote angiogenesis and metastasis (Grothey, 2006). The multiple siRNA strategy significantly reduced proliferation of the melanoma cells in mice. Proving this approach can work in complex biological systems. Changing Song *et al*'s delivery vector of a protamine-antibody fusion protein to a liposome based NP, Li *et al* where able to increase the potency of the siRNAs. Metastasis in the murine lung cancer model was reduced by 70-80% in comparison to free siRNA (without a delivery vector) (Li and Chono *et al.*, 2008). Therefore, combining multiple siRNAs with a NP delivery vector allowed Li *et al* to improve on Song *et al*'s previous work, by increasing the RNAi's potency whilst protecting the siRNA sequences through the properties of the nanocarrier.

1.1.3 Multivalency Leading Towards a Theranostic Nanoparticle

As described above, NPs can be functionalised with imaging molecules, such as fluorescent tags, targeting molecules and a therapeutic payload. This potential allows for NPs to be used with a view to simultaneously diagnose disease, and apply treatment therapeutically, coining the term "theranostic" NPs (Lee and Lee *et al.*, 2009.,Derfus

and Chen et al., 2007). A theranostic NP would aim to *target* a specific disease site, report back *via imaging* the diseased cells and in turn *deliver* some form of treatment (eg. siRNA, peptides, molecules). Such a theranostic NP was reported in 2007 by Medarova *et al*, where a magnetic NP was designed to specifically associate with tumours, using a modified membrane translocation peptide (myristoylated polyarginine peptides) as detected by imaging using both an attached Cy5.5 dye and *via* MRI. The NPs successfully delivered siRNA sequences against green fluorescent protein (GFP) into GFP-expressing cells (Medarova and Pham *et al.*, 2007). The authors reported an accumulation of NPs within the tumours, due to the enhanced permeability effect (Kobayashi and Watanabe et al., 2014). Tumours tend to have high retention effects as a result of the highly leaky and vascularised tissue, known as the enhanced permeability and retention effect. The addition of tumour-targeting moieties should increase this targeting effect (Chauhan and Stylianopoulos *et al.*, 2011).

In 2009 Cheon *et al* created a theranostic magnetic NP, which featured a fluorescent dye, a cell-specific targeting motif and siRNA with a view to targeting, imaging and treating diseased cells *in vitro* (Lee and Lee *et al.*, 2009). Also in that year, Lee *et al* furthered the concept of a theranostic NP. They created a multifunctional NP that utilised (i) the integrin-binding motif Arg-Gly-Asp (RGD) as a means to increase cellular uptake; (ii) PEG to increase the stability of the NP; (iii) Cy5 to facilitate imaging; and (iv) siRNA against GFP as the therapeutic model. The NP was found to be less toxic than the popular delivery method of polyethyleneimine (PEI), with the authors concluding that creating synergy between diagnosis and treatment is the direction future medicine must take to increase potency and reduce off-target effects (Lee and Lee *et al.*, 2009).

1.2 Gold Nanoparticles

Gold NPs (AuNPs) have been used for centuries, such as colloidal gold in stained glass, but only in the last few decades has the extent of their abilities been realised for potential biomedical applications (Alkilany and Murphy, 2010.,Chithrani and Chan, 2007.,Cho and Cho et al., 2010.,Conde and Ambrosone et al., 2012.,Ghosh and Singh et al., 2012.,Oh and Delehanty et al., 2011.,Paciotti and Myer et al., 2004). As alluded to in section 1.1.2, gold nanoparticles can be easily synthesised, in a wide range of sizes, quite simply by changing the length of time a solution of gold salts are left to be reduced by sodium citrate. Gold is typically an inert metal that is biocompatible, eliciting no immune response. As described briefly when considering multivalency, gold can be easily functionalised by thiol-linkage and click chemistry (generation of substances quickly and reliably by joining small units together), allowing for the relatively simple design and construction of a diverse range of multifunctional AuNPs (Salem and Searson et al., 2003.,Sanvicens and Marco, 2008.,Chen and Li et al., 2012.,Cheng and Al Zaki et al., 2012.,Conde and Ambrosone et al., 2012). To protect the therapeutic payload and ensure NP stability, amphiphilic polymers such as PEG can be attached using thiol linkage directly onto the gold NP surface (Free and Shaw et al., 2009).

1.2.1 Gold Nanoparticle Uptake

1.2.1.1 Cellular Uptake of Gold Nanoparticles

As described in section 1.1.1, the success of any biomedical application employing NPs is dependent on the uptake of the particles into the cell body. The interplay between the size, shape and surface chemistry of the particle play a key role in determining this uptake

AuNPs can have a range of size dependent and tuneable physicochemical properties, such as surface reactivity, surface plasmon resonance, and surface functionalisation (Chithrani and Ghazani *et al.*, 2006., Liu and Shipton *et al.*, 2007., Free and Shaw *et al.*, 2009., Nel and Madler *et al.*, 2009., Chithrani, 2010., Cho and Cho *et al.*, 2010., Decuzzi and Godin *et al.*, 2010., Lee and Huh *et al.*, 2010., Cebrian and Martin-Saavedra *et al.*, 2011., Oh and Delehanty *et al.*, 2011., Kumar and Ma *et al.*, 2012a., Zhao and Zhao *et al.*, 2012). Studies have shown that AuNPs are readily taken up by cells by both passive (diffusion) and active mechanisms (endocytosis) (Figure 1-1), however the actual mechanisms have not been fully elucidated as of yet, and a mix of the latter two in Figure 1-1 appears most likely (Chithrani and Chan, 2007., Chithrani, 2010., Ma and Wu *et al.*, 2011., Oh and Delehanty *et al.*, 2011).

1.2.1.2 Influence of Nanoparticle Properties on Cellular Uptake

Non-specific interaction between the AuNPs and serum proteins, termed 'opsonisation', during cell culture has been suggested to have a major effect on the rate of uptake (Chen and Xu *et al.*, 2008). Opsonisation results in the coating of the nanoparticle surface with proteins that are free in the cell media (*via* FCS/FBS). Many researchers pre-coat their NPs with a passivating ligand in an attempt to reduce this effect (section 1.1.2.1). For example, the addition of PEG to the surface of a AuNP prevents any non-specific interactions between the serum proteins and the functionalised AuNPs (Free and Shaw *et al.*, 2009)

It should also be noted that the type of reactive group attached to the NP will result in a different surface chemistry layer, with functional groups such as COOH and NH₂ inducing significantly different rates of uptake (Clift and Rothen-Rutishauser et al., 2008). However, Ehrenberg *et al* found that incubation in FCS/FBS for several hours levels out the differences in the uptake rates for these functional groups *in vitro* (Ehrenberg and Friedman *et al.*, 2008). In comparison Giljohan *et al* (2007) produced AuNPs (13nm) with a mixed monolayer of oligonucleotides. They observed that greater amounts of oligonucleotides on the particle surface increased cellular uptake upon serum exposure *in vitro* (Giljohann and Seferos *et al.*, 2007). This could be due to the negative charge of the oligonucleotides no longer being masked by the passivating ligand, in turn creating a charged NP that directly interacts with serum proteins.

The overall charge of the NP is also an important consideration for efficient uptake (Chompoosor and Han et al., 2008). The cell plasma membrane is negatively charged, and maintains a negative membrane potential for efficient ion uptake. Due to this negative potential across the membrane a NP with a positive charge would be attracted to the membrane and uptake would be facilitated. Amine functional groups and peptides with arginine exhibit positive charges that have been used to alter the surface charge of the NP (Clift and Rothen-Rutishauser et al., 2008).

In addition to the chemistry, NP size is known to influence uptake. The diameter of the NP core can heavily influence the rate of uptake. Chithrani *et al* (2006) observed that core sizes below 100nm allowed for a greater uptake of particles per cell, with sizes above 100nm having greatly reduced uptake in HeLa cells (Chithrani and Ghazani et al., 2006). The actual NP shape is also known to influence cellular uptake. AuNPs can be made into a vast array of shapes, however data has indicated that spherical AuNPs have the greater uptake potential than rod shaped particles (Chithrani and Ghazani et al., 2006). A report by

(Alkilany and Nagaria *et al.*, 2009) indicated a greater cytotoxic effect exhibited by rods in comparison to spherical gold.

1.2.1.3 Endosomal Uptake

Cellular uptake of AuNPs results in endosomal localisation. This can be problematic due to the acidic nature of the endosomal environment, that can range from \sim pH6 in the early endosome to \sim pH4.5 in the late endosome (Sorkin and Von Zastrow, 2002). This low pH can therefore cause the degradation of any attached drug or gene cargo. Thus, much effort is concentrated on tracking and localising NPs within the cell body. The time taken for cellular uptake to occur has been reported for different cell lines and particle types, with the uptake being described with as short as 30 seconds incubation (Sorkin and Von Zastrow, 2002).

1.2.1.4 Nanotoxicology

With the exponential use in NP bioapplications and the implications for human health, The Royal Society and The Royal Academy of Engineering published a report in 2004 dedicated entirely to the opportunities and potential dangers of NPs. The report concluded that all newly synthesised NPs must be viewed as a new chemical and all the necessary precautions must be taken (Dowling and Clift *et al.*, 2004). The report led to the creation of a new discipline; nanotoxicology. Nanotoxicology aims to assess the safety issues concerned with the use of NPs, by evaluating the risks involved in exposure to NPs and the mechanisms involved in NP toxicity (Fischer and Chan, 2007.,Oberdorster and Maynard *et al.*, 2005). Nanotoxicological studies are of a pressing concern at present, as multiple NPs are entering the clinical trial phase. The need for studies is compounded by growing public concern and awareness of NPs in everyday items, such as sun creams, food packaging and cosmetics, and their potential impact on the environment and our health (Miller, 2006).

Nanotoxicology studies to date have produced mixed results, with a review by Sanvicens and Marco reporting effects at the cellular, subcellular, protein and gene levels (Sanvicens and Marco, 2008). Lovric *et al* (2005) found green mercaptopropionic acid-coated CdTe QDs (2nm diameter) damaged not only the plasma membrane but also the mitochondria and nucleus (Lovric and Cho *et al.*, 2005). AuNPs have also been assessed in terms of nanotoxicology (Alkilany and Murphy, 2010). A report by Su *et al* (2007) described a toxic dose dependant effect of Au-nanoshells in BALBc mice (Su and Sheu *et al.*, 2007). However a subsequent study by Qian *et al* (2008) showed that PEGylated AuNPs administered to mice produced no cytotoxic effects or tissue damage, demonstrating the importance of passivating NP ligands (Qian and Peng *et al.*, 2008). The NP size of gold has created some concern that cellular barriers would not be able to stop AuNP infiltration into cells, which could potentially lead to unintended cytotoxic effects (Connor and Mwamuka *et al.*, 2005). Based on these concerns, a group by Pan *et al* (2007) demonstrated that AuNP cytotoxicity is indeed size dependant. Four cell lines were studied: Hela (cervical carcinoma epithelial cells), Sk-Mel-28 (melanoma cells), L929 (mouse fibroblasts), and J774A11 (mouse monocytic/macrophage cells). The authors systematically increased the size of the AuNPs and observed for signs of toxicity. Results indicated that AuNPs with a diameter of 1-2nms displayed high levels of cytotoxicity (Pan and Neuss *et al.*, 2007). Another study by Chen *et al* indicated that AuNPs with a diameter of 15nm were not toxic in human hepatoma cell culture (Chen and Xu *et al.*, 2008).

There are other studies that have highlighted additional factors such as NP concentration (Kirchner and Liedl *et al.*, 2005), geometry (Cui and Tian *et al.*, 2005), ligand side chains (Goodman and McCusker *et al.*, 2004) and surface modifications (Hoshino and Manabe *et al.*, 2007) all play a crucial role in the potential nanotoxicity of a AuNP.

The nanotoxic properties must be assessed on a particle-to-particle basis, using adsorptions tests, distribution analysis, particle excretion, metabolism and the physiochemistry or toxicological properties of the AuNP *in vitro* (Sanvicens and Marco, 2008). This allows for a quick and easy assessment of NP toxicology, before moving into more complex risk assessment with *in vivo* studies. This conclusion was echoed by Conner *et al* (2003), who emphasised that AuNPs nanotoxicity was dependant on AuNP size and surface coating.

1.2.2 Regulation of Cells by RNA

1.2.2.1 RNA Interference (siRNA)

RNA interference, (RNAi) is a natural function of the intra-cellular machinery affecting gene expression (Figure 1-4) (Fire and Xu *et al.*, 1998). Originally thought of as 'co-suppression' and attributed to another mechanism of antisense silencing (van der Krol and Mur *et al.*, 1990., Napoli and Lemieux *et al.*, 1990). However in 1998, Fire and Mello proved that this 'co-suppression' idea was incorrect and that this new mode of silencing was something new. They concluded that dsRNA sequences are understood in eukaryotic cells as specific signals that can inhibit mRNA expression (Fire and Xu *et al.*, 1998). This revelation resulted in both Fire and Mello receiving the Nobel Prize in Physiology or Medicine in 2006 (Zamore, 2006).

Double-stranded RNA (dsRNA) >30nucleotides (nt) in length are exported by exportin 5 from the nucleus into the cytoplasm and cleaved by DICER (a ribonuclease enzyme), into 21-23nt fragments of small interfering RNAs (siRNAs) (Bernstein and Caudy *et al.*, 2001., Elbashir and Harborth *et al.*, 2001., Ohrt and Merkle *et al.*, 2006., Lommatzsch and Aris, 2009). In the cytoplasm, these siRNAs interact with the RNA-induced silencing complex, RISC (Rand and Ginalski *et al.*, 2004), becoming single stranded (Matranga and Tomari *et al.*, 2005) and binding with complete complementarity to the mRNA sequence (Ameres and Martinez *et al.*, 2007). Argonaute 2 (AGO2), a multi-functional protein found within RISC, is responsible for cleaving the bound mRNA between the 10th and 11th nucleotide from the 5' end (Whitehead and Langer *et al.*, 2009a). Cleaving and degrading the bound mRNA transcript effectively silences the gene.

Over recent years RNAi has become the favoured method for gene knockdown studies in research. The advantages of RNAi over more traditional methods include the ability to target a broader range of genes and portions of regulatory code than classical drug inhibition

would facilitate. This is due to the very nature of RNAi, as any known portion of genetic code can be used to design a set of perfectly complimentary double stranded siRNA sequences (Huang and Li *et al.*, 2008). Chemical inhibitors can be very time-consuming to produce, costly and are generally more toxic than RNAi sequences. These advantages have led RNAi to emerge as an attractive therapeutic tool for clinical treatment of human genetic disease caused by abhorrent gene expression (Kurreck, 2009).

1.2.2.2 MicroRNA

MicroRNAs (miRNAs) were first discovered in 1993 in *C. elegans*, and have since become a key frontier for biomedical research, particularly in diseases such as cancer, but also in regenerative medicine using stem cells (Figure 1-3).

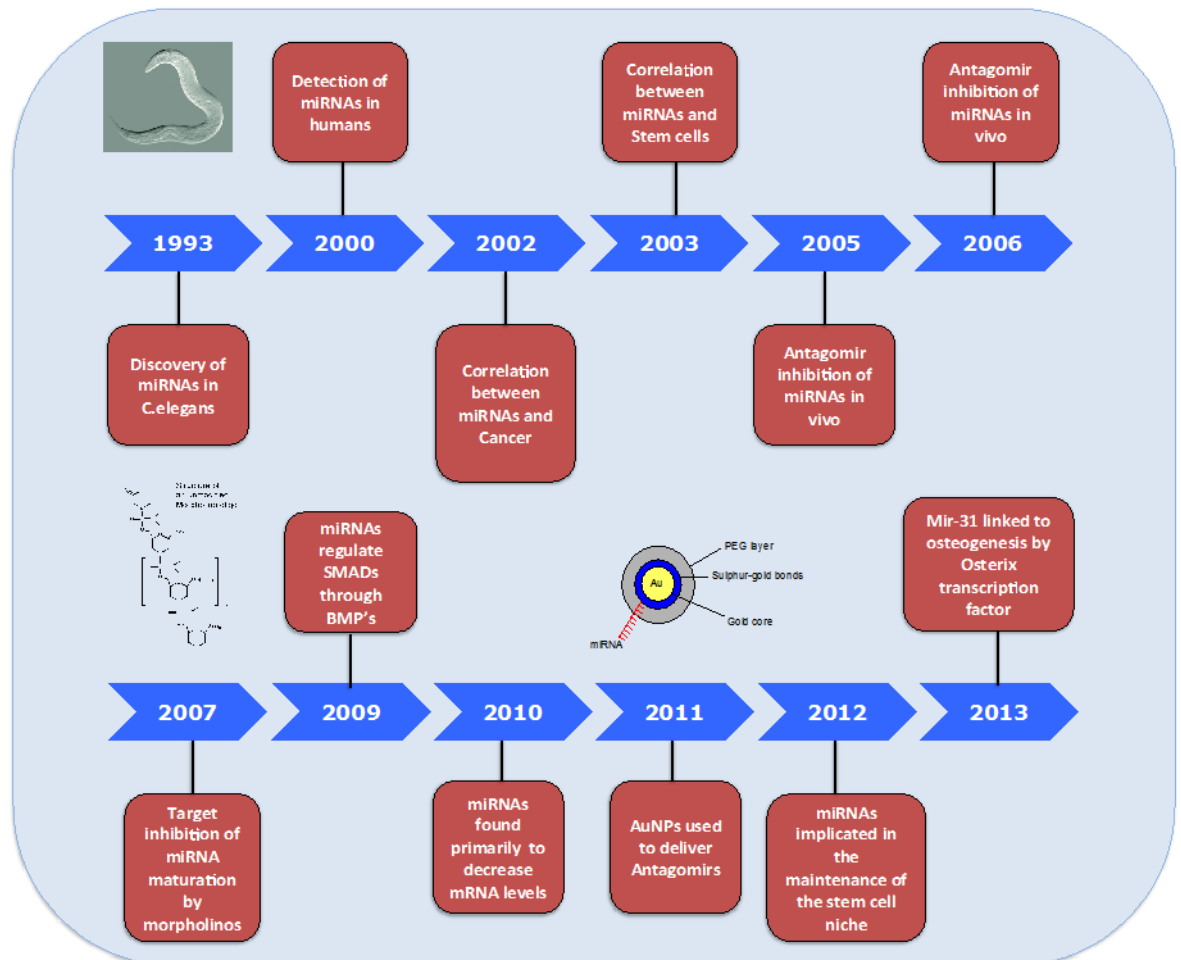


Figure 1-3. Timeline of major advances for miRNA studies, with particular focus on stem cells and osteogenesis (personal image).

MiRNA differs from siRNA in the method of generation, as summarised in Figure 1-4. Where siRNA is normally double stranded and produced outside of the cell, miRNA is produced within the nucleus. It is exported and processed from pre-miRNA into a mature miRNA form. Both siRNA and miRNA form RISC complexes with AGO2 to target mRNA. However miRNA primarily represses mRNA transcript translation and only induces degradation when bound with a high degree of complementarity (Guo and Ingolia *et al.*, 2010), whereas siRNA only acts to degrade mRNA transcripts with perfect complementarity,

As described previously, siRNA binds with complete complementarity to its intended mRNA transcript, whereas miRNAs bind imperfectly to the 3' untranslated region (UTR) of mRNA. The UTR region is important for

mRNA stability and sub-cellular location. This miRNA/mRNA interaction represses the translation of a whole family of mRNA transcripts, providing less specificity, but a broader range. Translational repression by miRNA depends on the binding free energy of the first 8 nucleotides located at the 5' end of the miRNA and the target mRNA (Doench and Sharp, 2004). MiRNAs have a major role in the regulation of many cellular processes; such as apoptosis, stem cell differentiation and proliferation (Zeng and Qu et al., 2012.,Wu and Xie et al., 2012.,van Wijnen and van de Peppel et al., 2013.,Sun and Wang et al., 2009b.,Seca and Almeida et al., 2010.,Sartipy and Olsson et al., 2009).

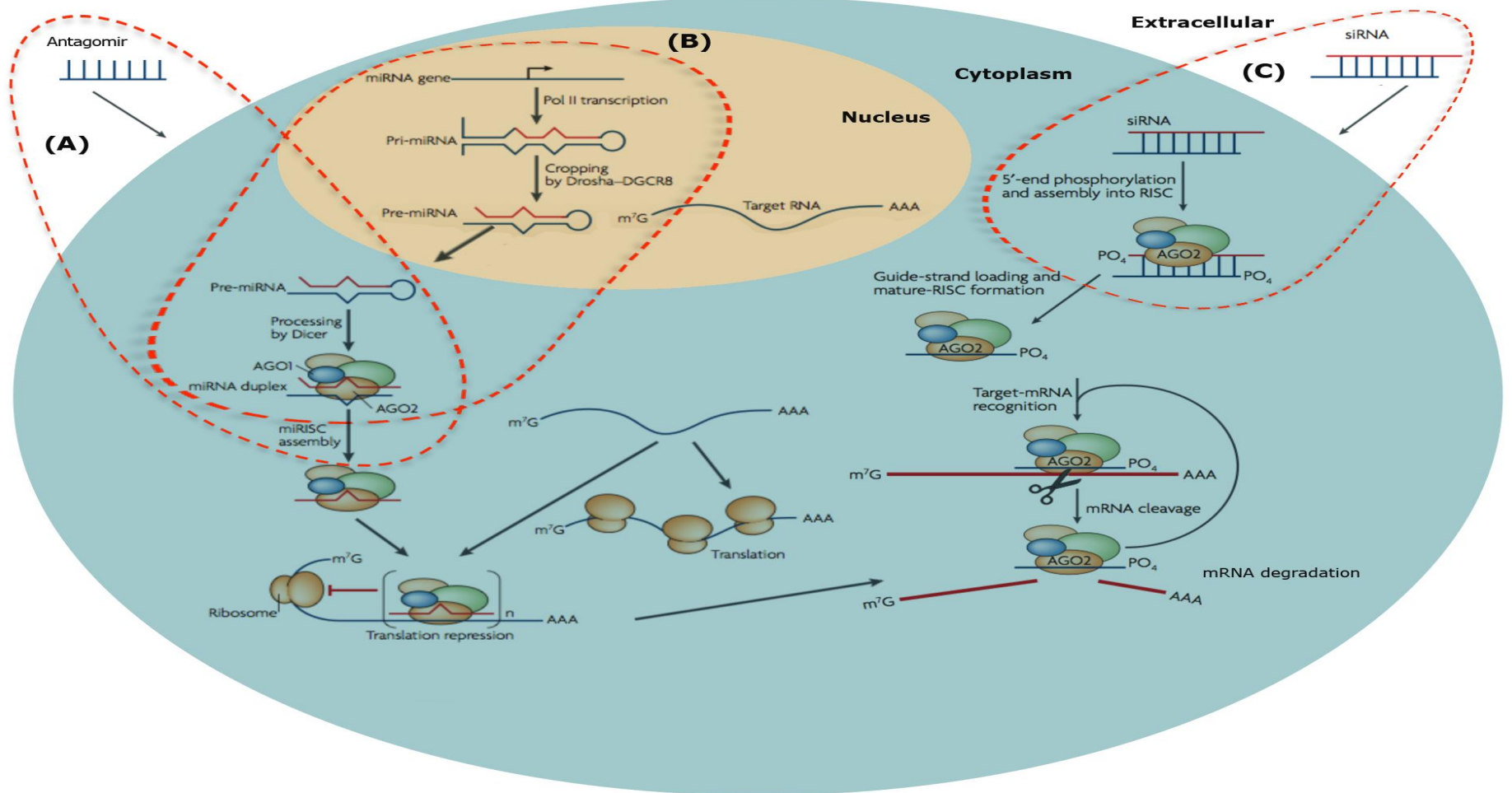


Figure 1-4 Diagram comparing antagomir, miRNA and siRNA pathways and routes. SiRNA and antagomirs are made exogenously. A) Antagomirs enter the cell and bind to miRNA, blocking miRNA expression. B) MiRNA made in the nucleus are processed into hairpin structures, exported from the nucleus and cut with dicer to silence mRNA. C) SiRNA enters the cell and is processed by dicer, cutting the double stranded RNA into single stranded RNA. This RNA is loaded into the RISC complex silencing mRNA targets. Routes A and C will be used in this thesis. Adapted from (Rana, 2007).

1.2.2.3 Blocking miRNA with Antagonists

Recent advances in our understanding of small RNAs have shown the wide-ranging and dynamic effects that these small RNAs have on cells; from disease progression through to cell growth and apoptosis. From this new understanding people have sought to target miRNAs with possible therapeutic potential. To date, two methods of miRNA targeting have been successfully trialled:

Morpholinos; modified nucleic acid analogues containing a morpholino ring (Kloosterman and Lagendijk *et al.*, 2007)

Antagomirs; usually containing a 2'-methoxy group or phosphorothioates as a method to prevent sequence degradation (Kruzfeldt and Rajewsky *et al.*, 2005b)

Morpholinos and antagomirs act by similar principles of blocking, that is to say that they tightly bind to the guide strand of the mature miRNA and prevent access of the miRNA to the mRNA (Schöniger and Arenz, 2013).

1.2.2.4 Delivery of Therapeutic siRNA and miRNA/Antagomirs

Using siRNA therapeutically relies upon the transfection of mammalian cells with designed double stranded sequences that can bind to and silence the target genes' mRNA with perfect complementarity. Sequences of siRNA are designed and created *ex-vivo*, however generally these sequences have a short half-life and are easily degraded. An alternative to conventional double stranded siRNA is short-hairpin RNA (shRNA) (~29nt long), which is capable of providing a longer lasting and higher stability of silencing (Shi, 2003.,Huang and Li *et al.*, 2008.,Siolas and Lerner *et al.*, 2005). ShRNA can be produced inside the cell with a DNA construct, but requires a viral vector. As with other viral technologies, the presence of the virus limits the potential clinical use of the shRNA. In 2010 Ryou *et al* reported the successful

silencing of the p53 gene in HEK293 cells using shRNA against p53 conjugated to gold nanoparticles. Due to the lack of viral DNA, knockdown decreased from 97% to 35% after 72 hours.

MiRNAs and antagomirs can be synthesised into single strands and subsequently delivered into the cells. However as with siRNA, naked miRNAs have a short half-life and are also easily degraded. To bring this technology into more widespread therapeutic use, a reliable, non-viral and non-toxic method for siRNA and miRNA/antagomir delivery must be developed with a view for potential use *in vivo*, as the half-life and degradation of naked siRNA is a major hurdle to overcome. This method of delivery must:

- 1) Protect the sequence from degradation once introduced into the body (Dykxhoorn and Lieberman, 2005., Kim and Yeom *et al.*, 2011),
- 2) Be able to target specific cells e.g. the disease phenotypic cells (Derfus and Chen *et al.*, 2007., Doench and Sharp, 2004)
- 3) Mask the negative charge of the sequences for efficient membrane crossing (Akhtar and Basu *et al.*, 1991., Wittung and Kajanus *et al.*, 1995., Suh and Lee *et al.*, 2013),
- 4) Avoid endosomal degradation (Lee and Huh *et al.*, 2010., Ghosh and Singh *et al.*, 2012)

NPs therefore offer the ideal platform for delivery of such small regulatory molecules. The ability of NPs to meet and surpass the four criteria mentioned above creates numerous opportunities for biomedical science. However some challenges still need to be meet. For example, rapid excretion by the kidney, complex extracellular matrices, poor vascular permeability and clearance of NPs by the reticuloendothelial system (a collection of phagocytic cells that target and remove foreign objects) present complex challenges for the systemic delivery of

therapeutic payloads (Barry, 2008.,Juliano and Alam *et al.*, 2008.,Gao and Dagnaes-Hansen *et al.*, 2009).

Within the cell, efficient delivery requires both (i) efficient cellular uptake levels, and (ii) availability of free siRNA within the cell to allow interaction with the RISC complex, which may depend on endosomal escape (Juliano and Alam *et al.*, 2008). Creating a multi-functional vehicle to deliver therapeutic payloads such as siRNA or miRNA could be the panacea needed to overcome the aforementioned technical problems. Moderate success has been achieved by using some transfection methods (liposomal, polymer capsules) delivering siRNA *in vivo*. Indeed, Hepatitis B has been treated by reducing the FAS protein in mice by delivering an injection of siRNA with no delivery vector intravenously (Song and Lee *et al.*, 2003). Although successful, this study required large volumes of siRNA to achieve protein knockdown, which in a clinical setting would be prohibitively expensive, with the potential for numerous off-target effects. Injection of siRNA into tissue can induce some limited therapeutic benefit (e.g. slow cancer progression), however a systemic approach to siRNA delivery and administration using a delivery vector could significantly enhance the therapeutic potential, and reduce the associative cost of delivery (Kurreck, 2009).

1.2.3 Nanoparticle-Mediated Delivery of Oligonucleotides

Progress within gene discovery and analysis, has begun to investigate the link between gene dysfunction and disease phenotype. As the previous section has shown, targeting diseases at the genetic level is an attractive opportunity currently receiving a lot of attention within medical research. However, problems surrounding the delivery and functional activity of the oligonucleotide payload have to date hindered the developing technology.

The combination of therapeutic siRNA with the adaptability of AuNPs creates an attractive platform for successful and targeted gene therapy. To date, there have been many studies to this effect. Derfus *et al* demonstrated that one siRNA per particle conjugated with >15 tumour homing peptides (F3) produced optimal knockdown and targeting (Derkus and Chen *et al.*, 2007). Subsequently, Lee *et al* (2008) reported that PEG-siRNA (against GFP) complexes conjugated to AuNPs functionalised with amines group, could efficiently enter the cell whilst significantly knocking down the expression of GFP in carcinoma cells without producing any severe cytotoxicity (Lee and Bae *et al.*, 2008). Other reports have shown that siRNA attached to AuNPs by thiol linkage are efficiently uptaken by cells and consistently knockdown the expression of the targeted gene. A report by Acharya *et al* (2013), developed a AuNP conjugated with KDEL peptides and siRNA against Nox4, delivered to C2C12 myoblasts. The authors reported a 55% knockdown of Nox4 at the gene level at 24 hours (Ryou and Kim *et al.*, 2010., Giljohann and Seferos *et al.*, 2009., Dreaden and Mackey *et al.*, 2011). Therefore the potential for using NPs to deliver therapeutic siRNA is apparent.

The delivery of multivalent NPs has also been achieved. Kim *et al* successfully demonstrated the potential of targeting cells using a combination of folate (FOL) and PEG attached to polyethylenimine (PEI) to significantly reduce GFP gene expression by siRNA (targeted against

GFP) loaded into polymer NPs (PEI-PEG-FOL) (Kim and Mok *et al.*, 2006). When applied to folate expressing cells these NPS were more readily uptaken as compared to control NPs lacking any folate or PEG. Despite the differences in NP type, cell type, study time courses *etc.*, when taken together, along with the multiple other studies in this field, there is certainly promise for siRNA functionalised NPs in nanomedicine.

Some studies have been advanced to the *in vivo* stage. For example Schiffelers *et al* (2004) created self-assembling polymer NPs with PEI-PEG, in addition to the RGD ligand, to enhance delivery of siRNA into cancer cells in mice. The authors reported successfully reducing the VEGF R2 oncogene, and *in vivo* prevented an increase in tumour size. (Schiffelers and Ansari *et al.*, 2004).

Ghosh *et al* (2013) addressed a number of issues surrounding miRNA delivery. Most miRNAs require expensive modifications to increase stability, and some delivery method such as lipofectamine, which is toxic to cells. The author's developed a system using AuNPs, conjugated with PEG and miRNA (mir-31,-1323), attached by ionic bonds to the gold surface. They reported a higher payload density than lipofectamine, efficient uptake and low cytotoxicity compared to lipofectamine (~98% cell survival). In 2011 Kim *et al*, developed a system that targeted mir-29b with antisense RNA (antagomir-29b). The antagomirs were conjugated to AuNPs (13nm) and delivered to HeLa cells. The authors reported an increase of MCL-1 at the protein and mRNA level upon addition of the antagomir-AuNPs. However the authors did not report the use of any polymer coating, which could have limited the success of the delivery (Kim and Yeom *et al.*, 2011).

Conde *et al* (2013) developed upon this system for targeting miRNAs. Using AuNPs (~15nm) they targeted mir-21 with antisense RNA and protected the AuNP with PEG. The antisense RNA was created as a hairpin structure with the 3' end containing a cy- dye and the 5' end containing a thiol group allowing for covalent attachment to the AuNP.

The authors successfully reported a ~89% knockdown of mir-21 by RT-qPCR in HCT-116 cells (a colorectal carcinoma).

These studies are excellent examples of the scope of using NP multifunctionality to successfully deliver siRNA and miRNA/antagomirs.

1.3 Targeting Cancers Using an siRNA-Nanoparticle Delivery Platform

1.3.1 Targeting Genetic Disease

Damaged or dysregulated expression of one or more genes is responsible for a wide range of human diseases. Nanomedicine is currently geared towards the targeting and treatment of known genetic aberrations in disease. Huntington's disease has received a lot of media attention as an autosomal dominant disorder caused by lengthening of a CAG repeat sequence in the genetic code (Walker, 2007). Additionally cystic fibrosis is an autosomal recessive disorder in humans, produced by mutations in the gene cystic fibrosis transmembrane conductance regulator (CFTR) (Lommatzsch and Aris, 2009). With Duchenne muscular dystrophy, a mutation in the dystrophin gene produces an x-linked recess disorder (Odom and Banks *et al.*, 2010). One method of facilitating treatment is the delivery of novel oligonucleotides, to either silence or replace the dysfunctional genes.

Conjugating cholesterol directly to siRNA, targeting ApoB (a gene associated with heart disease), was found by Soutshek *et al* (2004) to enhance the pharmacokinetics of the siRNA and increase cellular uptake of the siRNA (Soutshek and Akinc *et al.*, 2004). This increase although impressive, was overshadowed by Zimmerman *et al* (2006), who conjugated siRNA onto stable nucleic acid lipid particles (SNALPs). These SNALPs were capable of even greater silencing in the same ApoB mouse model used by Soutshek *et al* (2004). Zimmerman *et al* (2006) demonstrated that a SNALP based delivery method was capable of reducing ApoB mRNA by up to 90% in non-human primates.

The above conditions, although serious, are fairly rare in comparison to global rates of cancer, which account for 13% of all deaths per year, thus cancer remains one of the major treatment goals in nanomedicine (Ferlay and Shin *et al.*, 2010).

Cancer is a multipoint disease, with many genetic mutations resulting in unregulated cell growth and consequential formation of tumours (Santarius and Shipley *et al.*, 2010). Within the human genome approximately 600 proposed genes are involved in cancer formation and progression. These genes are linked to angiogenesis, apoptosis, cell cycle control, DNA repair, metastasis (Pawaiya and Krishna *et al.*, 2011).

1.3.2 C-Myc Protein and Cancer

The C-Myc gene was first reported in a Burkett's Lymphoma patient (Dalla-Favera and Bregni *et al.*, 1982). Since its discovery, the gene has been cloned (C-Myc) and has become one of the most studied oncogenes to date (Beroukhim and Mermel *et al.*, 2010). C-Myc is an essential transcription factor that regulates signal transduction for proliferation pathways. Whilst being vital to healthy cell survival, deregulated C-Myc has been found in approximately 95% of human cancers (Figure 1-5) (Beroukhim and Mermel *et al.*, 2010).

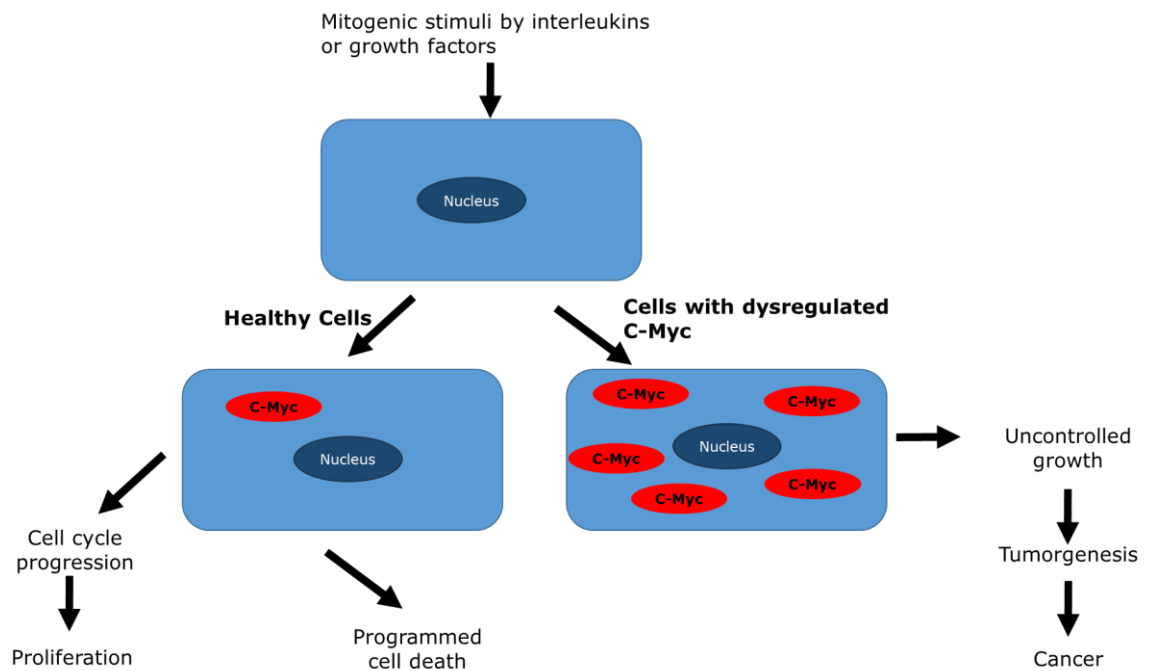


Figure 1-5. Effect of stimuli on C-Myc expression in healthy and dysregulated cells. Figure adapted from (Cassinelli and Supino *et al.*, 2004)

In healthy cells C-Myc expression is highly regulated by multiple feedback loops such as Arf and p53. Transcribed C-Myc forms a dimer with another transcription factor 'max'. This C-Myc/max complex can then bind to DNA (C-Myc-E Box 5'-CACGGTG-3'), activating a host of target genes (Liao and Dickson, 2000). To determine the exact number

of C-Myc target genes, a number of genome wide studies can be conducted (Li and Van Calcar *et al.*, 2003., Zeller and Zhao *et al.*, 2006). A study by Li *et al* (2003), found that approximately 726 binding sites bound to C-Myc. This was corroborated by another study by Zeller *et al* (2006) that found 700 genes responded to C-Myc activation (Zeller and Zhao *et al.*, 2006). Zeller *et al* (2006) used ChIP-PET (chromatin immunoprecipitation pair end tags) to map C-Myc binding sites. However a study by Ji *et al* (2011), identified a C-Myc core group of 50 gene targets by combining and correlating genome wide ChIP-chip, ChIP-seq and microarray data from multiple cell types (Ji and Wu *et al.*, 2011).

In 2012 a review by Dang, concluded that the majority of C-Myc studies suggested that C-Myc functioned as a master regulator, which was capable of affecting a broad spectrum of genes involved in energy metabolism, replication and division (Dang, 2012). Due to the high occurrence of C-Myc over-expression found in multiple types of cancerous cells, and the central role it plays in cell cycle regulation and proliferation, C-Myc is a very interesting candidate for gene therapy. Such a targeted approach should aim to normalise C-Myc levels and as a consequence slow down or halt the tumour formation and progression.

1.3.3 C-Myc Oncogene Addiction

A new approach for targeted cancer therapy is based on the theory that cancer cells become dependent on the expression of one main oncogene (Luo and Solimini *et al.*, 2009). This theory has been dubbed 'oncogene addiction', and has been described as the Achilles heel of cancer (Weinstein, 2002). C-Myc has been shown to be one of the major oncogenes that cells can become addicted to. To investigate this theory, Jain *et al* (2002) created a transgenic mouse model that, in the presence of doxycycline (dox) (an antibiotic that has shown promising anti-cancer properties), activated C-Myc expression. Their study found

that a brief inactivation of C-Myc lead to tumour regression and the transformation of osteogenic sarcoma cells to differentiate into mature osteocytes. Interestingly the authors noted that reactivation of C-Myc did not lead to the reactivation of the malignant tumour cells. They have proposed that the brief C-Myc inactivation has altered certain epigenetic features, desensitising the cells to C-Myc lead tumorigenesis (Jain and Arvanitis *et al.*, 2002). This study reinforced the theory that temporarily targeting key oncogenes can have a long-term beneficial therapeutic outcome. The limits for this study come from a clinical point of view, where oncogenes could not be manipulated by dox treatment alone. However sustained delivery of dox produces toxic off-target effects in normal cells. This type of off target effect is reduced in RNAi treatments, as there are a lot of overlapping and complementary molecules regulating essential pathways in healthy cells. So from a clinical aspect oncogene addiction treated by oligonucleotides offers a therapeutic with very limited side effects, facilitated by some form of NP delivery vehicle.

1.3.4 Targeting the C-Myc Protein by RNAi-siRNA

Fire and Mello used *C. elegans* treated with specific dsRNA molecules that resulted in potent and significant silencing (Fire and Xu *et al.*, 1998). Many studies afterwards have reiterated Fire and Mellos work, that dsRNA >30nts can silence genes in eukaryotes, such as *D. melanogaster* (Kennerdell and Carthew, 1998), and plants (Hamilton and Baulcombe, 1999). The breadth and diversity of life that exhibited some form of RNAi lead researchers to consider using RNAi to target human genes.

In mammalian cells however, the longer dsRNAs (>30nts) were found to produce a severe interferon (IFN) immune response, making them unacceptable for use in human targeted RNAi studies (Manche and Green *et al.*, 1992). This problem was solved in 2001, using small artificial, exogenous dsRNA molecules of approximately 21nts in length (Elbashir and Harborth *et al.*, 2001). The smaller lengths were able to

silence the intended genes whilst preventing any IFN immune response. Since then, the increase in bioapplications utilising RNAi has been exponential, growing into a multimillion-dollar business (Castanotto and Rossi, 2009).

Within 6 years from initial discovery in 1998, the first RNAi-based clinical trials began in 2004. The trial conducted by Acuity Pharmaceuticals targeted the expression of a VEGF receptor in the eye (Cand5) with siRNA, to treated patients with a form of macular degeneration that leads to adult blindness. The siRNA therapy reached phase III clinical trials and was reported by Bumcrot *et al* to reduce lesion size and improve near vision (Bumcrot and Manoharan *et al.*, 2006). This success led Acuity Pharmaceuticals to investigate if Cand5 silencing could be used to treat diabetic macular edema (DME). Other companies such as Merck-siRNA Therapeutics also started to bring their own versions of RNAi based therapeutics to clinical trials (Castanotto and Rossi, 2009). Alnylam Pharmaceuticals targeted respiratory syncytial virus (RSV) infections, using siRNA to reduce viral replication. They were the first antiviral siRNA therapy to make it to clinical trials (Castanotto and Rossi, 2009). To date, however, the therapies that have achieved clinical trial status mainly target easily accessible tissue, such as the lungs or the eyes, for siRNA delivery, and have not yet targeted more challenging tissue or diseases.

As explained previously, successful delivery of therapeutic siRNA to challenging sites within the body that cannot be reached by direct injection or inhalation, requires a suitable delivery vector, such as NPs. These NPs must protect the RNAi from degradation within the body; remain in the bloodstream without being cleared by the kidneys (Dykhorn and Lieberman, 2005); target a specific tissue or area (Derfus and Chen *et al.*, 2007) and be easily taken up by the target cells (Akhtar and Basu *et al.*, 1991., Wittung and Kajanus *et al.*, 1995). Bumcrot *et al* (2006) cite the 'Lipinski Rules' (a set of rules used to denote small molecule drug behaviour by the pharmaceutical industry),

for the poor uptake of siRNA into cells without the aid of a delivery vector. One of the rules states that: an octanol-water coefficient should be less than or equal to 5 and a molecular weight less than 500 Daltons (Da) are needed for successful uptake. SiRNA molecules break this rule with molecular weights of approximately greater than 13kDa and so require a delivery vector to circumvent this issue (Bumcrot and Manoharan *et al.*, 2006).

However siRNA have further issues, including their size, mainly that they are easily degraded *in vivo*, and rapidly excreted by the kidneys (Gao and Dagnaes-Hansen *et al.*, 2009). In addition, siRNA permeates poorly through vascular tissue and extracellular matrices, and is cleared rapidly by phagocytes in the reticuloendothelial system (RES) (Barry, 2008., Juliano and Alam *et al.*, 2008). Due to these drawbacks, naked siRNA molecules have very little practical applications for RNAi therapy. Therefore the design of a multifunctional NP has become key to resolving the above issues before RNAi therapy can become a wide scale therapeutic option.

1.3.5 Nanoparticles as siRNA Delivery Vehicles for Cancer

Zukiel *et al* (2006) clinically trialled RNAi therapy to treat human glioblastoma multiform brain tumours. The results concluded that although direct, localised injections of siRNA inhibited cancerous cells, there were differences in patient response. Additionally some patients had sections of the tumour removed, making direct comparisons of tumour regression difficult. The procedure itself was invasive and required a surgical team (Zukiel and Nowak *et al.*, 2006).

A growing volume of evidence indicates that attachment of siRNA onto a NP enhances siRNA administration and uptake (Bumcrot and Manoharan *et al.*, 2006). Numerous delivery agents have been studied, from liposomes to organic polymers and inorganic nanoparticles. Liposome delivery has been used within the last decade from ovarian cancer treatment (Halder and Kamat *et al.*, 2006., Landen and Chavez-Reyes *et*

et al., 2005) to liver metastasis in mice (Yano and Hirabayashi *et al.*, 2004). Cancerous bone tissue was administered with atelcollagen loaded with siRNA (Takeshita and Minakuchi *et al.*, 2005). However liposomal delivery has a number of significant drawbacks as summarised by Gabizon *et al* (2006): i) encapsulation of cargo can be difficult, ii) delivery and release is effected by serum proteins and can 'leak' through the liposomal layer, iii) cell targeting specificity, iv) half-life (Gabizon and Shmeeda *et al.*, 2006)

Conde *et al* (2012) created a multifunctional AuNP conjugated with siRNA against C-Myc, PEG to shield the siRNA and to stabilise the NP, biotin for imaging of the NP (*via* streptavidin linked fluorophores) and an RGD binding motif to increase cell uptake by integrin binding. The authors were the first to establish a NP system whereby functional siRNA was successfully delivered in three different models; *in vitro* human cell lines, a simple *in vivo* hydra model and an *in vivo* mouse model (Conde and Ambrosone *et al.*, 2012). With up to a 65% reduction of native C-Myc levels being reported by this delivery vector.

1.4 MiRNA and Mesenchymal Stem Cells

Aside from targeting dysregulated gene expression in disease, NPs also have potential for use in regenerative medicine.

1.4.1 Stem Cells

Stem cells are a unique and highly valuable subset of cells. By definition stem cells have the ability to self-renew in an undifferentiated state indefinitely, whilst simultaneously being able to differentiate into multiple highly specialised cells upon receiving the correct cues. Stem cells can have different levels of potency (Keller, 1995.,Pittenger and Mackay *et al.*, 1999.,Williams and Hilton *et al.*, 1988.,Clarke and Johansson *et al.*, 2000). Pluripotent stem cells can develop into any cell type within the three germ layers of mesoderm, ectoderm and endoderm, whereas multipotent stem cells can develop into multiple cell types but are limited by the lineage they form.

Stem cells have been classified into 3 main categories:

Adult stem cells

Embryonic stem cells

Induced pluripotent stem cells

Adult stem cells were first identified in the 1960s from bone marrow samples, and were further classified into hematopoietic stem cells (HSCs) and mesenchymal stem cells (MSCs) (Becker and McCulloch *et al.*, 1963); the differentiation capabilities of each is summarised in Table 1-1.

Table 1-1. Stem cell type, tissue of origin and differentiation potential.

Name	Tissue of Origin	Differentiated Cell Types
Hematopoietic	Bone marrow	All blood cells Osteoclasts
Mesenchymal	Adipose tissue Bone marrow Umbilical Cord	Bone Cartilage Connective tissue Fat Muscle Nerve

Embryonic stem cells (ESCs) were first isolated from mouse embryos in 1981; a discovery that led to the subsequent detection of stem cells in human embryos (Evans and Kaufman, 1981., Martin, 1981., Thomson and Itskovitz-Eldor *et al.*, 1998). More recently, the reprogramming of somatic cells into stem cells, known as induced pluripotent stem cells (iPSCs), became an area of intense study. However it was only with Yamanaka *et al* (2007) that real progress was made. The authors identified 4 key transcription factors (oct-3/4, sox2, klf-4 and C-Myc) that were required for reprogramming somatic cells back into a stem cell like state (Takahashi and Yamanaka, 2006., Yu and Vodyanik *et al.*, 2007). The initial studies used viral based vectors to introduce the reprogramming factors. Although this method was very efficient at reprogramming, it did however create several hazards including

increased oncogene activation and dangerous mutations caused by viral genome integration.

Recent advances for iPSC generation have moved away from viral based delivery methods and towards using RNAi. Although these methods are less risky, they also have much lower efficiencies (Kaji and Norrby *et al.*, 2009., Kim and Kim *et al.*, 2009., Woltjen and Michael *et al.*, 2009., Zhou and Wu *et al.*, 2009., Kim and Thier *et al.*, 2012). Stem cells, although unique, are not a homogenous population. Differences exist between the location of stem cells, their local niche microenvironment, the capacity to form different cell types and their suitability for regenerative applications. These differences have been summarized in Table 1-2.

Table 1-2. Advantages and disadvantages of different stem cell types and their origins.

Stem Cells	Origin	Potency	Advantages	Disadvantages
Adult Stem Cells	Adipose tissue Bone marrow Umbilical cord	Multipotent	Accessible Autologous Easy to culture Less ethical issues	Multipotent Spontaneous differentiation
Embryonic Stem Cells	Inner cell mass of a blastocyst	Pluripotent	Pluripotent	Complicated cell culture Ethical issues Immune rejection Tumorigenic
Induced Pluripotent Stem Cells	Reprogramming of somatic cells	Pluripotent	Autologous Pluripotent	Low efficiency Tumorigenic

Both ESCs and iPSCs can generate all three germ layers, a characteristic known as pluripotency. Pluripotency is seen as a very attractive tool for regenerative medicine research. ESCs culture well and multiply *in vitro*, however *in vivo*, these cells can form tumours including teratomas, due to unchecked division, and may produce an immune reaction. Additionally the ethical issues that surround ESCs make them unsuitable for therapeutic use.

Adult stem cells have several distinct advantages over ESCs and iPSCs. Adult stem cells such as mesenchymal stem cells (MSCs) are autologous, easily accessible for extraction and eliminate the risk of an immune response (Uccelli and Moretta *et al.*, 2008). Despite all these advantages, adult stem cells are more prone to spontaneous differentiation when cultured *in vitro*, from a stem cell state into a more fibroblast phenotype (Sherley, 2002., Sarugaser and Hanoun *et al.*, 2009).

1.4.2 Mesenchymal Stem Cells (MSCs)

MSCs have been discovered in adipose tissue, umbilical cord blood and Wharton's jelly of the umbilical cord tissue, however, the most studied and best-characterised population of MSCs to date are derived from the bone marrow (Zuk and Zhu *et al.*, 2001., Lee and Kuo *et al.*, 2004., Wang and Hung *et al.*, 2004). MSCs appear as large cells with a fibroblast-like morphology. Whilst the cells were initially discovered in HSC cultures, MSCs were noted to behave differently, by adhering to the tissue culture plates and forming clonogenic colonies known as colony forming unit-fibroblasts (CFU-Fs) (Becker and McCulloch *et al.*, 1963., Friedenstein and Gorskaja *et al.*, 1976., Owen, 1988., Owen and Friedenstein, 1988). Much work subsequently concentrated on improving the isolation and characterisation of MSCs.

The discovery of a definitive marker of MSCs is currently an elusive goal for stem cell scientists. At present MSCs are defined by a presence or absence of a range of cellular markers (cell surface receptors or intracellular protein expression), the main ones of which are highlighted in Figure 1-6 and Table 1-3. Positive markers include numerous surface markers (CD44, CD271), cell adhesion molecules (ALCAM) and cell surface proteins (Stro-1) (Casado-Díaz and Pérez *et al.*, 2011). Stro-1 is the most widely used marker to isolate MSCs from bone marrow, found in approximately 10% of the total cell population (Simmons and Torok-Storb, 1991.,Bakopoulou and Leyhausen *et al.*, 2013.,Stewart and Monk *et al.*, 2003).

Table 1-3. Common MSC stem cell markers used in biomedical research as described by Casado-Díaz *et al* (2011). Positive markers highlighted in yellow, are markers that have been selected and used for the experimental work carried out for this investigation.

Positive Markers	Negative Markers
CD29, CD44, CD71, CD73, CD90, CD105, CD106, CD120a, CD124, ICAM-1, MHC1, CD166 (ALCAM),CD271, STRO-1	CD11, CD14, CD18, CD34, CD40, CD45, CD80, CD86, MHCII

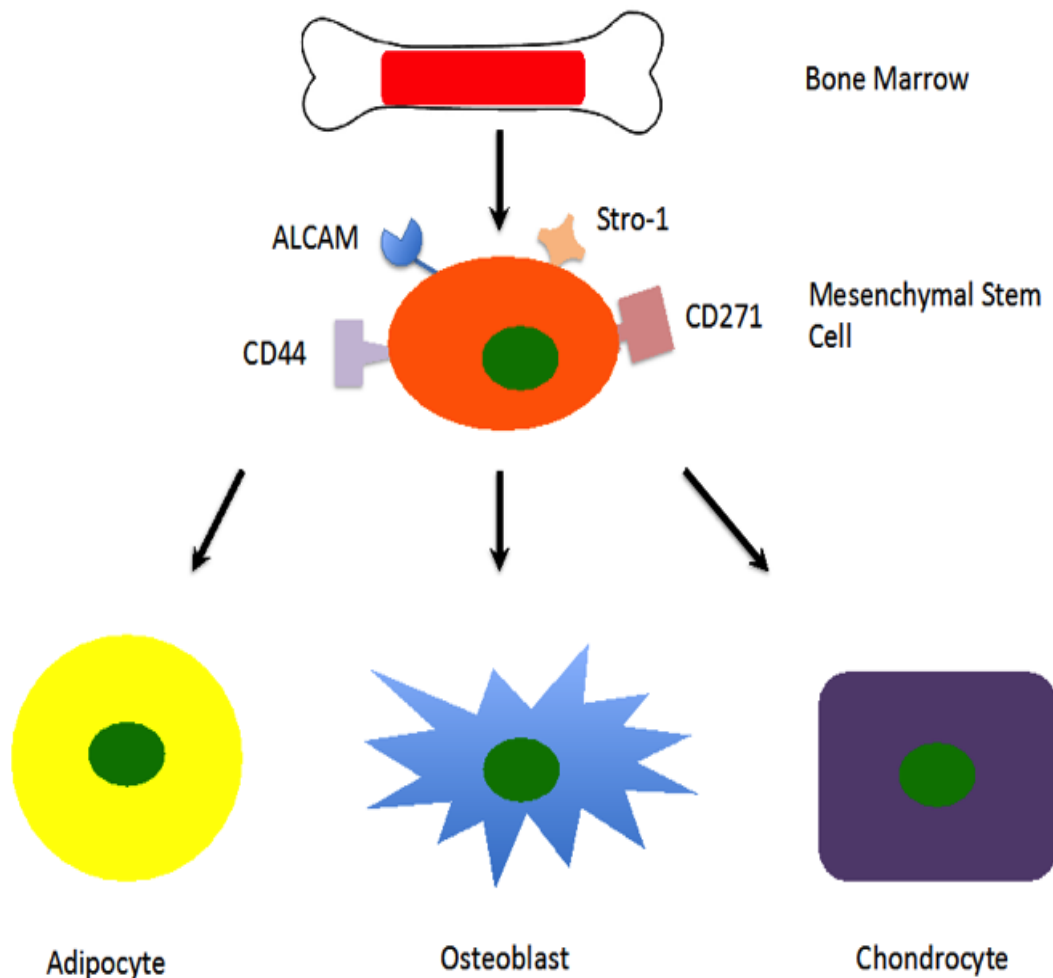


Figure 1-6. Differentiation potential of MSCs harvested from bone marrow, showing the most established stem cell positive cell markers

MSCs reside within a highly ordered environment known as the bone marrow niche. Within this area two individual niches exist; the endosteal niche (near the osteoblast lined endosteal bone, which supports MSC quiescence and self-renewal) and a peri-vascular/peri-sinusoidal niche (near blood vessels, supporting proliferation and differentiation). The endosteal niche, described by Zhang *et al* (2003) (Zhang and Niu *et al.*, 2003) is composed of multiple cell types including osteoblasts, HSCs, MSCs and endothelial cells (Wang and

Zhang *et al.*, 2012) (Figure 1-7). Signaling from the bone marrow can induce cycling of HSCs from the sinusoid to the outer bone marrow (Figure 1-7). Environmental signals ranging from the material stiffness and topography of the extracellular matrix to cell signaling (eg. cytokines, small RNAs and excreted proteins) can influence the proliferation, differentiation and migration of the MSCs (Laine and Hentunen *et al.*, 2012., Orford and Scadden, 2008).

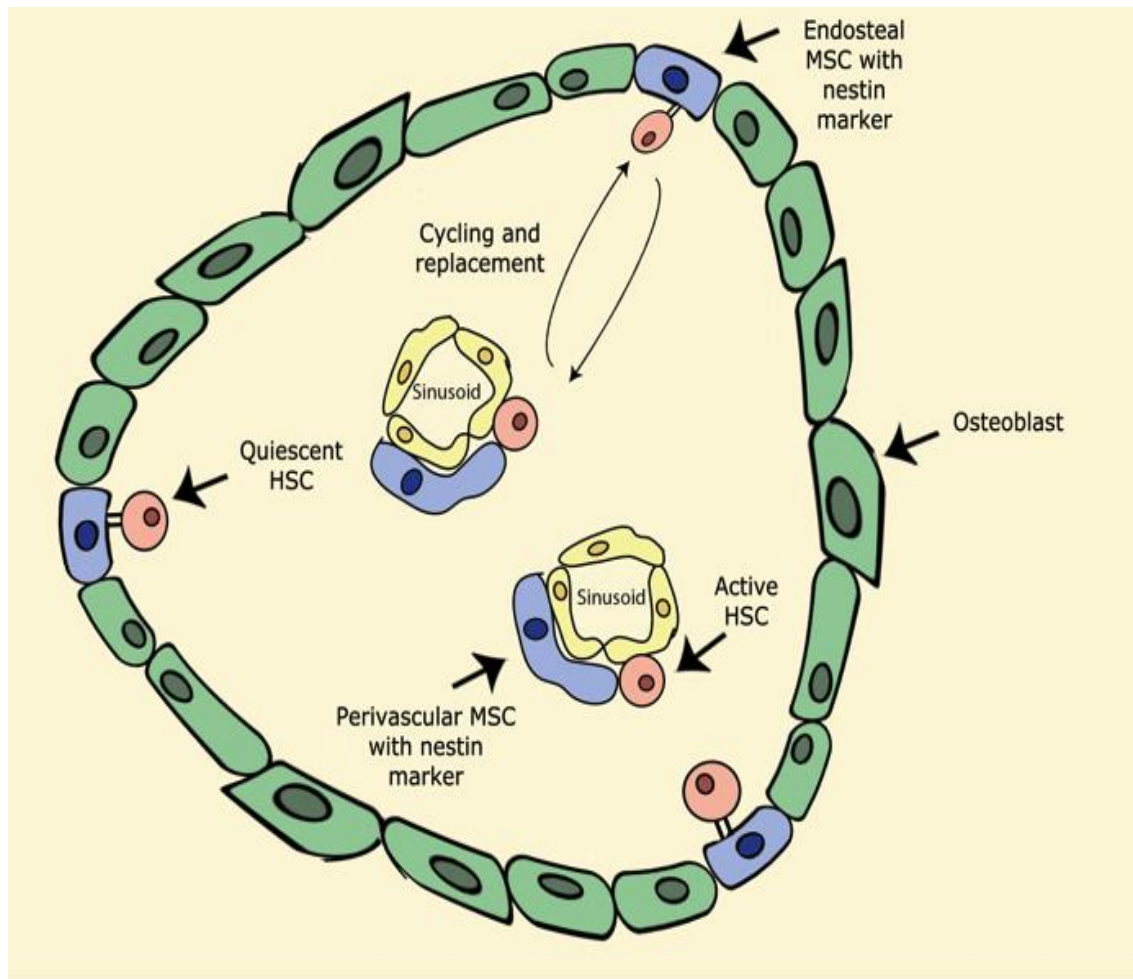


Figure 1-7. Interplay between the endosteal and sinusoid niches, in bone marrow. The endosteal niche is located near the osteoblast lined endosteal bone, which supports MSC quiescence and self-renewal. The sinusoidal niche normally located near blood vessels, supports proliferation and differentiation. HSCs migrate and bind to the nestin markers on MSCs. Blue cells show MSCs, pink indicate HSCs, Green osteoblasts and yellow endothelial capillary cells. Image adapted from Zhang *et al* (2003)

1.4.2.1 MSC Differentiation

MSCs are derived from the mesoderm layer. It is possible with chemically defined signals to induce MSC differentiation, to form a multitude of cell types ranging from adipocytes to chondrocytes, fibroblasts, myoblasts and osteoblasts (Figure 1-6) (Pittenger and Mackay *et al.*, 1999.,Majumdar and Thiede *et al.*, 2000.,Gang and Hong *et al.*, 2004).

Controversially some evidence has indicated that MSCs may have the potential to transdifferentiate across germ layers into ectoderm or endoderm cell types, potentially increasing the differentiation potential (Tropel and Platet *et al.*, 2006.,Woodbury and Schwarz *et al.*, 2000.,Wang and Bunnell *et al.*, 2005.,Jiang and Jahagirdar *et al.*, 2002).

1.4.2.2 Osteogenesis

MSC differentiation into a mature bone cell type requires a multistep process, from MSC to pre-osteoblast and finally to a mature osteoblast. The process of cellular differentiation reduces the rate of proliferation but increases the secretion of extracellular matrix proteins such as fibronectin (FN) and type I collagen. Osteoblast-type cells produce specific cell markers, including the enzyme alkaline phosphatase, and bone mineralisation proteins (in particular osteopontin and osteocalcin) (Stein and Lian *et al.*, 1990) . Key signalling pathways have since been identified, that are critical for osteogenesis, collated together in Figure 1-8.

Wnt (cell surface receptor) signalling was noted to alter osteogenic proteins levels, with Wnt3a thought to repress osteogenesis and increase proliferation (Boland and Perkins *et al.*, 2004.,Siddappa and Fernandes *et al.*, 2007).

The TGF-beta/BMP (bone morphogenic protein) pathway has also been identified to be critically important to the development of stem cells to a bone cell state (Linkhart and Mohan *et al.*, 1996.,Rickard and Sullivan *et al.*, 1994).

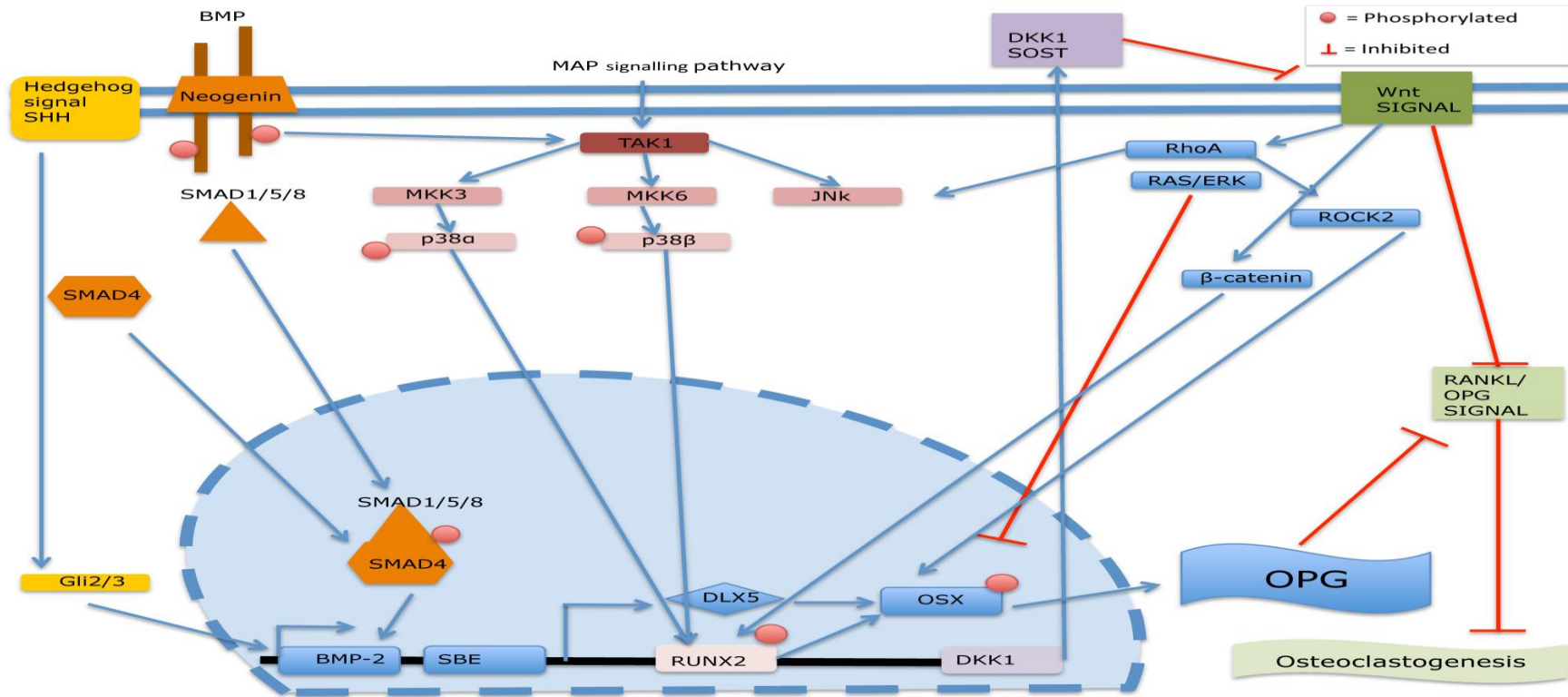


Figure 1-8. Osteogenic pathways found in hMSCs, combining BMP, Hedgehog, MAP and Wnt signalling. Red circles indicated a phosphorylated protein and red arrows indicate protein inhibition. This diagram is not an exhaustive list, and highlights only some of the complexity of signalling during osteogenesis. The area within the blue dotted line corresponds to the events within the nucleus, outside this represents the cytoplasm and the two parallel lines signify the plasma membrane.

1.4.2.3 Self-Renewal

Self-renewal in MSCs is currently not well understood at the molecular level. Self-renewal *in vivo* is governed by complex signals within the niche, such as mechanical properties of the extracellular matrix, cell cycle and hormonal signals. Within the niche, stem cells undergo either symmetrical division; whereby one stem cell divides creating two stem cells, and/or asymmetrical cell division; whereby one stem cell is produced and retained in the niche whilst a progenitor cell exits the niche and differentiates (Kiel and Morrison, 2006).

Asymmetrical cell division is thought to maintain tissue homeostasis and stem cell population within the niche environment, whereas symmetrical cell division is predominantly observed following an injury or during tissue development (Wilson and Laurenti *et al.*, 2008). Internal and external signalling controls both symmetrical and asymmetrical division. Factors within the cell such as the mitotic spindle orientation to the niche, the presence of differentiation factors and cell polarity are crucial to the choice of division (Wodarz, 2005., Beier and Rohrl *et al.*, 2008., Yamashita, 2009). Outside the cell, signals such as differentiation factors relatively closer to one daughter cell can produce an asymmetric division.

However, when cultured *in vitro*, MSCs are not subjected to this dynamic environment. MSC are traditionally cultured on a flat two-dimensional surface, with a steady supply of nutrients and growth factors. As a result, MSCs in culture tend to undergo asymmetric divisions, typically referred to as spontaneous differentiation. These daughter cells usually form a fibroblast-like cell, which over time deplete the stem cell population (Banfi and Muraglia *et al.*, 2000., Muraglia and Cancedda *et al.*, 2000., Siddappa and Licht *et al.*, 2007). Due to this loss of potency, the clinical potential of MSCs is

dependant on low passage numbers (Sherley, 2002.,Siddappa and Licht *et al.*, 2007.,Sarugaser and Hanoun *et al.*, 2009).

1.4.3 Artificial Control of MSC Differentiation

As mentioned previously, MSCs can respond to their environment through interactions with the extracellular matrix and signalling molecules. However MSCs can be artificially induced to differentiate by mimicking the properties of the extracellular matrix or by inducing chemical or small molecule signals.

1.4.3.1 Chemical induction

Dexamethasone (Dex) is a synthetic glucocorticoid that induces osteogenesis in MSCs. Although the pathway is still not fully understood several studies have linked Dex with regulation of hedgehog signalling (Siddappa and Licht *et al.*, 2007.,Rickard and Sullivan *et al.*, 1994). Other media supplements can stimulate adipogenesis with a combination of dexamethasone and indomethacin (Scott and Nguyen *et al.*, 2011) or chondrogenesis using GSK-3 (glycogen synthase kinase-3) inhibitors in MSCs (Eslaminejad and Karimi *et al.*, 2013).

1.4.3.2 Topographical induction

Cells, when cultured on surfaces, are capable of 'reading' topographies on surfaces just as they would identify and bind with extracellular matrix proteins. Controlling induction and differentiation by using specific topographical patterns is an exciting and rapidly advancing area of biomaterials. Authors Dalby *et al* (2007) found that disordered, nanoscale features (topographies) can alter MSC differentiation (Dalby and Gadegaard *et al.*, 2007.,). McMurray *et al* (2011) later demonstrated that these designed nanoscale topographies can maintain MSC self-renewal or produce osteoblast cells from MSCs (McMurray and Gadegaard *et al.*, 2011). Other groups demonstrated topographies improving cell adhesion, (Le Guehennec and Lopez-Heredia *et al.*, 2008.,Biggs and Richards *et al.*, 2009), gene expression(Gasiorowski

and Liliensiek *et al.*, 2010.,McNamara and McMurray *et al.*, 2010) and proliferation (Milner and Siedlecki, 2007).

1.4.4 Targeting MSC Differentiation by MiRNAs

As mentioned previously miRNAs regulate a plethora of metabolic and regulatory networks (Guo and Zhao *et al.*, 2011b.,Melton and Blelloch, 2010.,Sartipy and Olsson *et al.*, 2009.,Houbaviy and Murray *et al.*, 2003.,Dong and Yang *et al.*, 2012) These can be transiently altered to target MSCs to undergo differentiation or to maintain multipotency (Wu and Xie *et al.*, 2012.,Laine and Hentunen *et al.*, 2012.,Deng and Wu *et al.*, 2013.,Shi and Lu *et al.*, 2013.,van Wijnen and van de Peppel *et al.*, 2013)

Zeng *et al* (2013) found that under expressing mir-100 (a microRNA that regulates differentiation) induced an increase in osteogenesis, whereas overexpressing mir-100 significantly inhibited osteogenesis. Using dual luciferase reporter genes *in vitro* BMPR2 (bone morphogenic protein receptor 2), a protein kinase was found to interact with and be inactivated by mir-100. The mir-100 mimic and its inhibitor were transfected with Lipofectamine, into adipose derived MSCs (Zeng and Qu *et al.*, 2012). However, as mentioned with siRNA delivery, lipofectamine as a delivery agent tends to be cytotoxic and reduce the long term *viability* of the cells.

Deng *et al* 2013, furthered our understanding of the complexity between miRNAs and MSC differentiation (Deng and Wu *et al.*, 2013). They reported a regulatory mechanism whereby mir-31 (microRNA involved in proliferation and osteogenesis) expression inhibited osteogenesis through RUNX2 (an early time point osteogenic transcription factor) and SATB2. As MSC cultures grew and differentiated into bone they found a progressive decrease in mir-31 levels, with inhibition of mir-31 dramatically increasing alkaline phosphatase levels (a known bone protein marker, produced as a by-product of osteoblasts). Mir-31 overexpression was induced by the

introduction of plasmids encoded with the miRNA. Although plasmid vectors are highly effective delivery mechanisms the possibility of off-target effects, such as genome integration precludes this vector from clinical studies.

In the same year Suh *et al* (2013), attempted to promote osteoblastic differentiation by targeting mir-29b (an anti-apoptotic and osteogenic miRNA) (Suh and Lee *et al.*, 2013). Mir-29b was found to target anti-osteogenic factors and the authors hoped delivery of the miRNA into hMSCs would instigate bone formation. As with most RNA therapeutics, delivery was an issue, which the authors attempted to solve by creating a cell penetrating peptide that complexed with double-stranded miRNA using thiol bonds. Osteogenesis was confirmed with Alizarin red and osteocalcein staining.

MiRNA delivery to MSCs to maintain multipotency or induce a certain cell type is a very new, novel and dynamic frontier. The dosage of the miRNA, the duration of the dosage and the delivery vector are elements that need to be systematically investigated, to ensure we are developing successful and robust therapeutics for the clinic.

1.5 Project Outline and Aims

With regards to cell engineering, medical research advances in the last twenty years have focused on tissue engineering and materials science. However the advent of stem cell research and nanotechnology, in particular NPs, and the pace at which both research areas are moving, allows for the opening of new avenues in nanomedicine and therapeutics.

The mechanism of NP delivery is still an issue and there is still huge debate surrounding the potential toxicity of NPs *in vivo*. Delivery and release of the NPs cargo requires more optimisation, as there is significant difference between cell types, which affect the stability, and functionality of the cargo. Current research aims to resolve these issues and bring NP-mediated delivery of small molecules to the clinic.

This project concentrated on using AuNPs as a delivery platform for small regulatory RNAs into bone tissue. All AuNPs were designed and synthesised in collaboration with chemists in Zaragoza (Spain) and Lisbon (Portugal). Two different cell types were employed in the project; the human osteosarcoma cell line, MG63, and primary human mesenchymal stem cells. MG63s were chosen, as a cheap and easily cultured bone model.

Chapter 3, the first experimental chapter, concentrates on C-Myc silencing in cancer cells *via* siRNA functionalised AuNPs. There are contradictions in recent literature as to the benefits conferred by the passivating ligand, and how these benefits actually depend on the ligand density and arrangement on the NP surface. Therefore, the main aims of this chapter were to:

- Verify siRNA-AuNP delivery and uptake into MG63 cells
- Identify C-Myc silencing (indicative of successful delivery of functional siRNA)

- Compare two different passivating ligand (PEG) densities on C-Myc silencing.

Chapter 4 and chapter 5 moved focus to the artificial control of MSC differentiation *via* delivering miRNAs. Based on Cell Engineering lab data and a literature search, mir-31 was selected as a target in this regard, as it has been established that mir-31 is involved in osterix (osteogenic transcription factor) regulation. The AuNPs designed for this part of the project were functionalised with an antagomir sequence against mir-31 5' or a sequence against mir-31 3'. Whilst the delivery of miRNAs is a very recent field of study, there have been no studies to date that compare the possible difference in directionality of the miRNA used (i.e. whether 5' or 3'), therefore both sequences were used in both of these chapters.

Chapter 4 was a proof of concept study, and employed MG63 cells as an initial target. These cells are pre-osteoblastic cells, with relatively high levels of mir-31, and are therefore an excellent model to test the antagomir delivery. The main aims of this chapter were:

- Verify antagomir-AuNP delivery and uptake into MG63 cells.
- Assess osterix levels at the RNA and protein level (indicative of successful delivery).
- Identify any difference in potency between the 5' and 3' antagomir sequences.

Following the success of chapter 4, whereby osterix levels were altered with our antagomir-AuNPs, chapter 5 employed a more dynamic MSC population. Osterix is a major transcription factor in osteogenesis, therefore, any changes in osterix should lead to changes in stem cell phenotype. The main aims in this chapter were:

- Verify antagomir-AuNP delivery and uptake into MSC cells

- Assess osterix levels in MSCs (RNA and protein level)
- Assess long term (3 and 5 week) MSC phenotype following antagomir treatment (i.e. osteogenic differentiation).

The ability to guide osteogenesis of MSCs into osteoblasts, is a major goal for regenerative medicine and offers exciting avenues for the treatment of diseases such as osteoporosis.

2 Chapter 2: Materials and Methods

2.1 Materials

2.1.1 Antibodies

Primary Antibodies

- Anti-C-Myc antibody [9E10] **Abcam, UK**

Mouse ChIP Grade (ab32)

Used for In-Cell Westerns 1:2000

- Anti-GAPDH antibody **Abcam, UK**

Rabbit Monoclonal antibody (clone EPR6256)

Used for In-Cell Westerns 1:2000

- Amersham Monoclonal **GE Healthcare,
UK (GE)**

anti-Bromodeoxyuridine (clone BU-1) (murine)

Used to detect BrdU at 1:100

- Anti-Osterix (SP7, OSX) Antibody **Abcam, UK**

Rabbit polyclonal (ab22552)

Used for In-Cell Westerns 1:2000

- Anti-Osteocalcin (OCN) (sc-73464) **Santa Cruz
Biotechnology,
USA
(Santa Cruz)**

Used for Immunofluorescence 1:50

- Actin conjugated with Oregon Green

**Life
Technologies,
UK (Life Tech)**

Used for Immunofluorescence 1:1000

Secondary Antibodies

- Biotinylated anti-mouse

**Vector
Laboratories,Inc
UK (Vector)**

Used in BrdU assay at 1:50

- Texas Red anti-mouse

Vector

Used for Immunofluorescence assay at 1:50

- Donkey anti-Mouse IR Dye 680

Li-cor, UK

Used in In-Cell Western (C-Myv and GAPDH) at 1:2000

- Donkey anti-Rabbit IR Dye 800

Li-cor, UK

Used in In-Cell Western (C-Myc and GAPDH) at 1:2000

- Donkey anti-Rabbit IR Dye 680

Li-cor, UK

Used in In-Cell Western (C-Myc and GAPDH) at 1:2000

- Donkey anti-Mouse IR Dye 800 **Li-cor, UK**

Used in In-Cell Western (C-Myc and GAPDH) at 1:2000

- Cell Tag 700 **Li-cor, UK**

Used in In-Cell Western at 1:500

Tertiary Antibodies

- Streptavidin-FITC **Vector**

Used in BrdU assay at 1:50

2.1.2 Cell Culture

Trypsin **Sigma, UK**

Versine **(made in house)**

Fetal Bovine Serum (FBS) **Lonza, UK**

Needle (1.2mm x 40mm) **BD Microlance 3,
UK**

13mm glass coverslips **Chance Proper
LTD, UK**

Incubator (CO2 water jacketed incubator) **Forma Scientific,
UK**

Dulbeco's Modified Eagle Medium (DMEM) **Sigma, UK**

L-Glutamine 200mM (100x) liquid **Invitrogen, UK**

Sodium pyruvate	Life Tech
Penicillin streptomycin	Sigma, UK
MEM Non-Essential Amino Acids	Life Tech
Ficoll-Paque	GE
Opti-MEM® I Reduced Serum Media	Invitrogen, UK
Bone Marrow CD271+ Selected	Promocell, UK
Easy Sep CD271+	Stem Cell Technologies, UK
2.1.3 Electron Microscopy (EM)	
Thermanox coverslips	ThermoScientific , UK
Gluteraldehyde (25% aqua Pure, EM Grade)	Sigma, UK
Sodium cacodylate	Agar Scientific Ltd UK
Osmium tetroxide	Agar Scientific Ltd UK
Phosphate buffer	VWR International Ltd, UK (VWR)
Uranyl acetate	Agar Scientific Ltd UK

Propylene oxide	VWR
Resin (812 Kit E202)	TAAB Lab Equipment Ltd UK (TAAB)
Methanol	Sigma, UK
Reynolds lead citrate	Agar Scientific Ltd UK (Agar)
Alcohol increments (30-100% (dry))	AnalaR NORMAPUR, UK
Molecular sieve	Sigma, UK
Hexamethyl-disilazane	TAAB
Carbon coated grids	Agar
2.1.4 General Reagents	
5-Bromo-2'-deoxyridine (BrdU)	Calbiochem, UK
Dimethyl sulfoxide (DMSO)	Sigma, UK
Ethanol (absolute)	AnalaR NORMAPUR, UK
Lipofectamine 2000	Invitrogen, UK
LIVE/DEAD® Viability/Cytotoxicity kit	Invitrogen, UK
Methanol, analytical reagent grade	Fisher Scientific, UK

3-(4,5-Dimethylthiazol-2-yl)-2,5-diphenyltetrazolium bromide, a tetrazole (MTT)	Sigma, UK
Nitric acid (70%), analytical reagent grade	Fisher Scientific, UK
Hydrochloric acid, analytical reagent grade	Fisher Scientific, UK
Rhodamine phalloidin	Invitrogen Molecular Probes, UK
siRNA (C-MYC and nonsense) + miRNA	Thermo Scientific Dharmacon
Phosphate Buffer Solution(PBS) tablets	Sigma, UK
Sucrose	Fisher Scientific, UK
Sodium Chloride (NaCl)	AnalaR NORMAPUR, UK
Magnesium Chloride hexahydrate (MgCl ₂)	AnalaR NORMAPUR, UK
Hepes	Fisher Scientific, UK
Triton® X-100	Sigma, UK
Formaldehyde (40%)	Fisher Scientific, UK

Bovine serum albumin (BSA)	Sigma, UK
Tween® 20	Sigma, UK
Sodium deoxycholate	Sigma, UK
Sodium Dodecyl Sulphate (SDS)	BDH, UK
Protease inhibitor (10X)	Roche, UK
Phosphatase inhibitor (10X)	Roche, UK
β -mercaptoethanol	BDH, UK
Powdered milk (dried, skimmed)	Marvel, UK
Glycine	BDH, UK
Potassium Chloride (KCl)	BDH, UK
D-Glucose	Fisher Scientific, UK
Ethylenediaminetetraacetic acid (EDTA)	Sigma, UK
Phenol red	Sigma, UK
Sodium Hydroxide (NaOH) (powder)	Fisher Scientific

2.1.5 Microscopes

Axiovert 25 light microscope	Zeiss, UK
Axiophot fluorescence microscope	Zeiss, UK
Leitz DMRB fluorescence microscope	Leica, UK

LSM 510 META confocal microscope **Zeiss, UK**

Leo 912 AB TEM **Zeiss, UK**

Tecnai T20 **FEI, USA**

Jeol 6400 SEM **Jeol Ltd, UK**

2.1.6 Quantitative Real-Time PCR (qRT-PCR)

RNeasy® Micro kit **Qiagen, UK**

QuantiTect® Reverse Transcription kit **Qiagen, UK**

Taqman® master mix **Applied
Biosystems, UK**

Primers and Probes **Eurofins MWG
Operon, UK**

Abi Prism 96-well plates **Applied
Biosystems, UK**

Real-time PCR, 7500 System **Applied
Biosystems, UK**

2.1.7 Scientific Instruments

Inductively Coupled Plasma Mass Spectroscopy (ICP-MS) **THERMO
X Series II, UK**

NanoDrop-1000 V3.7.1 **Thermo
Scientific, UK**

Plate reader (Ch.3) **Dynatech
MR7000, UK**

Plate reader (Ch.4 & 5)

**FLUOstar
Omega, BMG
Labtech, UK**

Vortex

**Fisions
Whirlimixer, UK**

Zetasizer

Malvern, UK

Odessey SA

Li-cor, UK

2.2 General Solutions

PBS

1 x PBS tablet dissolved in 200ml H₂O

Permeabilising buffer

100ml PBS; 10.3g sucrose; 0.292g NaCl; 0.06g MgCl₂ (hexahydrae);
0.476g Hepes.

pH adjusted to 7.2, followed by the addition of 0.5ml Triton X.

Fixative

90ml PBS; 10ml (38%) formaldehyde; 2g sucrose.

PBS/BSA

100ml PBS, 1g BSA.

PBS/Tween

100ml PBS; 0.5ml Tween 20.

RIPA buffer

45ml H₂O; 150mM NaCl; 50mM TRIZMA® base; 0.5ml Triton 1% (t-Octyl phenoxy polyethoxy ethanol); 0.5g Sodium deoxycholate 1%; 0.05g SDS 1% (Sodium Dodecyl Sulphate).

Make up to 50ml with water (H₂O).

Protein Extraction Buffer (PEB)

1ml RIPA buffer; 100µl Protease inhibitor (10X stock); 100µl Phosphatase inhibitor (10X stock).

Blocking buffer

50ml PBS-Tween; 1.5g Marvel milk.

Versine

1L H₂O; 8g NaCl; 0.4g KCl; 1g glucose; 2.38g HEPES; 0.2g EDTA; 2ml 0.5% phenol red.

Adjusted to pH 7.5 with 5M NaOH, dispensed into 20ml aliquots and autoclaved. Stored at 4°C.

Electron Microscopy fixative (EM fixative)

1.5% glutaraldehyde in 0.1M sodium cacodylate

2.3 Cell Culture

2.3.1 Human Cell Lines

Fibroblast:

- **MG63** Osteosarcoma **Sigma, UK**
- **MCF-7** Breast Cancer **Sigma, UK**

- **HeLa** Cervical Cancer

**Gifted by Prof.
Gwyn Gould**

2.3.2 Primary Culture

Human Osteoprogenitor Stem Cells:

- Human Mesenchymal Stem Cells
- Bone Marrow from patients (hip surgery)

Promocell, UK

Gifted by Mr

Dominic Meek

2.3.3 Media

MG63 cells were expanded in Dulbecco's Modified Eagle Medium (DMEM) supplemented with 10% FBS and 1% penicillin streptomycin.

All stem cells were expanded in Dulbecco's Modified Eagle Medium (DMEM+) supplemented with 10% FBS and 1% penicillin streptomycin, 1% 100mM Sodium Pyruvate and 1% Non Essential Amino Acids.

Cells were cultured in T75 flasks in complete medium and passaged by trypsinisation when 80-90% confluent. Cells were cultured at 37°C with 5% CO₂.

2.4 General Methods

2.4.1 Synthesis and Functionalization of Gold Nanoparticles.

All gold nanoparticles (AuNPs) were prepared and characterised by collaborators in Zaragoza (C-Myc studies) and Lisbon (antagomir studies).

2.4.1.1 Synthesis of citrate-gold nanoparticles

Gold Nanoparticle Synthesis. Gold nanoparticles (AuNPs), with an average diameter of 14.4 ± 2.0 nm, were synthesized by the citrate reduction method, as described previously. Briefly, 225 mL of 1 mM hydrogen tetrachloroaurate (III) hydrate (Sigma) (88.61 mg) dissolved in 500 ml of distilled water were heated to reflux while stirring. Then, 25 mL of 38.8 mM sodium citrate dihydrate (285 mg) were added and refluxed for additional 30 minutes with vigorous stirring and protected from light. The resulting red solution was cooled down and kept protected from light. Citrate capped AuNPs were characterized by transmission electron microscopy (TEM) and UV-Vis spectroscopy (Figure 2-1).

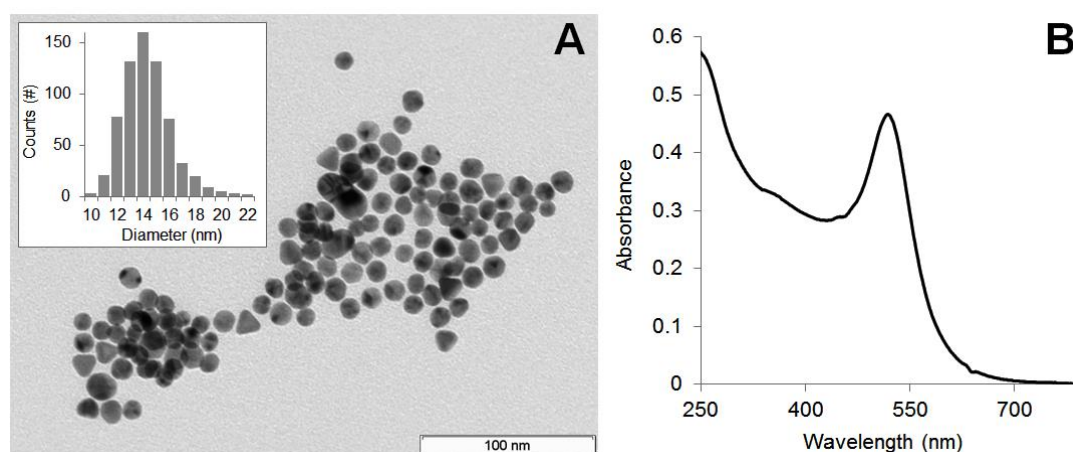


Figure 2-1. Gold nanoparticle characterization. (A) TEM image of citrate-gold nanoparticles (scale bar = 100 nm). Inset: size distribution histogram showing an average diameter of 14.4 ± 2.0 nm. (B) UV-Vis spectra of the synthesized gold nanoparticles with a characteristic surface plasmon resonance (SPR) peak at 519 nm. Provided by J. Conde (2015).

PEG Functionalization. Briefly, 10 nM of the AuNP solution were mixed with 0.003 mg/mL of a commercial hetero-functional poly (ethylene glycol) (PEG MW 2000) [O-(2-Mercaptoethyl)-O'-methyl-hexa (ethylene glycol), C₁₅H₃₂O₇S, 356.48 Da, Sigma] in an aqueous solution of SDS (0.028%). Then, NaOH was added to a final concentration of 25 mM and the mixture incubated for 16 hours at room temperature. Excess PEG was removed by centrifugation (21.460 ×g, 30 min, 4°C), and quantified by a modification of the Ellmans' Assay (Conde and Ambrosone et al., 2012). Briefly, Ellman's reagent (5,5'-dithiobis-(2-nitrobenzoic acid) quantifies the concentration of thiol bonds by being broken into 2-nitro-5-thiobenzoate (TNB⁻), which in the presence of water, forms the TNB²⁻ ion. This ion is yellow in colour and can be read on a spectrometer. The Ellman's method is a stoichiometric reaction, allowing for direct evaluation of the number of PEG molecules bound to the AuNP

The excess of thiolated chains in the supernatants is quantified by interpolating a calibration curve set by reacting 200 µL of stock solution of the O-(2-Mercaptoethyl)-O'-methyl-hexa (ethylene glycol) in 100 µL in phosphate buffer 0.5 M (pH 7) with 7 µL 5,5'-dithio-bis(2-nitrobenzoic) acid (DTNB, Sigma) 5 mg/mL in phosphate buffer 0.5 M (pH 7), and measuring the absorbance at 412 nm after 10 minutes. The linear range (see Figure 10 A-B) for the O-(2-Mercaptoethyl)-O'-methyl-hexa(ethylene glycol) chain obtained by this method is 0.0002-0.035 mg/mL ($Abs_{412} = 26.229 \times [HS-PEG, \text{mg/mL}] + 0.0671$). The number of exchanged chains is given by the difference between the amount determined by this assay and the initial amount incubated with the AuNPs. There is a point at which the nanoparticle becomes saturated with a thiolated layer and is not able to take up more thiolated chains - maximum coverage per gold nanoparticle, i.e. 0.01 mg/mL of O-(2-Mercaptoethyl)-O'-methyl-hexa (ethylene glycol) (Figure 10C). The AuNPs were functionalized with 0.003 mg/mL of O-(2-Mercaptoethyl)-O'-methyl-hexa (ethylene glycol) corresponding to 30% of PEG saturation of AuNPs' surface (200.16 ± 15.01 chains per nanoparticle).

Biotin was attached by EDC (1-ethyl-3-(3-dimethylaminopropyl)carbodiimide) (Sigma) and sulfo-NHS (sulfohydroxysuccinimide) (Sigma) chemistry at pH 6.1 (25 mM MES).

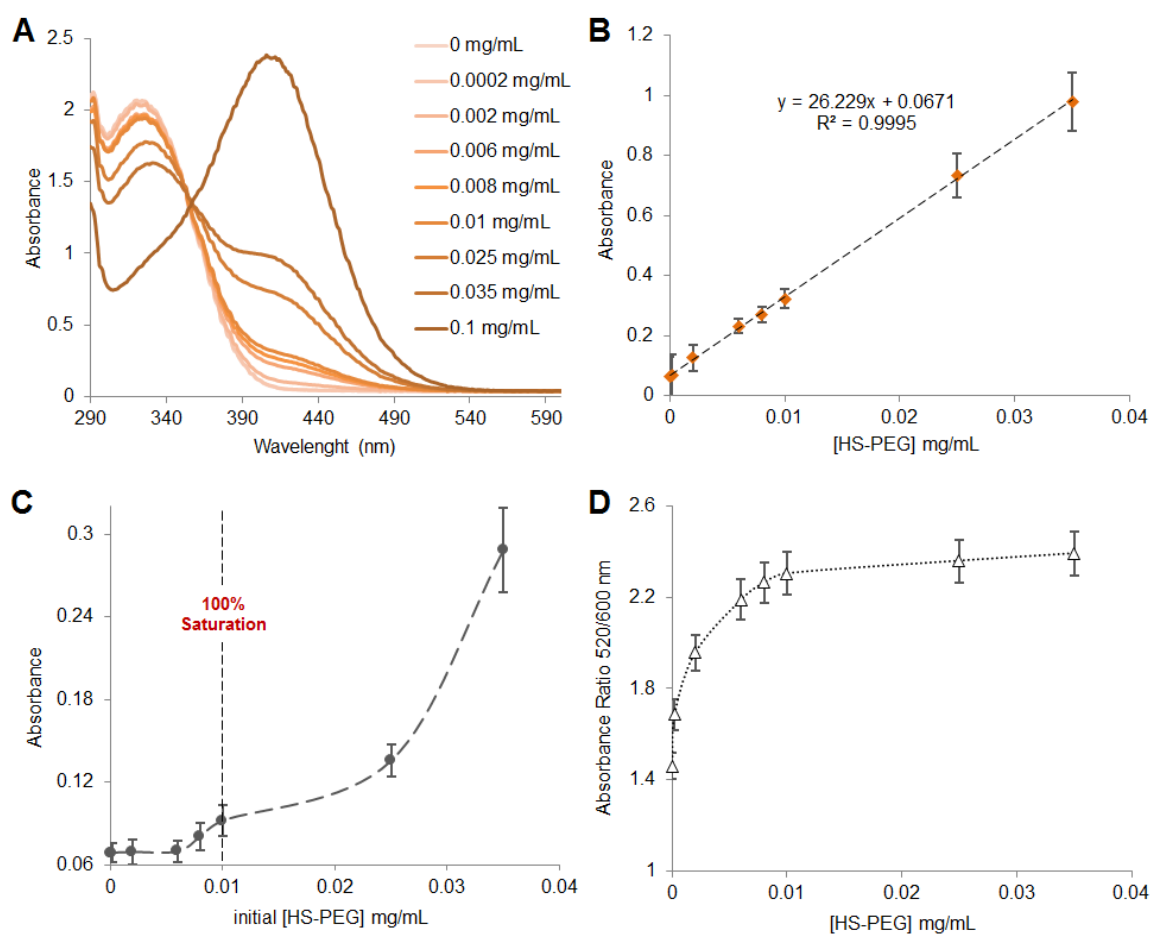


Figure 2-2. (A) Absorbance spectra of DTNB after reaction with the thiolated PEG. (B) Standard calibration curve for PEG chains, whose concentration can be calculated via the following equation $Abs_{412} = 26.229 \times [HS-PEG, \text{mg/mL}] + 0.0671$. (C) Variation of the excess of PEG thiolated chains as a function of the initial concentration in the incubation with 10 mM AuNPs. The dashed vertical line indicates the 100% saturation, i.e. the PEG concentration above which no more PEG can be bonded to the AuNPs surface. (D) Ratio between non-aggregated (at 520 nm) and aggregated NPs (at 600 nm) of AuNPs after functionalization with increasing amounts (0-0.035 mg/mL) of thiolated PEG. Provided by J. Conde (2015).

Finally, AuNP functionalisation with siRNA (Thermo Scientific Dharmacon) took place using thiolated siRNA incubated with NPs containing 0.028% SDS and 0.1 M NaCl. Excess siRNA was removed by centrifugation at 4°C. The siRNA quantification was carried out by fluorescence measurement (Perkin-Elmer LS55) using a GelRed (Biotium) acid nucleic intercalator.

2.4.1.2 NP Characterisation

A 2µl aliquot of each NP sample (0.1mg/ml in MilliQ H₂O) was dried onto a carbon-coated grid and viewed under the TEM at 120kV, at 40,000x magnification. In addition, NP size and charge were characterised by dynamic light scattering (DLS) and zeta potential respectively on a Malvern Zetasizer following manufacturers guidelines.

2.4.2 Toxicity Testing (MTT Assay)

MTT (3-(4,5-Dimethylthiazol-2-yl)-2,5-diphenyltetrazolium bromide) is a yellow tetrazole (550nm). The MTT assay is a colorimetric assay for measuring the activity of enzymes that reduce MTT to formazan dyes, producing a purple colour. The strength of this enzymatic activity and resulting purple colour is used to indicate cellular metabolic activity, viability, and indicate any cytotoxicity caused by a test substance, such as NPs. This technique is a quick and high throughput method to detect toxicity.

Cells were seeded at 1×10^4 cells per well in a 96 well plate and allowed to adhere overnight. AuNPs were diluted in appropriate cell media to a final working concentration per well and incubated with the cells for 1, 24 and 48 hours (control cells were incubated with media alone). After treatment incubation, cells were washed with warmed PBS; 100µl MTT solution was added per well (0.5mg/ml MTT powder in PBS) and cells were incubated for 1.5 h at 37°C. MTT solution was removed, and replaced with 100µl DMSO. Cells were left for 10 min at room

temperature and then the absorbance (Abs) was subsequently read via spectrophotometry at 550nm (Dyntech MR7000).

MTT data analysis: Percentage viability was calculated using the following equation: (Absorbance of NP-treated cells / Absorbance of control cells) x 100 = % viability) [n=3].

2.4.3 Uptake Analysis

2.4.3.1 Transmission Electron Microscopy (TEM)

TEM was used to observe the cells in cross section after NP treatment, to verify AuNP uptake into the cell body. Cells were seeded at 1×10^5 cells per well on Thermanox coverslips in a 24 well plate and allowed to adhere overnight. NP treatments were added to cells grown on coverslips at a stated concentration and incubated for 1, 24 or 48 hours (control cells were incubated with media alone). Following treatments, the cells were fixed in 1ml of 1.5% gluteraldehyde in sodium 0.1M cacodylate buffer at 4°C for 1 hour, then post fixed in 1% osmium tetroxide in phosphate buffer for 1 hour, followed by 0.5% uranyl acetate for 1 hour and then dehydrated through a series of alcohol increments (30 – 100%) and left in propylene oxide:Epon 812 resin araldite mix (1:1) overnight. At this point Margaret Mullen from the EM unit, continued the processing procedure. Samples were put into pure resin and kept in an oven for 24 hour to cure (at 60°C). Blocks were then cut into ultrathin sections, stained with 2% methanolic uranyl acetate and Reynolds lead citrate, and viewed under the TEM at 120kV for the LEO 912 (Chapter 3) and 200kV for the Tecnai T20 (Chapter 4 and 5).

2.4.3.2 Inductively Coupled Plasma Mass Spectrometry (ICP-MS)

ICP-MS, also known as element analysis, is a branch of mass spectrometry that can measure and quantify trace levels of a specified element. It is highly quantitative compared to microscopy. To facilitate this work, collaboration was set up with the chemistry department at

the University of the West of Scotland (UWS) in Paisley and Scottish Universities Environmental Research Centre (SUERC) in East Kilbride.

Cells were seeded at 1×10^4 in a 96 well plate and allowed to adhere overnight. Cell media was replaced with NP treatments the following day and the cells were cultured for a further 24 hours at 37°C in 5%CO₂. After incubation, the treatment media from each sample was removed and washed with sterile PBS, to remove extracellular AuNPs. Samples were treated 400 µl RIPA buffer, the lysate was put into a tube and a wash with 100 µl of sterile milliQ water was added to the wells and combined with the relevant tubes. To each tube 500 µl of milliQ water was added to get a volume of 1ml. To this, 1ml of AquaRegia was added (3:1 mix of HCL and 70% nitric acid) and then heated in a water bath at 70°C overnight. After heating, samples were cooled and then diluted to 50ml with H₂O (MilliQ H₂O used throughout). Samples were analysed by collaborators using ICP-MS at either the UWS or the SUERC.

2.4.4 Functional Assays

2.4.4.1 In-Cell Westerns (ICW)

Cells were seeded at 1×10^3 cells per well on a 96 well plate and allowed to adhere overnight. The AuNP treatments were added to coverslips at a stated concentration and incubated for a specified time (control cells were incubated with media alone). Cells were subsequently fixed in fixing buffer for 15 min at 37°C, and permeabilised for 5 min at room temperature. Non-specific binding sites were blocked by incubation with 1% (w/v) milk protein in PBS at 37°C for 1.5 hours. The PBS/milk Protein was removed and samples co-incubated with primary antibodies at 37°C for 1 hour. Free antibody was removed by washing three times in Tween/PBS (5 min/wash). Samples were co-incubated with Li-cor secondary antibodies, in PBS-1% milk protein and 0.2% Tween at 37°C for 1 hour, then washed three times in PBST (5 min/wash).

The plates were imaged by scanning simultaneously at 700 and 800 nm with an Odyssey SA at 100 μ m resolution, medium quality, focus offset of 3.53 mm, and an intensity setting of 7 for both 700- and 800-nm channels.

2.4.4.2 Fluidigm Analysis

Cells were seeded at 1×10^5 cells per well on glass coverslips in a 24 well plate and allowed to adhere overnight. The AuNP treatments were added to coverslips at a stated concentration and incubated for a specified time (control cells were incubated with media alone). After this, AuNPs were removed and RNA was extracted using an RNeasy Mini Kit. Reverse transcription was performed using a SuperScript III Reverse Transcriptase (Invitrogen). Each qRT-PCR reaction contained 10ng of cDNA. The cDNA was pre-amplified with a pool of selected 100 μ M forward and reverse primers. After pre-amplification the samples were then treated with Exonuclease I treatment, to clean up any unincorporated primers. After Exonuclease I treatment the amplified samples were diluted in TE buffer (TEKnova, PN T0224). The samples were prepared as two technical replicates for every three biological replicates. Samples were pre-mixed with 2xSsoFast Evagreen Supermix (Bio Rad, PN 172-5211) and 20x DNA binding dye sample loading reagent (Fluidigm, PN 100-3738). The stock primers, detailed in Table 2-1, were prepared separately, with 100 μ M of forward and reverse primers to a final concentration of 5 μ M in loading reagent. The plate was primed using an IFC controller MX and loaded with samples on one side and primers on the other. Afterwards the plate was run using the BioMark Fluidigm system. Data was obtained by Fluidigm Real-Time PCR Analysis Software. Heatmaps were produced using the software PermutMatrix v.1.9.3.

Table 2-1. Primer list used for fluidigm analysis, detailing the gene function and the forward and reverse sequences used. Those with * indicate housekeeping genes.

Primer	Function	Sequence (5' to 3')
β -Actin*	Housekeeping Gene	Forward GTGGGCCCGCCCTAGGCACCAG Reverse CACTTTGATGTCACGCACGATTTC
RUNX2	Transcription factor associated with osteoblast differentiation	Forward CAGCAGCAGCAACAGCAG Reverse GGCGATGATCTCCACCAT
ACVR1A	Binds BMPs to then form complexes with SMADs	Forward GCCAAGGGGACTGGTGTAAC Reverse GAGAATAATGAGGCCAACCTCCA
SMAD1	Mediates signals with BMPs by receptors	Forward GCTGCTCTCCAATGTTAACCG Reverse CACTAAGGCATTCGGCATAAC
SMAD2	Mediates signals with BMPs by receptors	Forward CCACGGTAGAAATGACAAGAAGG Reverse GATTACAATTGGGGCTCTGCAC
SMAD3	Mediates signals with BMPs by receptors	Forward GTCTGCGTGAATCCCTACCAC Reverse GGGATGGAATGGCTGTAGTCG
GNB2L1*	Receptor for activated C kinase 1	Forward TCCATACCTTGACCAGCTTG Reverse GCAGATTGTCTCTGGATCTC
SMAD4	Common mediator SMAD, enhances SMAD signaling	Forward GGGTCAACTCTCCAATGTCCAC Reverse GTCACTAAGGCACCTGACCC
SMAD5	Mediates signals with BMPs by receptors	Forward TGGGTCAAGATAATTCCCAGCCT Reverse GGCTCTTCATAGGCAACAGGC
SMAD6	Inhibitory SMAD, block R-SMAD activation	Forward CTCCCTACTCTCGGCTGTCT Reverse AGAATTCACCCGGAGCAGTG

SMAD7	Inhibitory SMAD, block R-SMAD activation	Forward CCATCACCTTAGCCGACTCT Reverse CCAGGGGCCAGATAATTCGT
SMAD9	Mediates signals with BMPs by receptors	Forward CTTATCATGCCACAGAAGCCTCT Reverse GTCCTCGTAACAAACTGGTCG
BMPR1A	Bone morphogenetic protein receptor, type IA (CD292)	Forward ACGCCGGACAATAGAATGTTGTC Reverse GAGCAAACCAGCCATCGAATG
TWY1*	Wyosine biosynthesis protein	Forward ATTGTCATCAAGACGCAGGGC Reverse GTTGCGAATCCCTTCGCTGTT
BMPR1B	Bone morphogenetic protein receptor type-1B (CDw293)	Forward GGTTCAGACTTCTGCTGATTCAT Reverse CGCAAAGCATGTTATCAAGG
BMP2-EL	Osteoinductive cytokine, linked to hedgehog pathway and TGF beta signaling	Forward CTTCTAGCGTTGCTGCTTCC Reverse AACTCGCTCAGGACCTCGT
BMP2-HW	Osteoinductive cytokine, linked to hedgehog pathway and TGF beta signaling	Forward AGACCTGTATCGCAGGCACT Reverse CCACTCGTTTCTGGTAGTTCTTCC
BMPR2	Serine/threonine receptor kinase that binds bone morphogenetic proteins	Forward AGCCTCTCACCCCACTCC Reverse GCAGAACAACCGTGAGAGG
ACVR1B	Binds ACVR2A or ACVR2B to recruit SMADS 2/3.	Forward GACATTGCCCGAATCAGAGG Reverse GCCCGAGGGCATAAATATCAGC
BMP4	BMP4 is found in early embryonic development	Forward CAGCACTGGTCTTGAGTATCCT Reverse AGCAGAGTTTTCACTGGTCCC
CYCR*	Bacterial housekeeping gene with adenylate cyclase activity	Forward ACTGCGGGAAGGTCTCTACTT Reverse GGGTGCCATCGTCAAACCTCTA

BMP7	Phosphorylates SMAD1 and SMAD5	Forward CAGGCCTGTAAGAAGCACGA Reverse TGGTTGGTGGCGTTCATGTA
BMP10	Involved in the trabeculation of the heart	Forward ACCCACCAGAGTACATGTTGG Reverse GCCCATTA AAACTGACCGGC
Nestin	A type VI intermediate filament, mainly a nerve stem cells marker	Forward GCTCAGGTCCTGGAAGGTC Reverse AAGCTGAGGGAAGTCTTGGA
CD63	A transmembrane protein, signaling cell growth, development and motility	Forward CCCTTGG AATTGCTTTTGTT Reverse TATTCCACTCCCCCAGATGA
ALCAM	(CD166) A transmembrane glycoprotein, mediating adhesions	Forward TTCCAGTCCCTCTACTCAGAGC Reverse GCTAAGAAGGACTCGCAGGA
Osterix	A master regulatory transcription factor for osteogenesis	Forward TGGGCTCCCAACACTATTTTC Reverse GGGAAGACTGAAGCCTGGA
UBE2D2*	Ubiquitin-conjugating enzyme E2 D2	Forward CCATGGCTCTGAAGAGAATCC Reverse GATAGGGACTGTCATTTGGCC
RUNX1T1	A zinc finger transcription factor, that blocks hematopoietic differentiation	Forward ATCACAACAGAGAGGGCCAA Reverse CTGCAGGTTTCACTCGCTTT
SMURF1	E3 ubiquitin-protein ligase regulates SMAD proteins	Forward ATGCAGTTCGTGGCCAGATA Reverse CAGGCCCGGAGTCTTCATAC
SMURF2	E3 ubiquitin-protein ligase regulates SMAD proteins	Forward GACAGGATCCTCTCGAGTGC Reverse AGCTTTCATAGGGTGGAATGTCT
INHBA	Inhibin beta A, a differentiation factor	Forward AAGTCGGGGAGAACGGGTAT Reverse GGTCACTGCCTTCCTTGGA

ACVR2A	Forms a dimer to activate TGF-Beta pathway.	Forward ACCATGGCTAGAGGATTGGC Reverse GCCAACCCAAAGTCAGCAAT
ACVR2B	Forms a dimer to activate TGF-Beta pathway. Binds with a 3-4 higher affinity than ACVR2A	Forward CTGCAACGAACGCTTCACTC Reverse CAGGACGATGAGGGAAAGGC
RNF20*	E3 ubiquitin-protein ligase BRE1A	Forward GGTGTCTCTTCAACGGAGGAA Reverse TAGTGAGGCATCATCAGTGGC
TGFB1	Cytokine of the TGF-beta superfamily, that controls cell growth, differentiation and proliferation	Forward CGACTCGCCAGAGTGGTTATC Reverse GTTATCCCTGCTGTCACAGGAG
TGFBR1	The receptor for TGFB1, that transduces further signalling	Forward CGTTCGTGGTTCCGTGAGG Reverse TAATCTGACACCAACCAGAGCTG
TRAF6	Tumor necrosis factor receptor, transduces signaling for MAP3K pathways	Forward CGCACTAGAACGAGCAAGTGA Reverse GCCACACAGCAGTCACTTTCA
SNAIL2	Regulator of osteoblast differentiation	Forward TCCTTCCTGGTCAAGAAGCA Reverse GGTATGACAGGCATGGAGTA
Vimentin	A type III intermediate filament protein expressed in MSC	Forward GGAGAAATTGCAGGAGGAGA Reverse TGCGTTCAAGGTCAAGACGT
IL-08	Chemokine involved in immune response and angiogenesis	Forward GTGTGAAGGTGCAGTTTTGCC Reverse GTGGTCCACTCTCAATCACTC
B2M*	MHC class I molecule present on all nucleated cells	Forward TTGTCTTTCAGCAAGGACTGG Reverse ATGCGGCATCTTCAAACCTCC
CathepsinB	Marker for cell death and inflammation	Forward TGTGTATTCGGACTTCCTGC Reverse TTAAAGAAGCCATTGTCACCC

CathepsinD	A lysosomal aspartyl protease	Forward GGTGCTCAAGAACTACATGG Reverse ATTCTTCACGTAGGTGCTGG
CathepsinG	Protease found mainly in immuno cells	Forward AACAGATACACTCCGAGAGG Reverse ACGACTTTCCATAGGAGACG
CathepsinL	Lysosomal endopeptidase enzyme initiating protein degradation	Forward GACTCTGAGGAATCCTATCC Reverse CTTAGGGATGTCCACAAAGC
CathepsinS	lysosomal cysteine protease	Forward GCGTCATCCTTCTTTCTTCC Reverse CCAGCTGTTTTTCACAAGCC
GAPDH*	Enzyme catalyzing a step of the glycolysis pathway	Forward TCAAGGCTGAGAACGGGAA Reverse TGGGTGGCAGTGATGGCA

2.4.4.3 Brdu Analysis via Fluorescence

Cells were seeded for 24 hours at 1×10^5 cells per ml in DMEM, AuNPs were incubated for 42 hours. After this time 1mM, Brdu solution in DMEM was added and left for 6 hours. Media was removed and washed in PBS, Cells were fixed in fixative for 15 min at 37°C, and permeabilised for 5 minutes at room temperature. Non-specific binding sites were blocked by incubation with 1% (w/v) milk protein in PBS at 37°C for 1.5 hours. The BrdU primary antibody (1:100 cell proliferation kit RPN20,) diluted in DNase I, was added for 2.5 hours at 37°C. Samples were subsequently washed 3 times (5 min/wash in PBS-Tween) before incubating with anti-mouse Texas red secondary antibody (1:50) for 1 hour at 37°C, before co-staining with DAPI loaded mounting media (Vector Laboratories). All images were view under a Zeiss Axiophot fluorescence microscope.

2.4.5 Osteocalcin Nodule Formation via Fluorescence

The hMSCs (from Promocell) were seeded for 24 hours at 1×10^3 cells per cm^2 in DMEM+ on glass cover slips. AuNPs were added to cultures at 50nM, and left for 3 and 5 weeks. Media was changed every 3 days. Cells were fixed for 15 minutes at 37°C, and permeabilised for 5 min at room temperature. Non-specific binding sites were blocked by incubation with 1% (w/v) milk protein in PBS at 37°C for 1.5 hours. The osteocalcin primary antibody (1:50) was added for 1 hour at 37°C, simultaneously with Oregon green phalloidin (1:1000) for F-actin staining, before incubating with anti-mouse Texas red secondary antibody (1:50) for 1 hour at 37°C, before mounting with DAPI loaded mounting media (Vector Laboratories). All images were viewed under a Zeiss Axiophot fluorescence microscope.

3 Chapter 3: Gold Nanoparticle-mediated Knockdown of C-Myc in the Osteosarcoma Cell Line MG63 via siRNA

3.1 Introduction

siRNA are double stranded RNA's approximately 20-25 nucleotides long and are key components, involved in the RNA interference (RNAi) pathway (Chiu and Rana, 2003). They bind specifically and with complete complementarity to a target sequence. This complementarity forms a tightly bound unit that halts RNA expression by preventing access to the RISC complex (see section 1.2.2.1). This form of silencing offers a robust and attractive method of gene therapy (Whitehead and Langer et al., 2009b).

Our fundamental knowledge of siRNAs and their effect on cell phenotypes and disease remediation has been exponentially increasing in the last decade. However this breadth of information has not been translated into the clinic, mainly due to technical limits of therapeutic delivery. As described in chapter 1, the successful delivery of active siRNA involve four keys steps; (i) cellular localisation and binding, (ii) cell internalisation, (iii) subcellular trafficking and endosomal escape and (iv) release of functional siRNA, capable of interaction with the RISC complex (containing the cells machinery for silencing to progress) (Grigsby and Leong, 2010). Resolving the outlined issues will require the design of a multifunctional delivery vehicle and NPs have been postulated as meeting these challenging conditions. In this study we focus on the use of AuNPs, which have become very popular within biomedicine due to their unique physical and chemical properties as outlined in the introduction (Lévy and Shaheen *et al.*, 2010). AuNPs are bio inert with the added benefit of being easily synthesized and stable, allowing precise control of size and shape, with a multitude of ligands to choose from (Lévy and Shaheen *et al.*, 2010).

Derfus *et al* (2009) concluded that one single siRNA molecule per particle conjugated with cell penetrating peptides >15 produced optimal silencing conditions(Derfus and Chen et al., 2007). However, whilst ligand-based NPs are championed as holding great potential in future

cancer diagnosis and therapy, to date they deliver inconsistent results. One of the major factors contributing towards this is thought to be the differences in PEG density and conformation coating the NPs (Stefanick and Ashley *et al.*, 2013).

As described in the introduction (section 1.1.2.1), polyethylene glycol (PEG) has been successfully used to passivate AuNPs due to it being inherently protein repulsive. PEG can be used at various molecular weights that in turn can influence the conformational arrangement of the PEG on the surface of the AuNP. A high molecular weight produces long thin chains that fold back on themselves forming mushroom-like structures. However these are unordered and can sterically hinder a release of additional ligands, such as therapeutics. Shorter PEG molecular weight molecules maintain a linear conformation, which confer stability under physiological conditions (Stefanick and Ashley *et al.*, 2013). It is noted that the innate ability of PEG to repel protein adsorption does not depend on the chemical method of attachment, be it ionic or covalent (Karakoti and Das *et al.*, 2011).

As alluded to earlier, intracellular release of a functional therapeutic such as siRNA from the AuNP surface is a critical consideration when designing a delivery vector. Functional attachments are made to the gold surface with the aid of a thiol bond, and it's the exploitation of the thiol bond that allows for the efficient disassociation and release of the NP therapeutic (Oishi and Nakaogami *et al.*, 2001a). The thiol bond is cleaved by the intracellular antioxidant glutathione (GSH), located within the cytoplasm in the millimolar range, whilst in the extracellular space it is virtually absent (Lushchak, 2012).

Previous studies in our group have confirmed that AuNPs functionalised with siRNA were able to silence the cancer gene C-Myc in HeLa cells (Conde and Ambrosone *et al.*, 2012). PEG was used as a passivating ligand with these AuNPs, and it has been postulated in the literature that as well as the PEG length and presentation on NP surface, the PEG

ligand density also plays a role in NP uptake into cells, however to date this has not been studied. Therefore we designed AuNPs with two differing PEG densities, 40% and 25%, with a view to determining whether the ligand density would affect the silencing ability of the NPs. In addition, it is known that different cell types may have differing levels of intracellular GSH, thereby also affecting the silencing. Our previous studies employed HeLa cells, which have relatively high levels of GSH, so in this study we sought to test the robustness of the AuNP design by selecting a cancer cell line with a relatively low GSH concentrations.

3.2 Materials and Methods

3.2.1 Synthesis and Functionalisation of Gold Nanoparticles.

AuNPs with a diameter of 14nm were synthesised by our collaborators in Zaragoza by the citrate reduction method described by Turkevich and Frens and in chapter 2.4.1.1 (Frens, 1973.,Turkevich and Stevenson *et al.*, 1951.,Lee and Meisel, 1982). Subsequently, a mixture of AuNPs, 0.028% SDS, and HS-EG(8)-(CH₂)₂-COOH (Iris-Biotech) (MW 458 Da) and HS-(CH₂)₃-CONH-EG(6)-(CH₂)₂-N₃ (MW 452 Da) in a 1:1 ratio (7 and 10.5 μ M of each chain for 25% and 40% respectively) was combined under basic conditions for 16 hours.

AuNP functionalization with siRNA (Thermo Scientific Dharmacon) took place using thiolated siRNA previously reduced with dithiothreitol (DTT) incubated with AuNPs followed by the addition of 0.028% SDS and NaCl at a final concentration of 0.1 M (25% saturated AuNPs) or 0.3 M (40% saturated AuNPs). Excess siRNA was removed by centrifugation at 4°C. SiRNA quantification was carried out by fluorescence measurement of supernatants (Perkin-Elmer LS55) using GelRed (Biotium), an acid nucleic intercalator. The panel of four AuNPs employed in this study, with PEG chain densities, are detailed in Table 3-1 and Figure 3-1.

Table 3-1. The AuNPs used in this chapter with the corresponding PEG ligand densities and siRNA strands per nm². Please note that B denotes biotin and S denotes siRNA

	Nanoparticle Acronym	PEG Ligand Density (Chains per nm²)	siRNA Density (strands per nm²)
1	Au-B-25% PEG	~ 2.03	2.26×10^{-2}
2	Au-B-S-25% PEG	~ 2.03	2.26×10^{-2}
3	Au-B-40% PEG	~ 2.99	2.26×10^{-2}
4	Au-B-S-40% PEG	~ 2.99	2.26×10^{-2}

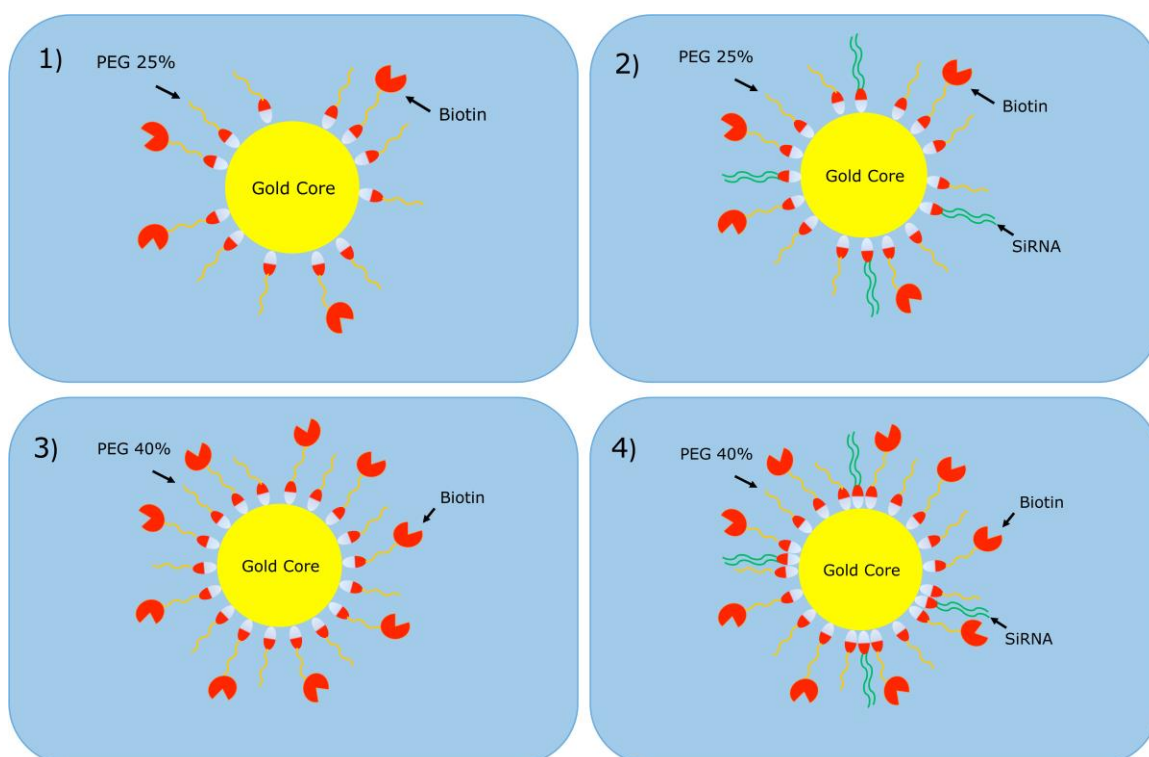


Figure 3-1 Panel of the four types of AuNP used: 1) Au-B-25% PEG, 2) Au-B-S-25% PEG, 3) Au-B-40% PEG, 4) Au-B-S-40% PEG.

3.2.2 Cell Culture

The human osteosarcoma cell line MG63, the human breast cancer cell line MCF-7 and HeLa cells were cultured in DMEM growth medium (10% FBS, 2 mM glutamine, 100 U/mL penicillin, and 100 µg/mL streptomycin) and maintained at 37°C in 5% CO₂ until ~90% confluent, after which time they were passaged and counted with a haemocytometer. The cells were seeded at a density of 1x10⁴ cells per ml for experiments unless stated otherwise. The cells were cultured for 24 hours before the addition of both the 25% and 40% PEG AuNP treatments at 2nM and 15nM. The concentrations of 2nM and 15nM were used throughout the experiments

3.2.3 Glutathione (GSH) Assay

The three cancer cell lines, MG63 (osteosarcoma), MCF-7 (breast cancer) and HeLa (cervical cancer), were assessed for their relative cytoplasmic levels of GSH. Cells were cultured and harvested (1x10⁶ cells were collected for each cell line) to determine cytoplasmic GSH levels. The cells were lysed by lysis buffer (GSH kit obtained from AbCam), incubated on ice for ten minutes and centrifuged at 13000g for ten minutes. A standard GSH curve was prepared alongside the samples. Monochlorobimane (McBeath and Pirone *et al.*), a dye that forms an adduct with GSH, was added to the well and the plate was left for 1 hour at 37°C. The fluorescence was measured on a plate reader with an EX/EM= 360/420 nm.

MG63 cells were deemed to have the lowest levels of GSH. With this in mind our aim for future studies was to test the robustness of siRNA release from AuNPs in a low level GSH cell type. Therefore MG63s were employed throughout the remainder of the study.

3.2.4 Nanoparticle Toxicity

The possible MG63 cytotoxicity response was assessed by standard MTT assay, as described in section 2.4.2.

3.2.5 Cellular Uptake of Gold Nanoparticles

3.2.5.1 Transmission Electron Microscopy (TEM)

MG63 cells were seeded at a density of 4×10^4 cells per mL onto Thermanox coverslips (13mm diameter) and cultured to develop a confluent monolayer of cells. At this point the AuNPs were added and cells further cultured for 24 hours. Cells were subsequently processed for TEM as described in chapter 2, section 2.4.3.1.

3.2.5.2 Inductively Coupled Plasma Mass Spectrometry

The MG63 cells were seeded (100 μ L/well) in a 96 well plate and incubated for 24 hours. AuNPs were added to cells for 48 hours and the cells were processed for ICP-MS as described in chapter 2, section 2.4.3.2. The converted values for gold uptake were averaged ($n=3$) and used for statistical analysis.

3.2.6 In Cell Western (ICW)

MG63 cells were seeded in a 96 well plate in triplicate, challenged with the AuNPs for 24 and 48 hours, then fixed, permeabilised and blocked as in chapter 2, section 2.4.4.1. Samples were then co-incubated with primary antibodies (1:10000 mouse anti-C-Myc, [9E10] - ChIP Grade (ab32), AbCam and 1:10000 rabbit anti-GAPDH, Epitomics) at 37°C for 1 hour. Following Tween washing, samples were subsequently co-incubated with secondary antibodies (1:10000 donkey anti-mouse IR680RD, Licor, UK and 1:10000 donkey anti-rabbit IR800CW, Licor, UK) at 37°C for 1 hour. All samples were finally washed three times in PBS/Tween (5 min/wash). The plates were imaged by scanning simultaneously at 700 and 800 nm with an Odyssey SA at 100 μ m resolution, medium quality, focus offset of 3.53 mm, and an intensity setting of 7 for both 700- and 800-nm channels.

3.2.7 Brdu Proliferation assay

MG63 cells were seeded onto 13 mm glass coverslips for 24 hours, and incubated with AuNPs for a further 42 hours. Cell proliferation was analysed via BrdU incorporation, as section 2.4.4.3. Cells were imaged using an Axiovert 200m fluorescence microscope (Carl Zeiss, Jena, Germany) equipped with ImagePro Plus Version 6.01 software (Media Cybernetics) and a sideport Evolution QEi Monochrome CCD camera (Media Cybernetics).

3.2.8 Statistics

Statistical analysis was performed in Graphpad using a one-way ANOVA with a Dunnett's test. In all figures * = $p < 0.05$, ** = $p < 0.01$, *** = $p < 0.001$ and **** = $p < 0.0001$. Two tailed T-Tests were performed where specifically mentioned, a welchs correction was used, # = $p < 0.05$, # # = $p < 0.01$

3.3 Results

3.3.1 Intracellular GSH Levels

The AuNPs were designed based on the established AuNP/GSH interaction within the cell cytoplasm, whereby GSH cleaves the thiol bonds that will in turn release the thiolated siRNA from the gold core. The levels of GSH in three established cancer cell lines were determined (Figure 3-2). MG63 cells were found to have relatively low GSH levels in comparison to both MCF-7 and HeLa cells, with HeLa approximately 4 times higher.

In previous studies we have demonstrated that C-Myc knockdown in HeLa cells using thiol exchange via GSH was achievable, therefore MG63 were selected to test the level of functionality we can achieve from our siRNA-AuNPs with a cancer cell line of known lower GSH concentration.

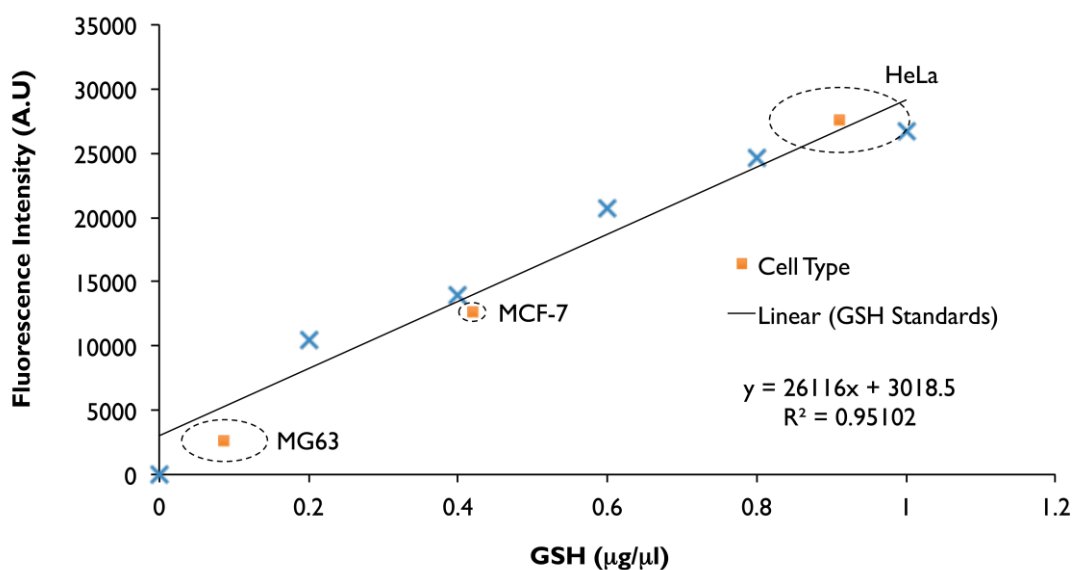


Figure 3-2. Glutathione (GSH) levels in MG63, MCF-7 and HeLa cancer cell lines. Cell number was normalised to 1×10^6 cells and values were plotted onto a GSH standard curve ($n=3$). Crosses indicate GSH standards, whilst the squares correspond to the cell type. Dashed areas around cell type indicate standard deviation. MTT Assay

The AuNPs were found to have no cytotoxicity over 24 hours incubation, as demonstrated with the MTT assay, showing no statistical difference between treatments (Figure 3 3).

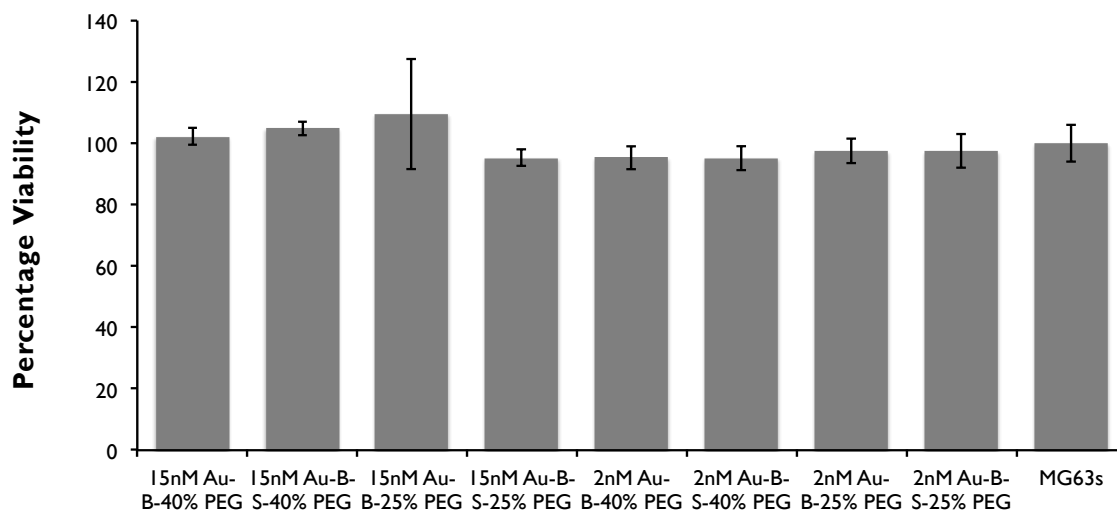


Figure 3-3. MTT analysis of MG63 cells treated with 15 nM and 2 nM of each AuNP, with 40% or 25% PEG coverage for 24 hours. (B = biotin; S = siRNA) (n=3; error bars indicate SD).

3.3.2 Cellular Uptake of AuNPs via TEM

AuNPs were initially screened for uptake using the biotin ligand attached to PEG on the AuNP, via streptavidin linked FITC (Supplemental figure 1, section 3.6 page 114)). However, this only provided images allowing confirmation of AuNP-cell interaction or attachment, to verify NP uptake had occurred, TEM was used with cross-sectional imaging.

At the lower 25% PEG saturation, the AuNPs were all distinctly located in the cell cytoplasm, as shown in Figure 3-4. The higher concentration (15nM) clearly demonstrated more tightly packed endosomes, reflecting the greater number of AuNPs present (Figure 3-4). The 40% PEG saturation proved similar, with AuNPs evident in the cell body (Figure 3-5). Therefore, after 24 hours incubation, NPs were clearly visible at both concentrations and both PEG densities within the cytoplasm, either free in the cytoplasm or packaged into endosomes.

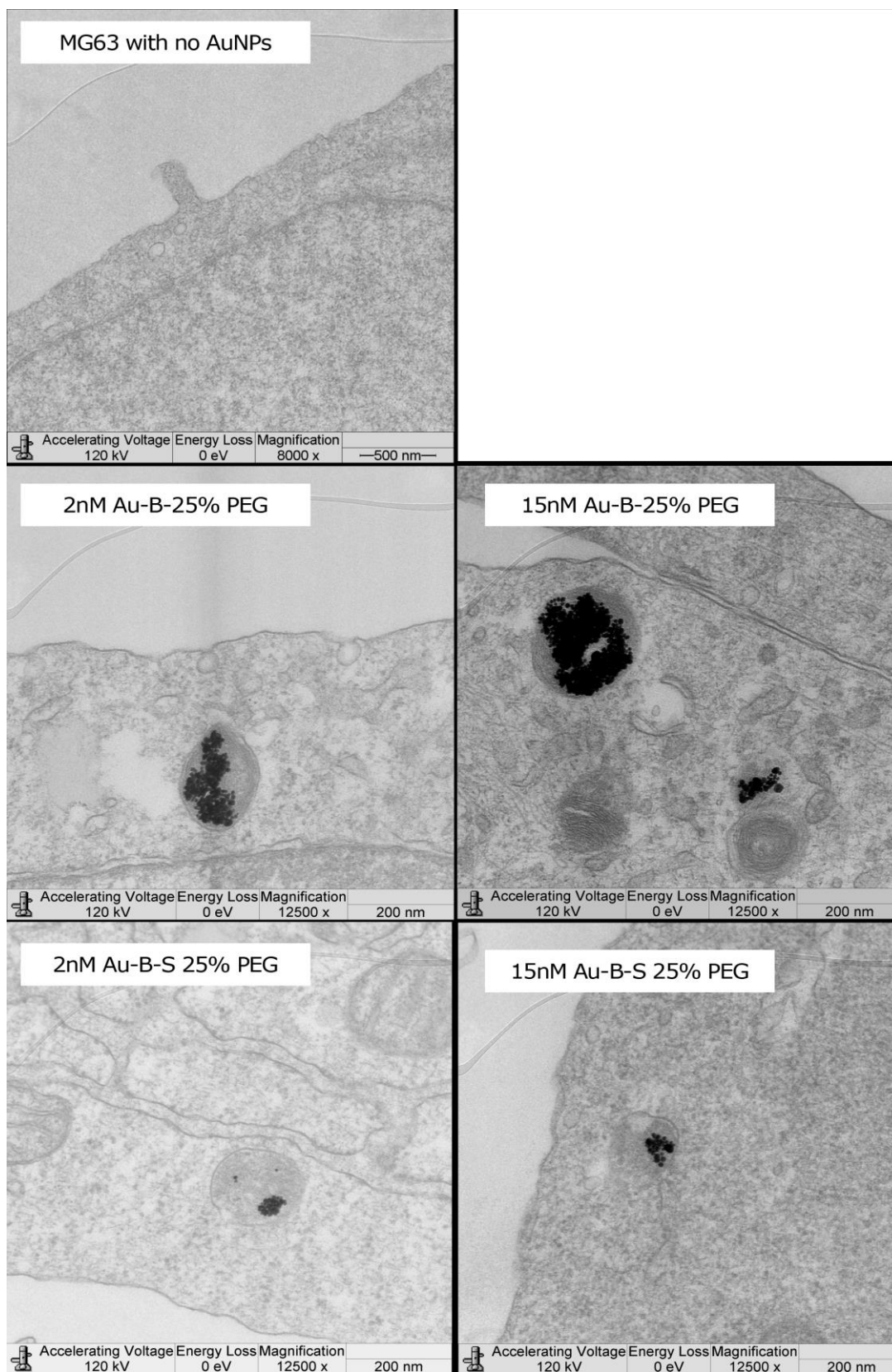


Figure 3-4. TEM images of MG63 cells treated with 15 nM and 2 nM AuNPs, with 25% PEG after 24-hour incubation. Clusters of the AuNPs are evident within the cell body. Scale bar = 1 μ m.

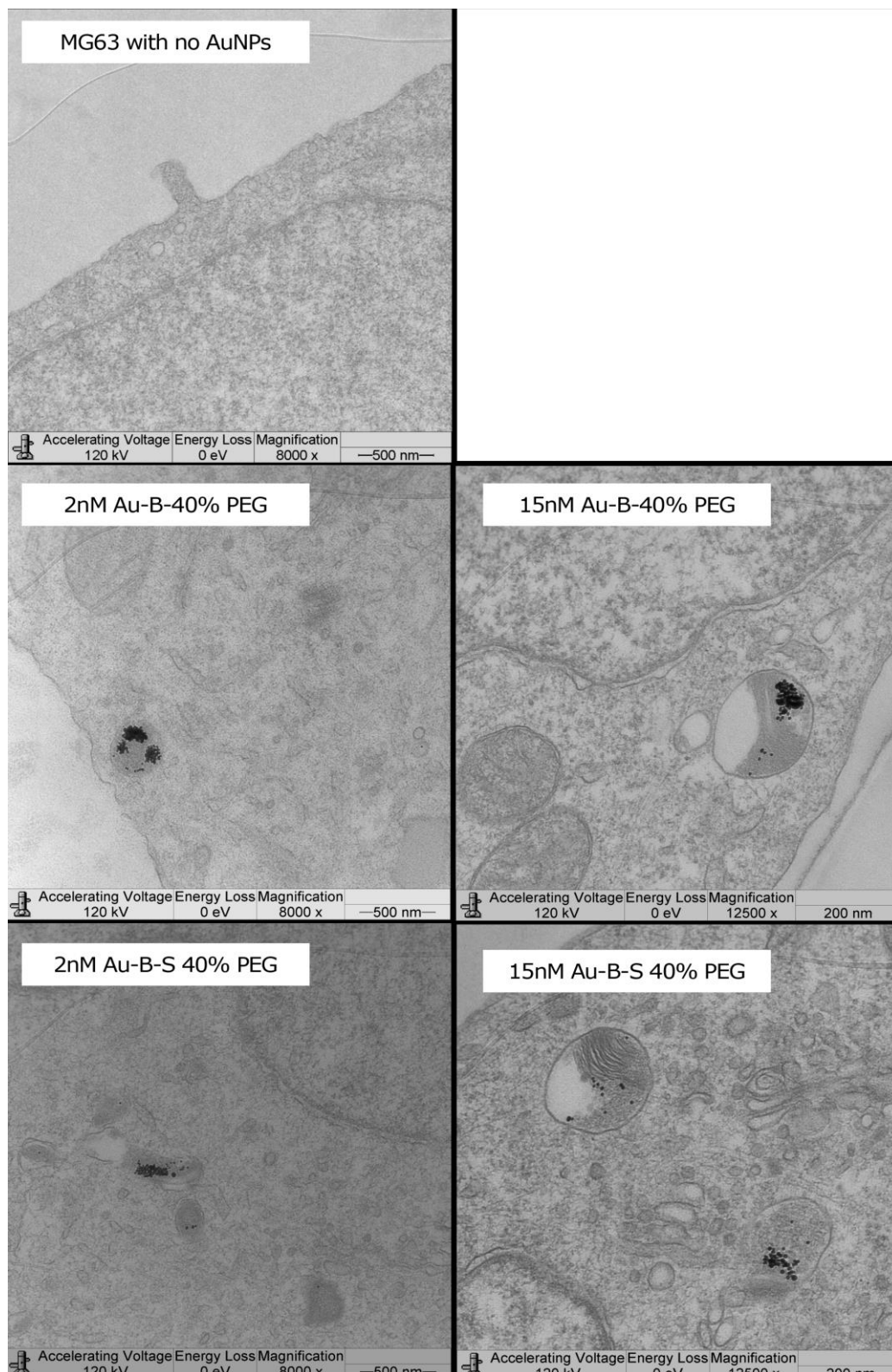


Figure 3-5. TEM images of MG63 cells treated with 15 nM and 2 nM AuNPs, with 40% PEG after 24-hour incubation. As with the 25%, clusters of the AuNPs are evident within the cell body.

3.3.3 ICP-MS

In parallel to qualifying AuNP uptake into cells, the amount of AuNPs within the cells was also quantified after 24 hours using ICP-MS to determine elemental gold levels in lysed cell samples (Figure 3 6). The AuNPs were clearly uptaken into the cells (ANOVA analysis $p < 0.0001$), with the higher concentration producing higher levels of internalised gold, verifying the methodology. Following an unpaired t-test, no significant difference was found between the different AuNP species with different PEG coverage.

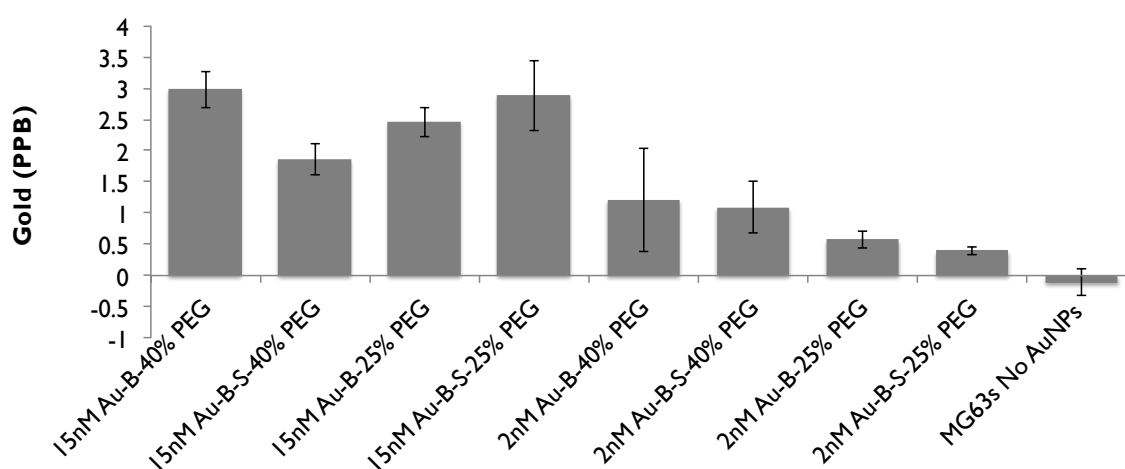


Figure 3-6. ICP-MS analysis of MG63 cells treated with 2nM and 15 nM of AuNPs, with 25% or 40% PEG coverage for 24 hours (each lysate has $n=3$, error bars denote SD). All values have been normalised to ultrapure water. ANOVA analysis comparing all treatments to MG63s without AuNPs, found a significant increase in elemental gold within cells treated with AuNPs $p < 0.0001$.

3.3.4 siRNA-mediated C-Myc Knockdown

Following verification and quantification of AuNP uptake into MG63 cells, the efficiency of siRNA-mediated C-Myc silencing was evaluated by ICW. The higher concentration of siRNA (15 nM) produced clear knockdown, at both PEG densities (40% and 25%), as indicated in the left side of the graph in Figure 3-7. The lower 25% PEG density also produced

strong down regulation of C-Myc protein, as indicated on the right side of the graph. The optimal silencing was achieved with a combination of both approaches, using the higher concentration (15 nM) and a lower PEG density (25%). There was also a significant reduction in C-Myc protein noted for one of the controls, Allstar nonsense siRNA with lipofectamine, however this may be due to the lipofectamine causing issues with cell viability.

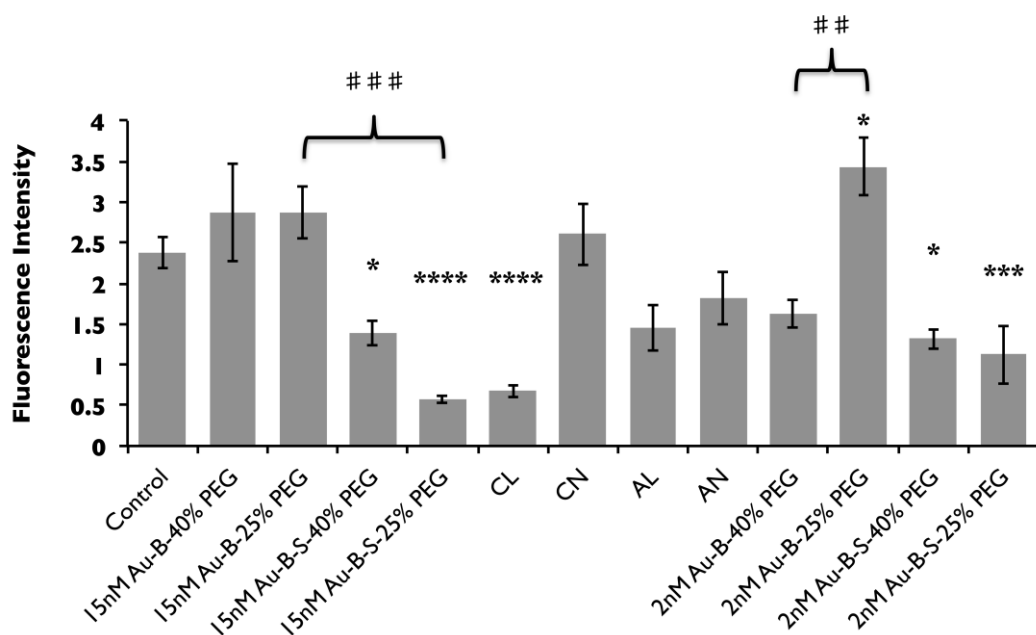


Figure 3-7. ICW data comparing C-Myc protein levels in MG63 cells with AuNP treatments, normalised to GAPDH. Cells were serum starved for 24 hours before treatment to synchronise cell division. The NPs were added at both 2nM and 15nM, with both 25% and 40% PEG coverage. The standard control reflects cells without AuNPs added, additional controls included lipofectamine treatment, C-Myc siRNA with lipofectamine (CL), Allstar nonsense siRNA with lipofectamine (AL), or C-Myc siRNA or Allstar siRNA added directly to the media (CN & AN) (n=6; error bars denote standard error, asterisk denotes significance based on Anova analysis, with a Dunnet post test normalising to control. Hash marks relate to an unpaired two tailed t-test, with a welchs correction ## = $p < 0.005$, ### = $p < 0.0005$).

3.3.5 BrdU Analysis

The synthetic nucleoside BrdU was used to analyse cells entering S-phase in the cell cycle, thus giving an indication of cell division in the sample population, allowing an estimation of cell proliferation rates. As shown in Figure 3-8, there were a higher proportion of cells in S-phase (red) in the standard control cells (no AuNPs) and cells treated with the additional control NPs (biotin & PEG only)., in contrast to the lack of cell division recorded in cells treated with the siRNA AuNPs (Figure 3-7). To quantify this, ten images were taken from each cell sample (n=3 samples). The proportion of cells in S-phase were determined using CellProfiler, which calculated the ratio of red (BrdU stained cells) to blue (nucleus) staining (Figure 3-9). Results demonstrated a significant decrease in cells entering S-phase when treated with siRNA at the higher concentration (15nM) at both densities (25% and 40%), but was only noted at the lower PEG density (25%) when tested at 2nM.

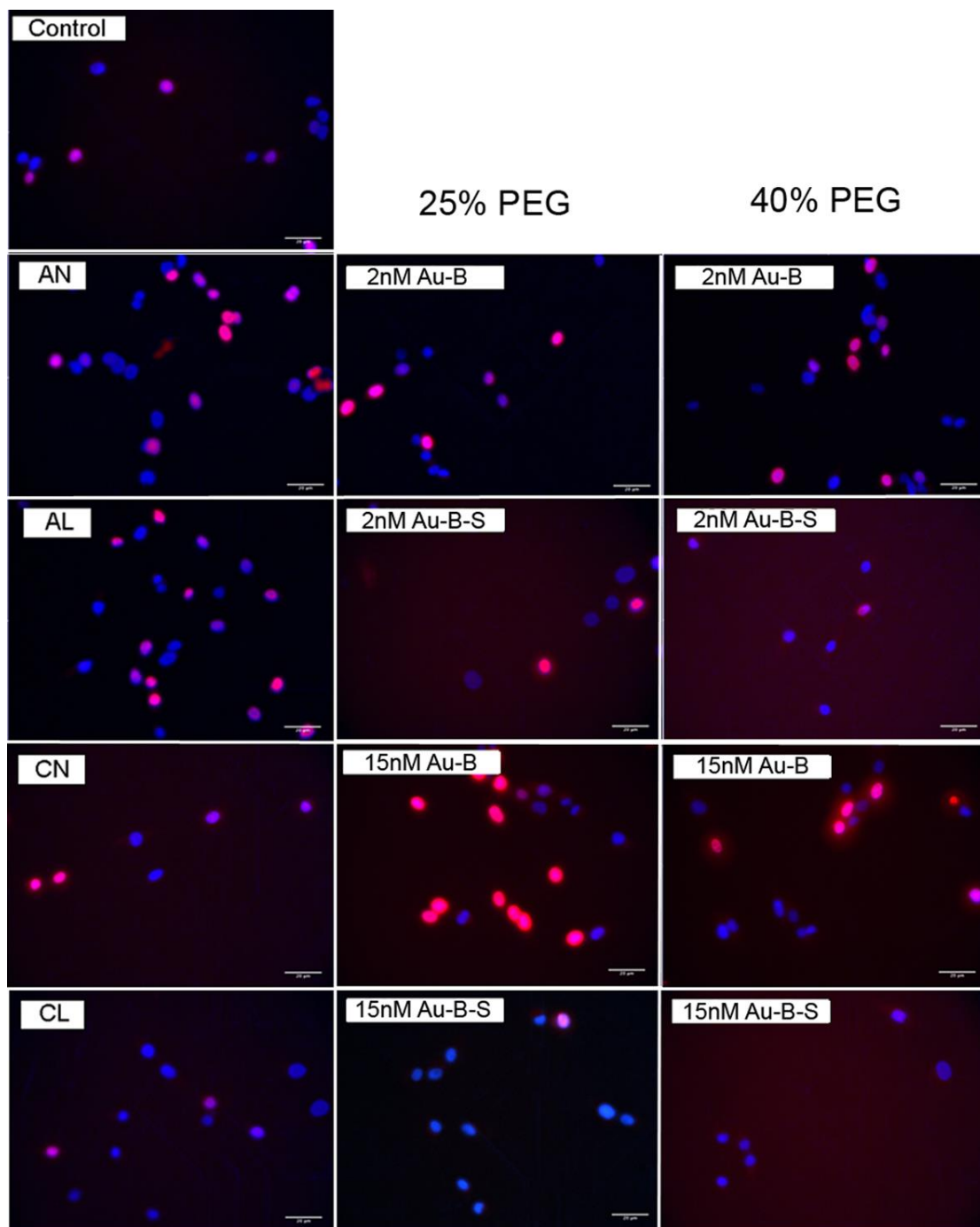


Figure 3-8. BrdU incorporation into cells treated with 2 nM and 15 nM of AuNPs, with either 40% or 25% PEG coverage for 48 hours. Cells were stained for nuclei (DAPI:blue) and actively dividing cells (BrdU:red). Additional controls included C-Myc with lipofectamine (CL), Allstar nonsense siRNA with lipofectamine (AL), or C-Myc and Allstar siRNA added directly to the media (CN & AN). Scale bar = 20 μm .

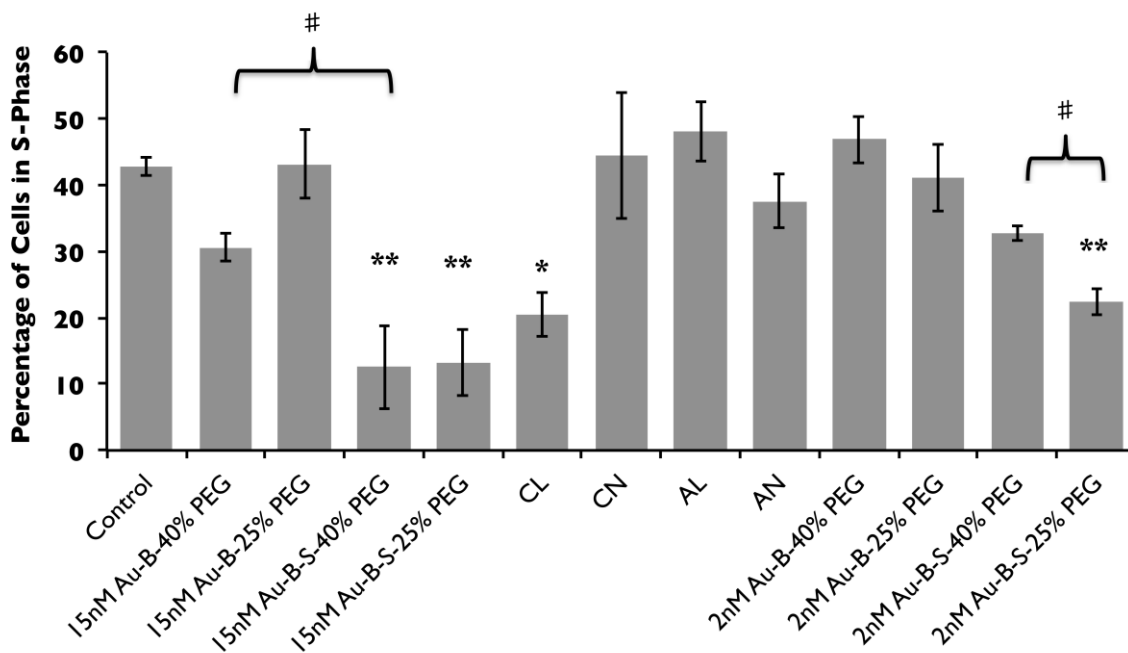


Figure 3-9. Graphical representation of the BrdU images as determined by CellProfiler, normalised to nuclei number, comparing the level of MG63 cells in S-phase with different treatments. Control cells are MG63s with AuNPs. CL= C-Myc siRNA with lipofectamine, CN= C-Myc siRNA only, AL= Allstar siRNA with lipofectamine, AN= Allstar siRNA only. Results from 10 images per sample, n=3 replicates, error bars denote standard error, asterisk denotes significance based on Anova analysis, with a Dunnet post test compared to control. Hash marks relate to an unpaired two tailed t-test, with a Welchs correction ($p < 0.05$).

3.4 Discussion

The use of intracellular GSH as a release mechanism has been capitalised upon to date with a view to thio-tethered ligand release from the surface of AuNPs. While there have been several recent studies into the influence of the PEG chain length and ligand release (Stefanick and Ashley *et al.*, 2013) the mixed reports on the effect of PEG density prompted this study; with a shorter chain length and higher density having been considered optimum for both ligand release and maintenance of the PEGylated NP stealth properties (Karakoti and Das *et al.*, 2011).

Previous work involving our group has shown that PEGylated AuNPs functionalized with siRNA against C-Myc can produce knockdown in HeLa cells (2 nM with a PEG ligand density of 25%) (Conde and Ambrosone *et al.*, 2012). This study was designed to assess both the potency of the AuNPs, by assessing the knockdown in a cancer cell line with a lower intracellular GSH level, and also the influence of PEG chain density on C-Myc knockdown. The NPs were PEGylated at both 25% and 40% saturation, and were used at two concentrations, 2 nM and 15 nM. Following cellular toxicity and AuNP uptake assessment, C-Myc knockdown was determined.

When investigating C-Myc knockdown at the protein level, the higher concentration (15 nM) achieved clear knockdown at both 25% and 40% PEG densities, with the lower 25% density achieving a significantly higher level of knockdown (Figure 3-7). Meanwhile, the lower concentration (2 nM) also achieved knockdown, but to a lesser extent. At the physiological level, however, when determining changes in cell proliferation, a comparable reduction was again noted for both higher concentration densities (ie. 15 nM at 40% and 25%), but with the lower concentration (2 nM) only the lower 25% PEG density indicated a reduction in proliferation. These results indicate that a variation in knockdown may be observed when adopting differing PEG saturation

densities, which may have consequences with regards to the therapeutic potential of siRNA.

GSH is an abundant thiol-cleaving antioxidant located within cells. During normal cellular processes GSH exists in two distinct forms, an oxidised (GSSG) and a reduced state (GSH). The oxidised form makes up <2% of total GSH levels (Meister and Anderson, 1983). GSH is used in many processes within the cells such as detoxification, removal of hydroperoxides and maintaining oxidation of protein sulfhydryls (Wu and Fang *et al.*, 2004., Lei, 2002., Fang and Yang *et al.*, 2002). Healthy cells tend to have GSH levels within 1-10 mM range, an order higher than the extracellular environment (Meister, 1988). Our AuNPs are designed with a view towards GSH interaction with the AuNP core, cleaving the thiol bound siRNA. In this study we have selected to use a cell type with a low concentration of intracellular GSH, to assess the robustness of our siRNA-NP delivery system. Despite this, C-Myc silencing was clearly observed in our MG63 cell line, indicating that the GSH concentration was perfectly sufficient to access and cleave the siRNA.

With our results we noted a difference in the potency of knockdown between siRNA concentrations, which cannot therefore be due to the low GSH concentration. Instead, we believe that increasing the PEG length, or in our case the PEG density, towards saturation can complicate access to the thiol (Stefanick and Ashley *et al.*, 2013), with greater ligand density or higher molecular weight polymers preventing GSH access to the core (Kah and Wong *et al.*, 2009). This is reflected in the results section 3.3.5, where a significantly better knockdown is recorded for the 15nM AuNPs at 25% density (as opposed to 40%), and also in section 3.3.6, where a significantly lower cell proliferation rate is noted for the 2nM AuNPs at 25%. Once released, the double stranded siRNA molecule is successfully loaded into the RISC complex. Within the RISC complex Ago2 cleaves the sense strand and dissociates it from the complex, where it will ultimately be degraded (Rana, 2007). The anti-

sense strand, which is complementary to the target mRNA, will remain bound to the RISC complex until it recognises the target sequence. Ago2 mediates the cleavage of the target mRNA ~10-11 nts upstream of the guide strands 5' end. After degradation the components of the RISC complex are recycled (Li and Rana, 2012).

As discussed in the introduction, the PEG chain length is known to influence the NP-cell interactions, however it is also well established that the PEG density on a NP surface can also affect the protein repelling capacity of the resultant NPs, and therefore influence the particles stealth properties (Unsworth and Sheardown *et al.*, 2005.,Knop and Hoogenboom *et al.*, 2010). The PEG density has also been identified as being key in determining cell uptake (Stefanick and Ashley *et al.*, 2013), although in this study, the AuNPs with 40% PEG coverage demonstrated marginally higher uptake levels to the 25% AuNPs (as demonstrated by ICP-MS results), and the TEM images indicated clear availability of the 40%-NPs in the cell cytoplasm. Thus, the 40% density did not appear to be hindering cellular uptake.

In summary, it is well established that ligand surface coverage, density and conformation on functionalized NPs is of critical importance to the success of the NP delivery system, however to date it is rarely reported. Until only very recently, data on ligand densities on AuNPs (in the 10-100 nm range) were seldom supplied (Hinterwirth and Kappel *et al.*, 2013). This may be due in part to the technical difficulties in determining such data, with X-ray crystallography and density functional theory studies being performed to derive theoretical considerations (Hakkinen, 2012). In this study, we surmise that the lower coverage of PEG potentially allowed greater access of the siRNA to the intracellular environment and the RISC complex, which was reflected in (i) the significantly higher C-Myc protein knockdown levels recorded with the 25% at 15 nM (Figure 3 6), and (ii) the reduction in cell proliferation observed with the 25% PEG at 2 nM whilst the 40% was similar to control levels (Figure 3-9). The most pronounced C-Myc

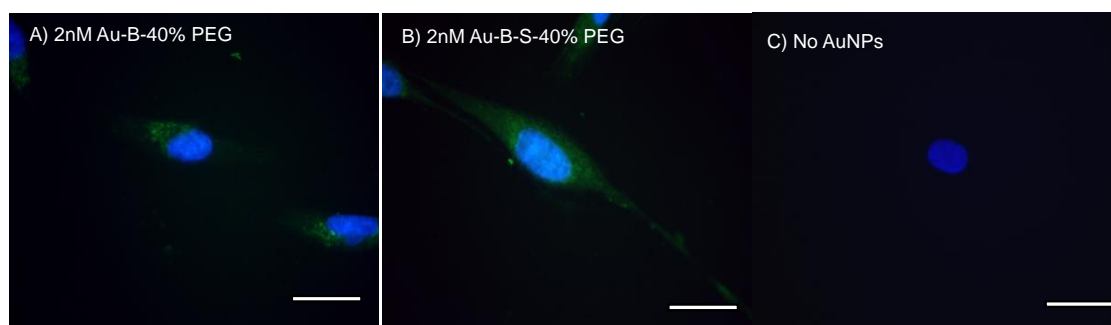
knockdown occurred using the increased concentration and the 25% PEG in tandem, producing better protein reduction than the positive control C-Myc Lipofectamine.

3.5 Conclusion

For siRNA to realise its therapeutic potential, it must be functional and freely available within the cell cytoplasm to interact with the RISC complex. When relying on a glutathione-based release strategy, this study highlights the importance of both particle design, in terms of passivating ligand densities such as PEG, and also intracellular glutathione levels, which differ between cell types. To tackle this, a multidisciplinary approach is strongly recommended, allowing a feedback loop between the cell biologists and synthesis chemists in order to redesign aspects of the NP, with a view to tailoring the particles for a specific cells and tissues.

3.6 Supplemental

Due to the expense of determining AuNP uptake via TEM, preliminary uptake studies were performed via fluorescence microscopy. Several AuNPs were selected to trial uptake in MG63s, after 24 hours incubation the cells were fixed and the particles were stained using streptavidin-FITC binding to the biotin attached to PEG on AuNP surface. The results indicated good uptake of the AuNPs into the cells, however, whether the NPs were internalised or merely attached onto the cell surface could not be determined by this method, thus uptake was measured qualitatively by TEM and quantitatively by ICP-MS.



Supplemental Figure 1. Fluorescent localisation of AuNPs, at 2nM, after 24-hour incubation. The green indicates the streptavidin-FITC binding to the biotin on the AuNPs (nucleus: blue). Scale bar = 5 μ m.

4 Chapter 4: Gold Nanoparticle-mediated Blocking of Mir-31 to Influence Osterix Expression in the Osteosarcoma Cell Line MG6

4.1 Introduction

MicroRNA's (miRNA) are single stranded RNA molecules approximately 20 nucleotides long, involved in the RNA interference (RNAi) pathway. MiRNA, unlike short interfering RNA (siRNA), do not innately bind with complete complementarity to targeted RNA sequences. This lack of complementarity allows miRNA to bind and halt the expression of a number of mRNA transcripts, thus offering an attractive mechanism for broad silencing of target genes.

Thompson *et al* (2006) performed the first global analysis of miRNA levels. Mature miRNAs were analysed and showed widespread post-transcriptional regulation of mRNAs (Thomson and Newman *et al.*, 2006). They have been shown to regulate a wide spectrum of biological processes from differentiation, (Bhushan and Grünhagen *et al.*, 2013.,Xie and Wang *et al.*, 2014) to tumorigenesis (Sun and Wang *et al.*, 2009b.,Liu and Li *et al.*, 2011b). Until lately, most miRNAs have been used diagnostically to identify cancerous cells in a number of tissues (Table 4-1). More recently, however, research is beginning to investigate miRNAs for their potential as therapeutic tools, with a view to influencing cell homeostasis and stem cell differentiation

Table 4-1 Specific miRNAs involved in different cancer types.

Cancer Tissue Types	Associated miRNAs with Cancer Cell Types	Reference
Bone	mir-31, mir-125b	Baglìo and DeVescovi <i>et al.</i> (2013) Liu and Li <i>et al.</i> (2011a)
Brain	mir-21, 221,181	Ciafre and Galardi <i>et al.</i> (2005)
Breast	mir-125b,145,21,155	Iorio and Ferracin <i>et al.</i> (2005)
Lymphatic	mir-15,16	Calin and Ferracin <i>et al.</i> (2005) Cimmino and Calin <i>et al.</i> (2005)
Colorectal	mir-143,145	Michael and SM <i>et al.</i> (2003)
Hepatocellular	mir-18,224,199,195,200,125	Murakami and Yasuda <i>et al.</i> (2006)
Lung	mir-17, mir-31	Zhong and Dong <i>et al.</i> (2013)
Mouth	mir-31	Chang and Kao <i>et al.</i> (2013)

Prostate	mir-31	Lin and Chiu <i>et al.</i> (2013)
Testicular	mir-372, 373	Voorhoeve and le Sage <i>et al.</i> (2006)
Thyroid	mir-221,222,146,181	He and Jazdzewski <i>et al.</i> (2005) Pallante and Visone <i>et al.</i> (2006)

MiRNAs are known to play a crucial role in bone formation and regulation (Lian and Stein *et al.*, 2012.,Ell and Kang, 2014). Bone tissue is made of several cell types, including osteogenic cells (stem cells); osteoblasts (form bone matix); osteocytes (maintain bone) and osteoclasts (resorb bone). Each different cell type has a miRNA profile, as detailed in Table 4-2. The osteogenic cells have sub-divisions of cell types, such as mesenchymal stem cells (MSCs) within the bone marrow, and pre-osteoblasts, which are cells that have begun to differentiate from MSCs and proliferate rapidly. As they proliferate, they mature into osteoblasts, reducing proliferation and creating layers of extracellular protein matrix. These cells can mature further into osteocytes, as they begin to mineralise and form functional ossified bone.

A final class of bone cell are osteoclasts, which are important for bone remodelling and are capable of digesting mineralised bone. Osteoclasts are slightly different, as they are generated from a hematopoietic stem cell (HSC; blood stem cells) cell maturing into a monocyte. The monocyte interacts with osteoblasts presenting the Receptor activator of nuclear factor kappa-B ligand (RANKI) protein. This protein-receptor interaction induces the monocyte to mature into an osteoclast (Lian and Stein *et al.*, 2012).

Table 4-2 Role of miRNAs in the different bone cell types. Adapted from Lain and Stein *et al*, 2012 and Baglio and DeVescovi *et al*, 2013.

Bone Cell Type	Role	miRNAs
MSCs	Proliferation and homeostasis	Mir-135, mir-138, mir-23a, mir-30c, mir-31, mir-196a, mir-204, mir-206, mir-335
Pre-osteoblast	Proliferation	Mir-23, mir-29, mir-34, mir-30, mir-31, mir-210, mir-218
Osteoblast	Matrix Maturation	Mir-125b, mir-138, mir-637, mir-29c
Osteocytes	Mineralization	Mir-23a~27a~24-2, mir-204, mir-205, mir-217, mir-133, mir-135
Osteoclast	Bone remodelling	Mir-155, mir-223, mir-21

Due to this wide range of regulation, miRNAs have recently become a potential target for future therapeutics. Mir-31 in particular has been linked to tumorigenesis, as mentioned in Table 4-1 (Zhong and Dong *et al.*, 2013., Hung and Tu *et al.*, 2014., Hua and Xiaotao *et al.*, 2012., Feng and Huang *et al.*, 2013., Chang and Kao *et al.*, 2013., Valastyan and Weinberg, 2011), angiogenesis (Liu and Cheng *et al.*, 2011) and Duchene muscular dystrophy (Cacchiarelli and Incitti *et al.*, 2011). More recently however mir-31 has been indicated to influence stem cell

osteogenesis by suppressing the master osteogenic transcription factor osterix (Baglìo and DeVescovi *et al.*, 2013.,Xie and Wang *et al.*, 2014.,Deng and Wu *et al.*, 2013.,Deng and Zhou *et al.*, 2013). A recent study by Baglìo *et al* (2013) introduced antagonists of mir-31 into the osteosarcoma cell line MG63s (pre-osteoblast), using linear sequences with a cholesterol attachment to aid cellular uptake, via the low density lipoprotein uptake pathway. Using quantities in the milimolar range, they demonstrated that by blocking mir-31, they increased the level of osterix in MG63s, and conversely, by increasing mir-31 they showed a reduction in osterix expression in SOAS-2 cells (a mature osteoblast cancer cell line). The authors concluded that osterix was a definite mir-31 target.

Another group in the same year linked mir-31 with the Runt-related transcription factor 2 (RUNX2) and Special AT-rich sequence-binding protein 2 (SATB2) regulatory network. The authors reported that mir-31 expression was progressively decreased in human bone marrow derived stem cells undergoing differentiation (Deng and Wu *et al.*, 2013). The authors used lipofectamine to transfect their cultures with mir-31, or mir-31 inhibitors. Increasing levels of mir-31 decreased SATB2 protein levels, however no notable changes were reported at the RNA level. The authors linked RUNX2, mir-31 and SATB2 together in a regulatory feedback system. By increasing RUNX2 levels (with transfected plasmids encoding RUNX2) they directly repressed mir-31. In addition, by overexpressing mir-31 they reduced osterix, osteocalcin, and osteopontin protein expression without effecting RUNX2 protein levels, suggesting that mir-31 can only target down stream targets of RUNX2. Using this collated evidence, I believe that mir-31 exists in a complex osteogenic pathway that represses several established factors (Figure 4-1).

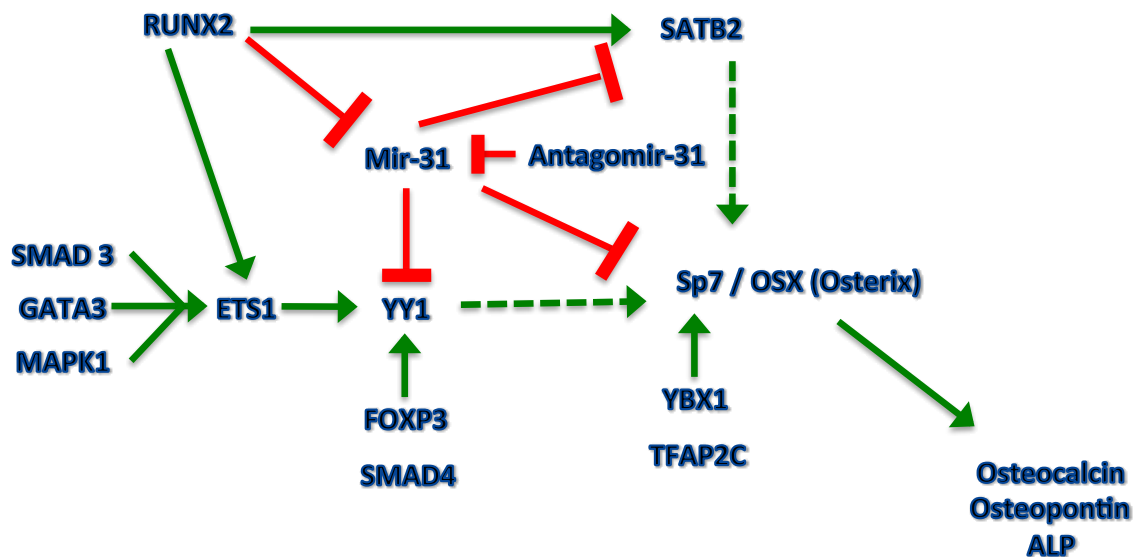


Figure 4-1. The interaction of mir-31 within an osteogenic pathway; green arrows indicate interacting factors, with a dashed line showing a simplified interaction, whilst red bars indicate an inhibitory effect (personal image).

The exploitation of miRNAs and their antagonists for widespread clinical treatment has to date been setback by technical problems, in particular their cellular delivery. In a manner similar to siRNA, miRNA and their antagomirs cannot enter cells easily and are rapidly degraded *in vivo*. It is important therefore that a delivery vector is used. As with the delivery of siRNA, the optimal delivery vector needs to, (i) target cells, (ii) cross the plasma membrane and (iii) release the functional miRNA/antagonist so that it can interact with the RISC complex (Grigsby and Leong, 2010). As described in section 1.2, AuNPs are excellent candidates, meeting all essential criteria. Therefore, this section of work focuses on the synthesis of AuNPs, which are designed with the aim to functionally inhibit mir-31 via antagomir sequences attached to the NP surface, and can bind to the mature mir-31 sequences by base-pair binding. The hypothesis therein being that such inhibition will lead to an increase in osterix expression.

This chapter aims to test this hypothesis using the osteosarcoma cell line MG63 (the same cell line used in chapter 3). Osteosarcoma cells are derived from malignant bone tumours. They share key osteoblastic

features, and are commonly used as osteoblastic models (Pautke and Schieker et al., 2004). The study aims to assess osterix levels in MG63 following treatment with antagomirs against mir-31 via AuNP delivery (Figure 4 1). A further facet to this study will be to identify any possible influence the antagomir sequence directionality has on function. To date, there have not been any specific studies addressing this issue, which is surprising given the possible differences in binding potency. Therefore, both the thiolated 5' and 3' sequences were conjugated onto the AuNP surface and tested independently.

4.2 Materials and Methods

4.2.1 Synthesis and Functionalisation of Gold Nanoparticles.

All AuNP synthesis and characterisation was carried out by our collaborators Professor Pedro Baptista and Dr. Joao Conde, based in Caparica, Portugal (section 2.4.1).

4.2.1.1 Assembly of Antagomirs to PEGylated gold nanoparticles

Four sets of NPs-Antagomirs were prepared using modified 2'-ACE (2'-bis(2-acetoxyethoxy)methyl) protected RNA oligonucleotides. 2'ACE is an orthoester group used to protect the 2'-OH of RNA monomers from degradation and can be used to store RNAs for extended periods prior to use. Three oligo sequences were synthesised as described in Table 4-3.

First, the RNA oligos were deprotected by adding 400 μ L of 2'-Deprotection buffer (100 mM acetic acid, adjusted to pH 3.8 with TEMED), dissolving the oligo completely by vortexing and centrifuge 10 seconds. Then, the oligos were incubated at 60°C for 30 minutes and SpeedVac to dryness before reduction and purification of thiol groups. Briefly, the thiolated RNA oligonucleotides were suspended in 1mL of 0.1M dithiothreitol (DTT), extracted three times with ethyl acetate and further purified through a desalting NAP-5 column (Pharmacia Biotech) using 10 mM phosphate buffer (pH 8) as eluent. Following oligonucleotide quantification via UV/Vis spectroscopy, each RNA oligonucleotide was added to the AuNP@PEG in a 100:1 ratio. AGE I solution (2% (w/v) SDS, 10 mM phosphate buffer (pH 8)) was added to the mixture to a final concentration of 10 mM phosphate buffer (pH 8), 0.01% (w/v) SDS, sonicated for 10 seconds using an ultrasound bath and incubated at room temperature for 20 minutes. Afterwards, the ionic strength of the solution was increased sequentially in 50 mM NaCl increments by adding the required volume of AGE II solution (1.5 M NaCl, 0.01% (w/v) SDS, 10 mM phosphate buffer (pH 8)) up to a final

concentration of 10 mM phosphate buffer (pH 8), 0.3 M NaCl, 0.01% (w/v) SDS. After each increment, the solution was sonicated for 10 seconds and incubated at room temperature for 20 minutes. The solution was allowed to rest for an additional 16 hours at room temperature. Then, the functionalized NPs-Antagomirs were centrifuged for 20 minutes at 21.460 $\times g$, the oily precipitate washed three times with DEPC-treated H₂O, and redispersed in the same buffer. The resulting NPs-Antagomirs, as listed in Table 4-4, were stored in the dark at 4 °C until further use.

Table 4-3. Oligomer sequences used for AuNPs-antagomir functionalization. GC % relates to the melting temperature, the greater the GC content the higher the melting temperature. Antagomir-31 5', is designed to bind with perfect complementarity to the corresponding mir-31 5' sequence. The same principle relates to antagomir-31 3', which binds with perfect complementarity to the mir-31 3' sequence.

Antagomirs	Sequences	GC %	Melting Temperature (°C)
antagomir non-targeting	S-S•GGAGAUUGGUUUUGACGUU UA	38	48.5
Antagomir-31 5'	S-S•AGCUAUGCCAGCAUCUUGCC U	52	54.4
antagomir-31 3'	S-S•AUGGCAAUAUGUUGGCAUA GCA	41	51.1

Physical characterization of the NPs-Antagomirs was performed by Dynamic Light Scattering (Zetasizer, Malvern), Zeta Potential

(Zetasizer, Malvern), UV/Vis Spectroscopy and Transmission Electron Microscopy (see Table 4-4 and Figure 4-2).

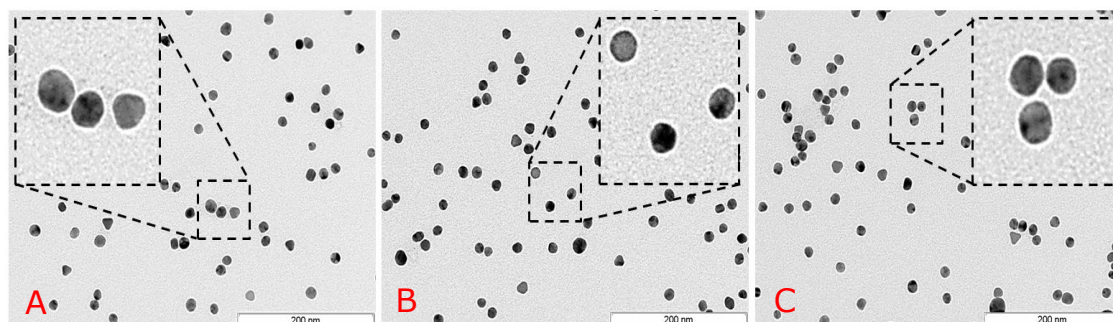


Figure 4-2. TEM image of antagomir-gold nanoparticles (scale bar = 200 nm). Panel A shows nonsense (NS)-AuNPs; B shows 5A-AuNPs, and C shows 3A-AuNPs.

In summary, the panel of four AuNPs employed in this study, with associated acronyms and PEG chain densities, is detailed in Table 4-4.

Table 4-4. Physical-chemical properties of the gold nanoparticles employed in this chapter. Please note that 5A denotes the 5' end of the antagonist sequence of mir-31, and 3A denotes the 3' end of the antagonist sequence of mir-31. NS is a nonsense strand used as a negative control. SPR corresponds to the AuNP surface plasmon resonance.

^a Determined by Dynamic Light Scattering (DLS).

^b Nanoparticles analysed at a concentration of 2 nM in water in a total volume of 1 mL, with 0.1 M KCl

NP Type	Acronym	SPR peak	Size (nm)^a	Zeta-Potential (mV)^b	PEG per NP	Antagomir (nM) per NP
	Uncoated NPs	519	14.4± 2.7	-19.2± 4.2	NA	NA
Au-30% PEG	PEG	521	18.5± 3.9	-25.2± 2.7	200.16 ± 15.01	NA
Au-NS-30% PEG	NS	523	39.75±1.2	-32.9± 1.4	200.16 ± 15.01	1123.81
Au-5A-30% PEG	5A	523	37.12±2.4	-34.3± 2.9	200.16 ± 15.01	965.35
Au-3A-30% PEG	3A	523	38.84±3.1	-32.3± 1.6	200.16 ± 15.01	1058.53

4.2.2 Cell Culture

The human osteosarcoma cell line MG63 was employed in this chapter, because of its innately high levels of mir-31. The cells were cultured in DMEM growth medium and maintained at 37°C in 5% CO₂ until ~90% confluent; after which time they were passaged and counted with a haemocytometer. The cells were seeded at a density of 1×10^4 cells per ml for experiments unless stated otherwise. The cells were cultured for 24 hours before the addition AuNPs treatments at 50nM of oligo.

4.2.3 Toxicity

MG63 cytotoxicity in response to the antagomir-AuNP treatments was assessed by standard MTT assay, as described in Chapter 2.4.2.

4.2.4 Cellular Uptake of Gold Nanoparticles

4.2.4.1 Transmission Electron Microscopy (TEM)

Cellular uptake of AuNPs was verified via TEM. MG63 cells were seeded at a density of 4×10^4 cells per mL onto Thermanox coverslips (13mm diameter) and cultured to develop a confluent monolayer of cells. At this point the AuNPs were added and cells further cultured for 24 hours. Cells were subsequently processed for TEM as described in chapter 2, section 2.4.3.1.

4.2.4.2 Inductively Coupled Plasma Mass Spectrometry (ICP-MS)

Cellular uptake of AuNPs was further quantified via ICP-MS. The MG63 cells were seeded (100 μ L/well) in a 96 well plate and incubated for 24 hours. AuNPs were added to cells for 48 hours and the cells were processed for ICP-MS as described in chapter 2, section 2.4.3.2. The converted values for gold uptake were averaged (n=3) and used for statistical analysis.

4.2.5 Fluidigm Analysis of Osterix and Related Gene RNA Levels

Analysis of MG63 cell RNA levels in response to antagomir-31-AuNP incubation was performed using the Fluidigm Biomark HD system. This system allows for automated PCR reactions to be carried out, using less samples and reagent, via a microfluidic design. This particularly suits experiments using NPs due to the typically large volumes required, and the expense this can lead to in terms of ordering sequences *etc.* A 48x48 array was used, allowing for multiple RNA targets to be assessed alongside several house keeping genes. The targets used are detailed in section 2.4.5.2. Aside from the principal target osterix, these additional primers were selected based on their possible link to mir-31 through osteoblast-like pathways including RUNX2, the bone morphogenic proteins (BMPs) and Mothers Against Decapentaplegic Homolog (SMADs) (intracellular signalling proteins).

To investigate the functionality of the antagomirs at the RNA level a fluidigm 48x48 well array was used, which quantified multiple targets after 48 hours of AuNP treatment. This robust, high throughput technique produced a snap shot of the effects of the AuNPs on selected RNA transcripts, including osterix, expressed in the MG63 cells (2.4.4.2, Table 2-1). From the qPCR data a heat map was created of the delta delta CT values :

$$((CT(\text{target}, \text{untreated}) - CT(\text{ref}, \text{untreated})) - (CT(\text{target}, \text{treated}) - CT(\text{ref}, \text{treated})))$$

From the samples normalised to multiple housekeeping genes, indicating increases or decreases in expression. MG63 cells were grown at 1×10^5 cells per well in a 24 well plate and allowed to adhere overnight. AuNP treatments were added (50nm oligo on AuNP surface) and incubated with the cells for 48 hours (control cells were incubated with media instead). After 48 hours samples were processed for fluidigm as per chapter 2, section 2.4.5.2.

4.2.6 In Cell Western Analysis of Osterix Protein Levels

The level of osterix protein in MG63 cells post AuNP treatment was further analysed via in-cell westerns. This allowed for both specific and high throughput analysis. Cells were seeded in a 96 well plate in triplicate, challenged with the AuNPs for 24 and 48 hours, then fixed, permeabilised and blocked as in section 2.5. Samples were then co-incubated with primary antibodies (1:2000 mouse OSX and 1:5000 Cell tag 700) at 37°C for 1 hour. Following Tween washing, samples were subsequently co-incubated with secondary antibody (1:2000 donkey anti-mouse IR800CW, Licor, UK) at 37°C for 1 hour. All samples were finally washed three times in PBS/Tween (5 min/wash). The plates were imaged by scanning simultaneously at 700 and 800 nm with an Odyssey SA at 100 µm resolution, medium quality, focus offset of 3.53 mm, and an intensity setting of 7 for both 700- and 800-nm channels.

4.2.7 Theoretical Binding of Antagomir-31 Sequences

Both the antagomir 5' and antagomir 3' (5A and 3A respectively) with the nonsense RNA sequences were run through the RNAhybrid programme developed by M. Rehmsmeier. RNAhybrid predicts the minimum free energy hybridization of two RNA sequences, allowing for miRNA target prediction. Hybridization is assessed by domain analysis with one sequence hybridized to the best fitting part of another (Rehmsmeier and Steffen *et al.*, 2004).

4.2.8 Statistics

Statistical analysis was performed in Graphpad using a one-way ANOVA with a Dunnett's test. In all figures * = $p < 0.05$, ** = $p < 0.01$, *** = $p < 0.001$ and **** = $p < 0.0001$. Two tailed T-Tests were performed where specifically mentioned, a welchs correction was used, # = $p < 0.05$, # # = $p < 0.01$

4.3 Results

4.3.1 Cell Toxicity : MTT Assay

The antagomir functionalised AuNPs were found to have no cytotoxicity over 24 hours incubation, as demonstrated with the MTT assay, showing no statistical difference between treatments (Figure 4 3).

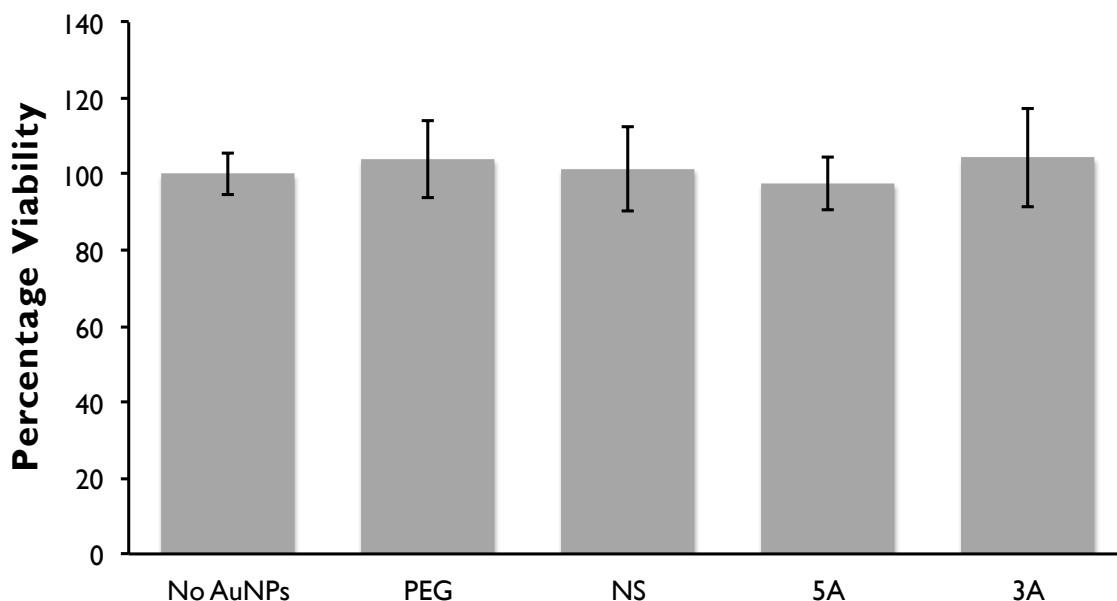
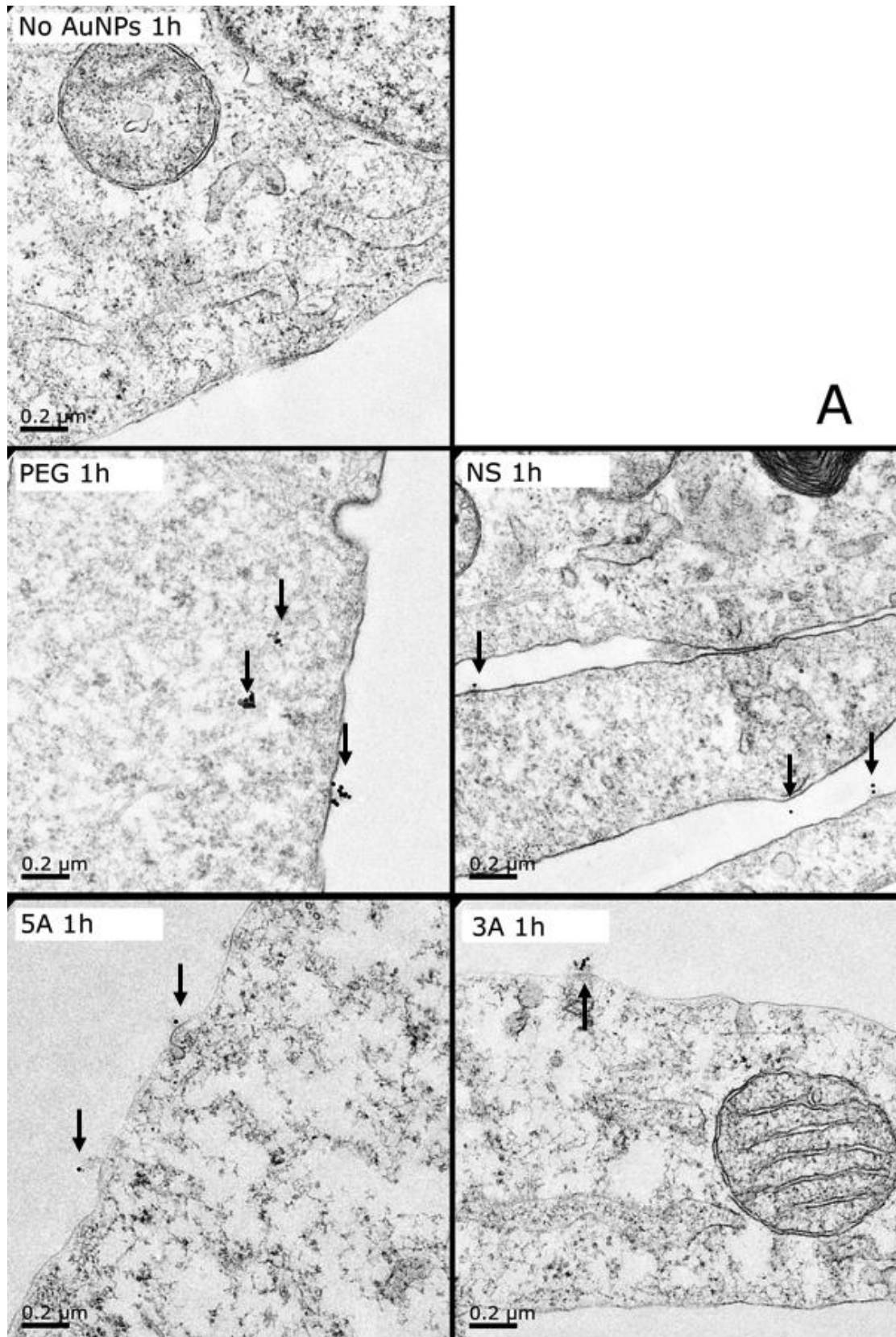


Figure 4-3. MTT analysis of MG63 cells treated with each AuNP (50nM oligo, 30% PEG) type for 24 hours (PEG, NS, 3A, 5A) (n=3; error bars indicate SD).

4.3.2 Cellular Uptake : TEM

Cross-sectional imaging by TEM was used to qualitatively analyse the cellular uptake and the intracellular location of the AuNPs after both 1 hour and 48 hour incubation. At the earlier time point of 1 hour, the AuNPs were observed interacting with the cell membrane and instigating cellular uptake, as denoted by arrowheads in Figure 4-4A, whilst at the latter 48-hour time point the NPs were clearly evident within the cell, mainly packaged into endosomes (Figure 4-4B).



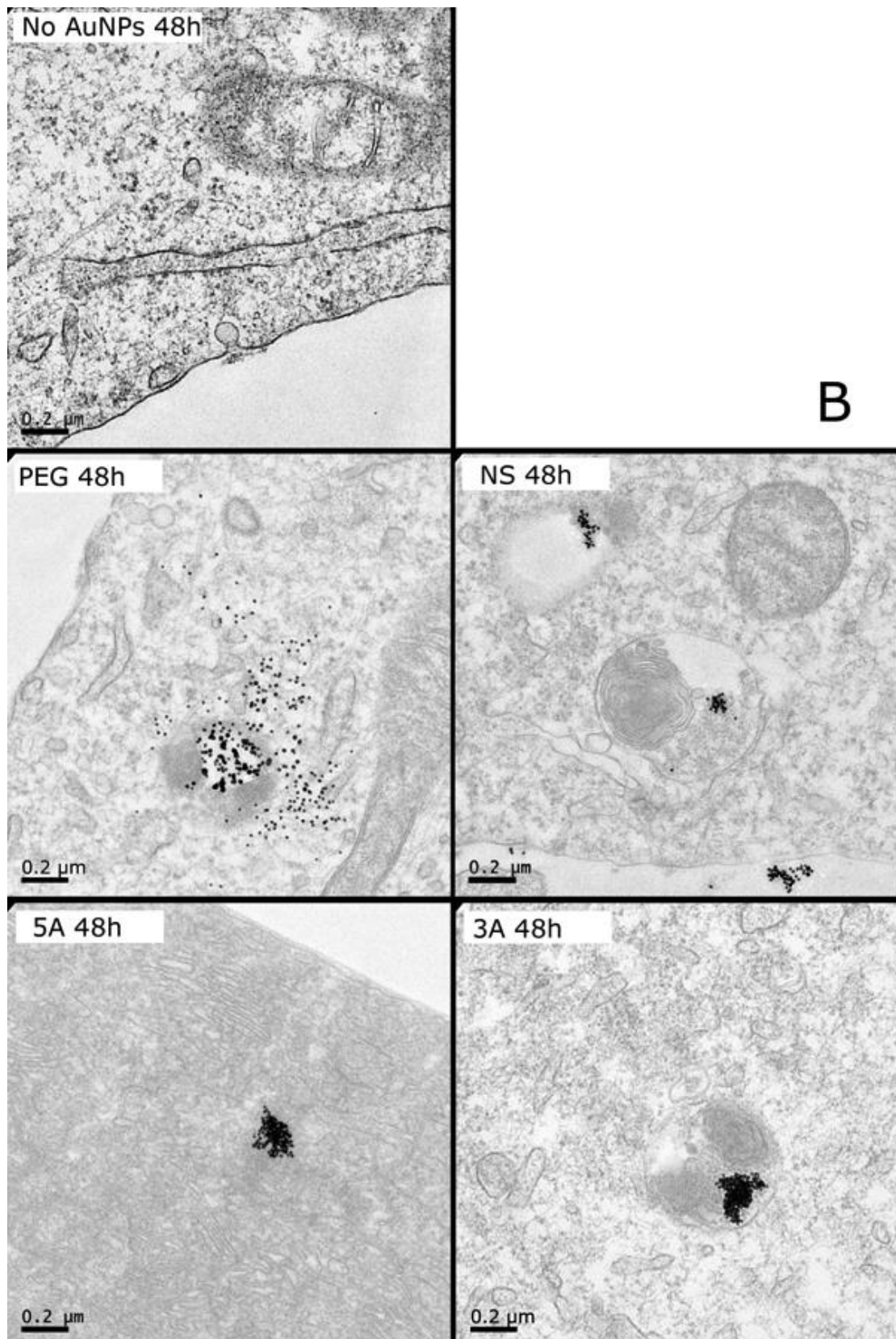


Figure 4-4. TEM images of MG63 cells treated with AuNPs (50nM, 30% PEG) after 1 (A) and 48 hours (B). Black arrowheads denote AuNPs. Scale bar =0.2μm.

4.3.3 Cellular Uptake : ICP-MS

In parallel to qualifying AuNP uptake into cells, the amount of AuNPs within the cells was quantified after 48 hours using ICP-MS to determine elemental gold levels in lysed cell samples. All four AuNPs types were recorded in the cells, with a notable increase in uptake with the 5A and 3A AuNP species compared to NS and PEG (Figure 4-5). This is unlikely to be due to either NP size or charge, as the NS functionalised AuNPs are very similar in both regards to the 5A and 3A NPs (Table 4-4). A possibility may be that the interaction of the antagonists, if still attached to the gold surface, with the target miRNAs may hinder possible exocytosis and NP turnover, in turn increasing the AuNP load within the cell. Repeat experiments at earlier time points would be required to verify this.

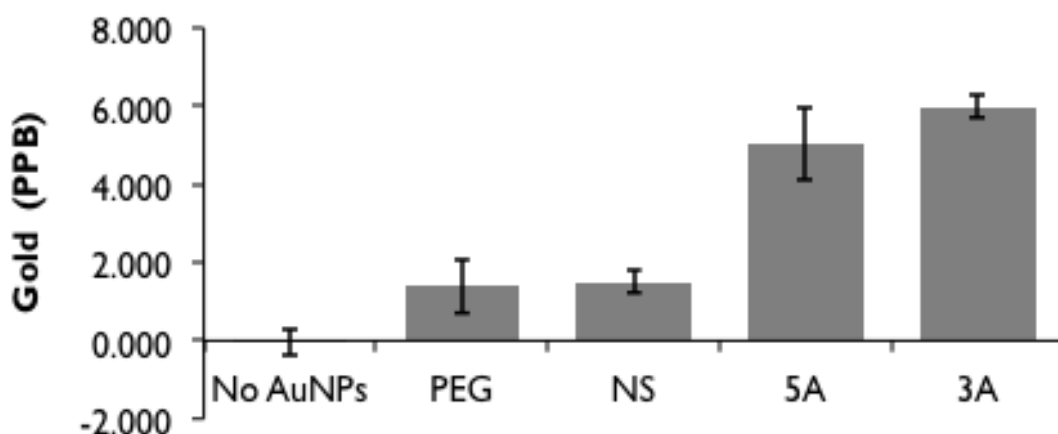


Figure 4-5. ICP-MS analysis of MG63s treated with AuNPs (50nM, 30%) for 48 hours. Each lysate has an n=3, error bars denote SD.

4.3.4 Osterix and Related Gene Expression via Fluidigm

From the raw fluidigm data, a hierarchical analysis was used to group the AuNPs together based on the similarity of the CT values (Figure 4-6). This separated out the NPs based on the influence they had on the 48 different target RNAs. The analysis identified a close relationship between 5A and 3A, with NS and PEG being more distantly related.

When considering targets that may be linked to mir-31, the 5A antagomir highly up regulated RUNX2 and SMAD3 after 48 hours in comparison to the other NP species; both of which were highlighted in Figure 4-6 as being involved in osteogenesis. Crucially however, osterix was not up regulated with 5A, yet the remaining three AuNPs (3A, the nonsense (NS) and PEG controls), appeared to upregulate osterix (Figure 4-6). This could be partly explained by off-target effects, as very few other osteogenic markers were up regulated. However, it may be due to the time point selected; 48 hours may be too late to identify changes at the RNA level. The RNA environment is highly dynamic, with many reactions and very quick RNA turnover. With this perspective it is possible that 5A may have up regulated osterix expression before the 48 hour time point and had been constitutively silenced by other intracellular factors balancing any changes, as seen in other pathways such as cyclin signalling; a pathway highly dependant on the interplay between positive and negative feedback loops (Murray, 2004). A study by Zhou *et al* (2012) have found that many miRNAs act in a bistable regulatory pattern, with transcription factors and miRNA levels oscillating in response to each other, as seen in cyclin signalling (Zhou and Cai *et al.*, 2012).

Interestingly, C-Myc expression (a proliferation gene; a target in siRNA studies in chapter 3) was only down regulated with 5A. C-Myc is typically highly overexpressed in cancer cell lines and undifferentiated cells. As MG63s are both a cancer cell line and a pre-osteoblast like cell, a reduction in C-Myc expression by 5A alongside an increase in RUNX2 and SMAD3 could indicate that the cells were slowing proliferation to focus on enhancing commitment down the osteoblast lineage

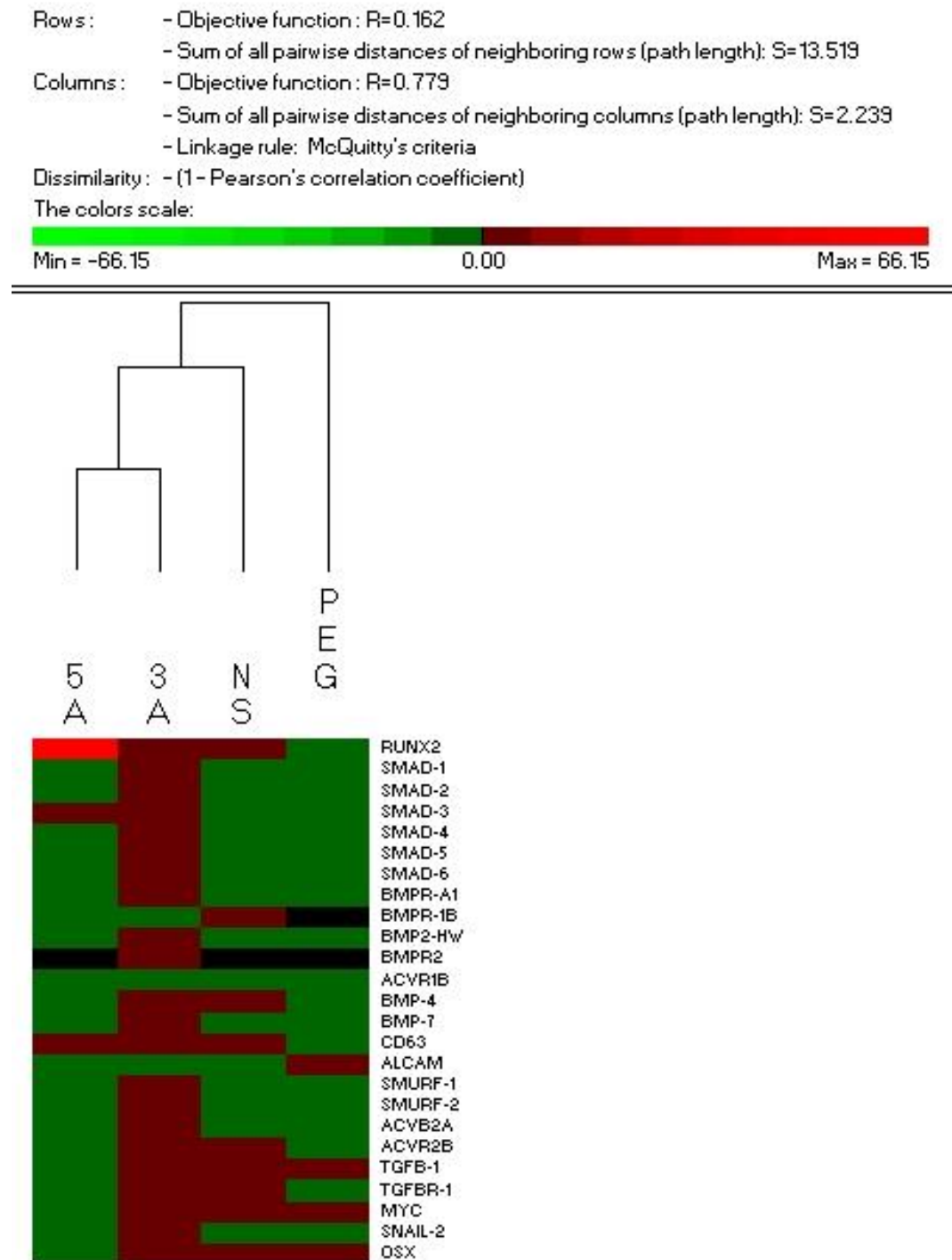


Figure 4-6. Heat-Map of MG63s treated with the AuNPs for 48 hours (green reflects a decrease in expression, whilst red reflects an increase). The data was analysed using PermutMatrix and ordered into hierarchy based on expression similarity using McQuitty's criteria. 5A and 3A are the most related. After 48 hours 3A appears to activate a wide array of osteogenic factors, whereas 5A has appeared to up-regulate RUNX2 very strongly whilst down regulating C-Myc expression.

4.3.5 Osterix Protein Levels via In-Cell Western

Due to the dynamic nature of RNA production, it is essential to also measure protein levels further downstream to further understand the effect of the antagomir functionalised AuNPs. Therefore, In-Cell Western was carried out to elucidate any changes in osterix at the protein level (Figure 4-7). After 48 hours of AuNP treatment osterix was significantly increased with both 5A and 3A treatment, compared to MG63s treated with no AuNPs, PEG or nonsense controls. The breast cancer cell line MCF-7 was used as a negative control, as this cell line is known to contain low levels of osterix; no difference was noted between these cells and the MG63 cells alone, or those incubated with the NS and PEG AuNPs. This suggests that the MG63 cells maintain a low background osterix expression level, which was increased in response to the antagomir functionalised AuNPs.

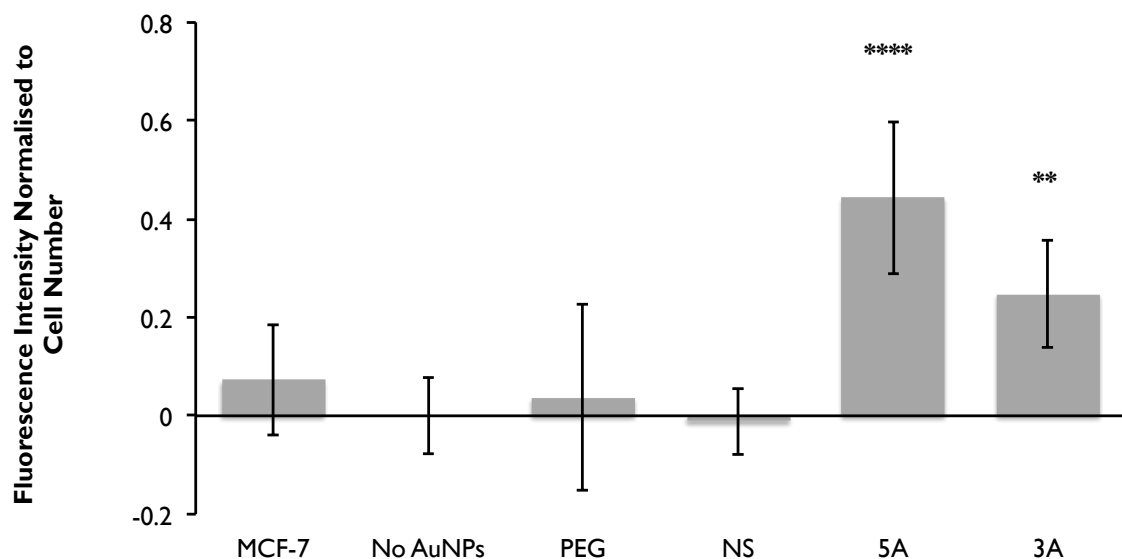


Figure 4-7. ICW data comparing osterix levels in MG63s after 48 hours with AuNP treatments normalised to cell number, and in MCF-7 cells. (n=6; error bars denote standard deviation)

4.4 Discussion

4.4.1 Mir-31 : Osterix and Osteogenesis

MiRNAs are becoming recognised as crucial regulatory molecules, as such, their dysregulation can lead to many disease phenotypes. Mir-31, for example, has been linked to numerous diseases including tumorigenesis (Liu and Sempere et al., 2010), as well as cellular processes such as adipogenesis (Sun and Wang et al., 2009a), and most recently osteogenesis (Xie and Wang et al., 2014.,Deng and Wu et al., 2013.,Guo and Zhao et al., 2011a.,Gao and Yang et al., 2011.,Deng and Zhou et al., 2013.,Baglìo and DeVescovi et al., 2013). Current papers by Baglìo et al (2013) and Deng et al (2013) found that mir-31 was linked to osterix expression; expression levels were generally found to decrease as a stem cell differentiates (Gao and Yang et al., 2011). This however is not the case for tumour cells lines, which had elevated levels of mir-31 in comparison to stem cells. This potential link with osteosarcomas has created a debate around mir-31 being described as both an oncogene (Liu and Sempere et al., 2010) and tumour suppressor (Lin and Chiu et al., 2013). The multifunctional aspect of miRNAs in general makes it possible that, depending on cell type and the point at which the dysregulation occurs, mir-31 may act as a tumour suppressor or oncogene and also influence osteogenesis.

However the link between mir-31 and osteogenesis is not without some controversy. Baglìo et al detected in their human mesenchymal stem cell (hMSC) cultures that mir-31 was upregulated in their differentiating cells in comparison to their undifferentiating cells. This is at odds with both Gao *et al* (2011) and Xie *et al* (2011), who both demonstrated that mir-31 decreases as a MSC continues down the osteogenic lineage. These conflicting results could be due to simple variation between experimental designs, for example differences in stem cell donor type, cell passage number, cell seeding density, culture times, culture media additives (eg. ascorbic acid), media changes and practices may have

produced such differences. Although this chapter employed MG63 cells as a proof of concept for our delivery system, the results in this chapter support the latter Gao and Xie papers, whereby when we block mir-31 via antagomir-AuNP delivery, we see an increase in osterix protein. This certainly suggests that the two are linked, and indicates that it may be possible to direct cells down an osteogenic lineage.

4.4.2 Antagomir Sequence Directionality: 5A Vs 3A

A further complication, when comparing research papers utilising miRNAs is the possible variation in the sequence origin. This study, whilst aiming to identify a link between mir-31 and osterix levels in a standard tumour cell line, also compared the differences between antagomir sequences with 5' (denoted 5A) and 3' (3A) directionality. Although both the 5A and 3A antagomir are antagonists of mir-31, the two species are from different sections of the mir-31 sequence. It appears from the fluidigm data and the ICW experiments that the two sequences behave slightly differently despite their origin. With this noted, questions about the binding of the sequences were raised.

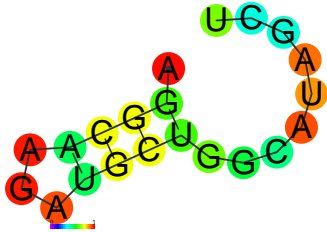
To investigate the antagomir binding potentials the RNAhybrid programme (designed by Rehmsmeier *et al* (2004)) was used, to determine the type and the strength of bond that both antagomirs would form with the corresponding and opposing strand (Rehmsmeier and Steffen *et al.*, 2004). The results are shown in Figure 4-8. Binding energies for both antagomirs to their respective mir-31 sequences (mir-31-5' with 5A and mir-31-3' with 3A) formed strong bonds that required $< \sim -40$ kcal/mol for dissociation. The antagomir 3' sequence (ie. 3A) was predicted to form a strong bond with the corresponding 5' sequence of mir-31 (-22.9 kcal/mol), whilst the 5' antagomir sequence (5A) was predicted to form a weaker structure with the opposing 3' mir-31 sequence (-12.6 kcal/mol). Weaker still were the nonsense strand's ability to bind to mir-31. This was expected, but was it was noted that a degree of potential binding was possible.

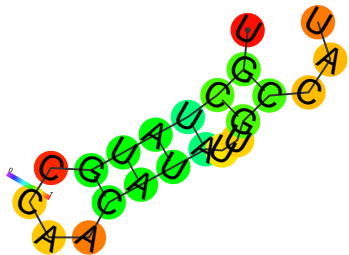
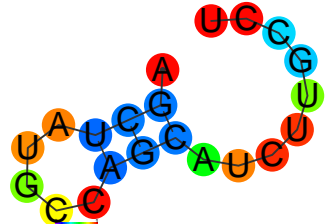
This differential between binding energies of the 5A and 3A with the different mir-31 stands could be a reason for the range of responses. A report by Chan *et al* (2013), found a range of concordant and discordant responses of mir-31 by shifting the sequence by one nucleotide; which was reported to repress dicer activity, whilst the nonshifted sequence could not. Recognising that other mechanisms apart from the seeding region can induce drastic change in properties by subtle variations in sequence length and position. This improved perspective could lead to better design of miRNA therapeutics.

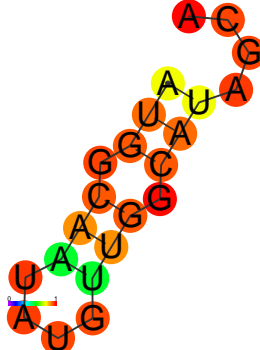
The difference between 5A and 3A in binding could also be due to differences in the structure of the primary RNA sequences, which, based on the minimum free energy method, are shown in Table 4-5. Mir-31 5' and the corresponding 5' antagomir (5A; the highest potency antagomir) form single stranded structures with large open unbound sequences of ~9 bp in length. This unbound section could allow for easier binding with targets, resulting in more efficient knockdown.

Very few antagomir studies focus on the origin of the sequence employed, and the possible differences having a sequence that targets the passenger strand over the guide strand might produce (Zhong and Dong *et al.*, 2013) (Chang and Kao *et al.*, 2013) (Chan and Lin *et al.*, 2013). This is certainly a facet of such studies that requires attention in future work.

Table 4-5. The predicted structures of the single stranded RNA sequences, based on the minimal free energy (MFE) method (an established method to predict RNA structure). Complimentary regions are evaluated to predict the most energetically stable molecule. The stability of the structure is given in kcal/mol, the more negative the value equates to a more stable structure.

Name	Sequence	MFE for optimal 2° structure kcal/mol	MFE structure drawing encoding base-pair probabilities 	Frequency of MFE structure
hsa-mir-31-5'	AGGCAAGAUGCUGGCAUAGCU	-2.00		18.96

Name	Sequence	MFE for optimal 2° structure kcal/mol	MFE structure drawing encoding base-pair probabilities 	Frequency of MFE structure
hsa-mir-31-3'	UGCUAUGCCAACAUAUUGCCAU	-1.10		39.35
antagomiR-31-5'	AGCUAUGCCAGCAUCUUGCCU	-1.20		24.65

Name	Sequence	MFE for optimal 2° structure kcal/mol	MFE structure drawing encoding base-pair probabilities 	Frequency of MFE structure
antagomiR-31-3'	AUGGCAAUAUGUUGGCAUAGCA	-3.30		45.78
nonsense	GGAGAUUGGUUUUGACGUUUA	0.00		47.20

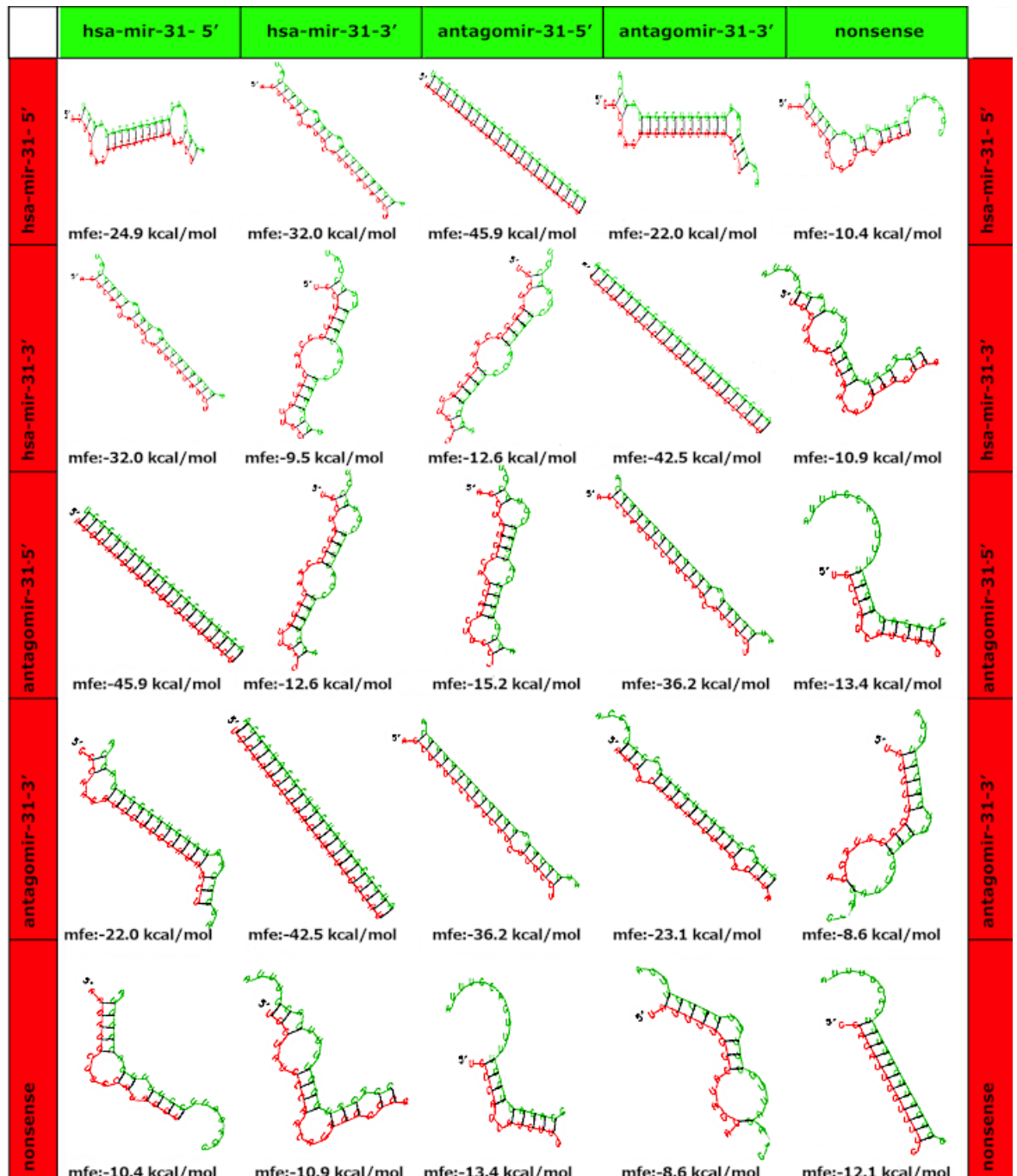


Figure 4-8. miRNA binding sequence geometries based on base pairing and minimum free energy using RNAhybrid. The stability of the structure is measured in kcal/mol (ie. the energy required to break the structure). The greater the energy needed the more stable the structure. Linearity infers stability, whilst loops indicate incompatibility and lack of binding. The antagomirs and their corresponding miRNA sequence form the strongest and most stable structure.

4.4.3 Off Target Effects

Fluidigm data demonstrated a host of up- and down-regulations for primers other than osterix. For example, it was noted that the nonsense strand up-regulated several genes, despite being a negative control. This suggested a general cell reaction to the AuNPs at the RNA level, which were not related to the intended antagomir target (osterix). This is not surprising, as the addition of NPs to the culture media, and their subsequent uptake into the cell would be expected to stimulate a variety of cell responses (Boisselier and Astruc, 2009). There is very little literature in this regard, as most reports using NPs focus on assessing functional delivery of the cargo, however recent work in our lab has noted several off target effects when using siRNA delivered to cells via AuNPs (Child et al, submitted).

From the fluidigm data in Figure 4-6, it was also notable that the 3A AuNPs up-regulated most genes shown on the heat map, in direct comparison to the 5A AuNP, that down regulated everything apart from RUNX2, SMAD3 and CD63. Typically, miRNAs repress protein levels, so it could be said that 5A behaviour is more true to type (Lian and Stein et al., 2012). The 3A antagomir may be non-specifically up regulating multiple RNAs by having more promiscuous binding, whilst 5A's more conservative binding (i.e. binding to one target very strongly and binding only very weakly to any other sequence) might enable for better, more consistent targeting, producing more osteogenic like cells with higher osterix levels (Figure 4-7).

The ICW data confirmed that blocking mir-31 with the antagomirs produced more osterix protein after 48 hours of treatment. The 3A indicated slightly less osterix in comparison to 5A, but both sequences significantly increased osterix levels in comparison to control cell populations.

4.5 Conclusion

Interfering with intracellular miRNA levels for therapeutics provides an exciting alternative to current drug delivery formulations for many diseases. Using AuNPs as the delivery vector within this section of work provided a stable delivery platform with low toxicity. A functional response to blocking mir-31 was noted, with an increase in osterix level in MG63 cells at the protein level. However some off target effects were noted in this study at the RNA level, which could potentially, cause issues for future studies. This investigation highlighted clear differences in results when using different miRNA sequences, and more research is needed to tackle the lack of knowledge surrounding miRNA sequence binding and its effects.

In spite of this, factors such as oligo concentration and duration of treatment proved challenging to achieve efficient silencing. With increased high throughput screening these variables could be fine-tuned, increasing our understanding of the complexities of miRNA therapeutics and delivery.

5 Chapter 5: Gold Nanoparticle-mediated Blocking of Mir-31 to Influence Osterix Expression in Human Mesenchymal Stem Cells

5.1 Introduction

The paradigm of using manmade synthetic materials to help support and restore functionality to injured tissues is being superseded by the potential of harnessing the body's natural ability to heal itself. The main drive behind this shift has been the breadth of recent research with stem cells, and our subsequent expansion of knowledge. As described in chapter 1 (section 1.4.2), MSCs are a subset of stem cells that are mainly located in the bone marrow, within their specialised niche environment, and they have the potential to differentiate and heal damaged tissue *in situ*. The more we understand about these processes, the better our chance of influencing MSC differentiation to our advantage to allow tissue regeneration and healing.

To this end, an expanding field of MSC research is concerned with bone regeneration. The main pathways involved in osteogenic differentiation are summarised in Chapter 1, (section 1.4.2). Committing MSCs to an osteogenic lineage produces a mineralized extracellular matrix of collagen, calcium and phosphorus. It has been established that diseases such as osteoporosis and osteogenesis imperfecta are underpinned by the dysregulation of components in osteogenic pathways (Heggebo and Haasters *et al.*, 2014). To date research has involved creating new tissue (Eslaminejad and Karimi *et al.*, 2013), repairing fractures (Chen and Deng *et al.*, 2012), and attempting to further understand the mechanisms of osteogenesis with a view to increasing bone density for osteoporosis patients (Zhu and Friedman *et al.*, 2012., Qiu and Andersen *et al.*, 2007., Heggebo and Haasters *et al.*, 2014., Benisch and Schilling *et al.*, 2012).

MSCs are highly regulated cells, in terms of self-renewal and differentiation, and it is becoming increasingly evident that miRNAs play a critical role in this regulation. Several key miRNAs involved in

osteogenic differentiation were noted in chapter 1, section 1.4.4, with the key ones identified to date highlighted in Figure 5-1.

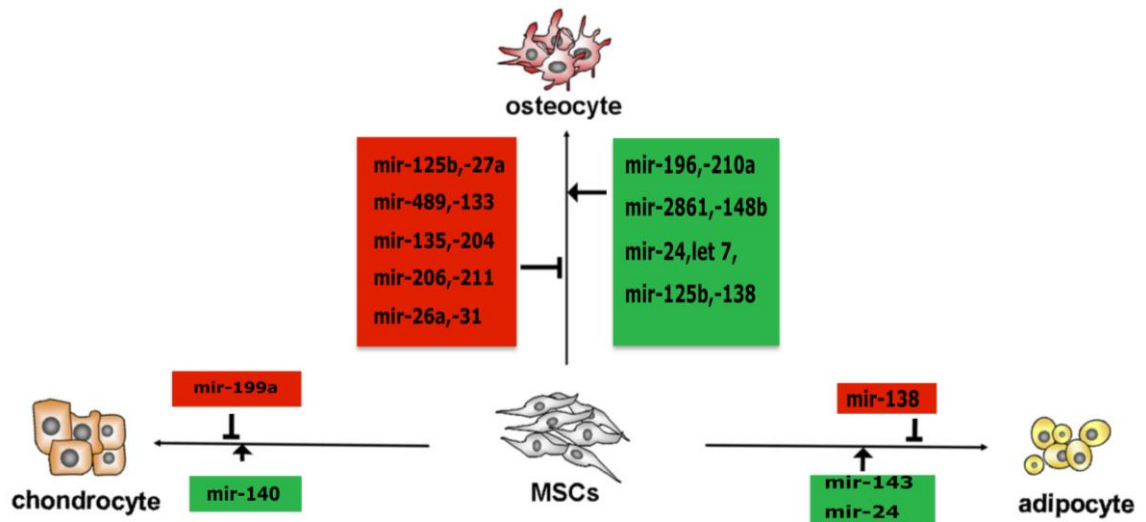


Figure 5-1 Key miRNAs involved in MSC differentiation. Figure adapted from Guo *et al* (2011) and Baglìo *et al* (2013).

As described in chapter 4, mir-31 has been linked to the inhibitory regulation of osterix in cells (Baglìo and DeVescovi *et al.*, 2013). Based on this, we designed antagomirs against mir-31 and tested their functionality in a simple bone cancer cell (MG63) model, using AuNPs as a delivery platform. Despite the RNA data proving more complex, results did demonstrate that introducing mir-31 antagomirs to our cell population for 48 hours was sufficient to reverse this inhibition and cause an increase in osterix protein levels.

When considering MSCs as a cell model as opposed to standard cell lines such as MG63, the effects of blocking a single miRNA which is known to affect osterix, may also affect other key factors in the osteogenic pathway. Authors Deng *et al* (2013), found that mir-31 expression was progressively decreased in human bone marrow derived stem cells undergoing differentiation (Deng and Wu *et al.*, 2013). The authors used lipofectamine to transfect their cultures with mir-31, or mir-31 inhibitors. Increasing levels of mir-31 decreased SATB2 protein

levels, however no notable changes were reported from the RNA level. The authors linked RUNX2, mir-31 and SATB2 together in a regulatory feedback system. Increasing RUNX2 levels with transfected plasmids encoding RUNX2 directly repressed mir-31. Whereas overexpressing mir-31 reduced osterix, osteocalcin, and osteopontin protein expression without affecting RUNX2 protein levels. This suggested that mir-31 can only influence downstream targets of RUNX2.

Dong *et al* (2015), investigated the role of SATB2 in MSCs. They found that the MSCs isolated from different sources had differential properties with regards to stemness, autophagy and senescence (Dong and Zhang *et al.*, 2015). MSCs harvested from the cranio-facial region tended to be more osteogenic and had increased levels of autophagy proteins, compared to MSCs harvested from tibia bone marrow. Autophagy, the organised destruction and recycling of cellular components; is a process of cell survival mediated through internal cellular recycling of surplus proteins, lipids and organelles. The interplay between autophagy and stemness has been discussed in several reviews (Vessoni and Muotri *et al.*, 2012., Phadwal and Watson *et al.*, 2013), with Oliver *et al* (2012), noting that reduction in the autophagy promoting protein Bcl-xL severely reduced cell survival (Oliver and Hue *et al.*, 2012). Our stem cells should exhibit high levels of autophagy, as a reduction could indicate differentiation or apoptosis.

The age of the patient derived MSCs is also an important factor, discussed by Heggrebo *et al* 2013. Differences in osteogenic potential by MSCs were noted from elderly patients compared to younger patients, in particular a lack of proliferation and osteogenic commitment. This presents a further challenge for patient specific tissue regeneration (Heggebo and Haasters *et al.*, 2014).

As the progressive loss of mir-31 has been demonstrated in differentiating MSCs (Deng and Wu *et al.*, 2013), we hypothesised that blocking mir-31 with antagomirs at an early time point, could kick start

the process of osteoblastic differentiation. We therefore progressed to use our antagomir functionalised AuNPs from chapter 4 with MSCs, to identify whether we could influence osteogenic differentiation by increasing osterix expression in cells.

5.2 Materials and Methods

The antagomir functionalised AuNPs were produced as described in Chapter 4, section 4.2.1.

5.2.1 Cell Culture

The human MSCs (hMSCs) were cultured in DMEM+ (section 2.3.3) maintained at 37°C in 5% CO₂ until ~70% confluent, after which time they were passaged and counted with a haemocytometer. The cells were seeded at a density of 1×10^3 cells per cm² for experiments unless stated otherwise. The cells were cultured for 24 hours before the addition AuNP antagomir treatments at 50nM.

MSCs gifted by Mr Dominic Meek were isolated and processed from bone marrow extracted from patients undergoing knee or hip operations. The MSC's were processed to remove any blood, fat or bone fragments present, by centrifugation with a ficoll-gradient. A heterogenous population of cells form an isolated band that contain MSCs. This band can be extracted and cultured in DMEM+ for a couple of days to allow cells to adhere. Adhered cells are further selected using the marker CD271, and a magnetic labelling separation kit (Cell technologies, UK), and seeded into a new flask. These MSCs were then treated as the MSCs from promocell.

Pilot studies used MSCs gifted by Mr Dominic Meek. Whilst the experiments described in this thesis used MSCs from Promo cell.

5.2.2 Toxicity

The hMSC cytotoxicity in response to the antagomir-AuNP treatments was assessed by standard MTT assay, as described in Chapter 2 section 2.4.3.

5.2.3 Cellular Uptake of Gold Nanoparticles

5.2.3.1 Transmission Electron Microscopy (TEM)

Cellular uptake of AuNPs was verified via TEM. The hMSCs were seeded at a density of 1×10^4 cells per mL onto Thermanox coverslips (13mm diameter) and cultured to develop a confluent monolayer of cells. At this point the AuNPs were added and cells further cultured for 24 hours. Cells were subsequently processed for TEM as described in chapter 2, (section 2.4.3.1).

5.2.3.2 Inductively Coupled Plasma Mass Spectrometry (ICP-MS)

Cellular uptake of AuNPs was further quantified via ICP-MS. The hMSCs were seeded (100 μ L/well) in a 96 well plate and incubated for 24 hours. AuNPs were added to cells for 48 hours and the cells were processed for ICP-MS as described in chapter 2 (section 2.4.3.2). The converted values for gold uptake were averaged ($n=3$) and used for statistical analysis.

5.2.4 Fluidigm

The hMSCs were cultured with antagomir functionalised AuNPs after 5 days. Fluidigm (as explained in chapter 4, section 4.2.5) analysis was carried out as described in chapter 2 (section 2.4.4.2).

5.2.5 In Cell Western

The level of osterix protein in MSCs cells post antagomir-AuNP treatment was further analysed via in-cell western, as described in chapter 4 (section 4.2.6).

5.2.6 Osteocalcin Nodule Formation by Immuno Fluorescence

The production of osteocalcin (OCN) nodules as a late marker for osteoblast cell phenotype was carried out as described in chapter 2 (section 2.4.5).

5.2.7 Statistics

Statistical analysis was performed in Graphpad using a one-way ANOVA with a Dunnett's test. In all figures * = $p < 0.05$, ** = $p < 0.01$, *** = $p < 0.001$

5.3 Results

5.3.1 Cell Toxicity: MTT Assay

MSCs exposed to antagomir functionalised AuNPs produced no statistical significant cytotoxic effect based on the MTT assay after 48 hours incubation (Figure 5-2). In fact, cells appeared to be increasing their metabolic activity when compared to control cells.

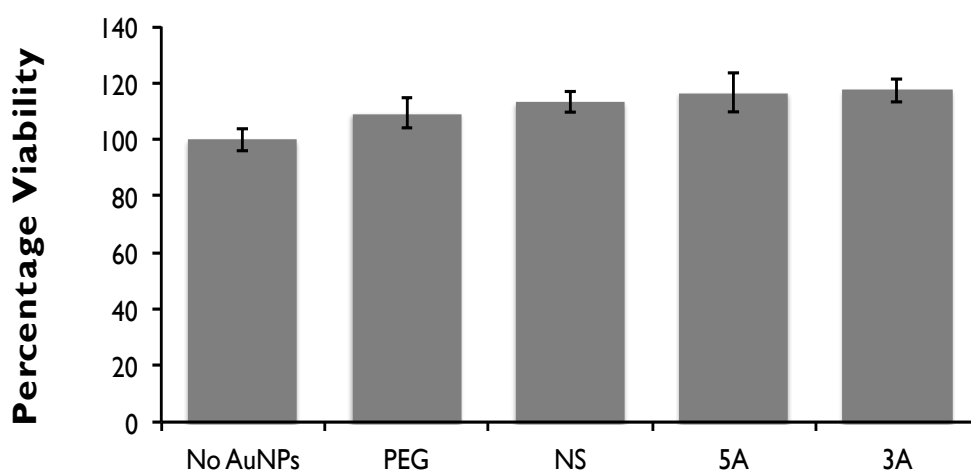
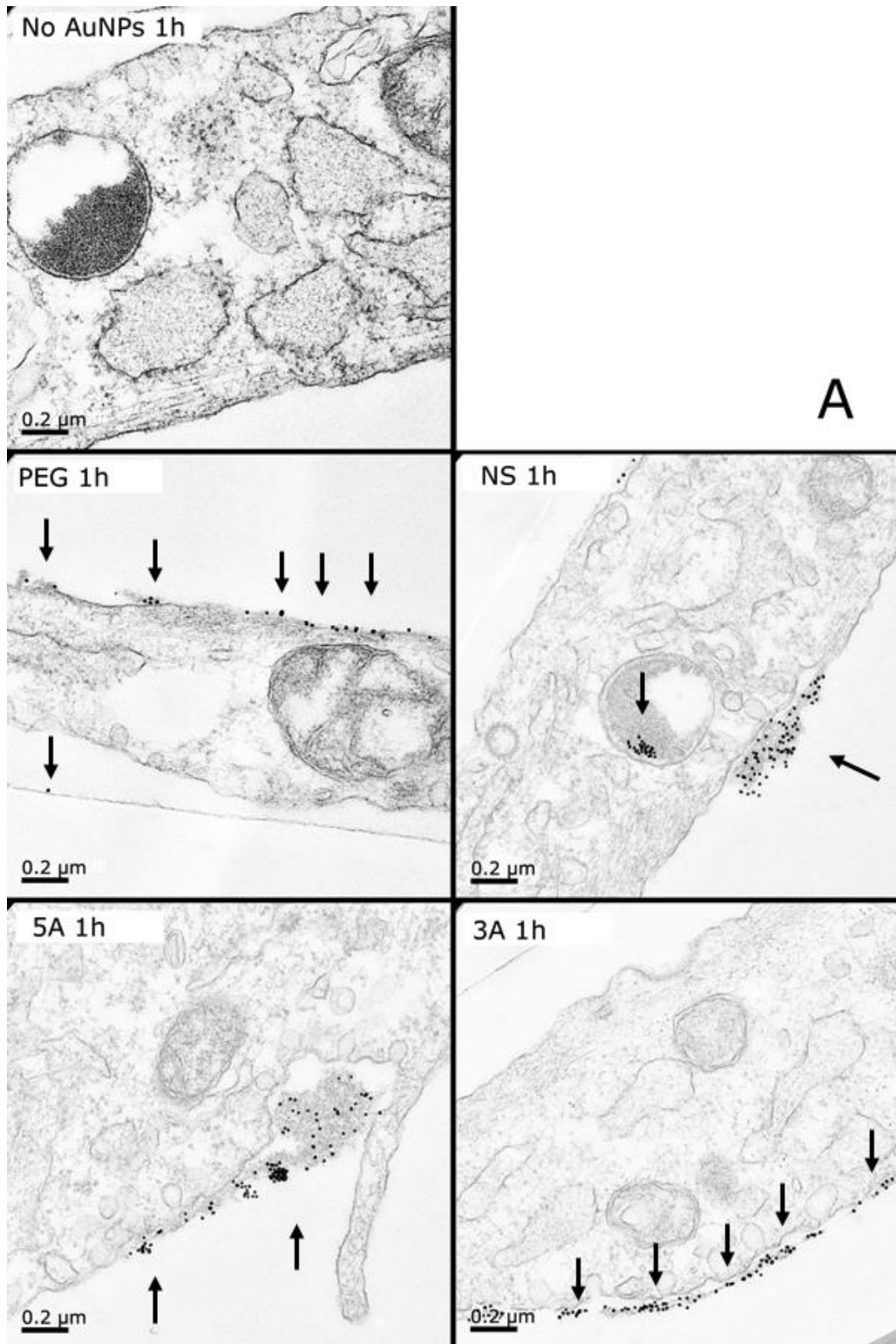


Figure 5-2. MTT analysis of hMSCs treated with each AuNP type (50nM oligo, 30% PEG saturation) for 48 hours (PEG, NS, 5A, 3A) (n=3; error bars indicate SD).

5.3.2 Cellular Uptake : TEM

The intracellular location of the AuNPs were qualitatively assessed by TEM after a 1 hour and 48 hour incubation. As with the MG63 cells, after 1 hour incubation the AuNPs appeared predominantly at the cell membrane, in the initial stages of uptake (Figure 5-3A). After 48 hours large accumulations of AuNPs can be seen within the cell (Figure 5-3B), in endosomes or free within the cytoplasm.



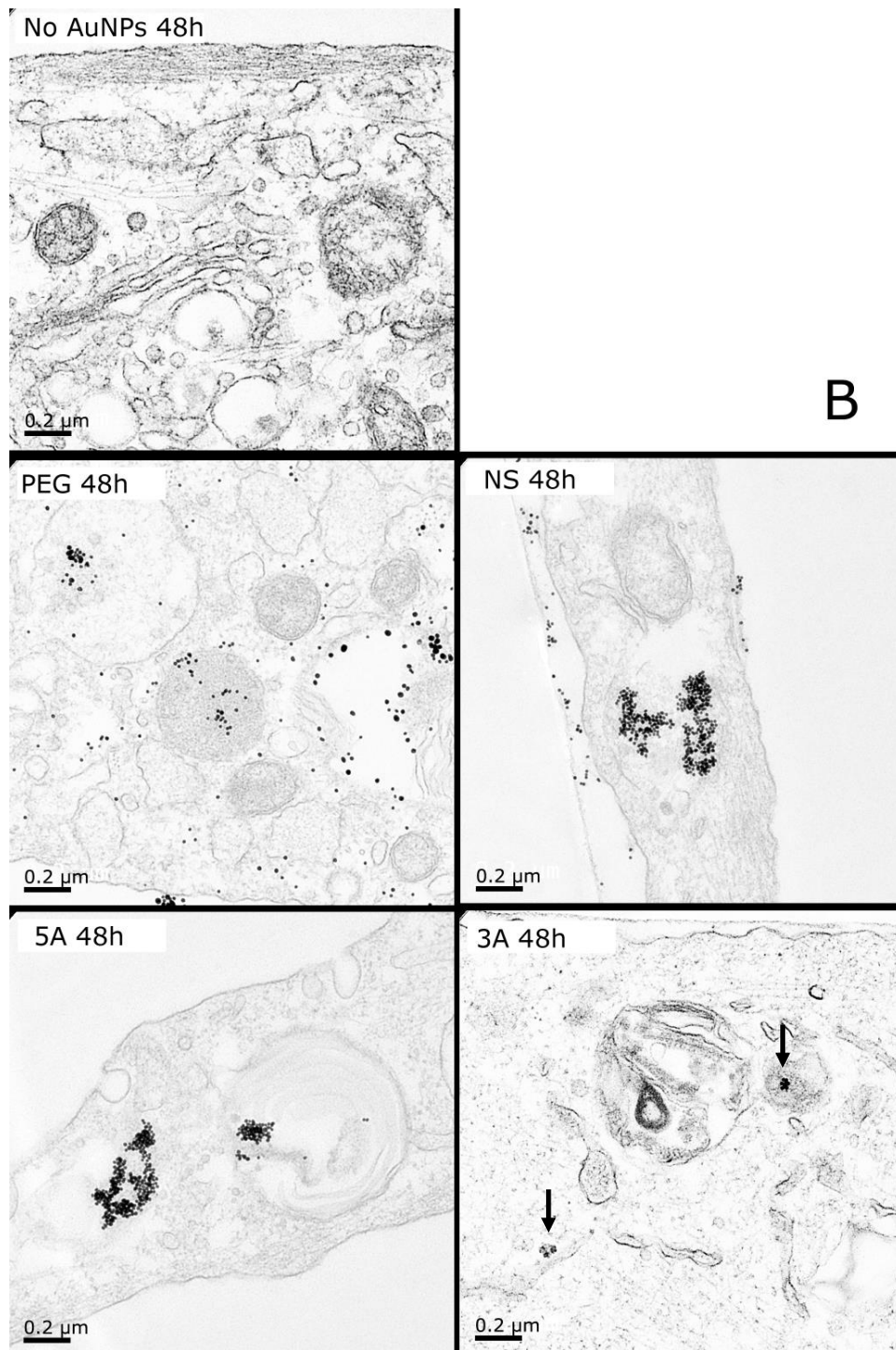


Figure 5-3. TEM images of hMSCs cells treated with AuNPs (50nM, 30%) after 1 (A) and 48 (B) hours. PEG=Cells treated with AuNPs functionalised with PEG only. NS=AuNPs with PEG and nonsense antagomir strands. 5A= AuNPs with PEG and antagonist sequences targeting 5' of mir-31. 3A=AuNPs with PEG and antagonist sequences targeting 5' of mir-31. Scale bar =0.2μm. Arrows indicate AuNP clusters.

5.3.3 Cellular Uptake : ICP-MS

To quantify the level of gold within the hMSCs, samples were incubated with AuNPs for 48 hours, and elemental gold levels were analysed by ICP-MS. All AuNP species were found within the hMSCs after 48 hours, with PEG-AuNPs demonstrating the highest level of uptake (Figure 5-4).

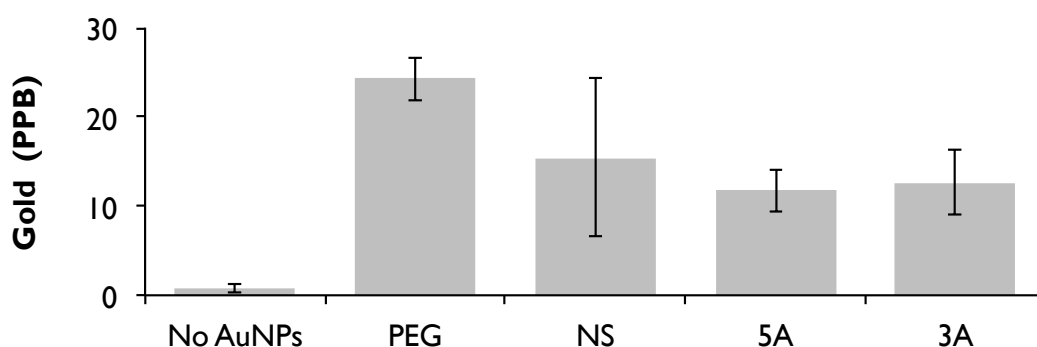


Figure 5-4. ICP-MS analysis of hMSCs treated with AuNPs (50nM, 30% PEG saturation) for 48 hours. Each lysate has an n=3, error bars denote SD.

5.3.4 Osterix and Related Gene Expression via Fluidigm

Changes at the RNA level were examined by a fluidigm 48x48 well array. This array was able to quantify multiple targets after 5 days of antagomir treatment. The data was expressed as a heat map, and subdivided into stem cell factors (Figure 5-5) and osteogenic factors (Figure 5-6). The brighter the shade of red correlates to a greater abundance of RNA transcripts in comparison to the RNA levels measured in the control samples. The reverse is true for RNA transcripts coloured green, with brighter green signal correlating to a reduction in RNA in comparison to control (No AuNPs). The heat map data was arranged into a hierarchy based on AuNP response similarity. The data from Figure 5-5 and Figure 5-6 were taken from the same plate, but split into two separate figures for convenience.

When considering the day 5 data, overall the 5A, 3A and NS seemed to produce a similar down regulatory response of key stem cell markers, with PEG AuNPs producing the opposite (Figure 5-5). The fact that nestin, alcam, CD63 and CD44 (established MSC markers, chapter 1, Figure 5-6) are all decreased indicates a shift away from the retention of stem cell factors, whilst the decrease noted with C-Myc suggests the cells are reducing proliferation, which commonly occurs during differentiation (Figure 5-5). The 5A antagomir was the only treatment that demonstrated a decrease in vimentin, an intermediate filament expressed in mesenchymal cells which is considered a stem cell marker, again indicative of a shift away from 'stemness'.

However both the 3A and the 5A induced a general decrease in most osteogenic-related genes analysed (Figure 5-6). There were increases for the bone morphogenic protein receptors (BMPR-2 and BMP-R1A), which are co-involved in the early cell signalling pathways for osteogenesis amongst other roles, and this may suggest that at day 5, the cells are in the early stages of osteogenesis, however this is purely hypothetical. A decrease in osterix was noted, across all AuNP treatments. As mentioned previously the RNA level is a very dynamic and ever changing environment. Further investigation would be required to see if this down regulation of osterix at the RNA level in comparison to control hMSCs, was a result of the time point selected or the cells reacting to the AuNPs in some manner.

5.3.5 Osterix Protein Levels via ICW

Following from the RNA analyses, which highlighted the difficulty in selecting the correct time point with hMSCs to detect changes in expression levels with differentiation, a time course experiment measuring the protein level of osterix was performed. The hMSC cells were cultured with the antagomir-AuNPs for 3, 5, 7 and 10 days, fixed and stained for osterix and normalised to cell number. The active AuNP treatments (5A, 3A and NS) were subsequently normalised to control NPs (ie. Au-PEG), with control cells (no AuNPs) acting as an osterix protein baseline level over time.

During the time course, levels of osterix in control cells begins to increase at day 5, indicating that differentiation is starting to occur, rising at day 7 and beginning to plateau at day 10 (Figure 5-7A). However the trend is very different when the AuNPs are added. Osterix levels begin to rise immediately and rapidly, peaking by day 5. The levels subsequently drop down at day 7, before picking up again and returning to starting levels at day 10.

This rapid and cyclic level of osterix expression, compared to the gradually rising expression found in control hMSCs (Figure 5-7B), may indicate an overall general cellular response to the presence of AuNPs, as the NS sequence also records an increase in osterix levels. This could potentially be due to some form of non-specific binding. However, both the 5A and the 3A had significantly higher levels osterix expression compared to the NS sequence. The cyclic nature of the response to the AuNPs is interesting, as it mimics many other gene expression responses to stimuli (Murray, 2004., Zhou and Cai *et al.*, 2012)

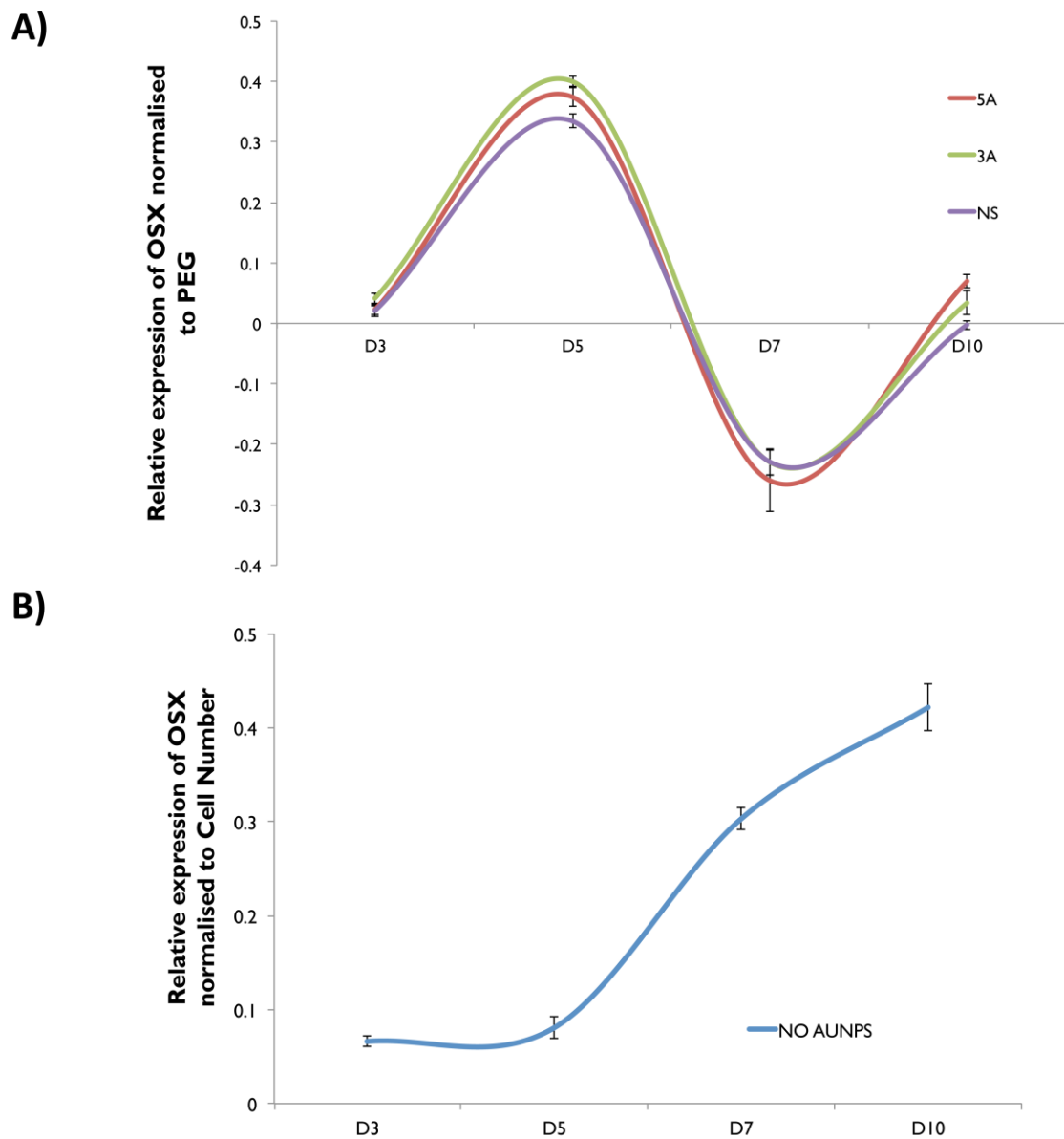


Figure 5-7. ICW data comparing osterix levels in hMSCs over several time points. A) AuNP treatments are shown as 5A= Red, 3A Green, NS= Purple (normalised to cell number and then PEG-AuNPs) B) Control cells (no AuNPs) normalised to cell number are shown in (n=6; error bars denote standard error).

5.3.6 Osteocalcin Nodule Formation by Immunofluorescence

The increase in osterix protein expression in response to the 5A and 3A (and the NS sequence) suggest that the antagonists may be having an effect by blocking the mir-31 and therefore increasing osterix. Based on this, it was hypothesised that, with such a dramatic increase in MSC

osterix at day 5, this may in turn have effects further downstream, whereby the peak at day 5 may produce an earlier peak of late osteogenic markers. To assess this hMSCs were cultured with all AuNPs for both 3 and 5 weeks, and stained for osteocalcin, a late osteogenic cell marker. Figure 5-8 and Figure 5-9 demonstrate several example images at both time points, whilst Figure 5-10 is a graphical representation of a series of images to allow semi-quantification of osteocalcin staining.

Osteocalcin is a downstream target of osterix and an established positive marker for osteogenesis. Osteocalcin protein levels were determined by immunostaining and quantified via Fiji, with normalisation of osteocalcin nodules to cell number. The 5A antagomir functionalised AuNPs produced a dramatic increase of osteocalcin compared to the other AuNP treatments and to the control cells at week 3 (Figure 5-10A). From the corresponding panel of images (Figure 5-9) the red osteocalcin can clearly be observed. By 5 week the accelerated osteogenic effect of the 5A treatment remains, but it is less dramatic, suggesting that the increase has peaked and the other cell populations are slowly catching up (Figure 5-9 and Figure 5-10B).

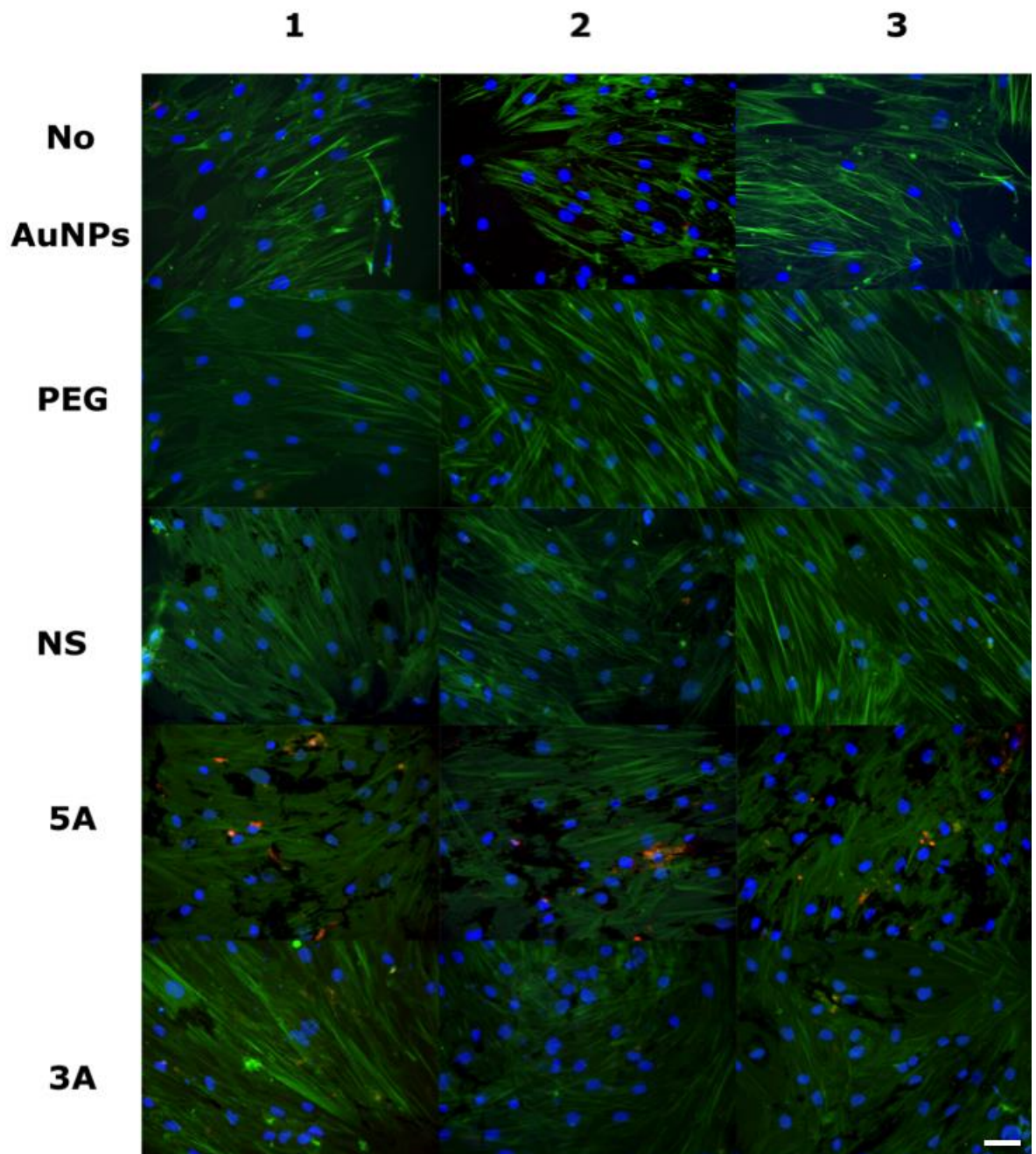


Figure 5-8 Representative images from each replicate of AuNP treatment cultured with hMSCs after 3 weeks. Staining indicates actin (green), nucleus (blue) and osteocalcin nodules (red). Scale bar= 5 μ m.

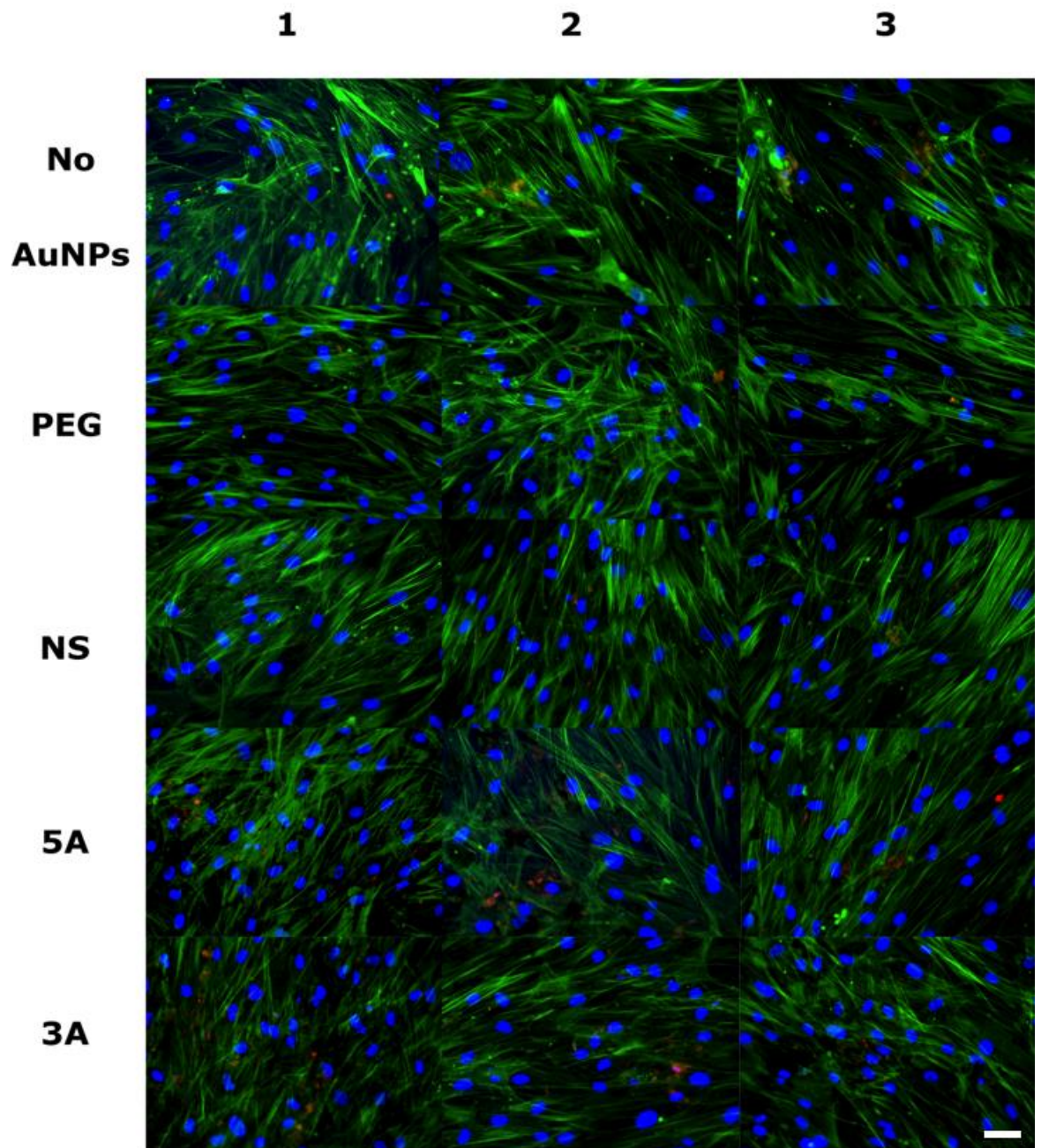


Figure 5-9 Representative images from each replicate of AuNP treatment cultured with hMSCs after 5 weeks. Staining indicates actin (green), nucleus (blue) and osteocalcin nodules (red). Scale bar= 5 μ m.

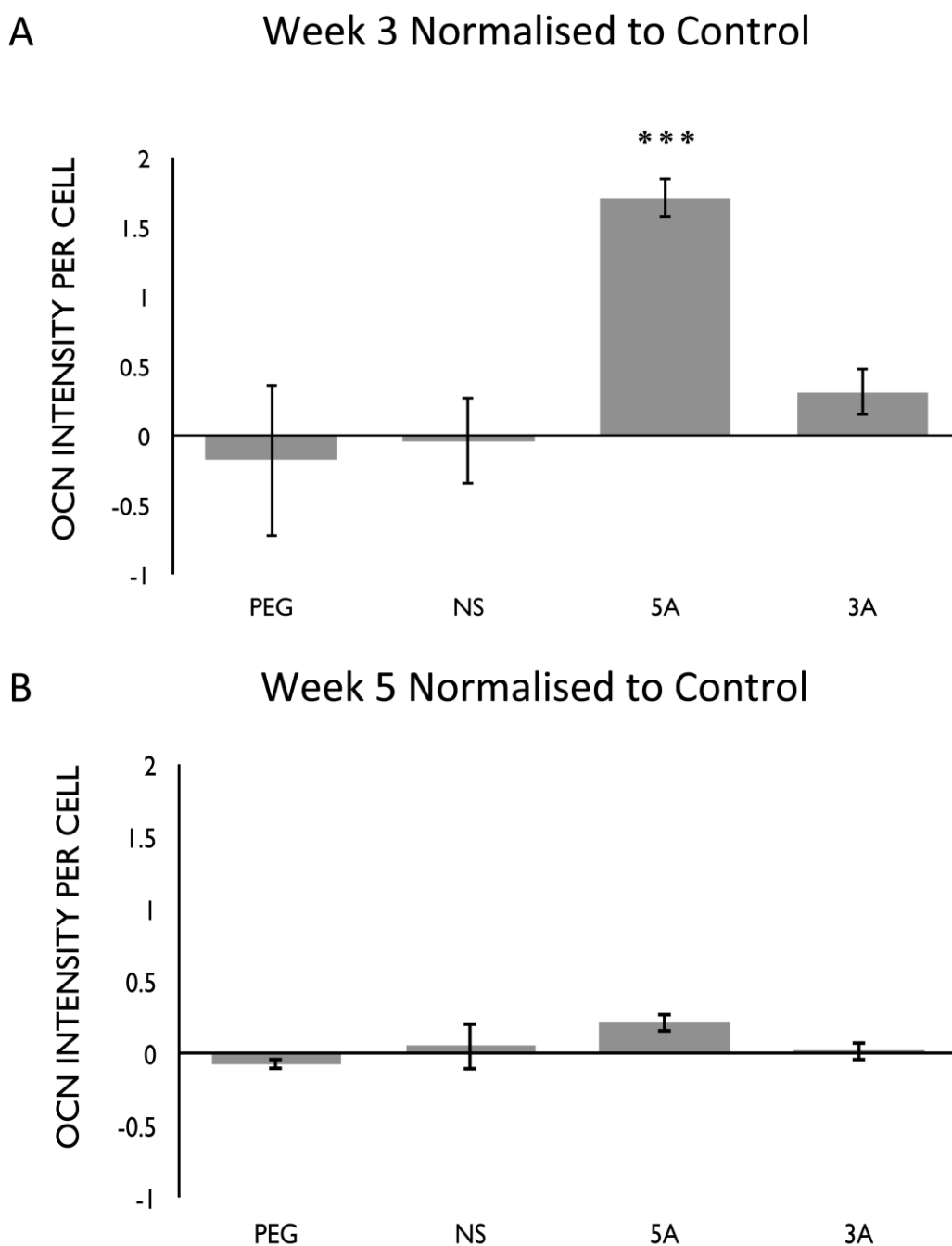


Figure 5-10 Semi-quantification of osteocalcin staining in hMSCs after treatment with AuNPs for 3 and 5 weeks (A and B respectively). All treatments have been normalised to control cells treated with no AuNPs. (n=3, error bars denote SEM) ***= $p < 0.001$.

5.4 Discussion

5.4.1 Influencing Differentiation

MSC differentiation is a hugely important area of research. Studies have shown that chemical induction using dexamethasone and ascorbic acid can create osteoblast-like cells *in vitro* (Heggebo and Haasters *et al.*, 2014). Similarly, specific nanotopographies on cell growth surfaces have been proven capable of either maintaining stemness of hMSCs or producing accelerated osteogenesis (McNamara and McMurray *et al.*, 2010., McMurray and Gadegaard *et al.*, 2011). However, whilst both technologies are well established, neither is without its inherent difficulties.

Chemical induction is limited predominately to *in vitro* studies, although some studies have shown the effectiveness of BMP-2 administered to patients to improve bone density (Rickard and Sullivan *et al.*, 1994., Heggebo and Haasters *et al.*, 2014). However the effectiveness of this treatment has been shown to be time dependant, with prolonged exposure diminishing any osteogenic effect produced within the first few days.

The nanotopographies used by McNamara *et al* (2010) and McMurray *et al* (2011) produced clear effects on the hMSCs cultured on them. However, the influence of topography on cells is known to be highly cell density dependent, and as the cells proliferate and also begin to deposit extracellular matrix, the monolayer becomes more complex and the effects of the topography are weakened. Therefore, when used *in vivo*, this could prove challenging to the formation of functional bone around nano-patterened implants. Therefore, using miRNA therapeutics with a suitable delivery vector and targeting mechanism to influence stem cell differentiation, while in its infancy, holds great potential could solve the non-specificity of chemical induction and the lack of signal transduction experienced by topographies.

As alluded to previously, the location and source of the hMSCs plays a critical role in tissue regeneration, as not all MSCs are created equal (Heggebo and Haasters *et al.*, 2014., Dong and Zhang *et al.*, 2015). The location of the MSC population has been shown to confer very specific differences in osteoblast formation, cell survival by the cellular process of autophagy and senescence (Dong and Zhang *et al.*, 2015). The age of the patient is also crucial for effective bone formation. As a patient ages, the MSCs become less proliferative and have a reduced capacity to form functional bone tissue (Chen and Lee *et al.*, 2012., Baxter and Wynn *et al.*, 2004). The elderly, therefore, are in much greater need of recapitulation of hMSC function, which primarily affects this section of the population e.g., osteoporosis.

5.4.2 Why Do PEG AuNPs Affect MSC Cell Gene Expression?

The fluidigm data indicated a wide range of general changes in gene expression responses for hMSCs when incubated with all of the AuNPs. Although gold is considered bio-inert, the very presence of the NPs and resultant AuNP-filled vesicles is likely to be producing a cellular response. It is conceivable that these vesicles could be altering an autophagy response or non-specifically influencing multiple pathways within the cell, in particular cellular trafficking.

The PEG AuNPs have no attached RNA sequences, and therefore exhibit a more neutral charge when compared to the other AuNPs. This could potentially lead to a higher uptake (as observed in the ICP-MS data) and increased intracellular trafficking, degradation and recycling when compared to the 5A, 3A and NS AuNPs. TEM images from the hMSCs treated with PEG for 48 hours showed that the majority of the AuNPs were free in the cytosol, rather than packaged into endosomes as seen with the other AuNPs. This difference in spatial organisation could be responsible for this increased metabolic activity seen in Figure 5-5 and Figure 5-6 by putting the cell under some form of stress response. However further experiments would be required to validate this

assumption. Ding *et al* (2014) found a differential effect of AuNPs on human kidney cells (HK-2), with the AuNPs up regulating autophagy in normoxic conditions, whilst under hypoxic conditions an increase in reactive oxygen species and programmed cell death was noted (Ding and Li *et al.*, 2014). With this information and the distribution of PEG AuNPs in the cytosol, it is conceivable that the PEG AuNP could be causing an increase gene expression by autophagy pathways as seen by the fluidigm data (Figure 5-6).

5.4.3 The Variability Between Osterix RNA and Protein Levels

The results in this chapter are variable. Fluidigm analysis at the RNA level did not demonstrate an increase in osterix levels with the 5A and 3A antagonists, however there was a suggestion of a cellular shift away from proliferation and towards differentiation when observing changes in other gene expression profiles. This may be due to the time points selected for analysis. As mentioned previously the RNA environment is a highly unstable and dynamic environment, with RNA's having a half-life anywhere between a couple of minutes and a few days (Fabian and Sonenberg *et al.*, 2010). This vast range means that there can be a lag time when comparing the RNA levels and the transcribed protein levels, with proteins tending to be far more stable. RNA transcription complexes can only produce one functional mRNA per read, however this mRNA can then go on to transcribe its protein a multitude of times, allowing for amplification. However mRNA can undergo many post-transcriptional modifications, which can degrade, make them dormant or enhance their stability. This makes understanding the RNA environment extremely complex, with the outcome being that only 40% of RNAs that change at the RNA level correspond to a change at the protein level (Vogel and Marcotte, 2012). This discrepancy means that it is simply not sufficient to look at the RNA level for miRNA therapeutic studies but a range of levels, such as the protein and physiological level. To confuse matters further, Wang *et al* (2010) demonstrated that a proportion of the 60% of RNAs mentioned by Vogel *et al* (2012) did

correlate with a change at protein level when a lag time was included (Wang and Wang *et al.*, 2010). This lag between the RNA and protein levels could be a reason for the seemingly contradictory results observed in the fluidigm and in-cell western data.

Due to the variable RNA levels, the protein environment is also dynamic. Over time, protein levels can fluctuate in delayed response to RNA signals. It is therefore prudent to measure proteins of interest over time. From Figure 5-7, we can see a dramatic increase in osterix levels at day 5, which drop off by day 7 and then recover and start to rise again by day 10, producing a cyclical response to osterix over time. The control hMSC, without any NPs, produce a far more stable and steady increase in osterix, rising exponentially from day 7 to 10 where it begins to plateau off. It could be reasonable to assume that given a longer time series, we would have observed the control cells and AuNP treated cells equilibrating together, suggesting that the antagomir treatment allowed for an initial spike in osterix, where cells then returned to control conditions.

5.4.4 Positive Downstream Effects of Increased Osterix

Osterix is the master transcriptional regulator of osteogenesis, to assess whether the antagomirs, after instigating a spike in osterix protein levels at day 5, produced effects further down the pathway; we selected osteocalcin as a protein of interest. Osteocalcin is only present during calcium nodule formation; these nodules are crucial for functional bone formation. Other assays could have been deployed to assess the downstream effectiveness of the antagomirs, however the presence of gold inside the cells produced a level of complexity that had to be resolved. Von Kossa staining, a gold standard for osteogenesis uses silver nitrate to stain calcium found in nodules. This stain colours calcium black, thus it would have been impossible to differentiate AuNPs and Von Kossa staining, giving false positives. The same is true for Alizarin Red, a stain measured by absorbance. The AuNPs within the

cells would block some of the light, reducing absorbance and again producing false positives. It was therefore only possible to elucidate functional osteogenesis by immuno-staining of late osteogenic markers (Figure 5-8 and Figure 5-9)

The staining showed a dramatic increase in 5A treatment of cells at week 3 and a sustained significant increase with 5A at week 5 of culture. This strongly suggests that the spike in osterix protein observed at day 5 was sufficient to accelerate those MSCs down the osteoblastic lineage at 3 and 5 weeks when compared to cells incubated with NS and PEG AuNPs, and control cells. This positive result is entirely novel, as to date no other studies have used AuNPs to delivery miRNA or antagomirs designed against specific miRNAs to influence MSC differentiation.

As reminiscent with the results for MG63 cells in the previous chapter, whereby a difference in efficacy was noted between the 3A and 5A sequences, with 5A producing a higher increase in osterix. Again, in this chapter, the 5A sequence initiates the better cell response in terms of increased osterix than the 3A.

5.5 Conclusion

The use of antagomirs against specific miRNAs known to be involved in stem cell differentiation has wide therapeutic potential. Whilst this study has indicated that such techniques should be possible, there are a number of issues that make successful deployment of antagomirs via NPs challenging. Elucidating the periodicity of the targeted miRNA is vitally important, in terms of when to apply the treatments and how long for; the length of exposure and duration of treatment must be systematically investigated. The direction of the antagomir sequence used should also be noted, as there are obvious differences in efficacy depending on whether a 5' or 3' sequence was used, both with a standard cells line (MG63 in chapter 4) and MSCs in this study. In addition, it should be noted that the variation of the cell type response must be considered, as identical cell types at different stages of aging can produce vastly different responses to the therapeutic.

6 Chapter 6: Discussion

6.1 Gold Nanoparticles: A Future in Clinic?

This thesis seeks to understand the practicality of delivering small molecules using gold AuNPs, and their potential therapeutic use in clinic. The underlying theme of the thesis has focused on the delivery of small RNAs with a view to influencing cellular behaviour in vitro. The initial experimental chapter 3 concentrated on reducing bone cancer cell growth, via delivery of siRNA against C-Myc, whilst the latter chapters (4 and 5) targeted an identified microRNA, mir-31, via antagomir delivery in both bone cancer cells and mesenchymal stem cells (MSCs) with a view to influencing osterix levels and ultimately stimulating bone differentiation. Generally, in each case, the original objective was attained, and the desired cell outcome was determined. However, from the literature and our own experimental discoveries, it is clear that further primary research must be carried out in order to understand the relationship between AuNPs and their target cells and tissues.

In order to conclude the thesis, the following section of writing aims to scope the current situation regarding the use of gold nanoparticles for clinical use, and determine whether the types of studies carried out during this PhD will indeed influence the future design of particles, based on their interaction at the cellular level.

It is clear that environmental factors such as the frequency of media changes and the time points selected can greatly influence results. Differences in growth media can alter cellular physiology, in turn altering cellular metabolism. This alteration can silence or produce off target effects of small RNA therapeutics. This for example, may be a possible explanation for the decrease in mir-31 expression in hMSCs recorded in the Baglio study (Baglio and DeVescovi et al., 2013). In this study the author's pre-primed hMSCs with media supplemented with dexamethasone (an osteogenic initiator) until nearly confluent, before

changing to mineralisation media. This was in contrast to the Guo study, who used the same type of media throughout and whereby the reverse was noted for mir-31 levels (Guo and Zhao et al., 2011b).

MiRNAs are regulated both temporally and spatially (Bratkovič and Glavan et al., 2012). Due to this, the duration of treatment during in vitro studies is highly important. If a miRNA is up-regulated for too long the cell could stall in a particular state. For example, induction media supplemented with BMP2 (a powerful osteoinductive cytokine) for 21 days was noticed to have a drastically reduced osteogenic response in comparison to media only supplemented with BMP2 for 2-4 days (Heggebo and Haasters et al., 2014). Therefore, care should be taken when planning experiments.

In addition, at the cellular level, the intracellular concentration of GSH can have a major impact on the successful delivery of our RNA cargos, based on thiol exchange release, which may bias any subsequent analysis of RNA therapeutics. Exploiting the thiol cleaving glutathione release mechanism for AuNP delivery of small regulatory RNAs requires understanding the intracellular GSH concentration, which in turn will dictate the necessary concentration of si/miRNA needed (Meister, 1988.,Rosi and Giljohann et al., 2006.,Lushchak, 2012).

Finally I have also learned that the RNA environment is a diverse and dynamic place, allowing only a small, and often undefined, timeframe to determine if an introduced RNA molecule has an effect on its supposed target; the difference of a few hours may mask any positive interaction with its target.

At present only three AuNPs have made it to clinical trials, and of these three none are delivering siRNA or miRNA. At present, liposomal delivery appears to be the dominant choice for small RNA delivery. However liposomes, as discussed in section 1.1, are not without their inherent problems as they can be cytotoxic, difficult to make

multifunctional and can “leak” their cargo. AuNPs have been demonstrated *in vitro* to be relatively non-cytotoxic in short term experiments; are multivalent, allowing for additional ligands for visualisation and targeting; and are able to effectively protect their cargo from degradation prior to release in the cell. However there is a large gap in the literature surrounding the toxicity of AuNP delivery of small RNAs such as siRNA and miRNA in humans. The very limited nanotoxicology studies concerning AuNPs are only short term *in vitro* or *in vivo* with mice (Connor and Mwamuka et al., 2005). Until the excellent advantages of AuNPs can be capitalised on in the clinic, their behaviour *in vivo* must be further studied.

6.2 The Use of siRNA and miRNA in Current Therapies

6.2.1 SiRNA Therapeutics

Current siRNA therapeutics offers the potential to treat the “undruggable” diseases caused by RNA dysregulation. SiRNAs are designed to bind with perfect complementarity to their target, however siRNA are ultimately made from nucleotides and these nucleotide sequences can partially bind to other RNA sequences producing unknown and potentially dangerous off-target effects. This is a major drawback for siRNA therapeutics in comparisons to using or targeting innate miRNAs. Several studies (described in chapter 1.3.4) have shown the effectiveness of siRNA targeting oncogenes, including our own studies in chapter 3 (Li and Chono et al., 2008., Conde and Tian et al., 2013). The siRNA dosage must be carefully considered, as excess siRNA can overwhelm the endogenous RNAi machinery, which can lead to an inflammatory response (Kasinski and Slack, 2011). In spite of these challenges however, twenty two siRNA-based therapeutics have successfully made it to clinical trials, with a variety of outcomes, since 2005. These trials have been summarised in Table 6-1. A conclusive list of current siRNA treatments undergoing clinical trials. All information was taken from clinicaltrials.gov. SNALPs (Stable Nucleic Acid Lipid

Particles) LODER polymer (biodegradable polymeric matrix). Several studies were terminated due to potential inflammatory immune responses, whilst others failed to progress into more advanced clinical trials. Rather disappointingly, to date, no siRNA treatment has left the clinic and made it onto the market.

6.2.2 MiRNA Therapeutics

As discussed previously miRNAs regulate a vast network of cellular processes and responses (section 1.2.2.2). This expansive array of miRNA offers the potential for a wide scope of therapeutics. Our understanding of miRNAs and their subsequent implication for treating diseases or influencing cell types is an area that is expanding exponentially and updated rapidly. As such miRNAs have been implicated as a target for oncology studies and more recently their application for cellular engineering.

Table 6-1. A conclusive list of current siRNA treatments undergoing clinical trials. All information was taken from clinicaltrials.gov. SNALPs (Stable Nucleic Acid Lipid Particles) LODER polymer (biodegradable polymeric matrix).

Date	Candidate	Disease target	Delivery route	Vehicle	Phase stage	Status	Company	Clinical Trial Identifier
2005	Bevasiranib	Age-related macular degeneration	Intravitreal	Free siRNA	III	Terminated	Opko Health	NCT00306904
2006	AGN211745	Age-Related Macular Degeneration	Injection	Free siRNA	II	Terminated	Allergan	NCT00395057
2007	ALN-RSV01	Respiratory syncytial virus infections	Nebulization	Free siRNA	I Ib	Completed	Alnylam/ Cubist	NCT01065935

Date	Candidate	Disease target	Delivery route	Vehicle	Phase stage	Status	Company	Clinical Trial Identifier
2008	TD101	Pachyonychia congenita	Intralesional	Free siRNA	Ib	Completed	TransDerm/IPCC	NCT00716014
2008	I5NP	Delayed graft function	Intravitreal	Free siRNA	II	Completed	Quark Pharma	NCT00802347
2008	ALN-VSP02	Solid tumour	Intravitreal	SNALP	I	Completed	Alynlan/Tekmira	NCT01158079
2008	CALAA01	Solid tumor	Intravitreal	Polyplex	I	Terminated	Calando Pharma	NCT00689065

Date	Candidate	Disease target	Delivery route	Vehicle	Phase stage	Status	Company	Clinical Trial Identifier
2009	SPC3649	Hepatitis C	Subcutaneous	LNA siRNA	IIa	Completed	Santaris	NCT00979927
2009	QPI-1007	Non-arteritic anterior ischemic optic neuropathy	Intravitreal	Free siRNA	I	Completed	Quark Pharma	NCT01064505
2009	SYL040012	Intraocular pressure	Eye drop	Free siRNA	II	Recruiting	Sylentis	NCT02250612
2009	TKM-ApoB	High cholesterol	Intravitreal	SNALP	I	Terminated	Tekmira	NCT00927459

Date	Candidate	Disease target	Delivery route	Vehicle	Phase stage	Status	Company	Clinical Trial Identifier
2009	ALN-TTR01	Transthyretin mediated amyloidosis	Intravitreal	SNALP	I	Completed	Alnylam	NCT01148953
2009	Atu027	Advanced solid tumor	Intravitreal	Lipoplex	I	Completed	Silence Therapeutics	NCT00938574
2010	siG12D LODER	Advanced pancreatic cancer	Intratumoral injection	LODER polymer	I	Completed	Silenceed Ltd.	NCT01188785

Date	Candidate	Disease target	Delivery route	Vehicle	Phase stage	Status	Company	Clinical Trial Identifier
2011	PF-4523655	Diabetic macular edema	Intravitreal	Free siRNA	II	Completed	Quark/Pfizer	NCT01445899
2011	SYL1001	Dry eye/ocular pain	Eye drop	Free siRNA	I	Completed	Sylentis	NCT01438281
2011	ALN-PCS02	LDL-Cholesterol	Intravitreal	SNALP	I	Completed	Alynlan	NCT01437059
2011	TKM-080301 (PLK1)	Cancer	Injection	SNALP	I	Completed	National Cancer Institute (NCI)	NCT01437007

Date	Candidate	Disease target	Delivery route	Vehicle	Phase stage	Status	Company	Clinical Trial Identifier
2012	EphA2	Cancer	Injection	Liposomal	I	Recruiting	M.D. Anderson Cancer Center	NCT01591356
2014	APN401	Cancer	Injection	siRNA-transfected peripheral blood mononuclear cells	I	Recruiting	Comprehensive Cancer Center of Wake Forest University	NCT02166255
2014	DCR-MYC	Cancer	intravenous infusion	Lipoplex	Ib/II	Recruiting	Dicerna Pharmaceuticals, Inc.	NCT02314052

Date	Candidate	Disease target	Delivery route	Vehicle	Phase stage	Status	Company	Clinical Trial Identifier
2014	ND-L02-s0201 (HSP47)	Hepatic fibrosis	intravenous infusion	Lipoplex	Ib/II	Recruiting	Nitto Denko Corporation	NCT02227459

6.2.3 Oncology

Thousands of miRNAs have been screened by high throughput analysis. From these experiments hundreds of individual miRNAs have been found to cluster around specific genomic sections prone to cancerous mutations, suggesting that miRNAs from these areas could be potential targets for cancer treatments (Calin and Sevignani et al., 2004). In fact, miRNAs are becoming so associated with cancer diagnostics, that miRNA expression profiles are being used to identify the type and stage of certain cancers (Ryan and Robles et al., 2010., Esquela-Kerscher and Slack, 2006., Calin and Croce, 2006). This in itself offers a fantastic advantage in the initial early diagnosis and follow-up treatment.

As described in section 1.3.3, cells can become addicted to certain oncogenes. Mir-21 over-expression has been reported in mouse models to induce multiple tumours and is found in many human tumour and serum samples (Medina and Nolde et al., 2010). However, blocking mir-21 expression in the mice models induced complete tumour regression, validating the theory that cells become addicted to only a few oncomirs and their subsequent silencing can halt cellular dysregulation (Medina and Nolde et al., 2010).

The therapeutic future of miRNAs looks promising with regards to oncology. Several studies in primates and mice have shown that miRNA degradation by antagomirs have limited side effects and can effectively silence metastatic cancers (Lanford and Hildebrandt-Eriksen et al., 2010., Tsai and Hsu et al., 2009., Krutzfeldt and Rajewsky et al., 2005a)

MiRNAs have also been linked to sensitizing tumours that are resistant to chemotherapies. Supplementing mir-9 into cell growth media was noted to reduce SOX2 expression, which indirectly pumps out cytotoxic drugs used by chemotherapies. By increasing mir-9 expression aggressive cancerous cells became vulnerable to chemotherapies (Jeon and Sohn et al., 2011).

It is therefore clear that by understanding the particular mechanism of a miRNAs action will help us design specific treatments. This can be difficult, as some miRNAs can appear to be oncogenic and oncosuppressive, depending on the context under which they are employed. For example mir-146 up regulation is associated with breast, thyroid and cervical cancer (Volinia and Calin et al., 2006.,Dahiya and Sherman-Baust et al., 2008). Conversely, however, over expressing mir-146 in hematopoietic cells seemed to provide a tumour suppressive role. As mir-146 knockout mice had a higher incidence of myeloid sarcomas and lymphomas (Zhao and Rao et al., 2011.,Boldin and Taganov et al., 2011.,Starczynowski and Kuchenbauer et al., 2011). Whereas other miRNAs are proving more straight forwards; mir-31 expression was noted to be down regulated in breast cancer cells, and over expressing mir-31 regressed the metastases of the tumour, switching the cancer from an aggressive, invasive tumour to a more benign phenotype. Suggesting a possible avenue for novel cancer therapeutics to use mir-31 in a supportive role for chemotherapies (Valastyan and Reinhardt et al., 2009.,Valastyan and Chang et al., 2011).

6.2.4 Encouraging Bone Formation

Dysregulation of miRNAs by diseases such as osteoporosis can lead to bone reabsorption creating weak, brittle bones. MiRNAs have been shown to maintain a fine controlled balance of ossification and reabsorption, and have therefore become a potential therapeutic opportunity. Reports to date have confirmed several miRNAs that inhibit osteogenic differentiation, such as mir-31, mir-206, mir-133, mir-125b and mir-135 (Guo and Zhao et al., 2011a.,Mizuno and Yagi et al., 2008.,van Wijnen and van de Peppel et al., 2013), whereas miRNAs such as miR-2861 and miR-3960 have been shown to promote calcification. (Scott and Goga et al., 2007.,Li and Xie et al., 2009.,Lee and Kim et al., 2005.,Mizuno and Yagi et al., 2008.,Inose and Ochi et al., 2009.,Kapinas and Kessler et al., 2009).

Our study in chapter 4 supported the increasingly established link between mir-31 expression and a decrease in osterix; we noted that blocking mir-31 in MG63 cells allowed for an increase in osterix. Whilst this result in itself is interesting, it is the potential use of the technology in MSCs that may prove to have potential. If we can artificially influence MSC differentiation towards the bone cell lineage, this will greatly benefit regenerative medicine and conditions such as osteoporosis and osteo imperfecta. In chapter 5 we carried on to demonstrate that blocking mir-31 did indeed encourage osteogenesis, with an early (day 5) increase in osterix providing a significant increase in bone forming osteocalcin further downstream at 3 weeks culture. These types of results are extremely encouraging, however it is the verification of these results in vivo that is now needed to progress the technology further towards the marketplace.

At last search, over 300 studies were found on clinicaltrials.gov linked to miRNAs. As was highlighted in the oncology section, all but one of the miRNAs currently undergoing clinical trials are being used as biomarkers for diagnostics. The exception to this is a miRNA mimic (MRX34, Clinical trial number NCT01829971). MRX34 is a liposomal-based injection designed to treat patients with advanced liver cancer. This is in complete contrast to siRNA, which is only used as a therapeutic. This disparity between the two small RNAs is probably in part due to the recent discovery of the depth and breadth miRNAs control and modulate cells.

6.3 Future Work

The experimental chapters in this thesis are all very encouraging with respect to the use of AuNPs in the delivery of small RNAs to cells in culture. The use of AuNPs as delivery agents for such therapeutics offer an immense potential to help remedy cellular dysregulation and “undruggable” diseases. However the use of siRNAs does prove problematic, as they present a very narrow field of blocking one target without considering the potential off-target effects. In contrast miRNA are known to block many mRNAs across a gene family, using miRNAs or their inhibitors could provide a safer therapeutic with less off-target effects.

All experimental work during this Ph.D. was performed *in vitro*. To advance this area of research further and develop AuNPs delivering siRNA and miRNA (including antagomirs) into a clinical setting, *in vivo* work will be required. This is needed to ensure that the early and promising studies *in vitro* follow through to the *in vivo* situation. Prior to this, however, certain considerations such as the duration of treatment, the treatment dose, the subsequent cytotoxicity and longer-term effects must all be considered. There is currently a wealth of information in the literature, and it is increasing exponentially. The collation of toxicological and efficacy data together with the development of therapeutic strategies would be of great benefit to this field of research. Whilst hurdles still remain, the delivery of small regulatory RNAs offers an exciting avenue for nanomedicine and the regenerative medicine field as a whole.

List of References

- AILI, D., GRYKO, P., SEPULVEDA, B., DICK, J. A., KIRBY, N., HEENAN, R., BALTZER, L., LIEBERG, B., RYAN, M. P. & STEVENS, M. M. 2011. Polypeptide folding-mediated tuning of the optical and structural properties of gold nanoparticle assemblies. *Nano Lett*, 11, 5564-73.
- AKHTAR, S., BASU, S., WICKSTROM, E. & JULIANO, R. L. 1991. INTERACTIONS OF ANTISENSE DNA OLIGONUCLEOTIDE ANALOGS WITH PHOSPHOLIPID-MEMBRANES (LIPOSOMES). *Nucleic Acids Research*, 19, 5551-5559.
- ALKILANY, A. M. & MURPHY, C. J. 2010. Toxicity and cellular uptake of gold nanoparticles: what we have learned so far? *J Nanopart Res*, 12, 2313-2333.
- ALKILANY, A. M., NAGARIA, P. K., HEXEL, C. R., SHAW, T. J., MURPHY, C. J. & WYATT, M. D. 2009. Cellular uptake and cytotoxicity of gold nanorods: molecular origin of cytotoxicity and surface effects. *Small*, 5, 701-8.
- AMERES, S. L., MARTINEZ, J. & SCHROEDER, R. 2007. Molecular basis for target RNA recognition and cleavage by human RISC. *Cell*, 130, 101-112.
- BAGLIÒ, S. R., DEVESCOVI, V., GRANCHI, D. & BALDINI, N. 2013. MicroRNA expression profiling of human bone marrow mesenchymal stem cells during osteogenic differentiation reveals Osterix regulation by miR-31. *Gene*, 527, 321-331.
- BAKOPOULOU, A., LEYHAUSEN, G., VOLK, J., KOIDIS, P. & GEURTSSEN, W. 2013. Comparative characterization of STRO-1(neg)/CD146(pos) and STRO-1(pos)/CD146(pos) apical papilla stem cells enriched with flow cytometry. *Arch Oral Biol*, 58, 1556-68.
- BANFI, A., MURAGLIA, A., DOZIN, B., MASTROGIACOMO, M., CANCEDDA, R. & QUARTO, R. 2000. Proliferation kinetics and differentiation potential of ex vivo expanded human bone marrow stromal cells: Implications for their use in cell therapy. *Exp Hematol*, 28, 707-715.
- BARRY, S. E. 2008. Challenges in the development of magnetic particles for therapeutic applications. *International Journal of Hyperthermia*, 24, 451-466.
- BAXTER, M. A., WYNN, R. F., JOWITT, S. N., WRAITH, J. E., FAIRBAIRN, L. J. & BELLANTUONO, I. 2004. Study of telomere length reveals rapid aging of human marrow stromal cells following in vitro expansion. *Stem Cells*, 22, 675-82.
- BECKER, A. J., MCCULLOCH, E. A. & TILL, J. E. 1963. Cytological demonstration of the clonal nature of spleen colonies derived from transplanted mouse marrow cells. *Nature*, 197, 452-454.
- BEIER, D., ROHRL, S., PILLAI, D. R., SCHWARZ, S., KUNZ-SCHUGHART, L. A., LEUKEL, P., PROESCHOLDT, M., BRAWANSKI, A., BOGDAHN, U., TRAMPE-KIESLICH, A., GIEBEL, B., WISCHHUSEN, J., REIFENBERGER, G., HAU, P. & BEIER, C. P. 2008.

- Temozolomide preferentially depletes cancer stem cells in glioblastoma. *Cancer Res*, 68, 5706-5715.
- BENFER, M. & KISSEL, T. 2012. Cellular uptake mechanism and knockdown activity of siRNA-loaded biodegradable DEAPA-PVA-g-PLGA nanoparticles. *Eur J Pharm Biopharm*, 80, 247-256.
- BENISCH, P., SCHILLING, T., KLEIN-HITPASS, L., FREY, S. P., SEEFRIED, L., RAAIJMAKERS, N., KRUG, M., REGENSBURGER, M., ZECK, S., SCHINKE, T., AMLING, M., EBERT, R. & JAKOB, F. 2012. The Transcriptional Profile of Mesenchymal Stem Cell Populations in Primary Osteoporosis Is Distinct and Shows Overexpression of Osteogenic Inhibitors. *Plos One*, 7.
- BERNSTEIN, E., CAUDY, A. A., HAMMOND, S. M. & HANNON, G. J. 2001. Role for a bidentate ribonuclease in the initiation step of RNA interference. *Nature*, 409, 363-366.
- BEROUKHIM, R., MERMEL, C. H., PORTER, D., WEI, G., RAYCHAUDHURI, S., DONOVAN, J., BARRETINA, J., BOEHM, J. S., DOBSON, J., URASHIMA, M., MC HENRY, K. T., PINCHBACK, R. M., LIGON, A. H., CHO, Y. J., HAERY, L., GREULICH, H., REICH, M., WINCKLER, W., LAWRENCE, M. S., WEIR, B. A., TANAKA, K. E., CHIANG, D. Y., BASS, A. J., LOO, A., HOFFMAN, C., PRENSNER, J., LIEFELD, T., GAO, Q., YECIES, D., SIGNORETTI, S., MAHER, E., KAYE, F. J., SASAKI, H., TEPPER, J. E., FLETCHER, J. A., TABERNERO, J., BASELGA, J., TSAO, M. S., DEMICHELIS, F., RUBIN, M. A., JANNE, P. A., DALY, M. J., NUCERA, C., LEVINE, R. L., EBERT, B. L., GABRIEL, S., RUSTGI, A. K., ANTONESCU, C. R., LADANYI, M., LETAI, A., GARRAWAY, L. A., LODA, M., BEER, D. G., TRUE, L. D., OKAMOTO, A., POMEROY, S. L., SINGER, S., GOLUB, T. R., LANDER, E. S., GETZ, G., SELLERS, W. R. & MEYERSON, M. 2010. The landscape of somatic copy-number alteration across human cancers. *Nature*, 463, 899-905.
- BERRY, C. C. 2008. Intracellular delivery of nanoparticles via the HIV-1 tat peptide. *Nanomedicine (Lond)*, 3, 357-65.
- BHUSHAN, R., GRÜNHAGEN, J., BECKER, J., ROBINSON, P. N., OTT, C.-E. & KNAUS, P. 2013. miR-181a promotes osteoblastic differentiation through repression of TGF- β signaling molecules. *Int J Biochem Cell Biol*, 45, 696-705.
- BIGGS, M. J. P., RICHARDS, R. G., GADEGAARD, N., WILKINSON, C. D. W., OREFFO, R. O. C. & DALBY, M. J. 2009. The use of nanoscale topography to modulate the dynamics of adhesion formation in primary osteoblasts and ERK/MAPK signalling in STRO-1+ enriched skeletal stem cells. *Biomaterials*, 30, 5094-5103.
- BOISSELIER, E. & ASTRUC, D. 2009. Gold nanoparticles in nanomedicine: preparations, imaging, diagnostics, therapies and toxicity. *Chemical Society Reviews*, 38, 1759.
- BOISVERT, M. & TIJSSEN, P. 2012. *Endocytosis of Non-Enveloped DNA Viruses*.
- BOLAND, G. M., PERKINS, G., HALL, D. J. & TUAN, R. S. 2004. Wnt 3a promotes proliferation and suppresses osteogenic differentiation of adult human mesenchymal stem cells. *J Cell Biochem*, 93, 1210-1230.

- BOLDIN, M. P., TAGANOV, K. D., RAO, D. S., YANG, L., ZHAO, J. L., KALWANI, M., GARCIA-FLORES, Y., LUONG, M., DEVREKANLI, A., XU, J., SUN, G., TAY, J., LINSLEY, P. S. & BALTIMORE, D. 2011. miR-146a is a significant brake on autoimmunity, myeloproliferation, and cancer in mice. *J Exp Med*, 208, 1189-201.
- BOSELNANN S FAU - WILLIAMS, R. O. & WILLIAMS, R. O. 2004. Has nanotechnology led to improved therapeutic outcomes? *Drug Development and Industrial Pharmacy*, 38.
- BRATKOVIČ, T., GLAVAN, G., ŠTRUKELJ, B., ŽIVIN, M. & ROGELJ, B. 2012. Exploiting microRNAs for cell engineering and therapy. *Biotechnology Advances*, 30, 753-765.
- BUMCROT, D., MANOHARAN, M., KOTELIANSKY, V. & SAH, D. W. Y. 2006. RNAi therapeutics: a potential new class of pharmaceutical drugs. *Nat Chem Biol*, 2, 711-719.
- CACCHIARELLI, D., INCITTI, T., MARTONE, J., CESANA, M., CAZZELLA, V., SANTINI, T., STHANDIER, O. & BOZZONI, I. 2011. miR-31 modulates dystrophin expression: new implications for Duchenne muscular dystrophy therapy. *EMBO Rep*, 12, 136-41.
- CALIN, G. A. & CROCE, C. M. 2006. MicroRNA signatures in human cancers. *Nat Rev Cancer*, 6, 857-66.
- CALIN, G. A., FERRACIN, M., CIMMINO, A., DI LEVA, G., SHIMIZU, M., WOJCIK, S. E., IORIO, M. V., VISIONE, R., SEVER, N. I., FABBRI, M., IULIANO, R., PALUMBO, T., PICHIORRI, F., ROLDO, C., GARZON, R., SEVIGNANI, C., RASSENTI, L., ALDER, H., VOLINIA, S., LIU, C. G., KIPPS, T. J., NEGRINI, M. & CROCE, C. M. 2005. A MicroRNA signature associated with prognosis and progression in chronic lymphocytic leukemia. *N Engl J Med*, 353, 1793-801.
- CALIN, G. A., SEVIGNANI, C., DUMITRU, C. D., HYSLOP, T., NOCH, E., YENDAMURI, S., SHIMIZU, M., RATTAN, S., BULLRICH, F., NEGRINI, M. & CROCE, C. M. 2004. Human microRNA genes are frequently located at fragile sites and genomic regions involved in cancers. *Proc Natl Acad Sci U S A*, 101, 2999-3004.
- CASADO-DÍAZ, A., PÉREZ, G. D. & QUESADA-GÓMEZ, J. M. 2011. 5.36 - Stem Cell Research and Molecular Markers in Medicine. In: MOO-YOUNG, M. (ed.) *Comprehensive Biotechnology (Second Edition)*. Burlington: Academic Press.
- CASSINELLI, G., SUPINO, R., ZUCO, V., LANZI, C., SCOVASSI, A. I., SEMPLE, S. C. & ZUNINO, F. 2004. Role of c-myc protein in hormone refractory prostate carcinoma: cellular response to paclitaxel. *Biochem Pharmacol*, 68, 923-31.
- CASTANOTTO, D. & ROSSI, J. J. 2009. The promises and pitfalls of RNA-interference-based therapeutics. *Nature*, 457, 426-33.
- CEBRIAN, V., MARTIN-SAAVEDRA, F., YAGUE, C., ARRUEBO, M., SANTAMARIA, J. & VILABOIA, N. 2011. Size-dependent transfection efficiency of PEI-coated gold nanoparticles. *Acta Biomater*, 7, 3645-55.
- CHAN, Y. T., LIN, Y. C., LIN, R. J., KUO, H. H., THANG, W. C., CHIU, K. P. & YU, A. L. 2013. Concordant and discordant regulation of target genes by miR-31 and its isoforms. *PLoS One*, 8, e58169.

- CHANG, K. W., KAO, S. Y., WU, Y. H., TSAI, M. M., TU, H. F., LIU, C. J., LUI, M. T. & LIN, S. C. 2013. Passenger strand miRNA miR-31* regulates the phenotypes of oral cancer cells by targeting RhoA. *Oral Oncol*, 49, 27-33.
- CHAUHAN, V. P., STYLIANOPOULOS, T., BOUCHER, Y. & JAIN, R. K. 2011. Delivery of molecular and nanoscale medicine to tumors: transport barriers and strategies. *Annu Rev Chem Biomol Eng*, 2, 281-98.
- CHEN, G., DENG, C. & LI, Y.-P. 2012. TGF- β and BMP Signaling in Osteoblast Differentiation and Bone Formation. *International Journal of Biological Sciences*, 8, 272-288.
- CHEN, H., LI, B., REN, X., LI, S., MA, Y., CUI, S. & GU, Y. 2012. Multifunctional near-infrared-emitting nano-conjugates based on gold clusters for tumor imaging and therapy. *Biomaterials*, 33, 8461-8476.
- CHEN, H. T., LEE, M. J., CHEN, C. H., CHUANG, S. C., CHANG, L. F., HO, M. L., HUNG, S. H., FU, Y. C., WANG, Y. H., WANG, H. I., WANG, G. J., KANG, L. & CHANG, J. K. 2012. Proliferation and differentiation potential of human adipose-derived mesenchymal stem cells isolated from elderly patients with osteoporotic fractures. *J Cell Mol Med*, 16, 582-93.
- CHEN, Z., XU, R., ZHANG, Y. & GU, N. 2008. Effects of proteins from culture medium on surface property of silanes- functionalized magnetic nanoparticles. *Nanoscale Res Lett*, 4, 204-9.
- CHENG, Y., MEYERS, J. D., AGNES, R. S., DOANE, T. L., KENNEY, M. E., BROOME, A.-M., BURDA, C. & BASILION, J. P. 2011. Addressing Brain Tumors with Targeted Gold Nanoparticles: A New Gold Standard for Hydrophobic Drug Delivery? *Small*, 7, 2301-2306.
- CHENG, Z., AL ZAKI, A., HUI, J. Z., MUZYKANTOV, V. R. & TSOURKAS, A. 2012. Multifunctional Nanoparticles: Cost Versus Benefit of Adding Targeting and Imaging Capabilities. *Science*, 338, 903-910.
- CHITHRANI, B. D. & CHAN, W. C. W. 2007. Elucidating the mechanism of cellular uptake and removal of protein-coated gold nanoparticles of different sizes and shapes. *Nano Lett.*, 7, 1542-1550.
- CHITHRANI, B. D., GHAZANI, A. A. & CHAN, W. C. 2006. Determining the size and shape dependence of gold nanoparticle uptake into mammalian cells. *Nano Lett*, 6, 662-8.
- CHITHRANI, D. B. 2010. Intracellular uptake, transport, and processing of gold nanostructures. *Mol Membr Biol*, 27, 299-311.
- CHIU, Y.-L. & RANA, T. M. 2003. siRNA function in RNAi: a chemical modification analysis. *RNA*, 9, 1034-1048.
- CHO, W.-S., CHO, M., JEONG, J., CHOI, M., HAN, B. S., SHIN, H.-S., HONG, J., CHUNG, B. H., JEONG, J. & CHO, M.-H. 2010. Size-dependent tissue kinetics of PEG-coated gold nanoparticles. *Toxicology and Applied Pharmacology*, 245, 116-123.
- CHOMPOOSOR, A., HAN, G. & ROTELLO, V. M. 2008. Charge dependence of ligand release and monolayer stability of gold nanoparticles by biogenic thiols. *Bioconjug Chem*, 19, 1342-5.

- CIAFRE, S. A., GALARDI, S., MANGIOLA, A., FERRACIN, M., LIU, C. G., SABATINO, G., NEGRINI, M., MAIRA, G., CROCE, C. M. & FARACE, M. G. 2005. Extensive modulation of a set of microRNAs in primary glioblastoma. *Biochem Biophys Res Commun*, 334, 1351-8.
- CIMMINO, A., CALIN, G. A., FABBRI, M., IORIO, M. V., FERRACIN, M., SHIMIZU, M., WOJCIK, S. E., AQEILAN, R. I., ZUPO, S., DONO, M., RASSENTI, L., ALDER, H., VOLINIA, S., LIU, C. G., KIPPS, T. J., NEGRINI, M. & CROCE, C. M. 2005. miR-15 and miR-16 induce apoptosis by targeting BCL2. *Proc Natl Acad Sci U S A*, 102, 13944-9.
- CLARKE, D. L., JOHANSSON, C. B., WILBERTZ, J., VERESS, B., NILSSON, E., KARLSTROM, H., LENDAHL, U. & FRISEN, J. 2000. Generalized potential of adult neural stem cells. *Science*, 288, 1660-3.
- CLIFT, M. J. D., ROTHEN-RUTISHAUSER, B., BROWN, D. M., DUFFIN, R., DONALDSON, K., PROUDFOOT, L., GUY, K. & STONE, V. 2008. The impact of different nanoparticle surface chemistry and size on uptake and toxicity in a murine macrophage cell line. *Toxicology and Applied Pharmacology*, 232, 418-427.
- CONDE, J., AMBROSONE, A., SANZ, V., HERNANDEZ, Y., MARCHESANO, V., TIAN, F., CHILD, H., BERRY, C. C., IBARRA, M. R., BAPTISTA, P. V., TORTIGLIONE, C. & DE LA FUENTE, J. M. 2012. Design of Multifunctional Gold Nanoparticles for In Vitro and In Vivo Gene Silencing. *ACS Nano*, 6, 8316-8324.
- CONDE, J., TIAN, F. R., HERNANDEZ, Y., BAO, C. C., CUI, D. X., JANSSEN, K. P., IBARRA, M. R., BAPTISTA, P. V., STOEGER, T. & DE LA FUENTE, J. M. 2013. In vivo tumor targeting via nanoparticle-mediated therapeutic siRNA coupled to inflammatory response in lung cancer mouse models. *Biomaterials*, 34, 7744-7753.
- CONNER, S. D. & SCHMID, S. L. 2003. Regulated portals of entry into the cell. *Nature*, 422, 37-44.
- CONNOR, E. E., MWAMUKA, J., GOLE, A., MURPHY, C. J. & WYATT, M. D. 2005. Gold nanoparticles are taken up by human cells but do not cause acute cytotoxicity. *Small*, 1, 1613-6829.
- CUI, D., TIAN, F., OZKAN, C. S., WANG, M. & GAO, H. 2005. Effect of single wall carbon nanotubes on human HEK293 cells. *Toxicol Lett*, 155, 73-85.
- DAHIYA, N., SHERMAN-BAUST, C. A., WANG, T. L., DAVIDSON, B., SHIH IE, M., ZHANG, Y., WOOD, W., 3RD, BECKER, K. G. & MORIN, P. J. 2008. MicroRNA expression and identification of putative miRNA targets in ovarian cancer. *PLoS One*, 3, e2436.
- DALBY, M. J., GADEGAARD, N., TARE, R., ANDAR, A., RIEHLE, M. O., HERZYK, P., WILKINSON, C. D. & OREFFO, R. O. 2007. The control of human mesenchymal cell differentiation using nanoscale symmetry and disorder. *Nat Mater*, 6, 997-1003.
- DALLA-FAVERA, R., BREGNI, M., ERIKSON, J., PATTERSON, D., GALLO, R. C. & CROCE, C. M. 1982. Human c-myc oncogene is located on

- the region of chromosome 8 that is translocated in Burkitt lymphoma cells. *Proc Natl Acad Sci U S A*, 79, 7824-7.
- DANG, C. V. 2012. MYC on the path to cancer. *Cell*, 149, 22-35.
- DAVIS, M. E., ZUCKERMAN, J. E., CHOI, C. H., SELIGSON, D., TOLCHER, A., ALABI, C. A., YEN, Y., HEIDEL, J. D. & RIBAS, A. 2010. Evidence of RNAi in humans from systemically administered siRNA via targeted nanoparticles. *Nature*, 464, 1067-70.
- DE NIGRIS, F., BALESTRIERI, M. L. & NAPOLI, C. 2006. Targeting c-Myc, Ras and IGF cascade to treat cancer and vascular disorders. *Cell Cycle*, 5, 1621-8.
- DECUZZI, P., GODIN, B., TANAKA, T., LEE, S. Y., CHIAPPINI, C., LIU, X. & FERRARI, M. 2010. Size and shape effects in the biodistribution of intravascularly injected particles. *J Control Release*, 141, 320-327.
- DENG, Y., WU, S., ZHOU, H., BI, X., WANG, Y., HU, Y., GU, P. & FAN, X. 2013. Effects of a miR-31, Runx2, and Satb2Regulatory Loop on the Osteogenic Differentiation of Bone Mesenchymal Stem Cells. *Stem Cells and Development*, 22, 2278-2286.
- DENG, Y., ZHOU, H., ZOU, D., XIE, Q., BI, X., GU, P. & FAN, X. 2013. The role of miR-31-modified adipose tissue-derived stem cells in repairing rat critical-sized calvarial defects. *Biomaterials*, 34, 6717-6728.
- DERFUS, A. M., CHEN, A. A., MIN, D. H., RUOSLAHTI, E. & BHATIA, S. N. 2007. Targeted quantum dot conjugates for siRNA delivery. *Bioconjugate Chem.*, 18, 1391-1396.
- DEXTER, D. L., KOWALSKI, H. M., BLAZAR, B. A., FLIGIEL, Z., VOGEL, R. & HEPPNER, G. H. 1978. Heterogeneity of tumor cells from a single mouse mammary tumor. *Cancer Res*, 38, 3174-81.
- DING, F., LI, Y., LIU, J., LIU, L., YU, W., WANG, Z., NI, H., LIU, B. & CHEN, P. 2014. Overendocytosis of gold nanoparticles increases autophagy and apoptosis in hypoxic human renal proximal tubular cells. *International Journal of Nanomedicine*, 9, 4317-4330.
- DOENCH, J. G. & SHARP, P. A. 2004. Specificity of microRNA target selection in translational repression. *Genes Dev*, 18, 504-11.
- DOHERTY, G. J. & MCMAHON, H. T. 2009. Mechanisms of Endocytosis. *Annual Review of Biochemistry*.
- DONG, S., YANG, B., GUO, H. & KANG, F. 2012. MicroRNAs regulate osteogenesis and chondrogenesis. *BIOCHEMICAL AND BIOPHYSICAL RESEARCH COMMUNICATIONS*, 418, 587-591.
- DONG, W. J., ZHANG, P., FU, Y., GE, J., CHENG, J., YUAN, H. & JIANG, H. B. 2015. Roles of SATB2 in Site-Specific Stemness, Autophagy and Senescence of Bone Marrow Mesenchymal Stem Cells. *Journal of Cellular Physiology*, 230, 680-690.
- DOWLING, A., CLIFT, R., GROBERT, N., HUTTON, D., OLIVER, R., O'NEILL, O., PETHICA, J., PIDGEON, N., PORRITT, J. & RYAN, J. 2004. Nanoscience and nanotechnologies: opportunities and uncertainties. *London: The Royal Society & The Royal Academy of Engineering Report*, 61-64.

- DREADEN, E. C., MACKEY, M. A., HUANG, X., KANG, B. & EL-SAYED, M. A. 2011. Beating cancer in multiple ways using nanogold. *Chem Soc Rev*, 40, 3391-404.
- DYKXHOORN, D. M. & LIEBERMAN, J. 2005. The Silent Revolution: RNA Interference as Basic Biology, Research Tool, and Therapeutic. *Annual Review of Medicine*, 56, 401-423.
- EHRENBERG, M. S., FRIEDMAN, A. E., FINKELSTEIN, J. N., OBERDÖRSTER, G. & MCGRATH, J. L. 2008. The influence of protein adsorption on nanoparticle association with cultured endothelial cells. *Biomaterials*, 30, 603-610.
- ELBASHIR, S. M., HARBORTH, J., LENDECKEL, W., YALCIN, A., WEBER, K. & TUSCHL, T. 2001. Duplexes of 21-nucleotide RNAs mediate RNA interference in cultured mammalian cells. *Nature*, 411, 494-498.
- ELL, B. & KANG, Y. 2014. MicroRNAs as regulators of bone homeostasis and bone metastasis. *Bonekey Rep*, 3, 549.
- ESLAMINEJAD, M. B., KARIMI, N. & SHAHHOSEINI, M. 2013. Chondrogenic differentiation of human bone marrow-derived mesenchymal stem cells treated by GSK-3 inhibitors. *Histochem Cell Biol*, 140, 623-33.
- ESQUELA-KERSCHER, A. & SLACK, F. J. 2006. Oncomirs - microRNAs with a role in cancer. *Nat Rev Cancer*, 6, 259-69.
- EVANS, M. J. & KAUFMAN, M. H. 1981. Establishment in culture of pluripotential cells from mouse embryos. *Nature*, 292, 154-6.
- FABIAN, M. R., SONENBERG, N. & FILIPOWICZ, W. 2010. Regulation of mRNA translation and stability by microRNAs. *Annu Rev Biochem*, 79, 351-79.
- FANG, Y.-Z., YANG, S. & WU, G. 2002. Free radicals, antioxidants, and nutrition. *Nutrition*, 18, 872-879.
- FENG, J., HUANG, C., DIAO, X., FAN, M., WANG, P., XIAO, Y., ZHONG, X. & WU, R. 2013. Screening biomarkers of prostate cancer by integrating microRNA and mRNA microarrays. *Genet Test Mol Biomarkers*, 17, 807-13.
- FERLAY, J., SHIN, H. R., BRAY, F., FORMAN, D., MATHERS, C. & PARKIN, D. M. 2010. Estimates of worldwide burden of cancer in 2008: GLOBOCAN 2008. *Int J Cancer*, 127, 2893-917.
- FERRARI, M. 2005. Cancer nanotechnology: opportunities and challenges. *Nat Rev Cancer*, 5, 161-71.
- FIRE, A., XU, S. Q., MONTGOMERY, M. K., KOSTAS, S. A., DRIVER, S. E. & MELLO, C. C. 1998. Potent and specific genetic interference by double-stranded RNA in *Caenorhabditis elegans*. *Nature*, 391, 806-811.
- FISCHER, H. C. & CHAN, W. C. 2007. Nanotoxicity: the growing need for in vivo study. *Curr Opin Biotechnol*, 18, 565-71.
- FREE, P., SHAW, C. P. & LEVY, R. 2009. PEGylation modulates the interfacial kinetics of proteases on peptide-capped gold nanoparticles. *Chem Commun (Camb)*, 5009-11.
- FRENS, G. 1973. Controlled Nucleation for Regulation of Particle-Size in Monodisperse Gold Suspensions. *Nature-Physical Science*, 241, 20-22.

- FRIEDENSTEIN, A. J., GORSKAJA, J. F. & KULAGINA, N. N. 1976. Fibroblast precursors in normal and irradiated mouse hematopoietic organs. *Exp Hematol*, 4, 267-274.
- GABIZON, A. A., SHMEEDA, H. & ZALIPSKY, S. 2006. Pros and cons of the liposome platform in cancer drug targeting. *J Liposome Res*, 16, 175-83.
- GANG, E. J., HONG, S. H., JEONG, J. A., HWANG, S. H., KIM, S. W., YANG, I. H., AHN, C., HAN, H. & KIM, H. 2004. In vitro mesengenic potential of human umbilical cord blood-derived mesenchymal stem cells. *Biochem Biophys Res Commun*, 321, 102-108.
- GAO, J., YANG, T., HAN, J., YAN, K., QIU, X., ZHOU, Y., FAN, Q. & MA, B. 2011. MicroRNA expression during osteogenic differentiation of human multipotent mesenchymal stromal cells from bone marrow. *J. Cell. Biochem.*, 112, 1844-1856.
- GAO, S., DAGNAES-HANSEN, F., NIELSEN, E. J. B., WENGEL, J., BESENBACHER, F., HOWARD, K. A. & KJEMS, J. 2009. The Effect of Chemical Modification and Nanoparticle Formulation on Stability and Biodistribution of siRNA in Mice. *Molecular Therapy*, 17, 1225-1233.
- GASIOROWSKI, J. Z., LILIENSIEK, S. J., RUSSELL, P., STEPHAN, D. A., NEALEY, P. F. & MURPHY, C. J. 2010. Alterations in gene expression of human vascular endothelial cells associated with nanotopographic cues. *Biomaterials*, 31, 8882-8888.
- GHOSH, P., HAN, G., DE, M., KIM, C. K. & ROTELLO, V. M. 2008. Gold nanoparticles in delivery applications. *Adv Drug Deliv Rev*, 60, 1307-15.
- GHOSH, R., SINGH, L. C., SHOHET, J. M. & GUNARATNE, P. H. 2012. A gold nanoparticle platform for the delivery of functional microRNAs into cancer cells. *Biomaterials*, 1-10.
- GILJOHANN, D. A., SEFEROS, D. S., PATEL, P. C., MILLSTONE, J. E., ROSI, N. L. & MIRKIN, C. A. 2007. Oligonucleotide loading determines cellular uptake of DNA-modified gold nanoparticles. *Nano Lett*, 7, 3818-21.
- GILJOHANN, D. A., SEFEROS, D. S., PRIGODICH, A. E., PATEL, P. C. & MIRKIN, C. A. 2009. Gene regulation with polyvalent siRNA-nanoparticle conjugates. *J Am Chem Soc*, 131, 2072-3.
- GOODMAN, C. M., MCCUSKER, C. D., YILMAZ, T. & ROTELLO, V. M. 2004. Toxicity of gold nanoparticles functionalized with cationic and anionic side chains. *Bioconjug Chem*, 15, 897-900.
- GRIGSBY, C. L. & LEONG, K. W. 2010. Balancing protection and release of DNA: tools to address a bottleneck of non-viral gene delivery. *J R Soc Interface*, 7 Suppl 1, S67-82.
- GROTHEY, A. 2006. Future directions in vascular endothelial growth factor-targeted therapy for metastatic colorectal cancer. *Semin Oncol*, 33, S41-9.
- GUO, H., INGOLIA, N. T., WEISSMAN, J. S. & BARTEL, D. P. 2010. Mammalian microRNAs predominantly act to decrease target mRNA levels. *Nature*, 466, 835-840.

- GUO, L., ZHAO, R. C. H. & WU, Y. 2011a. The role of microRNAs in self-renewal and differentiation of mesenchymal stem cells. *Experimental Hematology*, 39, 608-616.
- GUO, L., ZHAO, R. C. H. & WU, Y. 2011b. The role of microRNAs in self-renewal and differentiation of mesenchymal stem cells. *Experimental Hematology*, 39, 608-616.
- HAKKINEN, H. 2012. The gold-sulfur interface at the nanoscale. *Nat Chem*, 4, 443-55.
- HALABY, M. J. & YANG, D. Q. 2007. p53 translational control: a new facet of p53 regulation and its implication for tumorigenesis and cancer therapeutics. *Gene*, 395, 1-7.
- HALDER, J., KAMAT, A. A., LANDEN, C. N., JR., HAN, L. Y., LUTGENDORF, S. K., LIN, Y. G., MERRITT, W. M., JENNINGS, N. B., CHAVEZ-REYES, A., COLEMAN, R. L., GERSHENSON, D. M., SCHMANDT, R., COLE, S. W., LOPEZ-BERESTEIN, G. & SOOD, A. K. 2006. Focal adhesion kinase targeting using in vivo short interfering RNA delivery in neutral liposomes for ovarian carcinoma therapy. *Clin Cancer Res*, 12, 4916-24.
- HAMILTON, A. J. & BAULCOMBE, D. C. 1999. A species of small antisense RNA in posttranscriptional gene silencing in plants. *Science*, 286, 950-2.
- HE, H., JAZDZEWSKI, K., LI, W., LIYANARACHCHI, S., NAGY, R., VOLINIA, S., CALIN, G. A., LIU, C. G., FRANSSILA, K., SUSTER, S., KLOOS, R. T., CROCE, C. M. & DE LA CHAPELLE, A. 2005. The role of microRNA genes in papillary thyroid carcinoma. *Proc Natl Acad Sci U S A*, 102, 19075-80.
- HEGGEBO, J., HAASTERS, F., POLZER, H., SCHWARZ, C., SALLER, M. M., MUTSCHLER, W., SCHIEKER, M. & PRALL, W. C. 2014. Aged human mesenchymal stem cells: the duration of bone morphogenetic protein-2 stimulation determines induction or inhibition of osteogenic differentiation. *Orthopedic reviews*, 6, 5242-5242.
- HINTERWIRTH, H., KAPPEL, S., WAITZ, T., PROHASKA, T., LINDNER, W. & LAMMERHOFER, M. 2013. Quantifying thiol ligand density of self-assembled monolayers on gold nanoparticles by inductively coupled plasma-mass spectrometry. *ACS Nano*, 7, 1129-36.
- HOSHINO, A., MANABE, N., FUJIOKA, K., SUZUKI, K., YASUHARA, M. & YAMAMOTO, K. 2007. Use of fluorescent quantum dot bioconjugates for cellular imaging of immune cells, cell organelle labeling, and nanomedicine: surface modification regulates biological function, including cytotoxicity. *J Artif Organs*, 10, 149-57.
- HOUBAVIY, H. B., MURRAY, M. F. & SHARP, P. A. 2003. Embryonic stem cell-specific MicroRNAs. *Dev Cell*, 5, 351-358.
- HUA, S., XIAOTAO, X., RENHUA, G., YONGMEI, Y., LIANKE, L., WEN, G. & YONGQIAN, S. 2012. Reduced miR-31 and let-7 maintain the balance between differentiation and quiescence in lung cancer stem-like side population cells. *Biomed Pharmacother*, 66, 89-97.

- HUANG, C., LI, M., CHEN, C. Y. & YAO, Q. Z. 2008. Small interfering RNA therapy in cancer: mechanism, potential targets, and clinical applications. *Expert Opinion on Therapeutic Targets*, 12, 637-645.
- HUANG, X. & EL-SAYED, M. A. 2010. Gold nanoparticles: Optical properties and implementations in cancer diagnosis and photothermal therapy. *Journal of Advanced Research*, 1, 13-28.
- HUANG, X., JAIN, P. K., EL-SAYED, I. H. & EL-SAYED, M. A. 2007. Gold nanoparticles: interesting optical properties and recent applications in cancer diagnostics and therapy. *Nanomedicine (Lond)*, 2, 681-93.
- HUNG, P. S., TU, H. F., KAO, S. Y., YANG, C. C., LIU, C. J., HUANG, T. Y., CHANG, K. W. & LIN, S. C. 2014. miR-31 is upregulated in oral premalignant epithelium and contributes to the immortalization of normal oral keratinocytes. *Carcinogenesis*, 35, 1162-71.
- INOSE, H., OCHI, H., KIMURA, A., FUJITA, K., XU, R., SATO, S., IWASAKI, M., SUNAMURA, S., TAKEUCHI, Y., FUKUMOTO, S., SAITO, K., NAKAMURA, T., SIOMI, H., ITO, H., ARAI, Y., SHINOMIYA, K. & TAKEDA, S. 2009. A microRNA regulatory mechanism of osteoblast differentiation. *Proc Natl Acad Sci U S A*, 106, 20794-9.
- IORIO, M. V., FERRACIN, M., LIU, C. G., VERONESE, A., SPIZZO, R., SABBIONI, S., MAGRI, E., PEDRIALI, M., FABBRI, M., CAMPIGLIO, M., MENARD, S., PALAZZO, J. P., ROSENBERG, A., MUSIANI, P., VOLINIA, S., NENCI, I., CALIN, G. A., QUERZOLI, P., NEGRINI, M. & CROCE, C. M. 2005. MicroRNA gene expression deregulation in human breast cancer. *Cancer Res*, 65, 7065-70.
- IWASE, H., SHIMADA, M., TSUZUKI, T., OKEYA, M., KOBAYASHI, K., HIBINO, Y., WATANABE, H. & GOTO, H. 2006. A phase I study of S-1 administration and a 24-h infusion of cisplatin plus paclitaxel in patients with advanced gastric cancer. *Anticancer Res*, 26, 1605-9.
- JAIN, M., ARVANITIS, C., CHU, K., DEWEY, W., LEONHARDT, E., TRINH, M., SUNDBERG, C. D., BISHOP, J. M. & FELSHER, D. W. 2002. Sustained loss of a neoplastic phenotype by brief inactivation of MYC. *Science*, 297, 102-4.
- JEON, H. M., SOHN, Y. W., OH, S. Y., KIM, S. H., BECK, S., KIM, S. & KIM, H. 2011. ID4 imparts chemoresistance and cancer stemness to glioma cells by derepressing miR-9*-mediated suppression of SOX2. *Cancer Res*, 71, 3410-21.
- JI, H., WU, G., ZHAN, X., NOLAN, A., KOH, C., DE MARZO, A., DOAN, H. M., FAN, J., CHEADLE, C., FALLAHI, M., CLEVELAND, J. L., DANG, C. V. & ZELLER, K. I. 2011. Cell-type independent MYC target genes reveal a primordial signature involved in biomass accumulation. *PLoS One*, 6, e26057.
- JIANG, Y., JAHAGIRDAR, B. N., REINHARDT, R. L., SCHWARTZ, R. E., KEENE, C. D., ORTIZ-GONZALEZ, X. R., REYES, M., LENVIK, T., LUND, T., BLACKSTAD, M., DU, J., ALDRICH, S., LISBERG, A., LOW, W. C., LARGAESPADA, D. A. & VERFAILLIE, C. M. 2002. Pluripotency of mesenchymal stem cells derived from adult marrow. *Nature*, 418, 41-9.

- JOKERST JV FAU - GAMBHIR, S. S. & GAMBHIR, S. S. 2011. Molecular imaging with theranostic nanoparticles. *Acc. Chem. Res.*, 44, 1050-1060.
- JOKERST, J. V. & GAMBHIR, S. S. 2011. Molecular imaging with theranostic nanoparticles. *Acc Chem Res*, 44, 1050-60.
- JOKERST, J. V., LOBOVKINA, T., ZARE, R. N. & GAMBHIR, S. S. 2011. Nanoparticle PEGylation for imaging and therapy. *6*, 715-728.
- JULIANO, R., ALAM, M. R., DIXIT, V. & KANG, H. 2008. Mechanisms and strategies for effective delivery of antisense and siRNA oligonucleotides. *Nucleic Acids Research*, 36, 4158-4171.
- KAH, J. C. Y., WONG, K. Y., NEOH, K. G., SONG, J. H., FU, J. W. P., MHAISALKAR, S., OLIVO, M. & SHEPPARD, C. J. R. 2009. Critical parameters in the pegylation of gold nanoshells for biomedical applications: an in vitro macrophage study. *J Drug Target*, 17, 181-193.
- KAJI, K., NORRBY, K., PACA, A., MILEIKOVSKY, M., MOHSENI, P. & WOLTJEN, K. 2009. Virus-free induction of pluripotency and subsequent excision of reprogramming factors. *Nature*, 458, 771-5.
- KAPINAS, K., KESSLER, C. B. & DELANY, A. M. 2009. miR-29 suppression of osteonectin in osteoblasts: regulation during differentiation and by canonical Wnt signaling. *J Cell Biochem*, 108, 216-24.
- KARAKOTI, A. S., DAS, S., THEVUTHASAN, S. & SEAL, S. 2011. PEGylated inorganic nanoparticles. *Angew Chem Int Ed Engl*, 50, 1980-94.
- KASINSKI, A. L. & SLACK, F. J. 2011. MicroRNAs en route to the clinic: progress in validating and targeting microRNAs for cancer therapy. *Nature Reviews Cancer*, 11, 849-864.
- KELLER, G. M. 1995. In vitro differentiation of embryonic stem cells. *Curr Opin Cell Biol*, 7, 862-869.
- KENNERDELL, J. R. & CARTHEW, R. W. 1998. Use of dsRNA-mediated genetic interference to demonstrate that frizzled and frizzled 2 act in the wingless pathway. *Cell*, 95, 1017-26.
- KIEL, M. J. & MORRISON, S. J. 2006. Maintaining hematopoietic stem cells in the vascular niche. *Immunity*, 25, 862-864.
- KIM, B.-M., THIER, M.-C., OH, S., SHERWOOD, R., KANELLOPOULOU, C., EDENHOFER, F. & CHOI, M. Y. 2012. MicroRNAs Are Indispensable for Reprogramming Mouse Embryonic Fibroblasts into Induced Stem Cell-Like Cells. *PLoS ONE*, 7, e39239.
- KIM, D., KIM, C. H., MOON, J. I., CHUNG, Y. G., CHANG, M. Y., HAN, B. S., KO, S., YANG, E., CHA, K. Y., LANZA, R. & KIM, K. S. 2009. Generation of human induced pluripotent stem cells by direct delivery of reprogramming proteins. *Cell Stem Cell*, 4, 472-6.
- KIM, J.-H., YEOM, J.-H., KO, J.-J., HAN, M. S., LEE, K., NA, S.-Y. & BAE, J. 2011. Effective delivery of anti-miRNA DNA oligonucleotides by functionalized gold nanoparticles. *Journal of Biotechnology*, 155, 287-292.
- KIM, S. H., MOK, H., JEONG, J. H., KIM, S. W. & PARK, T. G. 2006. Comparative evaluation of target-specific GFP gene silencing

- efficiencies for antisense ODN, synthetic siRNA, and siRNA plasmid complexed with PEI-PEG-FOL conjugate. *Bioconjug Chem*, 17, 241-4.
- KIRCHNER, C., LIEDL, T., KUDERA, S., PELLEGRINO, T., MUNOZ JAVIER, A., GAUB, H. E., STOLZLE, S., FERTIG, N. & PARAK, W. J. 2005. Cytotoxicity of colloidal CdSe and CdSe/ZnS nanoparticles. *Nano Lett*, 5, 331-8.
- KLOOSTERMAN, W. P., LAGENDIJK, A. K., KETTING, R. F., MOULTON, J. D. & PLASTERK, R. H. A. 2007. Targeted inhibition of miRNA maturation with morpholinos reveals a role for miR-375 in pancreatic islet development. *PLoS* 5.
- KNOP, K., HOOGENBOOM, R., FISCHER, D. & SCHUBERT, U. S. 2010. Poly(ethylene glycol) in drug delivery: pros and cons as well as potential alternatives. *Angew Chem Int Ed Engl*, 49, 6288-308.
- KOBAYASHI, H., WATANABE, R. & CHOYKE, P. L. 2014. Improving Conventional Enhanced Permeability and Retention (EPR) Effects; What Is the Appropriate Target? *Theranostics*, 4, 81-89.
- KOHANE, D. S. 2007. Microparticles and nanoparticles for drug delivery. *Biotechnology and Bioengineering*, 96, 203-209.
- KRUTZFELDT, J., RAJEWSKY, N., BRAICH, R., RAJEEV, K. G., TUSCHL, T., MANOHARAN, M. & STOFFEL, M. 2005a. Silencing of microRNAs in vivo with 'antagomirs'. *Nature*, 438, 685-9.
- KRUTZFELDT, J., RAJEWSKY, N., BRAICH, R., RAJEEV, K. G., TUSCHL, T., MANOHARAN, M. & STOFFEL, M. 2005b. Silencing of microRNAs in vivo with 'antagomirs'. *Nature*, 438, 685-689.
- KUHN, D. A., VANHECKE, D., MICHEN, B., BLANK, F., GEHR, P., PETRI-FINK, A. & ROTHEN-RUTISHAUSER, B. 2014. Different endocytotic uptake mechanisms for nanoparticles in epithelial cells and macrophages. *Beilstein Journal of Nanotechnology*, 5, 1625-1636.
- KUMAR, A., MA, H., ZHANG, X., HUANG, K., JIN, S., LIU, J., WEI, T., CAO, W., ZOU, G. & LIANG, X.-J. 2012a. Gold nanoparticles functionalized with therapeutic and targeted peptides for cancer treatment. *Biomaterials*.
- KUMAR, A., MA, H., ZHANG, X., HUANG, K., JIN, S., LIU, J., WEI, T., CAO, W., ZOU, G. & LIANG, X. J. 2012b. Gold nanoparticles functionalized with therapeutic and targeted peptides for cancer treatment. *Biomaterials*, 33, 1180-1189.
- KUMAR, D., MEENAN, B. J. & DIXON, D. 2012. Glutathione-mediated release of Bodipy(R) from PEG cofunctionalized gold nanoparticles. *Int J Nanomedicine*, 7, 4007-22.
- KURRECK, J. 2009. RNA Interference: From Basic Research to Therapeutic Applications. *Angewandte Chemie-International Edition*, 48, 1378-1398.
- LAINE, S. K., HENTUNEN, T. & LAITALA-LEINONEN, T. 2012. Do microRNAs regulate bone marrow stem cell niche physiology? *Gene*, 497, 1-9.
- LANDEN, C. N., CHAVEZ-REYES, A., BUCANA, C., SCHMANDT, R., DEEVERS, M. T., LOPEZ-BERESTEIN, G. & SOOD, A. K. 2005. Therapeutic EphA2 gene targeting in vivo using neutral liposomal small interfering RNA delivery. *Cancer Research*, 65, 6910-6918.

- LANFORD, R. E., HILDEBRANDT-ERIKSEN, E. S., PETRI, A., PERSSON, R., LINDOW, M., MUNK, M. E., KAUPPINEN, S. & ORUM, H. 2010. Therapeutic silencing of microRNA-122 in primates with chronic hepatitis C virus infection. *Science*, 327, 198-201.
- LE GUEHENNEC, L., LOPEZ-HEREDIA, M. A., ENKEL, B., WEISS, P., AMOURIQ, Y. & LAYROLLE, P. 2008. Osteoblastic cell behaviour on different titanium implant surfaces. *Acta Biomater*, 4, 535-43.
- LEAMON, C. P. & LOW, P. S. 1991. Delivery of macromolecules into living cells: a method that exploits folate receptor endocytosis. *Proc Natl Acad Sci U S A*, 88, 5572-6.
- LEDUC, C., JUNG, J. M., CARNEY, R. P., STELLACCI, F. & LOUNIS, B. 2011. Direct investigation of intracellular presence of gold nanoparticles via photothermal heterodyne imaging. *ACS Nano*, 5, 2587-92.
- LEE, C. C., MACKAY, J. A., FRECHET, J. M. & SZOKA, F. C. 2005. Designing dendrimers for biological applications. *Nat Biotechnol*, 23, 1517-26.
- LEE, J. H., LEE, K., MOON, S. H., LEE, Y., PARK, T. G. & CHEON, J. 2009. All-in-one target-cell-specific magnetic nanoparticles for simultaneous molecular imaging and siRNA delivery. *Angew Chem Int Ed Engl*, 48, 4174-9.
- LEE, K.-D., KUO, T. K.-C., WHANG-PENG, J., CHUNG, Y.-F., LIN, C.-T., CHOU, S.-H., CHEN, J.-R., CHEN, Y.-P. & LEE, O. K.-S. 2004. In vitro hepatic differentiation of human mesenchymal stem cells. *Hepatology*, 40, 1275-1284.
- LEE, P. C. & MEISEL, D. 1982. Adsorption and surface-enhanced Raman of dyes on silver and gold sols. *The Journal of Physical Chemistry*, 86, 3391-3395.
- LEE, S.-Y., HUH, M. S., LEE, S., LEE, S. J., CHUNG, H., PARK, J. H., OH, Y.-K., CHOI, K., KIM, K. & KWON, I. C. 2010. Stability and cellular uptake of polymerized siRNA (poly-siRNA)/polyethylenimine (PEI) complexes for efficient gene silencing. *Journal of Controlled Release*, 141, 339-346.
- LEE, S. H., BAE, K. H., KIM, S. H., LEE, K. R. & PARK, T. G. 2008. Amine-functionalized gold nanoparticles as non-cytotoxic and efficient intracellular siRNA delivery carriers. *Int J Pharm*, 364, 94-101.
- LEE, Y. S., KIM, H. K., CHUNG, S., KIM, K. S. & DUTTA, A. 2005. Depletion of human micro-RNA miR-125b reveals that it is critical for the proliferation of differentiated cells but not for the down-regulation of putative targets during differentiation. *J Biol Chem*, 280, 16635-41.
- LEI, X. G. 2002. In vivo antioxidant role of glutathione peroxidase: evidence from knockout mice. *Methods Enzymol*, 347, 213-225.
- LEVY, R., SHAHEEN, U., CESBRON, Y. & SEE, V. 2010. Gold nanoparticles delivery in mammalian live cells: a critical review. *Nano Rev*, 1.
- LÉVY, R., SHAHEEN, U., CESBRON, Y. & SÉE, V. 2010. Gold nanoparticles delivery in mammalian live cells: a critical review. *Nano Reviews*, 1, 1-18.

- LI, H., XIE, H., LIU, W., HU, R., HUANG, B., TAN, Y. F., XU, K., SHENG, Z. F., ZHOU, H. D., WU, X. P. & LUO, X. H. 2009. A novel microRNA targeting HDAC5 regulates osteoblast differentiation in mice and contributes to primary osteoporosis in humans. *J Clin Invest*, 119, 3666-77.
- LI, S. D., CHONO, S. & HUANG, L. 2008. Efficient oncogene silencing and metastasis inhibition via systemic delivery of siRNA. *Mol Ther*, 16, 942-6.
- LI, Z. & RANA, T. M. 2012. Molecular Mechanisms of RNA-Triggered Gene Silencing Machineries. *Accounts of chemical research*, 45, 1122-1131.
- LI, Z., VAN CALCAR, S., QU, C., CAVENEE, W. K., ZHANG, M. Q. & REN, B. 2003. A global transcriptional regulatory role for c-Myc in Burkitt's lymphoma cells. *Proc Natl Acad Sci U S A*, 100, 8164-9.
- LIAN, J. B., STEIN, G. S., VAN WIJNEN, A. J., STEIN, J. L., HASSAN, M. Q., GAUR, T. & ZHANG, Y. 2012. MicroRNA control of bone formation and homeostasis. *Nat Rev Endocrinol*, 8, 212-27.
- LIAO, D. J. & DICKSON, R. B. 2000. c-Myc in breast cancer. *Endocr Relat Cancer*, 7, 143-64.
- LIN, P. C., CHIU, Y. L., BANERJEE, S., PARK, K., MOSQUERA, J. M., GIANNOPOULOU, E., ALVES, P., TEWARI, A. K., GERSTEIN, M. B., BELTRAN, H., MELNICK, A. M., ELEMENTO, O., DEMICHELIS, F. & RUBIN, M. A. 2013. Epigenetic repression of miR-31 disrupts androgen receptor homeostasis and contributes to prostate cancer progression. *Cancer Res*, 73, 1232-44.
- LINKHART, T. A., MOHAN, S. & BAYLINK, D. J. 1996. Growth factors for bone growth and repair: IGF, TGF beta and BMP. *Bone*, 19, 12.
- LIONG, M., LU, J., KOVOCHICH, M., XIA, T., RUEHM, S. G., NEL, A. E., TAMANOI, F. & ZINK, J. I. 2008. Multifunctional inorganic nanoparticles for imaging, targeting, and drug delivery. *Acs Nano*, 2, 889-896.
- LIU, L.-H., LI, H., LI, J.-P., ZHONG, H., ZHANG, H.-C., CHEN, J. & XIAO, T. 2011a. miR-125b suppresses the proliferation and migration of osteosarcoma cells through down-regulation of STAT3. *Biochem Biophys Res Commun*, 416, 31-38.
- LIU, L.-H., LI, H., LI, J.-P., ZHONG, H., ZHANG, H.-C., CHEN, J. & XIAO, T. 2011b. miR-125b suppresses the proliferation and migration of osteosarcoma cells through down-regulation of STAT3. *BIOCHEMICAL AND BIOPHYSICAL RESEARCH COMMUNICATIONS*, 416, 31-38.
- LIU, Q., YANG, T., FENG, W. & LI, F. 2012. Blue-emissive upconversion nanoparticles for low-power-excited bioimaging in vivo. *J Am Chem Soc*, 134, 5390-7.
- LIU, X., CHENG, Y., CHEN, X., YANG, J., XU, L. & ZHANG, C. 2011. MicroRNA-31 regulated by the extracellular regulated kinase is involved in vascular smooth muscle cell growth via large tumor suppressor homolog 2. *J Biol Chem*, 286, 42371-80.
- LIU, X., SEMPERE, L. F., OUYANG, H., MEMOLI, V. A., ANDREW, A. S., LUO, Y., DEMIDENKO, E., KORC, M., SHI, W., PREIS, M., DRAGNEV, K. H., LI, H., DIRENZO, J., BAK, M., FREEMANTLE, S.

- J., KAUPPINEN, S. & DMITROVSKY, E. 2010. MicroRNA-31 functions as an oncogenic microRNA in mouse and human lung cancer cells by repressing specific tumor suppressors. *J Clin Invest*, 120, 1298-309.
- LIU, Y., SHIPTON, M. K., RYAN, J., KAUFMAN, E. D., FRANZEN, S. & FELDHEIM, D. L. 2007. Synthesis, stability, and cellular internalization of gold nanoparticles containing mixed peptide-poly(ethylene glycol) monolayers. *Anal. Chem.*, 79, 2221-2229.
- LOMMATZSCH, S. T. & ARIS, R. 2009. Genetics of cystic fibrosis. *Semin Respir Crit Care Med*, 30, 531-8.
- LOVRIC, J., CHO, S. J., WINNIK, F. M. & MAYSINGER, D. 2005. Unmodified cadmium telluride quantum dots induce reactive oxygen species formation leading to multiple organelle damage and cell death. *Chem Biol*, 12, 1227-34.
- LU, A. H., SALABAS, E. L. & SCHUTH, F. 2007. Magnetic nanoparticles: synthesis, protection, functionalization, and application. *Angew Chem Int Ed Engl*, 46, 1222-44.
- LUO, J., SOLIMINI, N. L. & ELLEDGE, S. J. 2009. Principles of cancer therapy: oncogene and non-oncogene addiction. *Cell*, 136, 823-37.
- LUSHCHAK, V. I. 2012. Glutathione Homeostasis and Functions: Potential Targets for Medical Interventions. *Journal of Amino Acids*, 2012, 26.
- MA, X., WU, Y., JIN, S., TIAN, Y., ZHANG, X., ZHAO, Y., YU, L. & LIANG, X.-J. 2011. Gold Nanoparticles Induce Autophagosome Accumulation through Size-Dependent Nanoparticle Uptake and Lysosome Impairment. *ACS Nano*, 5, 8629-8639.
- MAJUMDAR, M. K., THIEDE, M. A., HAYNESWORTH, S. E., BRUDER, S. P. & GERSON, S. L. 2000. Human marrow-derived mesenchymal stem cells (MSCs) express hematopoietic cytokines and support long-term hematopoiesis when differentiated toward stromal and osteogenic lineages. *J Hematother Stem Cell Res*, 9, 841-848.
- MANCHE, L., GREEN, S. R., SCHMEDT, C. & MATHEWS, M. B. 1992. Interactions between double-stranded RNA regulators and the protein kinase DAI. *Mol Cell Biol*, 12, 5238-5248.
- MARTIN, G. R. 1981. Isolation of a pluripotent cell line from early mouse embryos cultured in medium conditioned by teratocarcinoma stem cells. *Proc Natl Acad Sci U S A*, 78, 7634-8.
- MATRANGA, C., TOMARI, Y., SHIN, C., BARTEL, D. P. & ZAMORE, P. D. 2005. Passenger-strand cleavage facilitates assembly of siRNA into Ago2-containing RNAi enzyme complexes. *Cell*, 123, 607-620.
- MCBEATH, R., PIRONE, D. M., NELSON, C. M., BHADRIRAJU, K. & CHEN, C. S. 2004. Cell shape, cytoskeletal tension, and RhoA regulate stem cell lineage commitment. *Dev Cell*, 6, 483-495.
- MCMILLAN, J. J., BATRAKOVA, E. E. & GENDELMAN, H. E. H. E. 2011. Cell delivery of therapeutic nanoparticles. *Progress in Molecular Biology and Translational Science*, 104, 563-601.
- MCMURRAY, R. J., GADEGAARD, N., TSIMBOURI, P. M., BURGESS, K. V., MCNAMARA, L. E., TARE, R., MURAWSKI, K., KINGHAM, E.,

- OREFFO, R. O. C. & DALBY, M. J. 2011. Nanoscale surfaces for the long-term maintenance of mesenchymal stem cell phenotype and multipotency. *Nat Mater*, 10, 637-644.
- MCNAMARA, L. E., MCMURRAY, R. J., BIGGS, M. J. P., KANTAWONG, F., OREFFO, R. O. C. & DALBY, M. J. 2010. Nanotopographical control of stem cell differentiation. *J Tissue Eng*, 2010, 120623-120623.
- MEADE, B. R. & DOWDY, S. F. 2008. Enhancing the cellular uptake of siRNA duplexes following noncovalent packaging with protein transduction domain peptides. *Adv Drug Deliv Rev*, 60, 530-6.
- MEDAROVA, Z., PHAM, W., FARRAR, C., PETKOVA, V. & MOORE, A. 2007. In vivo imaging of siRNA delivery and silencing in tumors. *Nat Med*, 13, 372-7.
- MEDINA, P. P., NOLDE, M. & SLACK, F. J. 2010. OncomiR addiction in an in vivo model of microRNA-21-induced pre-B-cell lymphoma. *Nature*, 467, 86-90.
- MEDINTZ, I. L., UYEDA, H. T., GOLDMAN, E. R. & MATTOUSSI, H. 2005. Quantum dot bioconjugates for imaging, labelling and sensing. *Nat Mater*, 4, 435-46.
- MEISTER, A. 1988. Glutathione metabolism and its selective modification. *J Biol Chem*, 263, 17205-17208.
- MEISTER, A. & ANDERSON, M. E. 1983. Glutathione. *Annu Rev Biochem*, 52, 711-760.
- MELLMAN, I. 1996. Endocytosis and molecular sorting. *Annual Review of Cell and Developmental Biology*, 12, 575-625.
- MELTON, C. & BLELLOCH, R. 2010. MicroRNA Regulation of Embryonic Stem Cell Self-Renewal and Differentiation. *Adv Exp Med Biol*, 695, 105-117.
- MICHAEL, M. Z., SM, O. C., VAN HOLST PELLEKAAN, N. G., YOUNG, G. P. & JAMES, R. J. 2003. Reduced accumulation of specific microRNAs in colorectal neoplasia. *Mol Cancer Res*, 1, 882-91.
- MILLER, G. 2006. Nanomaterials, sunscreens and cosmetics: Small Ingredients, big risks. *Friends of the Earth Australia Nanotechnology Project*.
- MILNER, K. R. & SIEDLECKI, C. A. 2007. Submicron poly(L-lactic acid) pillars affect fibroblast adhesion and proliferation. *J Biomed Mater Res A*, 82, 80-91.
- MIZUNO, Y., YAGI, K., TOKUZAWA, Y., KANESAKI-YATSUKA, Y., SUDA, T., KATAGIRI, T., FUKUDA, T., MARUYAMA, M., OKUDA, A., AMEMIYA, T., KONDOH, Y., TASHIRO, H. & OKAZAKI, Y. 2008. miR-125b inhibits osteoblastic differentiation by down-regulation of cell proliferation. *Biochem Biophys Res Commun*, 368, 267-72.
- MUKHERJEE, S., GHOSH, R. N. & MAXFIELD, F. R. 1997. Endocytosis. *Physiological Reviews*, 77, 759-803.
- MURAGLIA, A., CANCEDDA, R. & QUARTO, R. 2000. Clonal mesenchymal progenitors from human bone marrow differentiate in vitro according to a hierarchical model. *J Cell Sci*, 113 (Pt 7), 1161-6.
- MURAKAMI, Y., YASUDA, T., SAIGO, K., URASHIMA, T., TOYODA, H., OKANOUE, T. & SHIMOTOHNO, K. 2006. Comprehensive analysis

- of microRNA expression patterns in hepatocellular carcinoma and non-tumorous tissues. *Oncogene*, 25, 2537-45.
- MURRAY, A. W. 2004. Recycling the cell cycle: Cyclins revisited. *Cell*, 116, 221-234.
- NA, H. B., SONG, I. C. & HYEON, T. 2009. Inorganic Nanoparticles for MRI Contrast Agents. *Advanced Materials*, 21, 2133-2148.
- NAPOLI, C., LEMIEUX, C. & JORGENSEN, R. 1990. Introduction of a Chimeric Chalcone Synthase Gene into Petunia Results in Reversible Co-Suppression of Homologous Genes in trans. *Plant Cell*, 2, 279-289.
- NEL, A. E., MADLER, L., VELEGOL, D., XIA, T., HOEK, E. M. V., SOMASUNDARAN, P., KLAESSIG, F., CASTRANOVA, V. & THOMPSON, M. 2009. Understanding biophysicochemical interactions at the nano-bio interface. *Nat Mater*, 8, 543-557.
- OBERDORSTER, G., MAYNARD, A., DONALDSON, K., CASTRANOVA, V., FITZPATRICK, J., AUSMAN, K., CARTER, J., KARN, B., KREYLING, W., LAI, D., OLIN, S., MONTEIRO-RIVIERE, N., WARHEIT, D. & YANG, H. 2005. Principles for characterizing the potential human health effects from exposure to nanomaterials: elements of a screening strategy. *Part Fibre Toxicol*, 2, 8.
- ODOM, G. L., BANKS, G. B., SCHULTZ, B. R., GREGOREVIC, P. & CHAMBERLAIN, J. S. 2010. Preclinical studies for gene therapy of Duchenne muscular dystrophy. *J Child Neurol*, 25, 1149-1157.
- OH, E., DELEHANTY, J. B., SAPSFORD, K. E., SUSUMU, K., GOSWAMI, R., BLANCO-CANOSA, J. B., DAWSON, P. E., GRANEK, J., SHOFF, M., ZHANG, Q., GOERING, P. L., HUSTON, A. & MEDINTZ, I. L. 2011. Cellular Uptake and Fate of PEGylated Gold Nanoparticles Is Dependent on Both Cell-Penetration Peptides and Particle Size. *ACS Nano*, 5, 6434-6448.
- OHRT, T., MERKLE, D., BIRKENFELD, K., ECHEVERRI, C. J. & SCHWILLE, P. 2006. In situ fluorescence analysis demonstrates active siRNA exclusion from the nucleus by Exportin 5. *Nucleic Acids Res*, 34, 1369-1380.
- OISHI, M., NAKAOGAMI, J., TAKEHIKO ISHII, Y. & NAGASAKI, Y. 2001a. Smart PEGylated Gold Nanoparticles for the Cytoplasmic Delivery of siRNA to Induce Enhanced Gene Silencing. *Chemistry Letters*, 35, 1046-1047.
- OISHI, M., NAKAOGAMI, J., TAKEHIKO ISHII, Y. & NAGASAKI, Y. 2001b. Smart PEGylated Gold Nanoparticles for the Cytoplasmic Delivery of siRNA to Induce Enhanced Gene Silencing. 35, 1046-1047.
- OLIVER, L., HUE, E., PRIAULT, M. & VALLETTE, F. M. 2012. Basal autophagy decreased during the differentiation of human adult mesenchymal stem cells. *Stem Cells Dev*, 21, 2779-88.
- ORFORD, K. W. & SCADDEN, D. T. 2008. Deconstructing stem cell self-renewal: genetic insights into cell-cycle regulation. *Nat Rev Genet*, 9, 115-128.
- OWEN, M. 1988. Marrow stromal stem cells. *J Cell Sci Suppl*, 10, 63-76.
- OWEN, M. & FRIEDENSTEIN, A. J. 1988. Stromal stem cells: marrow-derived osteogenic precursors. *Ciba Found Symp*, 136, 42-60.

- PACIOTTI, G. F., MYER, L., WEINREICH, D., GOIA, D., PAVEL, N., MCLAUGHLIN, R. E. & TAMARKIN, L. 2004. Colloidal gold: a novel nanoparticle vector for tumor directed drug delivery. *Drug Deliv*, 11, 169-183.
- PALLANTE, P., VISIONE, R., FERRACIN, M., FERRARO, A., BERLINGIERI, M. T., TRONCONE, G., CHIAPPETTA, G., LIU, C. G., SANTORO, M., NEGRINI, M., CROCE, C. M. & FUSCO, A. 2006. MicroRNA deregulation in human thyroid papillary carcinomas. *Endocr Relat Cancer*, 13, 497-508.
- PAN, Y., NEUSS, S., LEIFERT, A., FISCHLER, M., WEN, F., SIMON, U., SCHMID, G., BRANDAU, W. & JAHNEN-DECHENT, W. 2007. Size-dependent cytotoxicity of gold nanoparticles. *Small*, 3, 1941-1949.
- PAUTKE, C., SCHIEKER, M., TISCHER, T., KOLK, A., NETH, P., MUTSCHLER, W. & MILZ, S. 2004. Characterization of osteosarcoma cell lines MG-63, Saos-2 and U-2 OS in comparison to human osteoblasts. *Anticancer Res*, 24, 3743-8.
- PAWAIYA, R. S., KRISHNA, L. & KUMAR, R. 2011. Genes responsible for cancer: a review. *The Indian Journal of Animal Sciences*, 81.
- PHADWAL, K., WATSON, A. S. & SIMON, A. K. 2013. Tightrope act: autophagy in stem cell renewal, differentiation, proliferation, and aging. *Cell Mol Life Sci*, 70, 89-103.
- PITTELLA, F., ZHANG, M., LEE, Y., KIM, H. J., TOCKARY, T., OSADA, K., ISHII, T., MIYATA, K., NISHIYAMA, N. & KATAOKA, K. 2011. Enhanced endosomal escape of siRNA-incorporating hybrid nanoparticles from calcium phosphate and PEG-block charge-conversional polymer for efficient gene knockdown with negligible cytotoxicity. 32, 3106-3114.
- PITTINGER, M. F., MACKAY, A. M., BECK, S. C., JAISWAL, R. K., DOUGLAS, R., MOSCA, J. D., MOORMAN, M. A., SIMONETTI, D. W., CRAIG, S. & MARSHAK, D. R. 1999. Multilineage potential of adult human mesenchymal stem cells. *Science*, 284, 143-147.
- QIAN, X., PENG, X. H., ANSARI, D. O., YIN-GOEN, Q., CHEN, G. Z., SHIN, D. M., YANG, L., YOUNG, A. N., WANG, M. D. & NIE, S. 2008. In vivo tumor targeting and spectroscopic detection with surface-enhanced Raman nanoparticle tags. *Nat Biotechnol*, 26, 83-90.
- QIU, W., ANDERSEN, T. E., BOLLERSLEV, J., MANDRUP, S., ABDALLAH, B. M. & KASSEM, M. 2007. Patients with high bone mass phenotype exhibit enhanced osteoblast differentiation and inhibition of adipogenesis of human mesenchymal stem cells. *Journal of Bone and Mineral Research*, 22, 1720-1731.
- RAHME, K., CHEN, L., HOBBS, R. G., MORRIS, M. A., O'DRISCOLL, C. & HOLMES, J. D. 2013. PEGylated gold nanoparticles: polymer quantification as a function of PEG lengths and nanoparticle dimensions. *RSC Advances*, 3, 6085.
- RANA, T. M. 2007. Illuminating the silence: understanding the structure and function of small RNAs. *Nat Rev Mol Cell Biol*, 8, 23-36.
- RAND, T. A., GINALSKI, K., GRISHIN, N. V. & WANG, X. 2004. Biochemical identification of Argonaute 2 as the sole protein

- required for RNA-induced silencing complex activity. *Proceedings of the National Academy of Sciences of the United States of America*, 101, 14385-14389.
- REHMSMEIER, M., STEFFEN, P., HOCHSMANN, M. & GIEGERICH, R. 2004. Fast and effective prediction of microRNA/target duplexes. *Rna*, 10, 1507-17.
- RICKARD, D. J., SULLIVAN, T. A., SHENKER, B. J., LEBOY, P. S. & KAZHDAN, I. 1994. Induction of rapid osteoblast differentiation in rat bone marrow stromal cell cultures by dexamethasone and BMP-2. *Dev Biol*, 161, 218-228.
- ROSI, N. L., GILJOHANN, D. A., THAXTON, C. S., LYTTON-JEAN, A. K. R., HAN, M. S. & MIRKIN, C. A. 2006. Oligonucleotide-modified gold nanoparticles for intracellular gene regulation. *Science*, 312, 1027-1030.
- RYAN, B. M., ROBLES, A. I. & HARRIS, C. C. 2010. Genetic variation in microRNA networks: the implications for cancer research. *Nat Rev Cancer*, 10, 389-402.
- RYOU, S. M., KIM, S., JANG, H. H., KIM, J. H., YEOM, J. H., EOM, M. S., BAE, J., HAN, M. S. & LEE, K. 2010. Delivery of shRNA using gold nanoparticle-DNA oligonucleotide conjugates as a universal carrier. *Biochem Biophys Res Commun*, 398, 542-6.
- SALEM, A. K., SEARSON, P. C. & LEONG, K. W. 2003. Multifunctional nanorods for gene delivery. *Nat Mater*, 2, 668-671.
- SANT, S., POULIN, S. & HILDGEN, P. 2008. Effect of polymer architecture on surface properties, plasma protein adsorption, and cellular interactions of pegylated nanoparticles. *Journal of Biomedical Materials Research Part A*, 87A, 885-895.
- SANTARIUS, T., SHIPLEY, J., BREWER, D., STRATTON, M. R. & COOPER, C. S. 2010. A census of amplified and overexpressed human cancer genes. *Nat. Rev. Cancer*, 10, 59-64.
- SANVICENS, N. & MARCO, M. P. 2008. Multifunctional nanoparticles--properties and prospects for their use in human medicine. *Trends Biotechnol*, 26, 425-33.
- SARTIPY, P., OLSSON, B., HYLLNER, J. & SYNNERGREN, J. 2009. Regulation of 'stemness' and stem cell differentiation by microRNAs. *IDrugs*, 12, 492-496.
- SARUGASER, R., HANOUN, L., KEATING, A., STANFORD, W. L. & DAVIES, J. E. 2009. Human mesenchymal stem cells self-renew and differentiate according to a deterministic hierarchy. *PLoS One*, 4.
- SCHIFFELERS, R. M., ANSARI, A., XU, J., ZHOU, Q., TANG, Q., STORM, G., MOLEMA, G., LU, P. Y., SCARIA, P. V. & WOODLE, M. C. 2004. Cancer siRNA therapy by tumor selective delivery with ligand-targeted sterically stabilized nanoparticle. *Nucleic Acids Res*, 32, e149.
- SCHÖNIGER, C. & ARENZ, C. 2013. Perspectives in targeting miRNA function. *BIOORGANIC & MEDICINAL CHEMISTRY*, 1-4.
- SCOTT, G. K., GOGA, A., BHAUMIK, D., BERGER, C. E., SULLIVAN, C. S. & BENZ, C. C. 2007. Coordinate suppression of ERBB2 and ERBB3

- by enforced expression of micro-RNA miR-125a or miR-125b. *J Biol Chem*, 282, 1479-86.
- SCOTT, M. A., NGUYEN, V. T., LEVI, B. & JAMES, A. W. 2011. Current methods of adipogenic differentiation of mesenchymal stem cells. *Stem Cells Dev*, 20, 1793-804.
- SECA, H., ALMEIDA, G. M., GUIMARÃES, J. E. & VASCONCELOS, M. H. 2010. miR signatures and the role of miRs in acute myeloid leukaemia. *European Journal of Cancer*, 46, 1520-1527.
- SHERLEY, J. L. 2002. Asymmetric cell kinetics genes: the key to expansion of adult stem cells in culture. *ScientificWorldJournal*, 2, 1906-1921.
- SHI, K., LU, J., ZHAO, Y., WANG, L., LI, J., QI, B., LI, H. & MA, C. 2013. MicroRNA-214 suppresses osteogenic differentiation of C2C12 myoblast cells by targeting Osterix. *Bone*, 55, 487-494.
- SHI, Y. 2003. Mammalian RNAi for the masses. *Trends in Genetics*, 19, 9-12.
- SIDDAPPA, R., FERNANDES, H., LIU, J., VAN BLITTERSWIJK, C. & DE BOER, J. 2007. The response of human mesenchymal stem cells to osteogenic signals and its impact on bone tissue engineering. *Curr Stem Cell Res Ther*, 2, 209-220.
- SIDDAPPA, R., LICHT, R., VAN BLITTERSWIJK, C. & DE BOER, J. 2007. Donor variation and loss of multipotency during in vitro expansion of human mesenchymal stem cells for bone tissue engineering. *J Orthop Res*, 25, 1029-41.
- SIMMONS, P. J. & TOROK-STORB, B. 1991. CD34 expression by stromal precursors in normal human adult bone marrow. *Blood*, 78, 2848-2853.
- SIMPSON, C. A., AGRAWAL, A. C., BALINSKI, A., HARKNESS, K. M. & CLIFFEL, D. E. 2011. Short-Chain PEG Mixed Monolayer Protected Gold Clusters Increase Clearance and Red Blood Cell Counts. *ACS Nano*, 5, 3577-3584.
- SIOLAS, D., LERNER, C., BURCHARD, J., GE, W., LINSLEY, P. S., PADDISON, P. J., HANNON, G. J. & CLEARY, M. A. 2005. Synthetic shRNAs as potent RNAi triggers. *Nat Biotechnol*, 23, 227-31.
- SONG, E., ZHU, P., LEE, S. K., CHOWDHURY, D., KUSSMAN, S., DYKXHOORN, D. M., FENG, Y., PALLISER, D., WEINER, D. B., SHANKAR, P., MARASCO, W. A. & LIEBERMAN, J. 2005. Antibody mediated in vivo delivery of small interfering RNAs via cell-surface receptors. *Nat Biotechnol*, 23, 709-17.
- SONG, E. W., LEE, S. K., WANG, J., INCE, N., OUYANG, N., MIN, J., CHEN, J. S., SHANKAR, P. & LIEBERMAN, J. 2003. RNA interference targeting Fas protects mice from fulminant hepatitis. *Nature Medicine*, 9, 347-351.
- SORKIN, A. & VON ZASTROW, M. 2002. Signal transduction and endocytosis: close encounters of many kinds. *Nat Rev Mol Cell Biol*, 3, 600-14.
- SOUTSCHEK, J., AKINC, A., BRAMLAGE, B., CHARISSE, K., CONSTIEN, R., DONOGHUE, M., ELBASHIR, S., GEICK, A., HADWIGER, P., HARBORTH, J., JOHN, M., KESAVAN, V., LAVINE, G., PANDEY, R. K., RACIE, T., RAJEEV, K. G., ROHL, I., TOUDJARSKA, I., WANG,

- G., WUSCHKO, S., BUMCROT, D., KOTELIANSKY, V., LIMMER, S., MANOHARAN, M. & VORNLOCHER, H. P. 2004. Therapeutic silencing of an endogenous gene by systemic administration of modified siRNAs. *Nature*, 432, 173-8.
- SPREMULLI, E. N. & DEXTER, D. L. 1983. Human tumor cell heterogeneity and metastasis. *J Clin Oncol*, 1, 496-509.
- STARCZYNOWSKI, D. T., KUCHENBAUER, F., WEGRZYN, J., ROUHI, A., PETRIV, O., HANSEN, C. L., HUMPHRIES, R. K. & KARSAN, A. 2011. MicroRNA-146a disrupts hematopoietic differentiation and survival. *Exp Hematol*, 39, 167-178.e4.
- STEFANICK, J. F., ASHLEY, J. D., KIZILTEPE, T. & BILGICER, B. 2013. A systematic analysis of peptide linker length and liposomal polyethylene glycol coating on cellular uptake of peptide-targeted liposomes. *ACS Nano*, 7, 2935-47.
- STEIN, G. S., LIAN, J. B. & OWEN, T. A. 1990. Bone cell differentiation: a functionally coupled relationship between expression of cell-growth- and tissue-specific genes. *Curr Opin Cell Biol*, 2, 1018-1027.
- STEWART, K., MONK, P., WALSH, S., JEFFERISS, C. M., LETCHFORD, J. & BERESFORD, J. N. 2003. STRO-1, HOP-26 (CD63), CD49a and SB-10 (CD166) as markers of primitive human marrow stromal cells and their more differentiated progeny: a comparative investigation in vitro. *Cell Tissue Res*, 313, 281-90.
- SU, C. H., SHEU, H. S., LIN, C. Y., HUANG, C. C., LO, Y. W., PU, Y. C., WENG, J. C., SHIEH, D. B., CHEN, J. H. & YEH, C. S. 2007. Nanoshell magnetic resonance imaging contrast agents. *J Am Chem Soc*, 129, 2139-46.
- SUH, J. S., LEE, J. Y., CHOI, Y. S., CHONG, P. C. & PARK, Y. J. 2013. Peptide-mediated intracellular delivery of miRNA-29b for osteogenic stem cell differentiation. *Biomaterials*, 34, 4347-4359.
- SUN, F., WANG, J., PAN, Q., YU, Y., ZHANG, Y., WAN, Y., WANG, J., LI, X. & HONG, A. 2009a. Characterization of function and regulation of miR-24-1 and miR-31. *Biochem Biophys Res Commun*, 380, 660-5.
- SUN, F., WANG, J., PAN, Q., YU, Y., ZHANG, Y., WAN, Y., WANG, J., LI, X. & HONG, A. 2009b. Characterization of function and regulation of miR-24-1 and miR-31. *BIOCHEMICAL AND BIOPHYSICAL RESEARCH COMMUNICATIONS*, 380, 660-665.
- SUN, Q., KANDALAM, A. K., WANG, Q., JENA, P., KAWAZOE, Y. & MARQUEZ, M. 2006. Effect of Au coating on the magnetic and structural properties of Fe nanoclusters for use in biomedical applications: A density-functional theory study. *Physical Review B*, 73.
- SWANSON, J. A. & WATTS, C. 1995. Macropinocytosis. *Trends in Cell Biology*, 5, 424-428.
- TAKAHASHI, K. & YAMANAKA, S. 2006. Induction of pluripotent stem cells from mouse embryonic and adult fibroblast cultures by defined factors. *Cell*, 126, 663-76.
- TAKESHITA, F., MINAKUCHI, Y., NAGAHARA, S., HONMA, K., SASAKI, H., HIRAI, K., TERATANI, T., NAMATAME, N., YAMAMOTO, Y.,

- HANAI, K., KATO, T., SANO, A. & OCHIYA, T. 2005. Efficient delivery of small interfering RNA to bone-metastatic tumors by using atelocollagen in vivo. *Proc Natl Acad Sci U S A*, 102, 12177-82.
- THOMSON, J. A., ITSKOVITZ-ELDOR, J., SHAPIRO, S. S., WAKNITZ, M. A., SWIERGIEL, J. J., MARSHALL, V. S. & JONES, J. M. 1998. Embryonic stem cell lines derived from human blastocysts. *Science*, 282, 1145-7.
- THOMSON, J. M., NEWMAN, M., PARKER, J. S., MORIN-KENSICKI, E. M., WRIGHT, T. & HAMMOND, S. M. 2006. Extensive post-transcriptional regulation of microRNAs and its implications for cancer. *Genes Dev*, 20, 2202-7.
- TORCHILIN, V. P. 2005. Recent advances with liposomes as pharmaceutical carriers. *Nat Rev Drug Discov*, 4, 145-60.
- TROPEL, P., PLATET, N., PLATEL, J.-C., NOEL, D., ALBRIEUX, M., BENABID, A.-L. & BERGER, F. 2006. Functional neuronal differentiation of bone marrow-derived mesenchymal stem cells. *Stem Cells*, 24, 2868-2876.
- TSAI, W. C., HSU, P. W., LAI, T. C., CHAU, G. Y., LIN, C. W., CHEN, C. M., LIN, C. D., LIAO, Y. L., WANG, J. L., CHAU, Y. P., HSU, M. T., HSIAO, M., HUANG, H. D. & TSOU, A. P. 2009. MicroRNA-122, a tumor suppressor microRNA that regulates intrahepatic metastasis of hepatocellular carcinoma. *Hepatology*, 49, 1571-82.
- TURKEVICH, J., STEVENSON, P. C. & HILLIER, J. 1951. A Study of the Nucleation and Growth Processes in the Synthesis of Colloidal Gold. *Discussions of the Faraday Society*, 55-&.
- UCCELLI, A., MORETTA, L. & PISTOIA, V. 2008. Mesenchymal stem cells in health and disease. *Nat Rev Immunol*, 8, 726-736.
- UNSWORTH, L. D., SHEARDOWN, H. & BRASH, J. L. 2005. Protein resistance of surfaces prepared by sorption of end-thiolated poly(ethylene glycol) to gold: effect of surface chain density. *Langmuir*, 21, 1036-41.
- VALASTYAN, S., CHANG, A., BENAICH, N., REINHARDT, F. & WEINBERG, R. A. 2011. Activation of miR-31 function in already-established metastases elicits metastatic regression. *Genes Dev*, 25, 646-59.
- VALASTYAN, S., REINHARDT, F., BENAICH, N., CALOGRIAS, D., SZASZ, A. M., WANG, Z. C., BROCK, J. E., RICHARDSON, A. L. & WEINBERG, R. A. 2009. A pleiotropically acting microRNA, miR-31, inhibits breast cancer metastasis. *Cell*, 137, 1032-46.
- VALASTYAN, S. & WEINBERG, R. A. 2011. Tumor metastasis: molecular insights and evolving paradigms. *Cell*, 147, 275-292.
- VAN DER KROL, A. R., MUR, L. A., BELD, M., MOL, J. N. & STUITJE, A. R. 1990. Flavonoid genes in petunia: addition of a limited number of gene copies may lead to a suppression of gene expression. *Plant Cell*, 2, 291-9.
- VAN WIJNEN, A. J., VAN DE PEPEL, J., VAN LEEUWEN, J. P., LIAN, J. B., STEIN, G. S., WESTENDORF, J. J., OURSLER, M. J., IM, H. J., TAIPALEENMAKI, H., HESSE, E., RIESTER, S. & KAKAR, S. 2013.

- MicroRNA functions in osteogenesis and dysfunctions in osteoporosis. *Curr Osteoporos Rep*, 11, 72-82.
- VESSONI, A. T., MUOTRI, A. R. & OKAMOTO, O. K. 2012. Autophagy in stem cell maintenance and differentiation. *Stem Cells Dev*, 21, 513-20.
- VOGEL, C. & MARCOTTE, E. M. 2012. Insights into the regulation of protein abundance from proteomic and transcriptomic analyses. *Nat Rev Genet*, 13, 227-32.
- VOLINIA, S., CALIN, G. A., LIU, C. G., AMBS, S., CIMMINO, A., PETROCCA, F., VISIONE, R., IORIO, M., ROLDO, C., FERRACIN, M., PRUEITT, R. L., YANAIHARA, N., LANZA, G., SCARPA, A., VECCHIONE, A., NEGRINI, M., HARRIS, C. C. & CROCE, C. M. 2006. A microRNA expression signature of human solid tumors defines cancer gene targets. *Proc Natl Acad Sci U S A*, 103, 2257-61.
- VOORHOEVE, P. M., LE SAGE, C., SCHRIER, M., GILLIS, A. J., STOOP, H., NAGEL, R., LIU, Y. P., VAN DUIJSE, J., DROST, J., GRIEKSPoor, A., ZLOTORYNSKI, E., YABUTA, N., DE VITA, G., NOJIMA, H., LOOIJENGA, L. H. & AGAMI, R. 2006. A genetic screen implicates miRNA-372 and miRNA-373 as oncogenes in testicular germ cell tumors. *Cell*, 124, 1169-81.
- WALKER, F. O. 2007. Huntington's Disease. *Semin Neurol*, 27, 143-50.
- WANG, G., BUNNELL, B. A., PAINTER, R. G., QUINIONES, B. C., TOM, S., LANSON, N. A., JR., SPEES, J. L., BERTUCCI, D., PEISTER, A., WEISS, D. J., VALENTINE, V. G., PROCKOP, D. J. & KOLLS, J. K. 2005. Adult stem cells from bone marrow stroma differentiate into airway epithelial cells: potential therapy for cystic fibrosis. *Proc Natl Acad Sci U S A*, 102, 186-91.
- WANG, H., WANG, Q., PAPE, U. J., SHEN, B., HUANG, J., WU, B. & LI, X. 2010. Systematic investigation of global coordination among mRNA and protein in cellular society. *BMC Genomics*, 11, 364.
- WANG, H., ZHANG, P., LIU, L. & ZOU, L. 2012. Hierarchical organization and regulation of the hematopoietic stem cell osteoblastic niche. *Critical Reviews in Oncology / Hematology*, 1-8.
- WANG, H.-S., HUNG, S.-C., PENG, S.-T., HUANG, C.-C., WEI, H.-M., GUO, Y.-J., FU, Y.-S., LAI, M.-C. & CHEN, C.-C. 2004. Mesenchymal stem cells in the Wharton's jelly of the human umbilical cord. *Stem Cells*, 22, 1330-1337.
- WANG, W., WEI, Q.-Q., WANG, J., WANG, B.-C., ZHANG, S.-H. & YUAN, Z. 2013. Role of thiol-containing polyethylene glycol (thiol-PEG) in the modification process of gold nanoparticles (AuNPs): stabilizer or coagulant? *Journal of Colloid And Interface Science*, 404, 223-229.
- WEINSTEIN, I. B. 2002. Cancer. Addiction to oncogenes--the Achilles heel of cancer. *Science*, 297, 63-4.
- WENG, J., SONG, X., LI, L., QIAN, H., CHEN, K., XU, X., CAO, C. & REN, J. 2006. Highly luminescent CdTe quantum dots prepared in aqueous phase as an alternative fluorescent probe for cell imaging. *Talanta*, 70, 397-402.

- WHITEHEAD, K. A., LANGER, R. & ANDERSON, D. G. 2009a. Knocking down barriers: advances in siRNA delivery. *Nat Rev Drug Discov*, 8, 129-138.
- WHITEHEAD, K. A., LANGER, R. & ANDERSON, D. G. 2009b. Knocking down barriers: advances in siRNA delivery. *Nature reviews. Drug discovery*, 8, 129-138.
- WILLIAMS, R. L., HILTON, D. J., PEASE, S., WILLSON, T. A., STEWART, C. L., GEARING, D. P., WAGNER, E. F., METCALF, D., NICOLA, N. A. & GOUGH, N. M. 1988. Myeloid leukaemia inhibitory factor maintains the developmental potential of embryonic stem cells. *Nature*, 336, 684-687.
- WILSON, A., LAURENTI, E., OSER, G., VAN DER WATH, R. C., BLANCO-BOSE, W., JAWORSKI, M., OFFNER, S., DUNANT, C. F., ESHKIND, L., BOCKAMP, E., LIO, P., MACDONALD, H. R. & TRUMPP, A. 2008. Hematopoietic stem cells reversibly switch from dormancy to self-renewal during homeostasis and repair. *Cell*, 135, 1118-29.
- WITTUNG, P., KAJANUS, J., EDWARDS, K., HAAIMA, G., NIELSEN, P. E., NORDEN, B. & MALMSTROM, B. G. 1995. Phospholipid membrane permeability of peptide nucleic acid. *FEBS Lett*, 375, 27-9.
- WODARZ, A. 2005. Molecular control of cell polarity and asymmetric cell division in *Drosophila* neuroblasts. *Curr Opin Cell Biol*, 17, 475-481.
- WOLTJEN, K., MICHAEL, I. P., MOHSENI, P., DESAI, R., MILEIKOVSKY, M., HAMALAINEN, R., COWLING, R., WANG, W., LIU, P., GERTSENSTEIN, M., KAJI, K., SUNG, H. K. & NAGY, A. 2009. piggyBac transposition reprograms fibroblasts to induced pluripotent stem cells. *Nature*, 458, 766-70.
- WOODBURY, D., SCHWARZ, E. J., PROCKOP, D. J. & BLACK, I. B. 2000. Adult rat and human bone marrow stromal cells differentiate into neurons. *J Neurosci Res*, 61, 364-70.
- WU, G., FANG, Y.-Z., YANG, S., LUPTON, J. R. & TURNER, N. D. 2004. Glutathione metabolism and its implications for health. *J Nutr*, 134, 489-492.
- WU, T., XIE, M., WANG, X., JIANG, X., LI, J. & HUANG, H. 2012. miR-155 modulates TNF- α -inhibited osteogenic differentiation by targeting SOCS1 expression. *Bone*, 51, 498-505.
- XIE, Q., WANG, Z., BI, X., ZHOU, H., WANG, Y., GU, P. & FAN, X. 2014. Effects of miR-31 on the osteogenesis of human mesenchymal stem cells. *Biochem Biophys Res Commun*, 446, 98-104.
- YAMASHITA, Y. M. 2009. The centrosome and asymmetric cell division. *Prion*, 3, 84-88.
- YANO, J., HIRABAYASHI, K., NAKAGAWA, S., YAMAGUCHI, T., NOGAWA, M., KASHIMORI, I., NAITO, H., KITAGAWA, H., ISHIYAMA, K., OHGI, T. & IRIMURA, T. 2004. Antitumor activity of small interfering RNA/cationic liposome complex in mouse models of cancer. *Clinical Cancer Research*, 10, 7721-7726.
- YU, J., VODYANIK, M. A., SMUGA-OTTO, K., ANTOSIEWICZ-BOURGET, J., FRANE, J. L., TIAN, S., NIE, J., JONSDOTTIR, G. A., RUOTTI, V., STEWART, R., SLUKVIN, II & THOMSON, J. A. 2007. Induced

- pluripotent stem cell lines derived from human somatic cells. *Science*, 318, 1917-20.
- ZAMORE, P. D. 2006. RNA interference: big applause for silencing in Stockholm. *Cell*, 127, 1083-1086.
- ZELLER, K. I., ZHAO, X., LEE, C. W., CHIU, K. P., YAO, F., YUSTEIN, J. T., OOI, H. S., ORLOV, Y. L., SHAHAB, A., YONG, H. C., FU, Y., WENG, Z., KUZNETSOV, V. A., SUNG, W. K., RUAN, Y., DANG, C. V. & WEI, C. L. 2006. Global mapping of c-Myc binding sites and target gene networks in human B cells. *Proc Natl Acad Sci U S A*, 103, 17834-9.
- ZENG, Y., QU, X., LI, H., HUANG, S., WANG, S., XU, Q., LIN, R., HAN, Q., LI, J. & ZHAO, R. C. 2012. MicroRNA-100 regulates osteogenic differentiation of human adipose-derived mesenchymal stem cells by targeting BMPR2. *FEBS Lett*, 586, 2375-2381.
- ZHANG, J. W., NIU, C., YE, L., HUANG, H. Y., HE, X., TONG, W. G., ROSS, J., HAUG, J., JOHNSON, T., FENG, J. Q., HARRIS, S., WIEDEMANN, L. M., MISHINA, Y. & LI, L. H. 2003. Identification of the haematopoietic stem cell niche and control of the niche size. *Nature*, 425, 836-841.
- ZHAO, E., ZHAO, Z., WANG, J., YANG, C., CHEN, C., GAO, L., FENG, Q., HOU, W., GAO, M. & ZHANG, Q. 2012. Surface engineering of gold nanoparticles for in vitro siRNA delivery. *Nanoscale*, 4, 5102.
- ZHAO, J. L., RAO, D. S., BOLDIN, M. P., TAGANOV, K. D., O'CONNELL, R. M. & BALTIMORE, D. 2011. NF-kappaB dysregulation in microRNA-146a-deficient mice drives the development of myeloid malignancies. *Proc Natl Acad Sci U S A*, 108, 9184-9.
- ZHONG, Z., DONG, Z., YANG, L., CHEN, X. & GONG, Z. 2013. MicroRNA-31-5p modulates cell cycle by targeting human mutL homolog 1 in human cancer cells. *Tumour Biol*, 34, 1959-65.
- ZHOU, H., WU, S., JOO, J. Y., ZHU, S., HAN, D. W., LIN, T., TRAUGER, S., BIEN, G., YAO, S., ZHU, Y., SIUZDAK, G., SCHOLER, H. R., DUAN, L. & DING, S. 2009. Generation of induced pluripotent stem cells using recombinant proteins. *Cell Stem Cell*, 4, 381-4.
- ZHOU, P., CAI, S., LIU, Z. & WANG, R. 2012. Mechanisms generating bistability and oscillations in microRNA-mediated motifs. *Physical Review E*, 85.
- ZHU, F., FRIEDMAN, M. S., LUO, W., WOOLF, P. & HANKENSON, K. D. 2012. The transcription factor osterix (SP7) regulates BMP6-induced human osteoblast differentiation. *Journal of Cellular Physiology*, 227, 2677-2685.
- ZUK, P. A., ZHU, M., MIZUNO, H., HUANG, J., FUTRELL, J. W., KATZ, A. J., BENHAIM, P., LORENZ, H. P. & HEDRICK, M. H. 2001. Multilineage cells from human adipose tissue: implications for cell-based therapies. *Tissue Eng.*, 7, 211-228.
- ZUKIEL, R., NOWAK, S., WYSZKO, E., ROLLE, K., GAWRONSKA, I., BARCISZEWSKA, M. Z. & BARCISZEWSKI, J. 2006. Suppression of human brain tumor with interference RNA specific for tenascin-C. *Cancer Biol Ther*, 5, 1002-7.